



UNIVERSITÄT
DES
SAARLANDES



Dynamic
Biomaterials

Optoregulation of collagen biosynthesis and remodeling in collagen associated diseases

Dissertation

zur Erlangung des Grades

des Doktors der Ingenieurwissenschaften

der Naturwissenschaftlich-Technischen Fakultät

der Universität des Saarlandes

von

Essak Khan

Saarbrücken, 2019

Tag des Kolloquiums: 25. November 2019

Dekan: Prof. Dr. Guido Kickelbick

Berichterstatter: Prof. Dr. Aránzazu del Campo

Prof. Dr. Ingrid M Weiss

Vorsitz: Prof. Dr. Albrecht Ott

Akad. Mitarbeiter: Dr. Indra Navina Dahmke

Optoregulation of collagen biosynthesis and remodeling in collagen associated diseases

Essak Khan

geb. in Mumbai, India

DISSERTATION

INM-Leibniz Institut für neue Materialien, Saarbrücken

“A scientist in his laboratory is not a mere technician: he is also a child confronting natural phenomena that impress him as though they were fairy tales”.

-Marie Curie

Abstract

Tissue regeneration and remodeling after damage requires enhanced collagen deposition at the site of damage. In collagen disorders like keratoconus and brittle bone disease this ability is lost due to collagen misfolding, poor crosslinking and deposition. For this purpose, tools that allow to control and regulate collagen biosynthesis and folding are required. Ideally, such tools should be collagen-specific and allow remote control, which available strategies fail to fulfill. In this context, a collagen-specific molecular chaperone, Hsp47, was chosen as it has multiple roles in collagen biosynthesis. Recombinant Hsp47 can be delivered in the endoplasmic reticulum of mammalian cells via KDEL receptor mediated endocytosis. Exogenous delivery of Hsp47 stimulates fibrillar collagen I, III and V in cells. A photoactivatable derivative of Hsp47 (H_{47Y<ONBY}) was developed containing an un-natural light-responsive tyrosine (o-nitro benzyl tyrosine (ONBY)), which renders Hsp47 inactive toward collagen binding. On-demand, localized and in situ activation of this tool, stimulating collagen production in disease-state cells, was tested in vitro. Also, this tool can be easily delivered precisely in cells of damage corneal tissue from keratoconus patients. Site-selective exposure after H_{47Y<ONBY} treatment, allowing localized remodeling of the extracellular collagen matrix, was demonstrated ex vivo. This tool has potential to trigger collagen deposition in collagen deficient disorders.

Zusammenfassung

Eine lokal erhöhte Kollagenablagerung ist für die Geweberegeneration und den Gewebenaufbau nach einer Schädigung notwendig. Bei Kollagenstörungen wie Keratokonus und Brittle Bone Disease geht diese Fähigkeit durch Fehlfaltung und schlechte Vernetzung verloren. Mittel und Wege werden benötigt, um die Kollagenbiosynthese und -faltung zu regulieren. Im Idealfall sind solche Werkzeuge kollagenspezifisch und von außen steuerbar, was derzeitige Strategien nicht erfüllen. In dieser Arbeit wurde das kollagenspezifische Chaperon Hsp47 ausgewählt, da es mehrere Rollen bei der Kollagenbiosynthese hat. Rekombinantes Hsp47 kann im endoplasmatischen Retikulum von Säugetierzellen über KDEL-Rezeptor-vermittelte Endozytose abgegeben werden. Die exogene Gabe von Hsp47 stimuliert in Zellen die Bildung von fibrillärem Kollagen I, III und V. Ein neues Hsp47 (H_{47Y} <ONBY) wurde entwickelt mit nicht-natürlichem o-Nitro-Benzyltyrosin (ONBY) an der Tyr383-Position, die inaktiv ist für die Bindung und Bildung von Kollagen. In vitro wurde in Hsp47-defizienten Zellen bewiesen, dass die kontrollierte lokale Photoaktivierung dieser Variante die Ablagerung von Kollagen stimuliert. Außerdem wurde das neue HSP47 ex vivo in Zellen von Hornhautgewebe von Keratokonus-Patienten angewendet. Hier wurde nachgewiesen, dass durch lokale Belichtung nach H_{47Y} <ONBY-Anwendung Kollagenfasern wiederhergestellt werden. Das neue HSP47 hat das Potential, gezielte Kollagenablagerungen bei Störungen mit Kollagenmangel auszulösen.

Acknowledgments

These 3 years have been an incredible journey of my life, which would not have been pleasant, nor as fun without encouragement, support and presence of several people. I would like to take this opportunity to thank all of you to help me grow as a researcher.

First I would like to thank you, Prof. Aránzazu Del Campo (Arancha) for giving me an opportunity to pursue this crucial phase of my education in your team. I very much enjoyed working with you in such an interdisciplinary environment which allowed me to explore my assets with open minded, enthusiastic, collaborative and critical individuals carefully populated in this group. I have enjoyed being given the opportunity to go for best conferences in the community, being able to have many collaborations and immense resources to carry out my research. Your balance between an open minded approach while still providing subtle guidance to keep me on path to success have increased my confidence throughout my PhD work. I have learnt so many things from you not just about managing science but also look forward in the career path. Thank you for trusting me and bringing best out of me.

Dr. Shrikrishnan Sankaran (Shirish), I thank you for always been supporting my work, encouraging me to learn new opportunities, helping me overcome my difficulties, been accessible and most importantly for mentoring me not just as a colleague but a good friend. Thanks for been critical when I am super excited about my results while always motivating in days when I am low.

Christina Muth, I would like to thank you for always been encouraging, supportive and appreciating my work. I am grateful to you in assisting my projects with all your knowledge. You have always been a dearest friend to not just discuss the projects but also personal life.

Lorena L Alzamora, Tressa Sunny and Simon Hehn, I thank you three for helping me in my experiments and I enjoyed working with all three of you.

Dr. Roshna Vakkeel, you were one of the first people who I know since day one in Saarbrücken. Thank you for supporting me in settling down in Saarbrücken. You have always been a great friend who has helped me in my difficulties and I am very happy to maintain that strong trust with you. I thank you for your advice on protein engineering, correcting my drafts from protein engineering point of view.

Dr. Bin Li, I thank you for your advice on how to draft figures. I really enjoyed working with you on the AFM project and I am happy it turned out to be successful.

Dr. Jennifer Kasper (Jenni), I thank you for your suggestions and inputs in keratoconus project.

Dr. Julieta Paez (Julie), thank you for always advising me right on the chemistry part, contributing your inputs in my research, for always learning about how am I progressing and advising me for my next career.

Prof. Ingrid M Weiss, you were supposed to co-supervise me at the starting of my PhD. I thank you for helping me design my initial experimental plans. I thank you for your help when I arrived to Saarbrücken. You have always been encouraging, supportive, for your positive vibes. I thank you for your advice on protein engineering and polarization microscopy.

Dr. Mitchell Han, I thank you for your advice on image analysis and quantification. Your critical comments on my data, presentations and constructive advices have always added cheer on top of the cake in my manuscripts.

Dr. Malgorzata Wlodarczyk-Biegun (Gosia), thanks for always been sporty, sharing your thoughts and advices in personal, social and scientific roles.

I thank Dr. Annette Kraegeloh, Jana Fleddermann, Dr. Aleeza Farrukh and Dr. Emmanuel Terriac for their advice and technical support. I also thank Dr. Jenny Brinkmann for designing template for this thesis.

I thank our collaborator Tanja Stachon and Dr. Lorenz Latta, Klinik für Augenheilkunde, UKS, Homburg, (DE) for their suggestions and providing me cornea for my experiments.

I also thank Prof. Ulrich Baumann, Cologne University (DE) for sharing Hsp47 pJExpress plasmid; Prof. Jason Chin, University of Cambridge (UK) for sharing psfGFP150TAGPyIT-His6pBad and pBK-ONBYRS plasmids; Prof. Kazuhiro Nagata, Kyoto University (JP) for sharing MEF Hsp47 (+/+) and (-/-) cell lines, Prof. Mathias Laschke, Institut für Klinisch-Experimentelle Chirurgie, UKS, Homburg, (DE) for sharing HDMEC cell line.

I thank Prof. Ulrich Baumann for discussion on molecular design, Prof. Kazuhiro Nagata for discussion on cell assays, Prof. Jesús Merayo, University of Oviedo, ESP for discussions on KC and Prof. Karl Kadler, University of Manchester, UK for discussions on tissue applicability of this tool.

I thank Stefan Brück and Martina Bonnard for always helping me in tackling social issues at INM and outside. Stefan, I appreciate your help, for being dearest friend and office mate.

Maria Villiou, Desna Joseph, Vaishali Chopra, Qiyang Jiang and Priyanka Dhakane, thanks all of you for been part of this journey. I enjoyed your company and friendship.

Finally, I thank my parents, family and friends. Without your support and encouragement, I would not have succeeded until this point.

-Essak Khan

Motivation and aim of this Thesis

Collagen is a structural protein whose fibrillar organization is crucial for the mechanical integrity of tissues. In case of injury or tissue damage, the restoration of tissue homeostasis is very much dependent on the directional deposition of collagen at the tissue site. In collagen-related disorders like keratoconus, brittle bone disease or Ehlers–Danlos syndrome, alteration in the expression profiles of collagen subtypes or their supramolecular organization in cornea, bones or skin respectively, have dramatic implications on the tissue function. Changes in collagen deposition also occur with aging, but in a highly regulated manner. Excessive collagen deposition occurs in pathologies like fibrosis or cancer.

The development of strategies to understand and treat collagenopathies requires tools that allow the regulation of collagen biosynthesis and folding. Ideally, such tools are collagen specific and allow remote control. Available strategies (treatment with ascorbate, retinol or growth factors like TGF β or VEGF) are neither specific, nor easy to regulate. In this context, the collagen specific chaperone Hsp47 seems to be an ideal candidate. Hsp47 is an endoplasmic reticulum resident protein and plays a fundamental role in the folding, stability and intracellular transport of procollagen triple helices. Existing information on the structure and interactions at the Hsp47-collagen binding site allows the design of molecular strategies to regulate Hsp47 bioactivity and consequently collagen production. In this context, the aim of this Thesis was to find a strategy for photo regulation of Hsp47, and to demonstrate its use to regulate collagen synthesis in mammalian cells and tissues. The focus of this study was to develop and test a molecular tool that enables manipulation of collagen synthesis at cell level using a remote trigger. To achieve this, a key player in the collagen biosynthesis machinery, Hsp47, was targeted and strategies to render it responsive to an external trigger were explored.

This work details important fundamental aspects in developing strategies to manipulate collagen biosynthesis *in situ* and provides a glimpse into possible applicability of the developed tool. In particular, the photoactivatable Hsp47 contains a non-natural light-responsive tyrosine at 383 position which renders Hsp47 inactive towards collagen binding. The inactive, photoactivatable protein is easily up taken by cells within a few hours of incubation, and accumulated at the endoplasmic reticulum (ER) via retrograde KDEL receptor-mediated uptake in corneal tissues. Upon light exposure, the photoactivatable Hsp47 is converted into functional Hsp47 *in situ*. This leads to increase in the intracellular concentration of Hsp47, resulting in stimulated deposition of collagen. The ability to promote collagen synthesis on-demand, with spatiotemporal resolution, and in disease state cells and tissues is demonstrated *in vitro* and in keratoconus cornea in *ex vivo* tissue.

These outcomes have been detailed in the following chapters of this thesis:

Chapter 1- Background and literature review describes the fundamentals of collagen as major ECM component, its molecular structure, collagen subtypes and biosynthesis, as well as advanced imaging techniques to study it. It also introduces Hsp47, its particular roles in

collagen biosynthesis, and how it is altered in different hereditary and non-Hereditary diseases. Finally, protein engineering strategies for regulating protein activity with light are also introduced and provide the theoretical basis for the next chapters.

Chapter 2 describes the selection and synthetic strategies for developing photoactivatable Hsp47, molecular design, results from these synthetic strategies and limitations of the strategies.

Chapter 3 shows the physicochemical characterization of the obtained photoactivatable variant and interaction with collagen compared to other Hsp47 variants.

Chapter 4 entails delivery of Hsp47 variants using KDEL receptor mediated endocytosis, different uptake capacity of Hsp47 in skin cells, stimulation of collagen deposition using exogenously-supplied Hsp47 in these cells and variation in the deposition of collagen subtypes depending upon cell types.

Chapter 5 describes on the bioactivity of Hsp47 in deposition of collagen subtypes in disease-state mammalian cell culture, the application of the photoactivatable variant of Hsp47 for spatial collagen deposition on light activation is demonstrated *in vitro* and on demand intracellular increase in collagen synthesis and distribution is also shown.

Chapter 6 describes applicability of photoactivatable Hsp47 in *ex vivo* keratoconus corneal tissue remodeling. It highlights the therapeutic potential of this tool and its advantages over existing methods, limitations of the tool and the potential applicability of this tool in other diseases as future outlook is also discussed in this chapter.

Table of Contents

Chapter 1:	Introduction	14
1.1.	Introduction	15
1.2.	Collagen	17
1.2.1.	Composition and Classification of Collagens	18
	a. Fibril forming collagen	
	b. Fibril-Associated Collagens (FACITs)	
	c. Network forming Collagens	
1.3.	Collagen Biosynthesis	20
1.3.1.	Prefolding of procollagen	
1.3.2.	Post transitional modifications	
	a. Hydroxylation	
	b. Glycosylation	
	c. Cis-trans isomerization	
1.3.3	Folding of procollagen	
1.3.4.	Trafficking, processing and secretion	
1.3.5	Extracellular deposition of collagen	
1.3.6	Assembly and collagen crosslinking	
1.4	Advances in imaging techniques for collagen	33
1.5.	Diseases due to defects in collagen production	38
	a Hereditary disorders due to genetic alternations in collagen	
	b Non-inherited genetically altered disorders	
1.6	Collagen disorder due to Hsp47 alterations	40
1.7	Hsp47 gene	40
1.8	Protein engineering strategies for localized manipulation	44
	a. Protein conjugation strategies	
	a1. Chemo selective reactions for modifications of proteins	
	a2. Native Chemical Ligation	
	a3. Enzyme-catalyzed ligations	
	b. Photoactivatable protein engineering strategies	
	b1. Oligomerization induced photo activation	
	b2. Regulation of protein accessibility (steric caging) and allosteric activity	
	b3. Light regulated photo activation of protein activity using non-canonical amino acids	
Chapter 2:	Synthesis of Photoactivatable Hsp47	54
2.1.	Introduction	55
2.2.	Results	57

2.2.1.	Strategy 1 : General molecular design	57
	a. Cloning and expression of truncated hHsp47 (human Hsp47) in pTXB1 and full length hHsp47	
	b. Cloning and expression of truncated hHsp47 (human Hsp47) in pRSETB and full length hHsp47	
	c. Cloning and expression of truncated hHsp47 (human Hsp47) in pTXB1 and full length hHsp47 along with p RARE plasmid	
2.2.2.	Strategy 2: General molecular design	64
	a. Canine Hsp47 gene optimized version construct & His-tag purification in T7 Express	
	b. Canine Hsp47 gene optimized version construct in PJExpress 411 & purification in Clear coli BL21 cells using Streptag2 purification	
2.3.	Discussion	68
<hr/>		
Chapter 3: Characterization of Photoactivatable Hsp47-Collagen interactions.		72
<hr/>		
3.1.	Introduction	73
3.2.	Results and Discussion	79
	3.2.1. Characterization of Photoactivatable Hsp47 interaction with collagen by binding assay	
	3.2.2. Characterization of Photoactivatable Hsp47 interaction with collagen by fibrillation assay	
	3.2.3. Characterization of collagen gelation by Rheology assay	
3.3.	Conclusions	84
<hr/>		
Chapter 4: Hsp47-induced stimulation of fibrillar collagen deposition in in vitro cultures of skin cells		86
<hr/>		
4.1.	Introduction	87
4.2.	Results	89
	4.2.1. Hsp47 variants can be delivered into ER via KDEL receptor-mediated Endocytosis	
	4.2.2. Increase in collagen production in skin cells in response to Hsp47	
	4.2.3. Increase in varying amount of collagen subtypes in response to Hsp47	
4.3	Discussion	94
4.4	Conclusions	95
<hr/>		
Chapter 5: Light regulated collagen deposition <i>in vitro</i>		97
<hr/>		
5.1.	Introduction	98
5.2.	Results and Discussion	102

5.2.1.	Increase in COL I, III and V deposition on Hsp47 delivery in Hsp47 -/- cells.	
5.2.2.	Increase in collagen production in Hsp47 -/- cell cultures in response to photo activation of H _{47Y<ONBY}	
5.2.3.	Controlled light exposure allows spatial regulation of collagen production	
5.2.4.	Procollagen and secretory organelles interactome on photo activation of H _{47Y<ONBY}	
5.3.	Conclusions	114
<hr/>		
Chapter 6:	Keratoconus corneal tissue remodeling using Photoactivatable Hsp47	118
<hr/>		
6.1.	Introduction	119
6.2.	Results	121
6.2.1.	Hsp47 uptake by NC and KC keratocytes in 2D cultures leads to increased collagen expression and secretion of fibrillar collagens I, III and V	
6.2.2.	Photoactivatable Hsp47 can be delivered to keratocytes in corneal explants	
6.2.3.	Light-stimulated deposition of matrix collagen in KC cornea after H _{47Y<ONBY} treatment	
6.2.4.	Deposited collagen in H _{47Y<ONBY} treated KC showed high degree of alignment	
6.2.5.	Fibrillar collagens type I, II and V are preferentially deposited in cornea tissue after treatment with H _{47Y<ONBY} and photo activation	
6.3.	Discussion	131
6.4.	Conclusions	133
<hr/>		
	Conclusion and Outlook	135
<hr/>		
	Annexure	138
	References	168
	List of publications	190
	Scientific talks and Poster presentation	191
	Curriculum Vitae	193

Chapter 1

Collagen is the most abundant structural protein in mammals and is crucial for the mechanical integrity of tissues. The tissue-specific morphology and arrangement of collagen fibers gives rise to mechanical toughness in bone, compliance in the skin and gradient mechanical properties in cartilage. The distribution and density of collagen plays a key role in branched tissue configurations like in the lung or mammary glands. This organization becomes distorted in pathologies like fibrosis and cancer. Collagen deposition supports tissue regeneration and remodeling after arterial or spinal cord injury. There are also several examples of collagen-related disorders like Osteogenesis Imperfecta, Ehlers Danlos Syndrome, Scurvy or Keratoconus, where collagen deposition and remodeling is distorted.

Collagen biosynthesis is a complicated process, involving different steps and different molecular players with roles and implications not yet fully understood. Progress in our understanding of collagen biosynthesis and possible treatment of collagen-related diseases requires the development of collagen-specific tools that allow interference with the secretion and/or assembly process. This chapter provides a brief introduction to collagen secretion and assembly pathways in natural tissues, to HSP47 as collagen-specific chaperone protein involved in collagen biosynthesis, and to synthetic biology approaches to develop light-responsive protein variants to be used for regulating collagen deposition in vitro and ex vivo.

1.1. Introduction

The extracellular matrix (ECM) is the matrix deposited by cells in their extracellular space which bestows physical scaffolding for cellular constituents and provides essential biomechanical and biochemical cues essential for tissue morphogenesis, remodeling and differentiation, thus maintaining tissue homeostasis¹. Fundamentally, ECM constitutes proteins, water and polysaccharides, which are not only tissue dependent but also heterogeneous creating unique compositions and topology which is generated through a reciprocal and dynamic, biomechanical, biochemical and biophysical dialogue between cells and their microenvironment². However, these properties can vary from one tissue to other, e.g. brain versus skin or within a tissue (e.g. Renal medulla versus cortex), as well in healthy state versus disease state (e.g. cancer and fibrosis)³⁻⁸. Additionally, beyond the structural function, the ECM component influences fundamental cellular processes like adhesion, migration or differentiation⁹⁻¹¹ by displaying growth factors and interacting with cell surface integrin's. ECM-cell interactions are crucial for the cohesion of tissues, preserving of tissue morphology and function¹²⁻¹⁴.

ECM is composed of proteoglycans (PGs), polysaccharides, extracellular vesicles and, most importantly, of structural proteins¹⁵ (See figure 1). PGs fill most of the space in the ECM by forming hydrated gel and have functions like hydration, buffering, and force –resistance properties^{3, 15}. Polysaccharide like Hyaluronic acid confers tissues property to resist compression in the form of swelling force by absorbing water molecules i.e. counteracting turgor. It is abundant in ECM of joints which are load bearing and also acts as an environmental clue like growth factors¹⁶. Exosomes are small vesicles which carry biological clues for intercellular and extracellular events for example. In cancer high number of exosomes are found in ECM carrying growth factors and RNA for promoting tumorigenesis¹⁷. The prominent component of ECM are structural proteins include collagen, fibronectin, elastin, laminin and tenascin. Amongst these, the most abundant is collagen, a structural protein that provides tensile strength to tissues, promotes cell adhesion, migration and guides tissue development¹⁸⁻¹⁹. It associates with other ECM proteins like

elastin and fibronectin. Elastin provides recoil to the tissues that undergoes stretch repeatedly. Elastin's are consist of elastin molecules sitting on microfibrillins which are essential for integrity of the elastin fibers²⁰. Fibronectin (FN) is involved in directing the organization of ECM, acts as a good adhesive substrate for cell attachment and can be stretched multiple times over its resting length by traction forces generated by cells²¹.

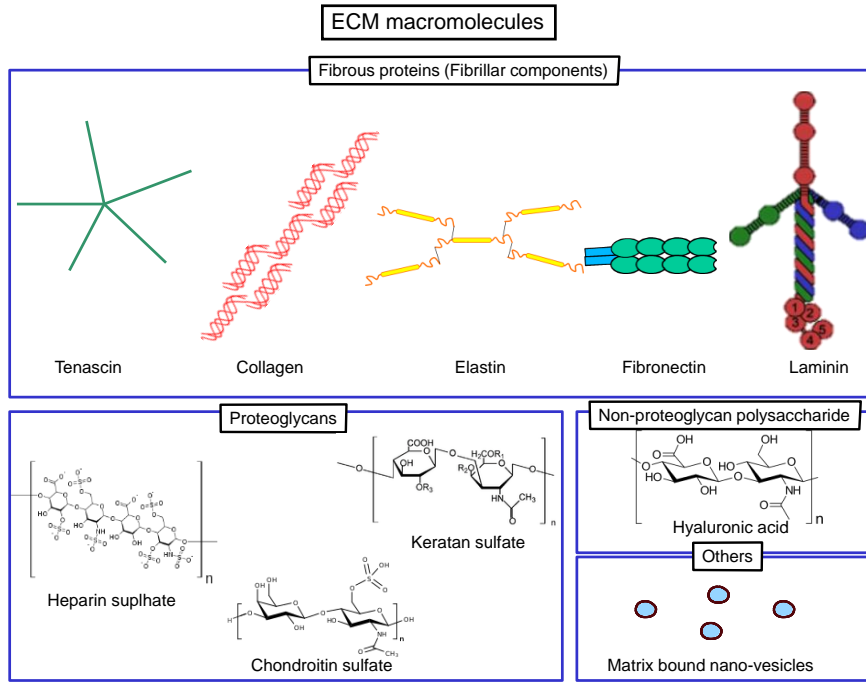


Figure1. Scheme showing ECM macromolecular components

1. Collagen:

Collagen is a structural protein which constitutes about a third of the total protein mass in the body. Collagen is vital in providing structural integrity to almost all tissues²². Collagen molecules are formed by the assembly of three protein α -chains (Figure2, 3) in a triple helix superstructure. Collagen helices self-assemble to form higher order structures, like collagen fibrils, beaded filaments or network structures depending on the collagen type. This assembly

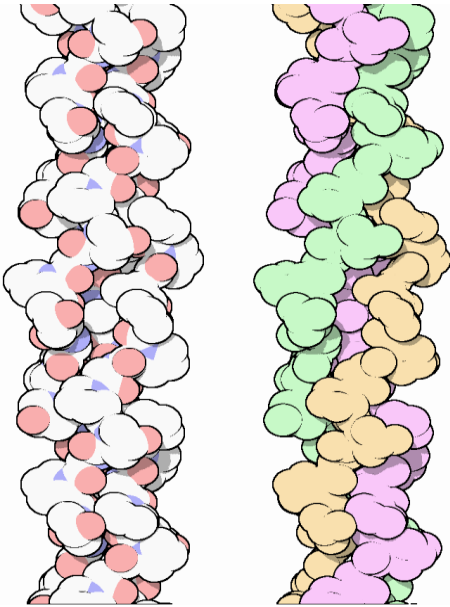


Figure 2. Triple helical structure of collagen.

is the basis for achieving tissue-specific mechanical properties: rigid bone, compliant skin, or gradient mechanics in cartilage tissue²³. Collagen assembly and deposition plays a crucial role in biological processes such as embryogenesis²⁴ and tissue regeneration²⁵, while it gets dysregulated in pathologies like brittle bone disease²⁶, fibrosis or tumor formation^{5, 27-29}.

1.1. Composition and Classification of Collagens

Collagen α -chains contain repetitive domains of the tripeptide sequence Gly-Xaa-Yaa. The Xaa amino acid is typically proline (28%) and Yaa is hydroxyproline (38%)³⁰. The left-handed α -chains form a right-handed left-handed triple helical structure. The H bonds between the backbone NH group of Gly and the CO group of the residue Xaa on adjacent chains stabilizes the triple helix structure. Non-collagenous domains are also intercalated in the collagen chains, and also at the N and C terminals (Figure 4).

Collagen subtypes:

There are 28 collagen types which are designated with Roman numerals (I-XXVIII). In humans 46 different types of α chains (named by Arabic numerals³¹) assemble to form collagen helices of 28 different types. Beyond the variability in the repetitive collagenous tripeptide sequence, the identity of the N and C

terminal domains varies among the different subtypes³² (Figure 3). Collagen supramolecular assemblies depend on the primary sequence of collagen and include fibrils, beaded filaments, anchoring filaments and networks³³⁻³⁴.

Fibril forming collagen

Fibril-forming collagens associate forms cross-striated fibrils with a characteristic axial periodicity of 67 nm. COL I, II, III, V and XI are fibril forming collagens, COL I being the most abundant one. In tissues, COL I forms heterotypic fibrils by associating with Col III in cartilage and skin, or with COL V in cornea³⁵. The nature of the associated collagens influences the crosslinking of the fibers, i.e. COL V and XIV influence the crosslinking of COL I³⁶⁻³⁷. The interactions with the matrix adhesive protein fibronectin and with integrin membrane receptors influences collagen deposition and assembly of COL V and XI with COL I and II during fibrillogenesis³⁸.

Fibril-Associated Collagens (FACITs)

COL IX, XII, XIV, XV, XVI and XIX are fibril-associated collagens. They do not form fibrils on their own, but they attach to the surface of fibrillar collagens. COL IX is mostly found cross-linked to COL II while COL XII and XIV are associated with COL I³⁹. COL XV is found mostly in basement membrane forming bridge between banded fibrils⁴⁰

Network forming Collagens

COL IV, IV, VI, VIII and X are network forming collagens. COL IV is also known as basement membrane collagen as it forms three dimensional structures associating chicken wire like two dimensional structure⁴¹ as shown in the figure.4 COL VI forms beaded filaments and COL VII connects epidermis and dermis by assembling into anchoring fibrils⁴²COL VIII and X forms hexagonal networks in cartilages and Descemet's membrane⁴¹ (Figure3).

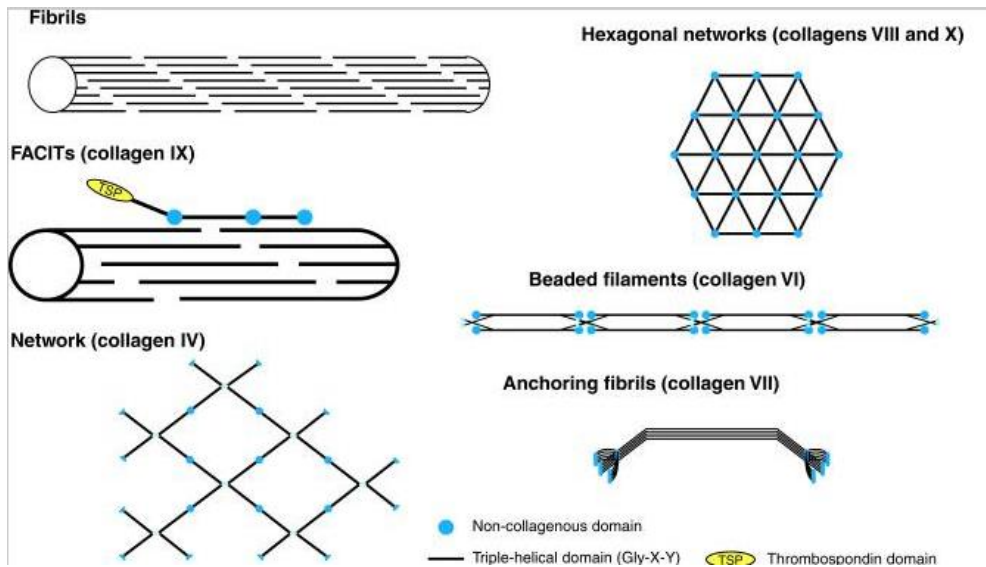


Figure 3. Supramolecular assemblies formed by collagens. Reproduced from ³⁵ with permissions from Cold Spring Harbor Laboratory Press.

1.3. Intracellular events in Collagen Biosynthesis

Collagen biosynthesis involves a complex orchestration of intracellular and extracellular⁴³ assembly events⁴⁴ regulated by specific enzymes and molecular chaperones³⁴. It starts with intracellular events like synthesis of the collagen α -chains, followed by folding and post translational modifications before its emergence as fibrillar structure to the extracellular space^{5, 22, 44-52}.

At first step, collagen is synthesized as pro α -chains by transcription and translation of collagen genes. Pro α -chains contain the same signal sequence at their N-terminals, by which they are co-translationally transferred into the lumen of the rough ER. Here, the triple helix of procollagen is formed with simultaneous post-translational modifications.

1.3.1. Pre folding of triple helix

Before the triple helix structure can be assembled, multiple steps are required to form a procollagen which functions properly in the ECM. This procedure starts with post translational modifications in parallel to chain selection.

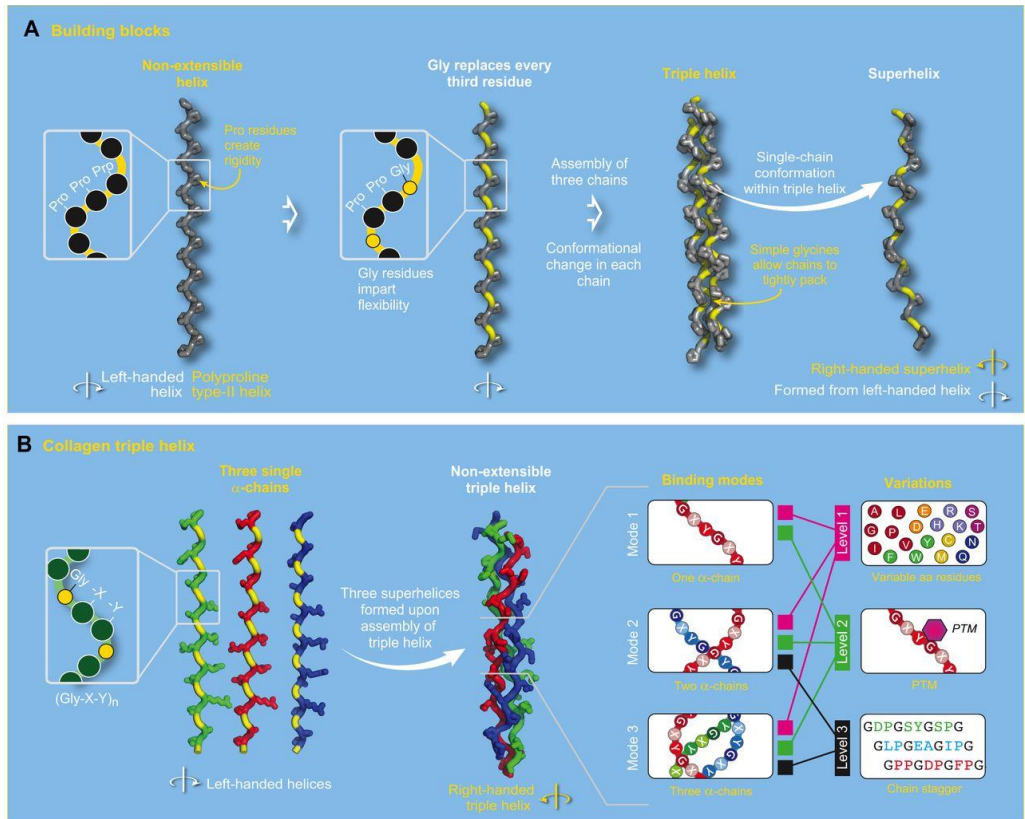


Figure 4. Collagen triple helix building blocks and the information encoded in it. (A) It shows general scheme of polypeptide chains of the triple helix which are left-handed polyproline type-II helices. At every third position is proline (Pro) residue with a glycine (Gly) residue at first position, it results in increased flexibility. Three α -helix chains come together to triple helix which promotes conformational changes in each chain forming right handed super helix. (B) In collagen, the super helices are wind together and tightly pack

due to the Gly residues. Once the non-extensible triple helix is formed, the combination of three chains shows either of three binding modes with three stages of variation to these modes, i.e. *level 1*: 20 amino acids, *level 2*: post-translational modifications and, *level 3*: chain staggered. Reproduced from ⁵³ with permissions from Cold Spring Harbor Laboratory Press.

Role of molecular chaperones and enzymes in Collagen assembly

1.3.2. Post translational modifications

Collagen modifying enzymes introduce post-translational modifications and have a chaperone function. This is a practical solution to avoid the aggregation of procollagen into large clusters. Most of these enzymes are not exclusive to collagens and often act as part of heterocomplexes to perform more than one function. Major roles of collagen-related chaperones are described below:

a. Hydroxylation

Collagen has Gly-X-Y repeats, where X and Y are typically Proline or Lysine. Prolyl 4-hydroxylation⁵⁴ at the Y-positions, prolyl 3-hydroxylation at the X-positions⁵⁵, and lysyl hydroxylation to form hydroxylysine (Hyl) are frequent post-translational modifications in collagen molecules. Hydroxylation is driven by three enzyme families: Prolyl 4-hydroxylases (P4Hs), Prolyl 3-hydroxylases (P3Hs) and Lysyl hydroxylases (LHs). These modifications are only possible on triple helices which are unfolded. All the three hydroxylases are part of Fe(II)- and 2-oxoglutarate-dependent dioxygenase family which contains a dioxygenase domain. Vitamin C acts as a co factor to oxidize the iron, especially for prolyl4-hydroxylases ⁵⁶. All the enzymes have three isoforms in invertebrates, which differs based on tissue distribution, and has potential for complex formation with other proteins. For example Prolyl 3-hydroxylase 1 (P3H1) forms a complex with other ER proteins like CRTAP and CypB for (3S) hydroxylation of prolines. Mutations in any member of this complex not only exile hydroxylation but also lead to non-specific over modification of collagens ⁵⁷. One function of this complex is to momentarily stabilize junctions between triple-helical and unfolded regions until other chaperones, such as Hsp47, takes over this function. However, this complex can hydroxylate other proteins as it

is not collagen specific. Lysine hydroxylases form similar multifunctional complexes together with FK506-binding protein 65 (FKBP65), 78kDa Glucose-regulated protein (GRP78, or BiP) and Hsp47⁵⁸⁻⁵⁹. They are peripheral membrane proteins which are lumenally oriented. 5-hydroxylysine helps in O-glycosylation and fiber-crosslinking at later stages of collagen maturation. GRP78 and HSP47 as the positive regulator of the complex formation whereas an ER homologue of HSP70, acting as a scaffold for the complex acts as a negative regulator for lysine hydroxylation⁵⁹.

b. Glycosylation

Many hydroxylysine residues are further modified by O-glycosylation. The attachment of β -galactose is catalyzed by the glycosyltransferases GLT25D1, GLT25D2 and LH3. GLT25D1 and GLT25D2⁶⁰, The attachment of glucose is catalyzed by LH3⁶¹. The role of O-linked sugars has not been fully elucidated yet. One study indicates that it is necessary for the interaction with the endocytotic collagen receptor uPARAP/Endo180⁶². The telopeptide domain is rich in mannose-rich oligosaccharides due to N-glycosylation. Glycosyltransferase specifically recognizes highly conserved Asn-Ile-Thr motif in fibrillar collagens. N-glycosylation at propeptide region helps in recognitions of propeptide regions for their cleavage and endocytosis.

c. Cis-trans isomerization

Peptidyl-prolyl cis-trans isomerase (PPI) isomerizes cis peptide bonds to trans, which is the rate limiting step in the triple-helix formation. It targets proline at the imidic peptide bond position which allows it to regulate protein folding of type I collagen³⁴. FKBP65 is one of the PPIs which promote cis-trans-isomerization⁶³⁻⁶⁴. This step is required for the stability of triple helices.

1.3.3. Folding of collagens

a. Folding of propeptides and chain selection.

Folding of collagen triple helix starts with the chain selection at the C-propeptides. Nucleation of triple helix occurs at the C-terminal propeptides. The

folding of these propeptides is initiated by rER-residing general chaperones like GRP78, PDI and CypB³⁴, and is followed by post translational modifications catalyzed by enzymes towards the N-terminus in a zipper-like fashion⁶⁵. The C-propeptides helps in procollagen folding by ensuring association between pre-procollagen chains⁶⁶ and maintaining chain selectivity⁶⁷(Figure.5). The association of procollagen chains is stabilized by disulfide bond formation. This step is initiated with PDI (Protein disulfide isomerase), which helps in intrachain and interchain disulfide bonds⁶⁸. The propeptides folding (at least for fibrillar collagens) is an important step for chain propagation. The chain selection at C- propeptides of COL I $\alpha 1$ and $\alpha 2$ chains occurs due to single N-linked glycosylation sites. The C-propeptides of the $\alpha 1$ and $\alpha 2$ chains of type I collagen contain a single N-linked glycosylation site having an Asn-Ile-Thr sequence, which is highly conserved among fibrillar collagens⁶⁹⁻⁷⁰. In FACIT COL IX, the NC2 domain is responsible for chain selection and trimerization of collagenous domains⁷¹.

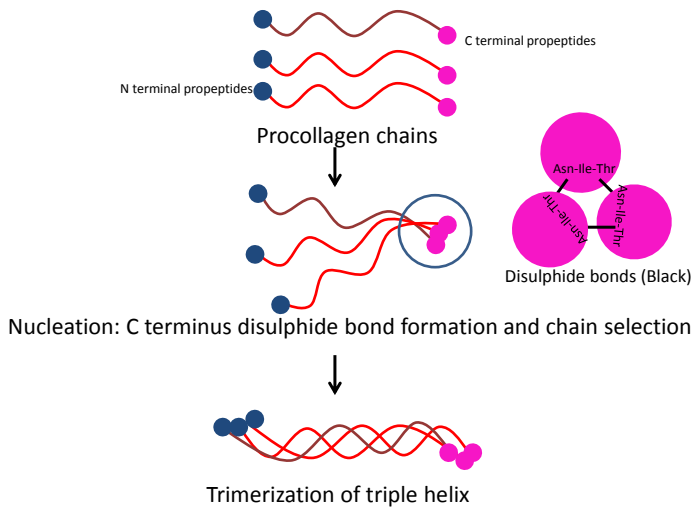


Figure5. Procollagen chains are brought to ER and interaction between C-propeptides helps in folding and folding of triple helices flanked by globular N- and C- propeptides.

b. Triple Helix trimerization of procollagen chains

After chain selection, fibrillar collagen starts folding from C to N terminus and this process is driven initially by P3H1/CRTAP/CypB complex as mentioned earlier and later by Hsp47 and FKBP65. During the zipper-like triple helix formation the state between folded and unfolded chains of procollagen is unstable. The P3H1/CRTAP/CypB complex interacts with triple helices at this site and helps in stabilization. The dissociation rate constant (kd) of this complex has been reported to be faster than that of collagen with Hsp47 ⁷². Therefore, the P3H1/CRTAP/CypB complex is considered as a molecular chaperone for this site until Hsp47 and/or FKBP65 further stabilize the triple helix.

c. Role of Hsp47 in Triple Helix trimerization

Hsp47, also called SERPINH1 or Colligin is a vital chaperone, specifically involved in collagen biosynthesis within cells ⁷³⁻⁷⁷. It is a highly conserved (see supporting information), 47-kDa endoplasmic reticulum (ER) resident protein that binds to collagen of at least types I to V ⁴⁹. Most interestingly, and in striking contrast to other chaperones, Hsp47 is specific for collagen and it preferentially recognizes the folded triple-helical conformation of its client.

Collagen molecules are often considered as “molecular rope”. Like flying capstan (a tool with helps in intertwining three coiled strands of rope in a controlled manner), Hsp47 trimerizes and binds to single collagen strands to promote the folding of triple helices. Hsp47 exists as structurally mesostable monomer and/or as hyper stable trimer ⁷⁸ (Figure 6). It stabilizes the procollagen triple helix, which is inherently unstable under physiological conditions, and protects it from intracellular degradation. It provides a quality control mechanism for correct helical folding and assembly, and prevents premature aggregation of procollagen molecules in the ER into large aggregates ⁷⁹. The highest-affinity sites for Hsp47 are located in the N-terminal region of procollagen. During triple-helix formation, binding of Hsp47 to the folded segments at the N terminus is believed to signal a successfully terminated folding event and mark this complex for passage to the Golgi. This

is in agreement with the finding that Hsp47^{-/-} cells secrete collagen much more slowly and are deficient in N-propeptide processing⁷⁷

Hsp47 binds at least to COL I, II, III, IV and V, as reported in studies based on surface plasmon resonance analysis⁸⁰. It has strongest affinity for sequences with Thr/Pro-Gly-Xaa-Arg-Gly, either of which is present in all types of collagens^{79, 81-82}. Hsp47 knock-out mice are embryonic lethal having misfolded collagen which highlights its role in quality control mechanism⁸³

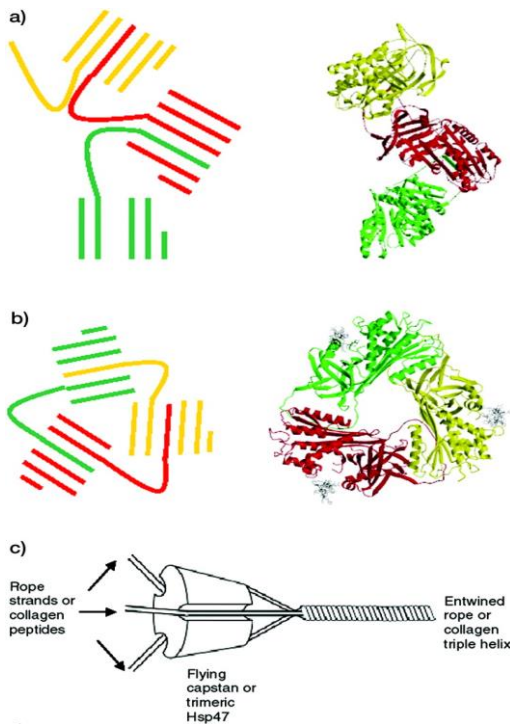


Figure6: Two possible variations of Hsp47 trimer. **a.** It shows an oligomer similar to α 1-antitrypsin polymerization. **b.** a closed trimer formed by RCL (loop). Diagram on the left-hand side shows monomers of Hsp47 in red, green, and yellow. **c.** Diagrammatic representation of collagen triple helix entwined and Hsp47 shown as a flying capstan (a piece of apparatus important to maintain strand order during rope making). Reproduced from⁸⁴ with permissions.

1.3.4. Trafficking, processing and secretion

Collagens are large proteins, often exceeding the length of 400nm⁸⁵. Folded procollagens are rigid rod-like elements^{32, 86}, which make their transport challenging. The transport of procollagen, therefore, requires special secretory

pathways. ³² COP-II vesicles responsible for the transport of Collagen to the Golgi have typical diameters of 90nm. Collagens are too large to fit into them⁸⁷. Moreover, the transport of Collagen between ER and Golgi occurs very rapid and has to be realized by a very efficient transfer pathway between compartments. The COPII vesicles have TANGO1 interacting with the inner coat components Sec23A and Sec24C, and additionally with the guanine nucleotide-exchange factor ⁸⁸.

Hsp47 and TANGO1 interaction for collagen packaging into COPII vesicles

Collagen loading into cargo vesicles is mediated by trans membrane protein transport and Golgi organization protein 1 (TANGO1) which reside at ER exit site ⁸⁹. The procollagen is packed by interaction Hsp47 and TANGO1 at the ER exit site. The SH3-domain of TANGO1 recognizes Hsp47 bound to collagens ⁹⁰. Blocking TANGO1 function in chondrocytes, fibroblasts, endothelial and mural cells was observed to hamper secretion of collagen types I, II, III, IV, VII and IX⁹¹. Next, the TANGO1 protrude and buds along with other chaperone mentioned above to form COPII vesicles while handling procollagen with the Hsp47 as a handle to pack it in this vesicles. Throughout the delivery of collagen from ER to Golgi Hsp47 remains bound to it.

Release of Hsp47 in the Golgi and retention

The interaction between Hsp47 and the collagen is stabilized by six histidine residues on Hsp47 that face towards the collagen–Hsp47 interface: His215, His216, His238, His273, His274, and His386. These are responsible for the stabilization of the Hsp47-Collagen complex at neutral pH in the Endoplasmic reticulum (ER)^{74, 79, 92-95}. Upon arrival at the Golgi apparatus, the acidic pH medium mediates protonation of Hsp47's histidine's and assists the release of Hsp47 from procollagen⁵⁰. When collagen-bound Hsp47 is carried to the Golgi body via vesicular transport, the KDEL sequence at its C-terminus is recognized by the KDEL receptor, which retrieves it and returns it to the ER. Artificial removal of this sequence results in the secretion of the protein from the cell by exocytosis⁹⁶.

Multiple roles of Hsp47

Constitutive expression levels of Hsp47 correlate strictly with the amounts of collagen being synthesized in the corresponding cells ^{77, 97}. Collagen biosynthesis therefore strongly depends on the correct expression and functions of Hsp47, and hence can be altered by interfering with Hsp47 expression. The specificity of Hsp47 for collagen, its interdependence with collagen expression, and its crucial role for collagen folding make it an ideal tool to manipulate and study collagen production and assembly at early stages of the biosynthesis process.

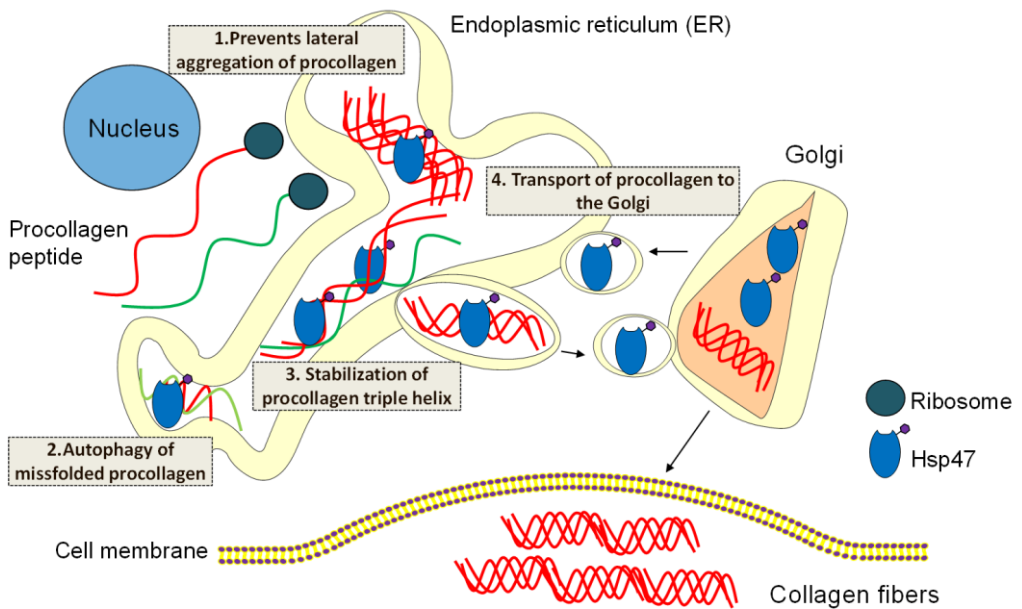


Figure7. Multiple roles of Hsp47 in collagen assembly. 1. Hsp47 prevents lateral aggregation of procollagen, 2. It promotes autophagy of miss-folded procollagen, 3. It stabilizes procollagen triple helix, 5. It helps in transporting procollagen from ER to Golgi.

The possible functions of Hsp47 have been known till date is as follows (Figure7):

1. Inhibition of intracellular procollagen degradation ^{74, 96, 98}.

2. Quality control of procollagen^{79, 98}.
3. Supports procollagen transport to Golgi apparatus⁹⁶.
4. Stabilization of triple helical folding intermediates of procollagen^{5, 26, 44, 99-100}.
5. Inhibition of procollagen aggregate formation in the ER^{75, 101}.
6. Promotion of autophagy of miss-folded collagen¹⁰².

1.3.5. Extracellular deposition of collagen

Processing of collagen for secretion in the ECM in the form of fibropositors

After transfer into golgi compartments the procollagen's are finally secreted into ECM. It is not entirely clear at what stages pre-fibril assembly of collagen occurs. Kadler and co-workers have performed serial block TEM experiments in embryonic mouse tendon and demonstrated that fibril assembly most likely occurs in a post Golgi compartment¹⁰³⁻¹⁰⁵. For COL VI it has already been shown that the assembly into tetramers is an intracellular event¹⁰⁶. The process of collagen secretion is mediated by formation of Fibripositors (a portmanteau of 'fibril' and 'depositors')¹⁰³ and in the cornea, by keratopodia¹⁰⁷. These are small vacuoles containing collagen fibrils as shown in the Figure 8, which help in the transfer of fibrils of collagen to the plasma membrane and expulsion in the ECM. It is therefore predicted that intracellularly procollagen associates to form ordered collagen superstructures, i.e. fibrils Figure9. Such fibrils can range from 15 to 500nm depending upon the tissue.

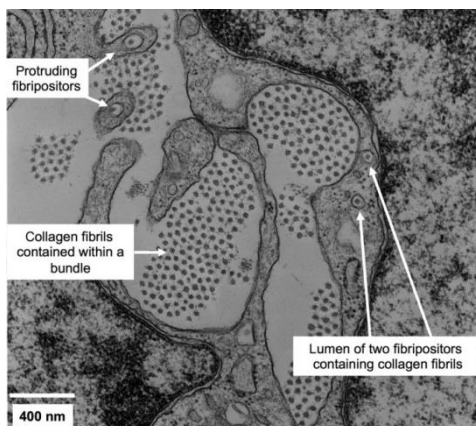


Figure8. Transmission electron microscopy (TEM) image of embryonic tendon shows bundles of collagen fibrils between two fibroblasts from embryonic mouse tail tendon. The image shows profiles of fibripositors. Reproduced with permissions from¹⁰³.

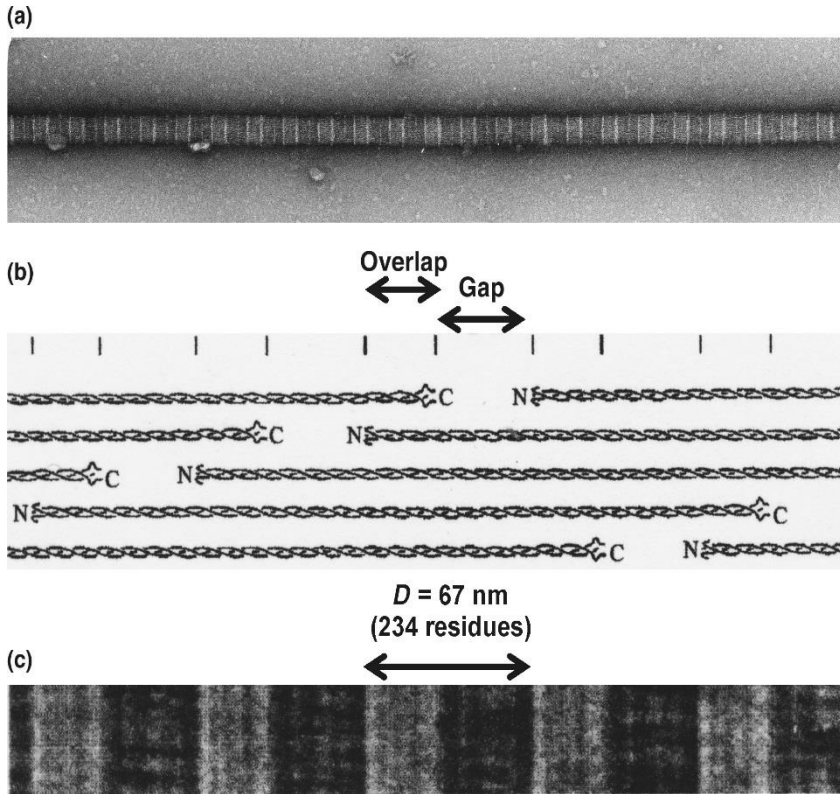


Figure 9. TEM of an individual collagen fibril. (a) 18 day chicken embryo metatarsal tendon extracted single collagen fibril negatively stained with 2% uranyl acetate showing the characteristic light and dark banding pattern. (b) Schematic represents the axial arrangement of collagen. Each collagen molecule shown with coiled chains. Each molecule is $4.4 \times D$ in length. The D-stagger of collagen molecules having 4.4 D leads to the formation of a gap zone in the axial structure. (c) The negative staining pattern of collagen fibrils. Figure reproduced with permissions from ¹⁰³.

The solubility of procollagen inside cells is due to the protecting propetides. These propetides are removed by molecular enzyme scissors called metalloproteases¹⁰⁸. The resulting structure is called tropocollagen. Fibrils generated *in vitro* from procollagen digested by metalloproteases initially have a near paraboloidal pointed tip and a blunt end, and growth occurs from the

pointed tip direction¹⁰⁹. As the growth proceeds the blunt tip becomes pointed tip and fiber starts growing in both direction which results in N-N bipolar structures in which a switch in molecular orientation occurs at a region along the fibril shown in figure 11¹¹⁰. *In vivo*, both unipolar and bipolar sets of populations have been observed. This step is required for axial continuity of the intermolecular cross-links in the fibrils outside. The N-N bipolar fibril see figure 10¹⁰⁸.

1.3.6. Stabilization of collagen fibers by crosslinking

Fiber-associated collagen types bind to the surface of fibrils and join neighboring fibrils. In order to mechanically stabilize the collagen fibers, enzyme-catalyzed crosslinking between collagen molecules occurs after assembly¹⁰⁸. The final mechanical properties of the collagen are directly linked to the cross-linking degree. In fibrillar collagens, the oxidation of lysine residues by lysyl oxidases helps cross linking and proteolytic cleavage of the propeptides for efficient fibril formation. The whole processes still include a lot of open questions and further study of proteins that assist in the maturation of procollagen are necessary.

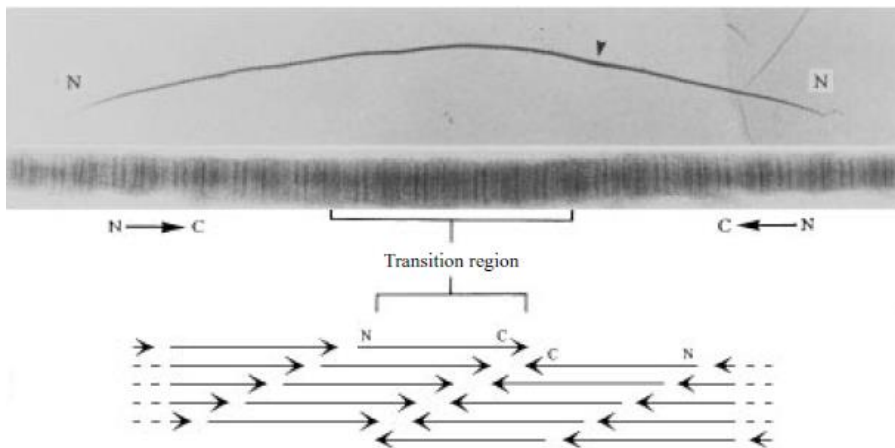


Figure10. This figure illustrates the TEM image of collagen fibril which is 10.5 μm long having polarity reversal 3.5 μm from one end (arrowhead). The braced region shows four

D-periods where pattern show molecules with anti-parallel arrangement. The analyzed region of the negative staining pattern in the transition region represents an anti-parallel arrangement of molecules. Reproduced from ¹⁰³.

Crosslinking reactions include (1) the N^ε(γ -glutamyl)lysine isopeptide which are formed from lysine residues by transglutaminase-2 (which acts a catalyst) in COL I, III, V/XI, and VII¹¹¹; (2) disulfide bonds between thiols in COL III, IV, VI, VII, and XVI; (3) mature and reducible cross-links produced via the lysyl oxidase pathway¹¹²; and (4) Glycation products. Intramolecular and intermolecular crosslinking are seen between lysine, hydroxylysine, and histidine residues. These are bifunctional crosslinks. They further form non-reducible trifunctional cross-links like pyridinoline and deoxypyridinoline in stiffer tissues like bone and cartilage and histidinohydroxylysinonorleucine in skin³⁵ (Figure11).

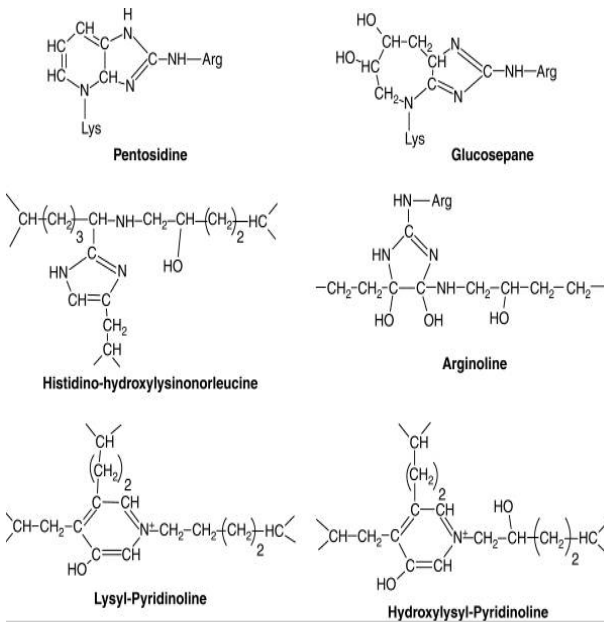


Figure11. Collagen cross-links are shown in this figure. Lysyl-mediated cross-links are arginine, deoxypyridinoline, pyridinoline. Glycation products like glucosepane and pentosidine. Reproduced from ³⁵ with permissions from Cold Spring Harbor Laboratory Press.

1.4. Label-free techniques to image collagen

Imaging techniques to study collagen superstructures ranges from non-staining approaches like SHG (Second harmonic generation) Imaging, Serial block TEM of fibrils from tissues or polarization microscopy to study fiber orientation, to genetically labeling of collagen genes with fluorescently-labeled proteins and photo switches. Staining approaches includes use of collagen-adhesive proteins, collagen hybridizing peptides with fluorophores and immunostaining with collagen-specific antibodies.

Collagen fibers are highly anisotropic which allows amplified SHG signals because of its repeating structures are tightly aligned within fibrils. SHG is defined as the processes in which two photons amalgamate in an optically nonlinear medium which lacks centro-symmetry (such as collagen), generating an SHG photon having a wavelength which is exactly half of the excitation wavelength (or twice the frequency, ω)¹¹³. This imaging is based on signal left after the phase-matched within the material i.e. a second harmonic wave generally co-propagates with the excitation beam, resulting in SHG signal in forward direction as the excitation beam. About, 80% to 90% of the signal from collagen in a tissue sample propagates in the forward direction and depends on how much light is scattered. A single collagen fiber having length of 40- to 300-nm is considered as a dipole which radiates in all directions apart from the normal to the incident beam. This is because of the peptide bonds within the collagen chains generates a permanent dipole characteristic allowing SHG to occur within collagen rich tissues¹¹⁴ (Figure 12).

Collagen fibers are optically birefringent due to their anisotropic nature. Birefringence is the materials optical property having a refractive index that depends on the polarization and propagation direction of light. Polarized light microscopy (PLM) is a technique used to examine birefringent material such as collagen, giving the information on the orientation and distribution of the collagen fibers. When polarized light is illuminated on the sample the ratio between incident to emergent light changes by the retardation, also known as the optical path difference (OPD) of the object¹¹⁵.

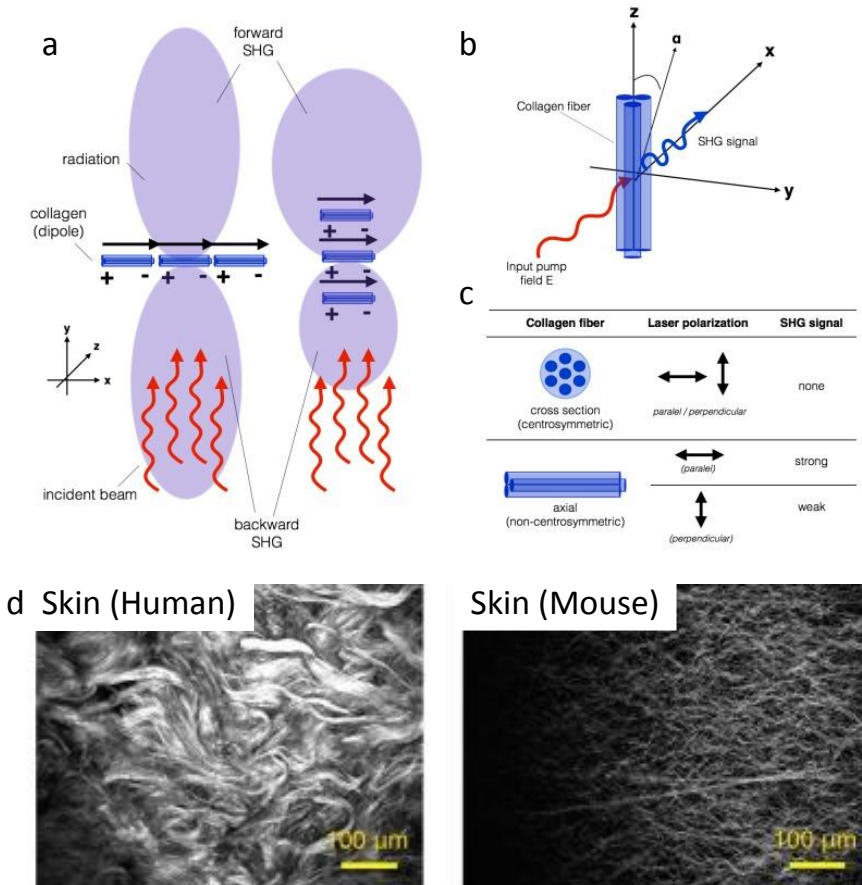


Figure 12 Schematic illustrating **a.** collagen fibers having dipoles radiating in all directions except in the direction of incident beams; **b.** it shows a single collagen fiber relative to an applied electric field. The emission of SHG signal is in blue; **c.** if the light is polarized along the collagen fiber axis (z) then maximum SHG signal will be observed and it is polarized perpendicular to the fiber axis (x), the weakest SHG signal will be shown. **d.** SHG images showing collagen fibers on Human and Mouse skin tissues. Reproduced from ¹¹³.

When light is incident on a birefringent material, the wave of light splits into two perpendicularly polarized beams having one beam polarized on the slowest direction and another on the fastest direction⁸⁰. When the incoming

light polarization is in the same direction with respect to the slowest or the fastest direction, the exiting light remains linearly polarized from the sample, showing a brighter image which is referred as birefringence brightness where δ is proportional to the thickness of the sample (L) and the difference in refractive indices (Δn) and it is inversely proportional to the wavelength of the light (λ): $\delta = (2\pi/\lambda) L\Delta n$. Here $L\Delta n$ is the optical retardation (OPD)¹¹⁶.

This OPD technique has been reported to allow quantitative analysis during the wound healing process in burned skin. Collagen fibers orientation and thickness can be studied using this technique. Imaging of collagen fibers using this technique without any labeling has already been reported in tissues like Skin, Muscle, Cornea and other parts of eye^{115, 117} (Figure 13). Both SHG and PLM technique are suitable for *in vivo* applications.

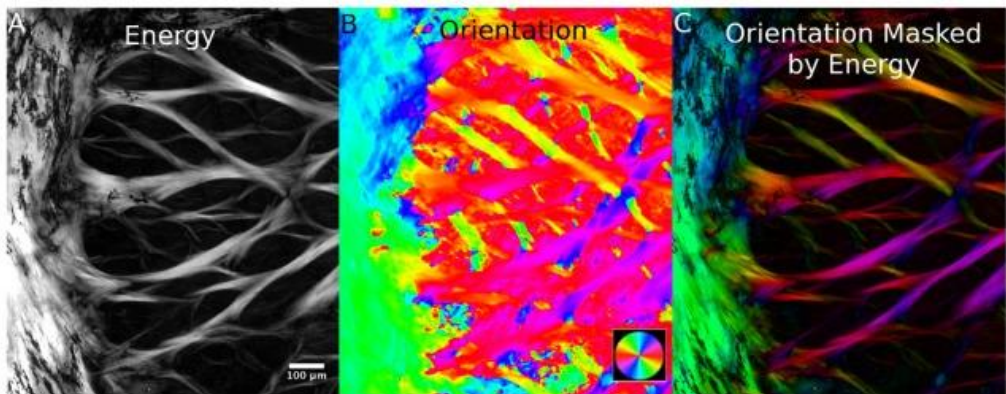


Figure 13. PLM microscopy images of the peripheral lamina cribrosa and sclera of eye. The pixel measure of orientation is shown in A. A direct plot of orientation with pseudo plots are shown in B and C. The colors in pie diagram in B shows the fibers orientation. Reproduced from ¹¹⁷.

Other techniques which are used to characterize collagen fibers in a biological samples or biomaterial at nano scale are atomic force microscopy (AFM), scanning electron microscopy (SEM), environmental scanning electron microscopy (ESEM), and light microscopy.

AFM is a nanometer-scale resolution technique. It uses a microscopic probe mounted on a cantilever to contact and scan the collagen substrate, and the topology and interactions between the tip and the substrate are followed by measurements of force deflection of the cantilever¹¹⁸. This technique can generate a readout of morphology and roughness of collagen-coated surfaces, for example deposited collagen during cell culture¹¹⁹. However, it cannot give information on a tissue stiffness and surfaces due to layers of structures interwoven on top of each other making it difficult to characterize which part of the material contributes to biomechanics of the tissue **Figure 14**.

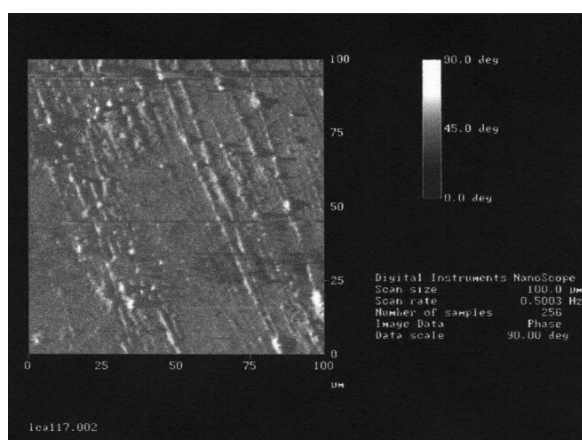


Figure 14. AFM image showing collagen surface. Showing 100-µm scan size, 0.5003-Hz scan rate, 256 samples, phase data image, 90° data scale. Reproduced with permissions from ¹¹⁹.

SEM is an electron microscopy technique that uses a highly focused electron beam to scan a sample. The incident electrons interact with the atoms in the sample and give information regarding the surface topography and composition of the sample¹²⁰. The electron beam is scanned in a raster scan pattern in which the position of the beam is combined with the intensity of the signal detected to produce an image. Magnification of 3000× to 30,000× can be achieved by SEM to image a collagen substrate (**Figure 15**). A thin layer of gold sputter-coated is required to facilitate imaging of the surfaces. ESEM has a high vacuum condition, high humidity chamber to image samples without any coating. Information about pore size of collagen hydrogels, orientation of collagen fibers on 2D cells can be observed can be quantified ¹²¹.

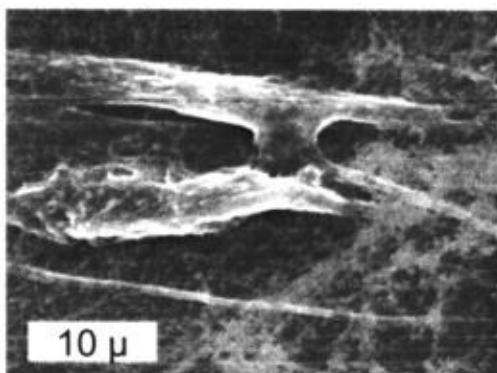


Figure15. SEM images showing collagen fibers deposited by cells after 3 days of culture. Reproduced with permissions from ¹¹⁹.

The limitations associated with SEM are that collecting SEM data requires precise sample preparation i.e. sputter coating with gold and this could dampen resolution of the surface. Strong beam of electrons can burn the samples as collagen is soft in nature. Collagen in a 2D or 3D hydrogel format can be damaged while imaging. Therefore, ESEM is preferred over SEM and resolution is good comparatively¹¹⁹.

TEM is a technique which works on imaging samples based on transmission of electron beam after passing through the sample. This is a label-free method but requires very thin samples to give surface topography of the collagen substrates. The Serial block imaging advancement to this technique boosts its applicability to gain insights into information on tissues and embryos¹²². The imaging involves serially imaging organized slices of the sample and compiling them to produce a 3D image. It has been extensively reported by Kadler and coworkers to study fibripositor formation in mouse embryonic tendons etc. (Figure 16) ^{103, 105, 108}.

Real-time intracellular tracing of collagen biosynthesis for multiple hours is quite challenging by immunofluorescence. Traditionally, labeling of collagen fibers have been done using collagen-specific antibodies, collagen adhesion proteins like CNA35¹²³ and collagen hybridizing peptides ¹²⁴.Recent advancements in gene editing technology has helped in understanding some key aspects of collagen biosynthesis.

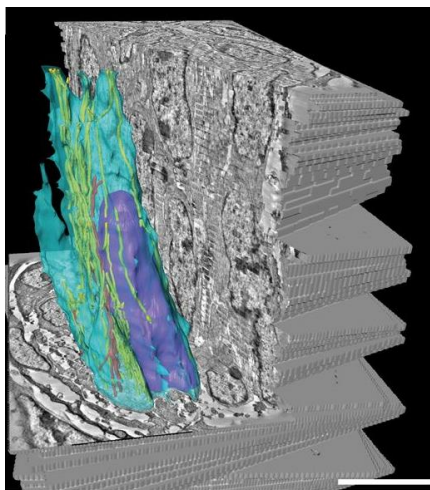


Figure16. Three dimensional reconstructed image showing stacked serial section tomogram where the components are highlighted with different colors (cell membrane (light blue), nucleus (purple), and fibripositor-associated fibrils (yellow) and fibrils in fibricarriers (red)). (Scale bar: 5 μm .). Reproduced from ¹⁰⁵.

Initially, Stephens and coworkers developed collagen plasmids labeled with fluorescent protein tags for intracellular imaging but the major limitation with this method is that these proteins were cleaved due to the propeptide cleavage step in the procollagen assembly ¹²⁵⁻¹²⁶. Recently, CISPR-based photo switchable protein-tagged COL I plasmids were developed by Kadler and co-workers, which has two advantages over this method - 1. It is a stable knock-in procedure 2. Newly synthesized procollagen can be separately quantified using the photo-switchability of the fluorescent protein, 3. The photo-switchable protein is introduced at a unique site after pro-peptide encoding which makes it even more powerful to trace collagen both intra and extracellularly ¹²⁷.

1.5. Diseases due to defects in collagen production:

a. Hereditary disorders due to genetic alternations in collagen

These disorders occur due to mutations in the genetic code of collagen proteins passed on from parents to progeny. Common examples of such disorders are Osteogenesis imperfecta (brittle-bone disease)¹²⁸, Ehlers-Danlos Syndrome, Chondrodysplasias (e.g. dwarfism), Alport syndrome and Knobloch syndrome¹⁸. Osteogenesis imperfecta is caused by COL I mutation, which causes weak bones and irregular connective tissues. Some cases can be mild,

with lowered levels of COL I, while others can be lethal, involving structural defects in collagen. Ehlers-Danlos Syndrome refers to a collection of connective tissue disorders, currently classified as 13 subtypes, each caused due to a different mutation in collagen. For example, 4 types of this disorder are caused by a mutation in COL III¹²⁹. These are characterized by hypermobility of joints and hyper extensibility of skin¹³⁰. Chondrodysplasias is a skeletal disorder caused by mutation in COL II, leading to long bones and abnormal cartilages¹²⁹. Alport syndrome is caused due to mutations in X chromosome and leads to problems in kidney function, eyesight, and hearing. Knobloch syndrome is caused by a mutation in the COL XVIII gene and can result in a protrusion of brain tissue through a defect in the skull and/or degeneration of the retina.

b. Non-inherited genetically altered disorders

These disorders occur during aging and are associated with reduced levels of collagen in the skin, bones and eyes like scurvy, osteoporosis and keratoconus are particular examples related to mutations in either collagen or enzymes involved in collagen biosynthetic pathway. Scurvy is a disease is caused due to poor hydroxylation of collagen. The main reason is Vitamin C i.e. ascorbate deficiency which acts a co-factor in hydroxylation enzymes mentioned earlier¹³¹. It causes bleeding from skin and gums, decreased red blood cells, weakness and fatigue¹³². Osteoporosis is a bone related disease related to mutation in COL I¹⁸. It causes fragility of bones which results in common injuries like wrist and hip fractures. It is responsible for chronic pain, in activity and invalidity in elderly. Worldwide every third women and every fifth men over the age of 50 is prone to this disorder. The existing therapy for this disease is growth hormone injections to counteract loss of collagen in bones, use of collagen supplements and peptides etc. Keratoconus a corneal disorder that causes corneal thinning and protrusion of the cornea leading to visual deterioration¹³³. The prevalence of keratoconus in white Europeans has been estimated to be 1 in 1750 and up to 1 in 450 in South Asians¹³⁴. Keratoconus is related to poor crosslinking of collagen and disturbance of the collagen fibril superstructure, which leads to blurred vision¹³⁵. The existing therapeutic approaches to treat this disease are

use of corneal implants or transplant and UV crosslinking of collagen matrix after riboflavin ultraviolet (UV) treatment¹³⁶.

Other disorders include muscular dystrophy¹³⁷, Knobloch syndrome¹³⁸, Aortic Aneurysms¹³⁹, osteoarthritis¹⁴⁰, and intervertebral disc disease¹⁴¹, Von brand Willebond syndrome¹⁴²(Blood Platelets clotting disorder¹⁴³) etc. All these can be genetically linked or acquired due to conditions like malnutrition, vitamin deficiency etc.

1.6. Collagen disorder due to Hsp47 alterations

Alterations in Hsp47 expression levels or mutations in Hsp47 correlate with pathological states¹⁴⁴. For example, expression of Hsp47 is up-regulated during the progression of various fibrotic lesions¹⁴⁵⁻¹⁴⁶. Studies have also shown that suppression of Hsp47 expression can reduce accumulation of collagens and can delay the progression of fibrotic diseases in experimental animal models¹⁴⁷. Recently, enhanced expression of Hsp47 has been found in cancer tissue.

Silencing of Hsp47 expression reprogrammed breast cancer cells to form polarized and/or non-invasive structures in 3D culture, which significantly inhibited tumor growth *in vivo* and reduced deposition of collagen¹⁴⁸. These results indicate that Hsp47 is relevant for cancer progression, and may represent a potential biomarker and therapeutic target. It is also involved in platelets disorder and neurodegenerative disorders like Parkinson¹⁴⁹ and neuronal cancer like Glioblastoma¹⁵⁰.

Hsp47 is down regulated in different types of Osteogenesis Imperfecta^{26, 151}, EDS⁷⁴, arterial disorders¹⁹, chondrodysplasia¹⁵² and Keratoconus¹⁵³. Details of all this disease are mentioned earlier. It is also known to rescue ER trafficking and unfolded protein response linked to other diseases¹⁴⁹.

1.7. Hsp47 gene

The Hsp47 gene contains a conserved HSE (Heat shock element) which is located -180bp upstream of transcription initiation site (Figure. 17). Hsp47 also has two glycosylation sites that are speculated to be glycosylated by mannose-

type sugar moieties. Both the ER-retention sequence and the glycosylation sites are present in Hsp47 gene which is a proof for Hsp47 localizing to the ER. The ER localization of Hsp47 was confirmed by Immunofluorescence and immunogold-electron microscopy and *in vivo* imaging¹⁵⁴. The expression of Hsp47 is induced by activation of HSE by HSF1 (Heat shock factor1)¹⁵⁵⁻¹⁵⁶.

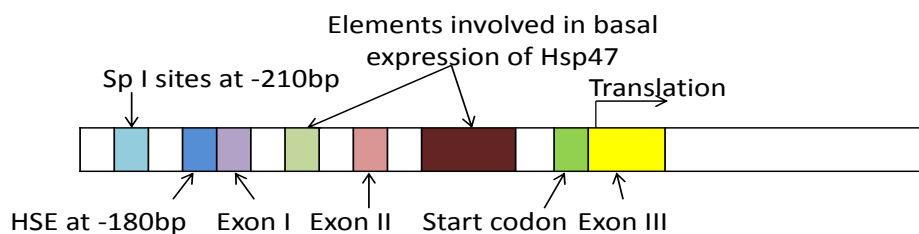


Figure17. Scheme shows Hsp47 gene and its functional elements for transcription. Adapted from ⁹².

As collagen molecular chaperones govern the assembly of collagen biosynthesis, controlling their function can be directly linked to controlling collagen production. Molecular engineering strategies to modify these proteins are described below.

1.8. Protein engineering strategies

Strategies to regulate protein functions activity

Understanding mechanistic principles of cell biology and physiology requires molecular tools to exploit the system and to assay the feedback in presence of such tools. This requires complex engineering to dissect the processes by understanding its components, connectivity and causation. One way to deduce the role of molecular components in biochemical pathways is by manipulating gene function through over expression, mutation or by deletion of the gene. It is quite robust and specific but poorly reversible and at times difficult to implement ¹⁵⁷. Another strategy is to control RNA stability through RNA silencing (RNAi) which is easier to implement but doesn't completely suppress the function and can result in off target effects¹⁵⁸. However, when it comes to understanding protein functions, it is insufficient to manipulate them at a

genetic level. Behaviors such as complex formation, allosteric effects, degradation kinetics, subcellular localization are necessary to be taken into account¹⁵⁹. Therefore, strategies to engineer structural characteristics of proteins are essential to answer complex biological questions. The existing strategies for such manipulation of proteins involves chemo selective labeling, protein ligation methods such as thiol-based or enzyme based coupling, arresting protein steric and allosteric effects by photo switchable groups and incorporation of chemical moieties that can temporarily arrest protein functions and can be cleaved by remote triggers like light.

A. Protein conjugation strategies

A1. Chemo selective reactions for covalent modifications of proteins

A chemo selective reaction is defined in as the selective reactivity of one functional moiety in the presence of others ¹⁶⁰. In the context of biology, chemo selective ligation of two uniquely reactive functional groups needs to selectively occur in an aqueous environment or in a biological material even when a multitude of potentially reactive functional groups available in the vicinity ¹⁶¹. In protein engineering, it is a method which selectively introduces a chemical moiety to arrest, label or amplify a protein and its function ¹⁶²⁻¹⁶³. This is broader definition of bio orthogonal reactions which includes different chemistries like Staudinger ligation and azide based cyclo-additions which can be triggered by light i.e. Photo-click cyclo-additions or by metal i.e. Cu-catalyzed¹⁶³. For example, of chemo selective reactions for protein modification is the reaction between azides and alkynes. It is a [3+2]-dipolar cycloaddition¹⁶⁴⁻¹⁶⁵ that leads to the formation of a triazole. It can happen at room temperature when an energy-rich cyclooctyne is used as substrate, or by using Cu (I) catalyst¹⁶⁶(Figure 18a). Alternatively, the Staudinger-phosphite reaction of azides with phosphite to form phosphoramidate¹⁶⁷⁻¹⁶⁸ (Figure8b) can also be used. These strategies have been widely used for the imaging¹⁶⁹. But, these techniques have limitations like toxicity induced by Cu(I) hampering various cellular protein functions¹⁷⁰. Cyclooctynes have huge hydrophobic unit between protein and probe and they are costly to synthesize¹⁷¹. Phosphine's are prone to

oxidation and Staudinger-phosphite reaction can be applied only at lower pH value than 7 (Figure 18.b).

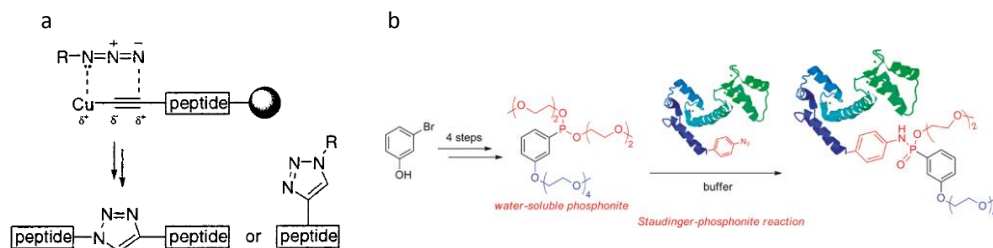


Figure 18. a. Scheme showing 1,3-Dipolar Cycloaddition of Alkynes to Azides by Copper (I)-Catalyzed reaction offering Peptidotriazoles or N-Substituted Histidine Analogs. Reproduced with permissions¹⁷² from ACS. b. Scheme showing Staudinger reaction of aryl-phosphonites for the functionalization of azido-peptides and proteins. Reproduced with permissions¹⁶⁸ from ACS.

The main advantage of this strategy is that it is robust and specific to chemically functional reactive partners for labeling or coupling proteins and peptides. However, it has limitations like a functional moiety is non-reversibly covalently coupled and also the functional activity of such proteins is not fully recovered sometimes because of steric hindrance.

A2. Native Chemical Ligation

Chemical ligation for the modification of proteins refers to the covalent coupling of two peptide sequences followed by intermolecular rearrangement to form a native amide bond¹⁷³⁻¹⁷⁵. This capture/rearrangement strategy is known as Native Chemical ligation (NCL) and was described first by Kent et al. 1994¹⁷⁶ by forming a amide bond next to a cysteine ligation site. In native chemical ligation, the thiol group of the N-terminal cysteine residue in second peptide attacks the C-terminal thioester of first peptide in an aqueous environment at pH 7.0 with temperature ranging between 20°C to 37 °C. This step is known as reversible transthioesterification step, which is regioselective and chemo selective to form a thioester intermediate. Next step is the rearrangement of intermediate forming an intramolecular S, N-acyl shift forming a native amide ('peptide') bond at the ligation site^{159, 162} (Figure19). The

advantage of this technique is its robustness, selectivity of ligation, which allows coupling peptides to another peptide, protein and oligonucleotides. The limitations are Cys required for thiol based coupling. In recent years, this strategy has been extended to enable ligation of other sequences not containing Cys at the ligation site¹⁷⁷⁻¹⁷⁸ but should be Cys mimetic. Other limitations of chemical synthesis are that large proteins (larger than 200 amino acids) cannot be achieved. To solve this problem, a derivative approach of using living machinery like bacteria is employed. This approach is called expressed protein ligation (EPL) where two proteins or a protein and peptide are conjugated¹⁷⁹.

This is the most commonly used approach following the protein trans-splicing principle by making use of engineered proteins called Intein's. Intein's are proteins having sequences embedded in-frame within a sequence of precursor protein that is excised during the post translational maturation of protein and this excising process is termed as protein splicing. They have both properties of protein splicing activity and an endonuclease activity. These proteins at the end of the target protein allows thiol mediated cleavage by creating a thiol handle at the end of the truncated protein, which on exposure to another peptide or a protein having Cys at the N terminal performs native chemical ligation. This semisynthetic strategy is known as EPL¹⁸⁰ (Figure 20a).

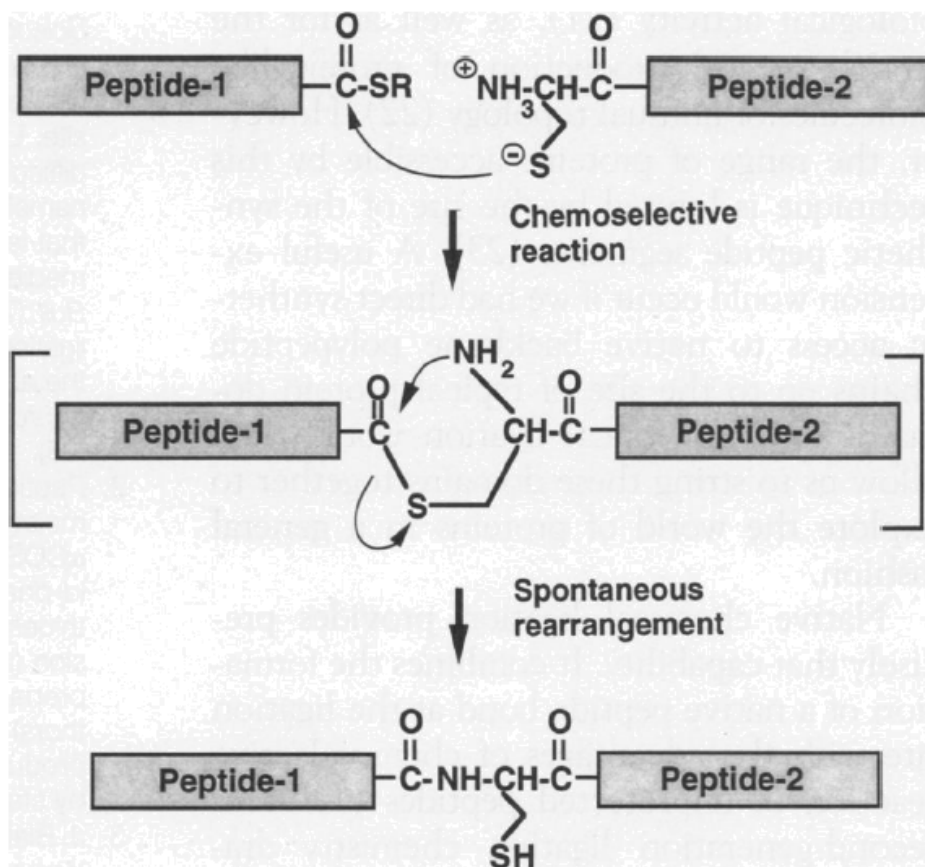


Figure 19. NCL scheme showing steps involved in peptide conjugation approach. The first peptide, which contains a thioester at the α -carboxyl group, undergoes nucleophilic attack by the side chain of the Cys residue at the amino terminal of second peptide (R is an alkyl group). This is followed by thioester ligation bond forming rapid intramolecular reaction due to favorable geometric arrangement of the amino group of second peptide yielding a product. The bond formed is a native peptide bond at the ligation site. Reproduced with permissions¹⁸¹ from The American association for advancement of Science.

A3. Enzyme-catalyzed ligations

Enzymatic reactions can also be applied to ligate proteins or peptides. Enzymes like subtiligase can be efficiently used to ligate Cys-free peptides to protein thioesters by recognizing LPXTG motif. However; these strategies require

specific motifs for identification of coupling sites¹⁷⁹ Other examples are Sortase¹⁸² and Butelase¹⁸³ (Figure 20b).

One major disadvantage of this system is it insert extra amino acid require in the protein which sometimes can alter the structure and function of the protein¹⁸⁴.

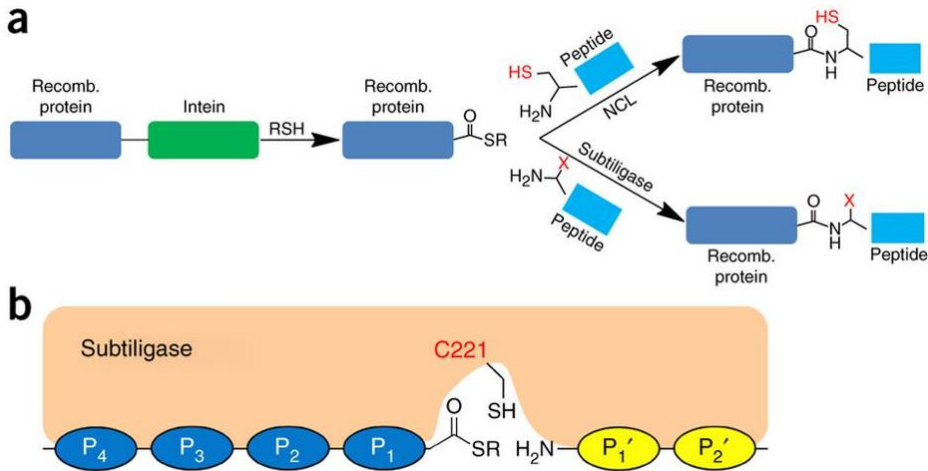


Figure 20.a. Scheme showing the intein-mediated protein thioester formation followed by ligation via (NCL) or subtiligase. **b** Figure shows a subtiligase is known to interact with four residues (P4–P1) N-terminal to and two residues (P1' and P2') C-terminal to the ligation site Reproduced by a sharable link <https://rdcu.be/bASg9>¹⁷⁹.

B. Introduction of light-regulated structural units in the protein structure for regulation of protein function

Light is excellent stimulus as it allows non-invasive, spatial and temporal activation, it can be tuned by varying exposure dose along with multiplexins at different wavelengths. Inspired by light activatable proteins in nature like Rhodopsin, photoactivatable proteins can be obtained by introducing photosensitive domains in the protein structure, which undergo conformational changes upon photo excitation resulting in activity changes in the protein. This can be done by different approaches detailed below.

B1. Photo activation of protein function by light induced oligomerization

Photo sensory domains are chromophores derived from photoreceptors or fluorescent proteins. These proteins absorb light through a chromophore, which has a light-sensitive cofactor or, in some cases, residues like tyrosine and tryptophan. Photon absorption results in conformational changes and structural rearrangement in this domain resulting in response. There are different photo sensory domains available with a wide range of binding affinities and reversion kinetics. A relevant example is the interaction between the light-oxygen-voltage (LOV) domain¹⁸⁵ and a C terminal α helix¹⁸⁵.

Proteins responsible for signal transduction undergo dimerization or oligomerization for signal transductions like receptor tyrosine kinases or serine/threonine kinases¹⁸⁶. To study such proteins, photo sensory domains that undergo light induced homodimerization or oligomerization such as VVD¹⁸⁷⁻¹⁸⁸ derived from *Neurospora crassa*, have been engineered (Figure 11). This strategy could be applied to study binding affinity of molecular chaperone to collagen which undergo dimerization and trimerization for specific function in collagen folding e.g. Hsp47 undergoes dimerization and trimerization states for folding and stabilizing procollagen triple helices. However, this strategy cannot specify or differentiate between the activity of monomeric and dimeric proteins. To study such functions a unique technique was established, 'Clustering Indirectly using Cryptochrome 2' (CLICR)¹⁸⁹. In this case, CRY2 is fused to adaptor that binds to target protein having low affinity in monomeric form. Light induces oligomerization of the CRY2-fused adaptor, which increases affinity for the target protein (Figure 21).

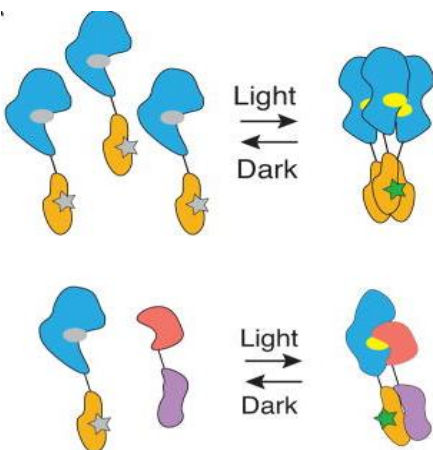


Figure 21. It shows light-induced oligomerization of proteins due to conformational changes within photo sensory domains. The homo oligomerization is shown above and hetero-oligomerization is shown below. Photo sensory in active domains are shown in grey and active in yellow. Reproduced with permissions from Elsevier's¹⁹⁰.

B2. Regulation of protein accessibility (steric caging) and allosteric activity

Steric caging approach involves blocking the active site of a target protein with a photo sensory domain via a conformational change that can be reversibly controlled by light (Figure 11). For example, an ATPase-inactive variant of Rac1 was arrested by AsLOV2 in the dark. Light triggers the unwinding of the Ja helix between LOV2 and Rac1, exposing the binding surface of Rac1 to downstream effectors¹⁹¹. The function of calcium channel regulator¹⁹² and transcription factors¹⁹³ have also been photo regulated using this approach. To cage large protein domains, photo dimers are fused at N and C terminus of the target protein. For example, a variant of Dronpa that tetramerizes in the dark but exhibits light-dependent monomerization was fused to hepatitis C virus protease allowing light control activity¹⁹⁴. This strategy has also been applied for photo-inhibition of protein activity using a light-dependent oligomerization system i.e. light-activated reversible inhibition by assembled trap' (LARIAT) (Figure22). This strategy can be useful for developing switchable chaperones having collagen regulatory functions like PPIs and Hsp47. The major limitations is the functionality of the protein could be lost by introducing photo sensory domain in between two domains and also the structure and functional information of each part of the protein should be clearly known which is most of chaperones case is yet to be understood.

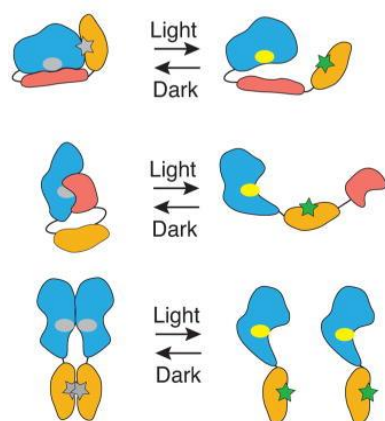


Figure22. Steric effects. The active site (indicated by a star: grey is inactive; green is active) of a protein (yellow) can be caged via intra- (top and middle) or inter- (bottom) molecular interaction by light. Reproduced with permissions from Elsevier's¹⁹⁰.

B3. Photoactivatable proteins by introducing un-natural amino acids

Site specific incorporation of un-natural amino acids (UAAs) with bio orthogonal reactive groups into proteins allows site-specific introduction of functional groups that can be used to control protein function. UAAs are amino acids which are synthetically designed having probes attached to them which can be triggered by external stimuli. Here, the UAAs which are light cleavable and can arrest the function of the proteins temporarily will be discussed. Till date ~ 50 amino acids have been successfully incorporated into proteins in bacteria, yeast and mammals¹⁹⁵⁻¹⁹⁷. Non-natural amino acids bearing functional groups like ketone, azide, alkyne and tetrazine side chains have been incorporated within proteins through genetic encoding¹⁹⁸. This method has already been established for few UAAs in bacteria, yeast and mammalian cells (Figure23).

Site specific incorporation of un-natural amino acids (UAAs) with bio orthogonal reactive groups into proteins allows site-specific introduction of functional groups that can be used to control protein function. UAAs are amino acids which are synthetically designed having probes attached to them which can be triggered by external stimuli. Here, the UAAs which are light cleavable and can arrest the function of the proteins temporarily will be discussed. Till date ~ 50 amino acids have been successfully incorporated into proteins in bacteria, yeast and mammals¹⁹⁵⁻¹⁹⁷. Un-natural amino acids bearing functional groups like ketone, azide, alkyne and tetrazine side chains have been incorporated within proteins through genetic encoding¹⁹⁸. This method has already been established for few UAAs in bacteria, yeast and mammalian cells¹⁹⁹⁻²⁰¹ (Figure12).

In this method a site specific incorporation of UAAs are possible. For this purpose, selection of a non-endogenous coding codon is required, an orthogonal t RNA which can be charged with UAAs and recognize this non-endogenous coding codon to selectively code UAAs for it and an orthogonal aminoacyl-tRNA synthetase i.e. aaRS (it is the enzyme that acylates the tRNA with a UAAs).

In nature, except for the stop codons amber (TAG), ochre, and opal, all other triplet codons are used to code for one of the 20 canonical amino acids by cellular systems. To engineer and direct the cells to encode a new amino acid in the translational machinery one of these three degenerate stop codons are used because these codons are not recognized by any endogenous t RNA in the host system. A t RNA is engineered to recognize this recognize a stop codon when changed with UAAs. This adds the UAA in the growing polypeptide chain by a commonly referred mechanism known as nonsense codon suppression. The most commonly used stop codon is the amber or TAG codon²⁰².

Firstly, the aaRS and t RNA both are engineered to recognize the UAA of interest. This is followed by both engineering t RNA and aaRS in such a way that neither the orthogonal t RNA should be non-specifically acylated by aaRS endogenous to the host nor the orthogonal aaRS should acylate the endogenous t RNA. This means the pair tRNA/aaRS should be orthogonal to the whole system. This can be done by using an orthogonal tRNA/aaRS pair from a very distant species. The recognition of t RNA to its client codon on m RNA is via codon recognition. Therefore, the anticodon in orthogonal t RNA is mutated to specifically recognize the stop codon that codes for the UAA (For example. If TAG is used then the tRNA anticodon is mutated to AUC).

Secondly, aaRS gene is modified to recognize the UAA specifically. For this a large library of aaRS active site mutants are engineered and screened. After multiple rounds trails a selection in bacteria or yeast the final aaRS is obtained. This involves considering a gene of interest as an antibiotic resistance gene having a TAG codons in reading frame, which is used as a resistance marker for bacterial selection procedure i.e. the bacteria producing a full-length antibiotic resistance gene survive in the selection media containing that specific antibiotic.

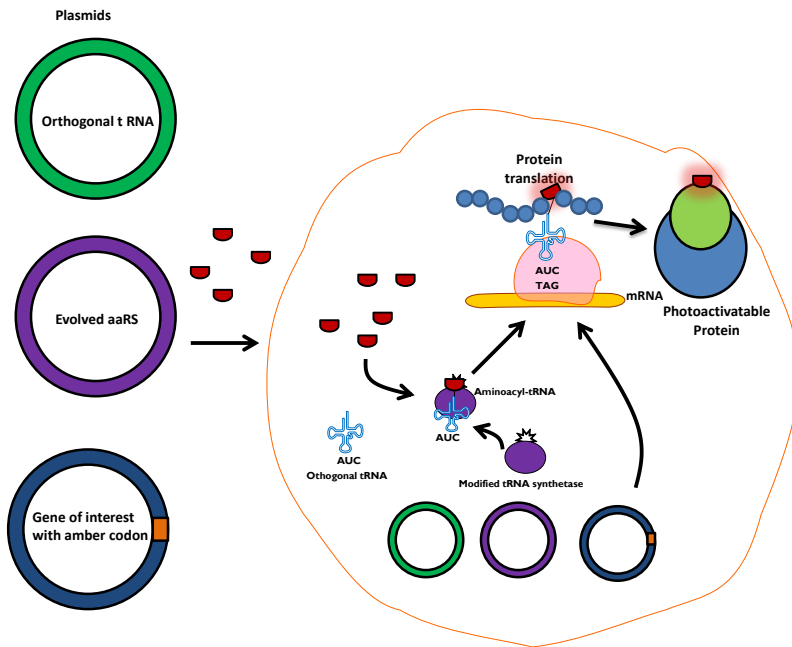


Figure 23. A schematic of UAA (Unnatural amino acid site specific incorporation (Red): Plasmids encoding the target protein gene, the Orthogonal tRNA CUA and the evolved amino acyl-tRNA synthetase (aaRS) are transfected or transformed into mammalian, yeast and bacterial cells. The media in which cells grow is supplemented with the UAA (shown in red). The aaRS catalyzes the acylation of the UAA with the orthogonal tRNA_{CUA}. When the mRNA of the gene of interest containing the amber codon is being translated in the ribosome (shown in yellow), the amber codon (TAG) is recognized by the tRNA_{AUC} charged with the UAA and this amino acid is incorporated into the growing polypeptide chain to give an photoactivatable protein.

If the aaRs has no ability to suppress TAG codon in a gene, it turns toxic to the bacteria, in the absence of the UAA incorporation resulting in no resistance mechanism because of truncated expression resulting in elimination of that clone. This is how the positive aaRs are selected exclusively²⁰³

This method works with multiple engineering steps, the gene of interest is engineered to have the amber codon by site directed mutagenesis approach, the orthogonal suppressor tRNA and the evolved aaRS are introduced into cells by transformation or transfection depending upon the cell type (Figure 12)²⁰⁴.

The UAAs are added in the media and these transformed cells are allowed to uptake it. The cells engineered with this orthogonal machinery is evolved to recognize the site specific mutated stop codon as coding codon with this evolved machinery and non-translation is terminated and the polypeptide chain grows until it encounters a stop codon distinct from this stop codon to eliminate the protein translation i.e. if this machinery recognizes the TAG codon to coding then the stop codon should be either TAA or TGA. After this protein having UAAs are engineered which can be used for in vitro studies inside the cells or can be extracted from the cells by protein purification methods²⁰⁵.

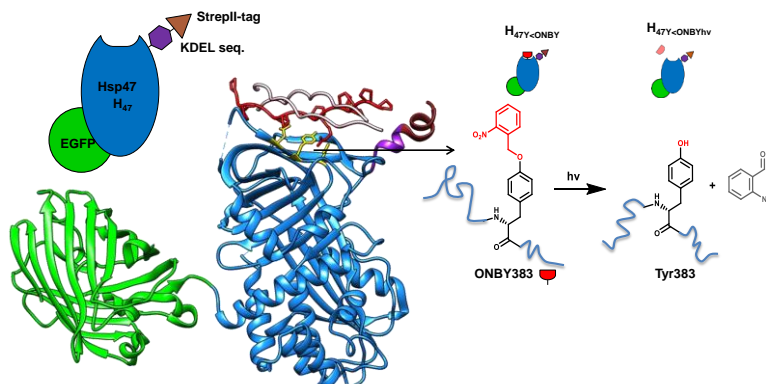
Incorporation of photoactivatable unnatural amino acids into proteins recombinantly in live cells using 'evolved' machinery was pioneered in the Peter Schultz lab, Scripps Research Institute²⁰⁶. Proteins can be engineered using this method to incorporate a light-removable protecting group within their active site that blocks the interaction to their clients for the biological activity. This blocking activity can be achieved by photo caged amino acids which arrest the protein function temporarily, but upon exposure to light, the blocking group in the amino acid is removed, exposing the native amino acid and thus the biological activity is retained. Till date photo caged versions of tyrosine²⁰⁷⁻²⁰⁹, cysteine²¹⁰, serine²¹¹ and lysine²¹² have been incorporated into proteins genetically.

The advantage of this approach is that the proteins can be site specifically arrested, it is tool which can be spatially and temporally controlled, and the production of orthogonal t RNA can be tuned by having a high copy number plasmid ^{200, 204, 210}. However, there are some limitations to this strategy like low yields on extraction, solubility issues with large amount of UAAs in the medium and more cell toxicity when large amount of by products are released ^{200-201, 204-206, 210}.

Chapter 2

Synthesis of Photoactivatable Hsp47 (H_{47Y<ONBY})¹

Molecular chaperones are folding modulators that play a central role in the conformational quality control of the proteome by interacting with, stabilizing and remodeling a wide range of specific proteins or non-native polypeptides. Hsp47/SERPINH1 is a collagen-specific molecular chaperone with a crucial role in collagen biosynthesis. Mutations in Hsp47 in the cell are associated with collagen disorders (i.e. osteogenic imperfecta, keratoconus), and overexpression of Hsp47 has been found in fibrotic diseases and cancer. In this chapter, synthetic biology approaches applied to obtain a photoactivatable variant of HSP47 are presented. This protein should be delivered to cells and allow external regulation of its intracellular activity by light exposure. The synthesis of the photoactivatable Hsp47 involves site-specific incorporation of non-natural amino acids at its collagen-binding site to render an inactive protein unless irradiated with 360 nm light. Two strategies were explored to replace either Asp385 or Tyr383 amino acids with photo-activatable analogues in the protein structure: (i) native chemical ligation and (ii) genetic encoding incorporation using *E. coli*. A photoactivatable Hsp47 was successfully synthesized by the second strategy, wherein o-nitro benzyl tyrosine (ONBY) replaced the tyrosine at position 383. In subsequent chapters the photoactivatable Hsp47 will be applied to manipulate collagen production and assembly¹



¹Parts of this chapter were published in Advanced Science (2019), 6,1801982, Essak S. Khan, Shrikrishnan Sankaran, Julieta I. Paez, Christina Muth, Mitchell K. L. Han, Aránzazu del Campo, "Photoactivatable Hsp47: A Tool to Regulate Collagen Secretion and Assembly"

2.1. Introduction

Hsp47 is a molecular chaperone that binds specifically to collagen and requires at least eight Gly-Xaa-Yaa amino acid repeat motifs. Hsp47 exhibits a typical serpin fold, consisting of three β -sheets (A, B, and C) and nine α helices and does not change its conformation upon collagen binding. Crystal structure analysis of the Hsp47-collagen complex⁷⁴ has shown that when the Yaa position in the collagen helix is occupied by Arg, the Asp385 of Hsp47 binds to the triple helix strand by forming a salt bridge. Further stabilization of this complex is provided through Tyr383 and Leu381 through hydrophobic interactions. In its triple helical form, collagen forms a complex with Hsp47 with a total solvent-accessible surface area of $1000 \pm 150 \text{ \AA}^2$ buried between them, indicating tight interactions within the binding site⁷⁴. Interestingly, while mutations in Hsp47's Asp385 and Leu381 seem to reduce its affinity with collagen, mutations in Tyr383 were shown to completely inhibit the interaction, indicating that this residue plays a major role in the binding^{74, 102}. Positions Asp385 and Tyr383 in Hsp47 are then regarded as suitable sites for the introduction of photoactivatable residues to control Hsp47 binding to collagen with light.

Controlling intracellular protein function by light is possible by introducing photoactivatable non-natural amino acids at the active site in the protein structure^{50, 213-215}. Photo activatable non-natural amino acids are amino acids which are engineered to have chemical moiety attaching to their functional amino acids to arrest its function which on light exposure is cleaved off temporarily controlling the functional amino acids. For developing photoactivatable proteins by introducing photo responsive amino acids different biochemical strategies are available, from which two are of special interest for this chapter:

Strategy 1: Intein protein ligation method

The Intein protein ligation (IPL) is an orthogonal recombinant protein coupling method which involves a transthioesterification step for coupling an unprotected peptide-thioester to a cysteine containing peptide or protein. With this method, it is possible to form a native amide bond next to a cysteine-

containing ligation site. First, a reversible transthioesterification step forms a thioester (capture) N → S shift, it further reacts to an intermolecular peptide bond by a S → N shift (rearrangement). Initially, this approach was developed for coupling two presynthesized peptide chains. Later, intein protein ligation (IPL) approach was developed^{162, 180, 184, 200}, where either a peptide was conjugated to a truncated protein or two truncated proteins were coupled using an intein splicing approach.

The advantage of this technique is its two hybrid proteins can be developed, due to covalent chemistry and native peptide bonds the protein is stable. This technique works powerful workhorses i.e. Inteins for multiple coupling of proteins and peptide fragments in larger yields¹⁹⁹⁻²⁰⁰. For this purpose mechanistic models and synthetic strategies have to be carefully planned. However, there are few limitations with this technique like cysteine at the first amino acids of second peptide is required. The peptide or protein conjugated with Intein should be cleavable at lower temperatures with thiol as many proteins degrade very fast at higher temperatures^{200, 204, 216}. The further development and understanding of intein-based splicing systems the progress of ligation strategies will certainly enlarge the repertoire of these interesting technique²¹⁶.

Strategy2: Genetic incorporation of photo responsive UAAs using *E. coli*

Genetic incorporation of non-natural amino acids employs orthogonal gene expression machinery engineered to incorporate UAAs at a specific site in the protein structure. In the past 28 years, bacteria, yeast and mammalian host specific aminoacyl-tRNA synthetase(aaRS)-tRNA pairs have been developed to enable facile incorporation of nnAAs into desired proteins. The aaRS are engineered by directed evolution to precisely recognize and attach the nnAA to the orthogonal tRNA without interfering with host tRNAs, aaRS or amino acids. The orthogonal tRNA is derived from organisms that encode a 21st amino acid, selenocysteine by recognizing the Amber stop codon (UAG) sequence on the mRNA. So, with the appropriate aaRS and tRNA, a nnAA can be incorporated at any site in a protein by including the codon, TAG, in its DNA sequence^{195, 217-}

²¹⁸(See figure2). The most common photoactivatable groups with which most of the amino acids have been modified and for which aaRS and tRNA pairs have been engineered are o-nitro benzyl groups and their derivatives²¹⁹. These groups can be installed on hydroxy, carboxy, thio, or amino side-chains of proteins and are cleaved upon irradiation with 365-nm light.¹⁹⁸

The advantage of this approach is that the photo responsive UAAs can be site specifically incorporated UAAs, and the production of orthogonal t RNA can be tuned by having a high copy number plasmid ^{200, 204, 210}. However, there are some limitations to this strategy, solubility issues of UAAs, limited yields and moreover for cell toxicity when large amount of by products are released after cleavage of this UAAs ^{200-201, 204-206, 210}.

2.2. Results and Discussion

2.1.1. Strategy 1: General molecular design

The procollagen-binding site in Hsp47 is located close to the C-terminus (residues 381-386) and contains an aspartic acid residue (Asp385) involved in collagen binding. This position was selected to be replaced by a photoactivatable aspartic acid (DMNPB-Asp). In order to site-specifically introduce the non-natural residue, a semisynthetic Human Hsp47 to be obtained by fusing two building blocks (BB, Figure1) using NCL was planned. The N-terminal block, a truncated version of the protein, should be produced recombinantly in *E. coli* (378-mer, BB1). The C-terminal block (BB2), a 40-mer containing the DMNPB-Asp residue, should be synthesized by solid phase peptide synthesis (SPPS). The IMPACT kit (New England Biolab) should be used for the ligation of the two blocks. BB1 would be produced as an intein-fusion protein, which, after intein-cleavage, would leave a C-terminal thioester that can react with the thiol of an N-terminal cysteine residue in BB2 to form a peptide bond ¹⁷³⁻¹⁷⁵ (Figure1).

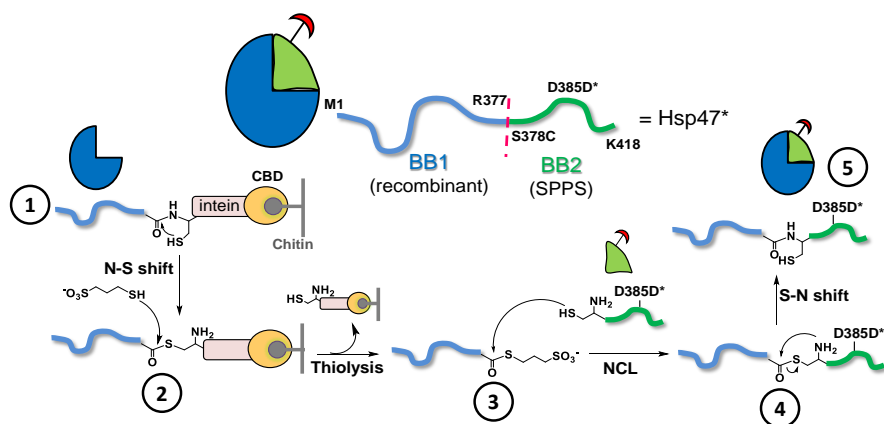


Figure 1. Scheme depicts semisynthetic recombinant approach for developing photoactivatable Hsp47 by intein protein ligation. Reversible trans thioesterification step forms a thioester (capture) 1. N-S Shift, 2. Thiol mediated cleavage, 3. Peptide attack and 4. Rearrangement of intermolecular peptide bond by a S \rightarrow N shift.

a. Cloning and expression of truncated hHsp47 (human Hsp47) in pTXB1 and full length hHsp47:

The Intein protein ligation-based approach was used for expression of truncated *hHsp47*, as it allows single step protein purification and subsequent ligation of photoactivatable C terminus peptide. This system exploits the facile cleavage of the guest protein i.e. truncated Hsp47 from a fusion adduct, intein, in the presence of thiols. The intein has a chitin binding domain which is used for purification on chitin beads. The protein of interest is cleaved off leaving a thioester handle for ligation of the BB2 peptide to the column-bound truncated protein (Figure 1)^{52, 75, 101}.

A custom made hHsp47 gene encoding human Hsp47 was cloned at the N terminus of intein protein gene with the chitin binding motif for affinity purification in pTXB1 vector. A truncated hHsp47 gene having 1-377 amino acids was also cloned into pTXB1 vector in front of Intein protein expressing gene. The arginine at 377 position was selected to attach the photoactivatable peptide handle to create the recombinant photoactivatable Hsp47 construct as

after this position the RCL loop starts which is just next to active site involved in the binding activity. Initial attempts to express truncated and full length hHsp47 using hHsp47pTXB1 and truncated hHsp47pTXB1 vectors in T7 express cells were unsuccessful. Most of the protein was found in inclusion bodies (Figure 2), despite screening different bacterial growth culture conditions (Incubation temperature (14°C-37°C), shaking speed (100rpm-250rpm, inducer concentration (0.001μM-1Mm) and duration of expression) for optimal protein production (Figure 2). This was most likely due to heterologous expression of hHsp47 in *E. coli* which was discovered later to have 31 rare codons which *E. coli* cannot recognize because of its less evolved machinery (Figure 3)

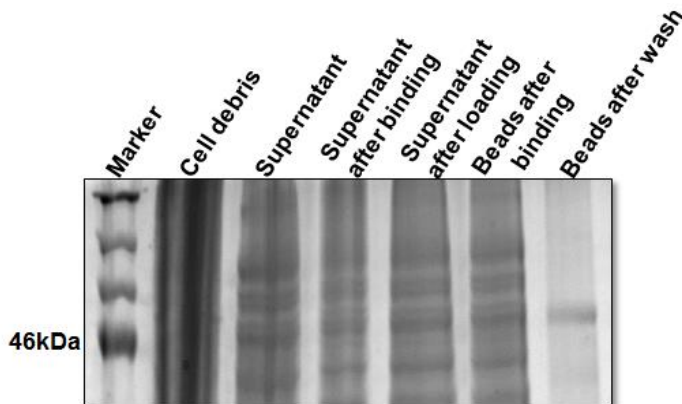


Figure2.12% SDS Page gel of full length hHsp47 p TXB1 in T7 express cells at 47kDa size.

b. Cloning and expression of truncated hHsp47 (human Hsp47) in pRSETB and full length hHsp47:

The full length hHsp47 was also cloned in pRSETB vector to and reduce basal expression of hHsp47 gene²²⁰, but this strategy did not help much in overcoming the solubility issue (Figure 5). The meagre soluble fraction of protein eluted or bounded to chitin beads was incubated at different thiol cleavage conditions by varying temperature and time. Due to low solubility and fast degradation of hHsp47 in the incubation conditions the native chemical ligation was unsuccessful. Moreover, this version has Arginine at the C terminal

cleavage site next to Intein protein site which was found to require 23h under cleavage condition at RT^{221b}. These reaction conditions were too harsh for hHsp47 as Hsp47 degrades very fast in vitro at RT. Trials were made with different thiol reagents such as DTT, MESNA and β -mercaptoethanol to test milder conditions for cleavage. Cleavage of truncated hHsp47 was possible using DTT at 23°C for 24 hrs. However, DTT does not promote Native chemical ligation as it cannot create a thioester handle in order to ligate the caged peptide (Figure 4)

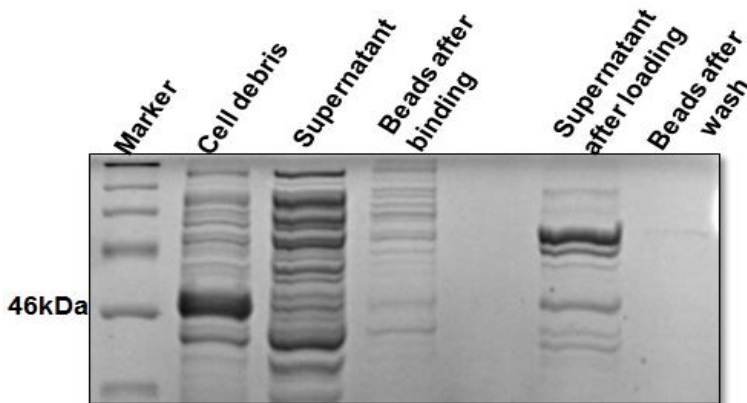


Figure3. 12% SDS Page gel of full length hHsp47 p RSETB in T7 express cells

c. Cloning and expression of truncated hHsp47 (human Hsp47) in pTXB1 and full length hHsp47 along with p RARE plasmid:

In an attempt to circumvent these issues, both truncated hHsp47 pTXB1 and full length hHsp47 were transformed into in Rosetta-gami 2(DE3) pLacI having pRARE plasmid for gene optimization. Rosetta-gami 2(DE3) strains were chosen to promote enhance Hsp47 protein expression by targeting rare condons. Rosetta-gami 2(DE3) are BL21 derivative cells that are designed to enhance the expression of eukaryotic proteins containing codons rarely used in *E. coli*. The strain supply tRNAs for AGG, AGA, AUA, CUA, CCC, GGA codons on a compatible antibiotic-resistant plasmid to promote the “universal” translation which is otherwise limited by the codon usage of *E. coli*. The tRNA genes are driven by their native promoters. In Rosetta(DE3)pLysS, the rare tRNA genes

are present on the same plasmids that carries the T7 lysozyme gen pRARE plasmid which was able to slightly enhance expression of truncated version of hHsp47. Fluorescent proteins like GFP and RFP are reported to improve the solubility of protein of interest like toxic proteins up to a certain extent and facilitate visualization of the expression and purification processes.²²²⁻²²³ Therefore, full length *hHsp47* at the C terminal of mcherry gene in pTriEx-mCherry plasmid was cloned. Also, truncated hHsp47 fused to intein protein was amplified from its pTXB1 vector and cloned into pTriEx-mCherry plasmid with mcherry tagged at the N terminus of hHsp47. However, this approach did not improve the solubility of hHsp47 (Figure 6).

During the expression and purification of pTriEx-hHsp47-intein-mcherry construct in T7 express, it was observed that mcherry gets cleaved from the hHsp47 (learnt via eluting fluorescent red color soluble fraction attributing to mcherry during harvesting). Phenylmethylsulfonyl fluoride (PMSF) a serine protease inhibitor (serine hydrolase inactivator) protease inhibitors was used in an attempt to overcome this problem, but this strategy remained unsuccessful. Amino acid at the protein of interest and intein protein play a key role in cleavage conditions, especially tyrosine promotes efficient cleavage²²⁴⁻²²⁶. Therefore, the arginine at the C terminus end of truncated hHsp47 was mutated with Tyrosine; thus helping on-column cleavage and ligation of hHsp47 with the peptide but with minute yield (confirmed by the western blot, Figure 6). However, this protein was unstable at even lower temperatures with negligible yields identified by running SDS PAGE.

In short, developing photoactivatable Hsp47 using IPL was unsuccessful mainly because of poor solubility of human Hsp47 protein having 31 rare codons, demand of cleavage conditions of protein from the intein at high temperature. This led to explore other photoactivatable protein engineering strategies to develop the protein using genetic engineering.

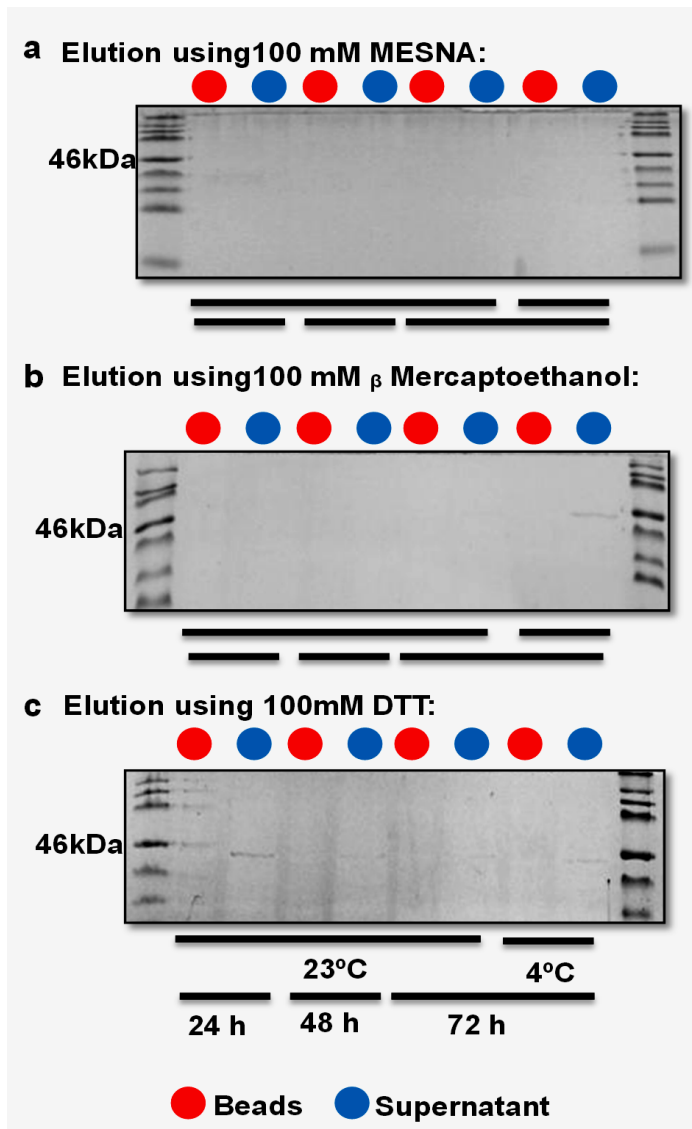


Figure.4. a.12% SDS PAGE Gel of Elution fractions at varying temperature and time using 100 mM MESNA; b.12% SDS PAGE Gel of Elution fractions at varying temperature and time using 100 mM β Mercaptoethanol; c. 12% SDS PAGE Gel of Elution fractions at varying temperature and time using 100 mM DTT.

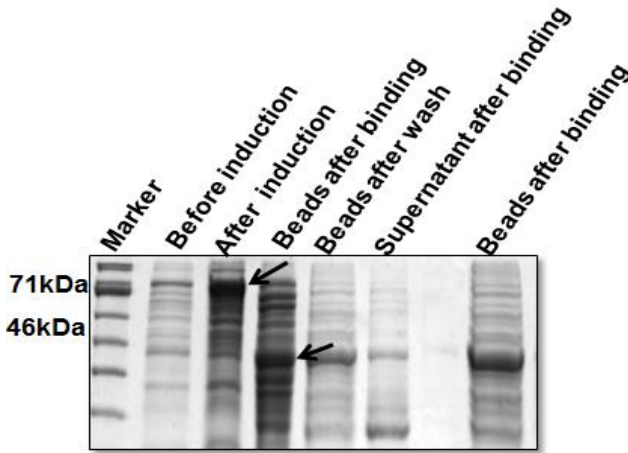


Figure5. 12% SDS Page gel of mcherry-full length hHsp47-pTriEX expressed in T7 express. Arrows indicate expected protein at 71kDa which gets cleaved during the bead binding step.

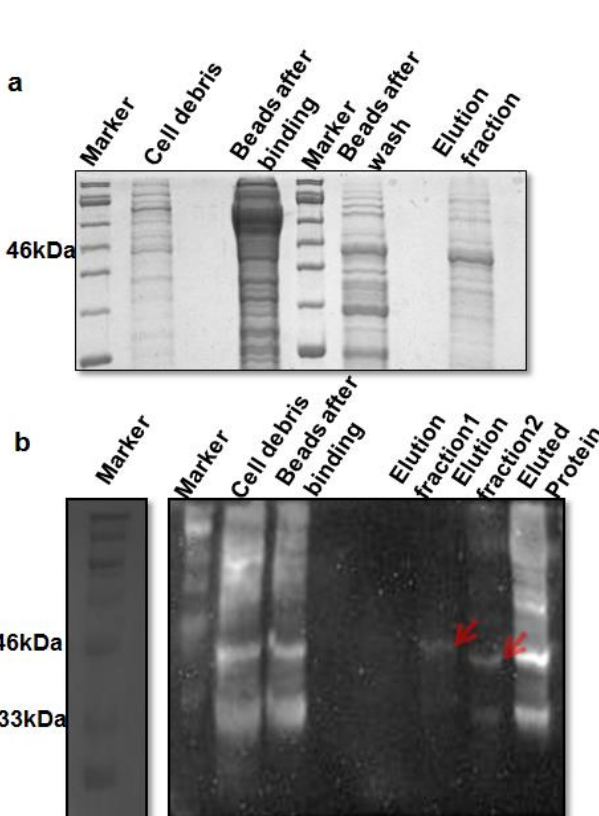


Figure6.A. 12% SDS PAGE Gel of purification of mcherry+ full length hHsp47pTriEX constructs along with pRARE plasmid using Rosetta-gami 2(DE3) pLacI; B. Western blot of hHsp47 showing truncated version hHsp47 ligation to 51 mer peptide.

2.2.2. Strategy 2: General molecular design

Synthetic tools to incorporate the non-natural light-responsive tyrosine (o-nitro benzyl tyrosine – ONBY) amino acid on recombinant proteins has been previously developed.²²⁷ It has been shown that replacement of Tyr by ONBY in Tyr-stabilized protein-protein or protein-DNA complexes lead to destabilization of the complex via steric hindrance and disruption of hydrophobic interactions due to the polar nitro group²²⁷. It was hypothesized that a similar effect would occur when replacing Tyr383 by ONBY in Hsp47 structure to obtain the photoactivatable variant i.e. $H_{47Y<ONBY}$ (Figure 7).

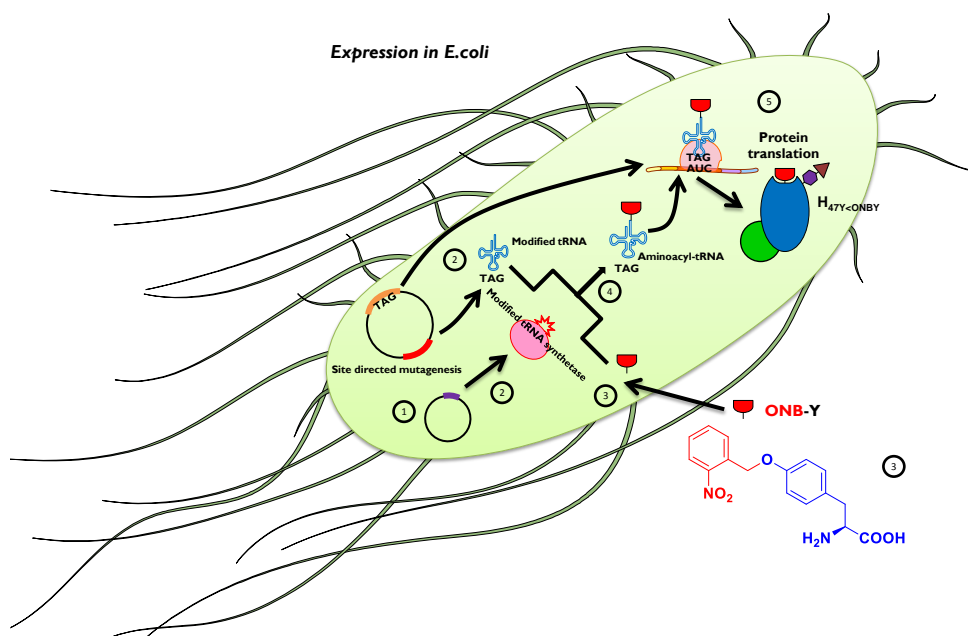


Figure 7. Scheme shows the synthesis of $H_{47Y<ONBY}$ in *E. coli*. Co-transformation of pBAD-Hsp47383TAG and pBK-ONBYRS, 2. Synthesis of orthogonal modified tRNA and tRNA synthetase, 3. uptake of ONBY by the *E. coli*, 4. Modified tRNA attached to ONBY, 5. protein translation.

a. Canine Hsp47 gene optimized version construct & His-tag purification in T7 Express:

A canine-derived synthetic Hsp47 (*cHsp47*) gene coding for residues 36-418, identical to hHsp47 sequence, a codon-optimized cDNA for *E.coli* having a C-terminal His-tag and cloned in pet22b was received from Prof. Dr. Ulrich Baumann, University of Cologne. Soluble Hsp47 purification had already been established using this construct⁷⁴. The N-terminal 1-36 amino acids, were removed due to hydrophobicity and solubility issues. This construct was cloned into T7 express cells for the expression of *cHsp47*. In this case, it was possible to purify *cHsp47* using His-tagged purification Figure 9. However, while scaling up from 200ml culture to 1 L culture, all non-specific proteins were eluted out during purification and most of the target protein was still found in inclusion bodies. Also, the yield was very low and *cHsp47* was less stable even after storing the protein at -80°C after running the entire purified protein on SDS PAGE gels at different time points. Induction studies at lower temperatures and IPTG concentration was performed but the yield only further reduced. (Figure 8)

b. Canine Hsp47 gene optimized version construct in PJExpress 411 & purification in Clear coli BL21 cells using Streptag2 purification:

A canine-derived synthetic Hsp47 gene coding for residues 36-418⁷⁴ which is a codon-optimized cDNA for *E.coli* having an additional C-terminal StrepII-tag and cloned in pJExpress 411 was also received from Prof. Dr. Ulrich Baumann, University of Cologne⁵⁰. StrepII-tag has been reported to promote efficient purification of Hsp47 avoiding non-specific protein elution. This construct was cloned in Clear Coli competent cells have a genetically modified lipopolysaccharide (LPS) that does not cause an endotoxic response in human cells. This BL21 strain also helps efficient protein expression²²⁸. Canine-derived Hsp47 was purified using StrepII-tag affinity purification method (IBA Life sciences Strep Tag II Purification protocol). Using this approach, it was possible to elute soluble *cHsp47* without non-specific proteins.

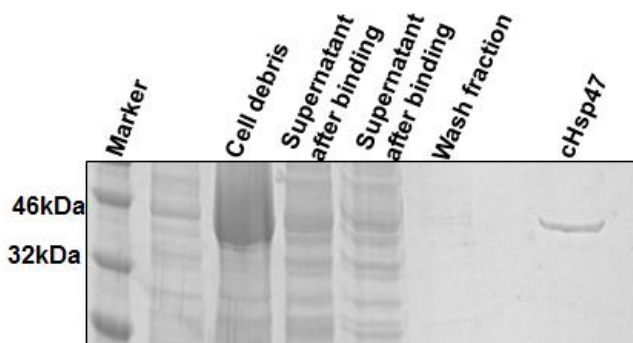


Figure 8. 12% SDS PAGE purification gel of cHsp47 using His tagged Ni NTA affinity chromatography

The soluble fraction was concentrated and purified further by gel filtration (Superdex S75; GE Healthcare) in buffer A [20 mM Hepes (pH 7.5), 300 mM NaCl, 4 mM DTT]. The purified protein was concentrated to ~15 mg/mL and stored at -80°C for further use. This method allowed us to reduce nonspecific binding of other proteins as observed during His-tagged purification as mentioned above. The *Clear coli* cells and streptag2 tag helped in making cHsp47 more pure and soluble of yield 183.26 ng (Figure 9).

In order to improve Hsp47's solubility for heterologous expression in *E. coli*, an enhanced green fluorescent protein (EGFP) and turquoise fluorescent protein (Turq) were genetically fused to its N-terminal²²⁹. This approach led to a significant increase in the synthesis yield (Table S1). A StrepII-tag was introduced at the C-terminal for affinity purification. This derivative of Hsp47 having EGFP and Turquoise was successfully obtained in 207.8 μg and 103.4 μg yield from 200mL culture, as confirmed by absorbance with UV-Vis spectrophotometer, and was named H_{47N} (N refers to native) (Figure 10). The o-nitro benzyl tyrosine (ONBY) residue was incorporated at 383 position by co-expressing the H_{47N} gene along with an appropriately engineered aaRS and tRNA^{196, 230} (see details in Figure 7). The H_{47N} gene was also mutated with an amber codon TAG at the 383rd position to site-specifically incorporate ONBY. This Hsp47 derivative was named $H_{47Y<ONBY}$

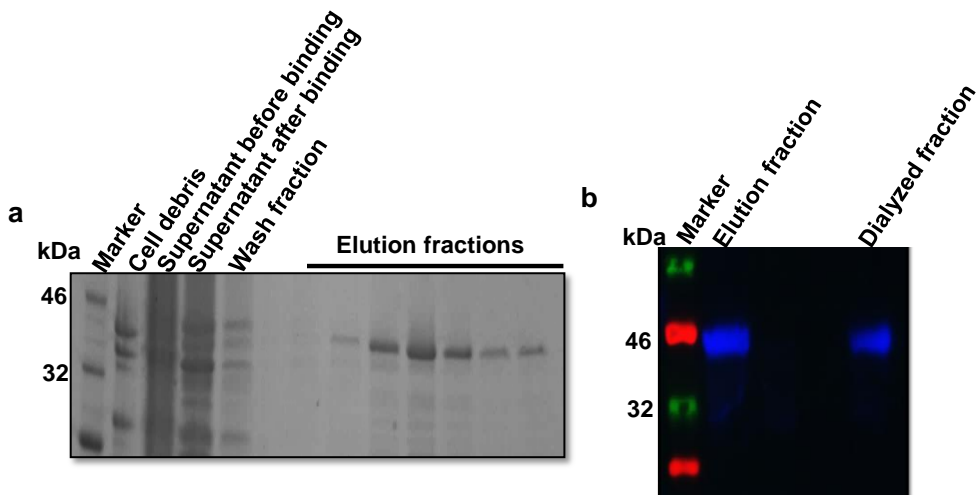


Figure 9. a. 12% SDS PAGE gel of canine Hsp47 produced in Clear coli and purified using Strep-Tag affinity chromatography b. Western Blot of purified H_{47N} (truncated and full) stained with Alexa 488 conjugated Streptavidin (blue).

In order to confirm the incorporation of ONBY, synthesis in the presence or absence of ONBY in the medium before induction was performed. In the presence of ONBY, the full protein would be expressed, whereas in the absence of ONBY, translation should terminate at the 383rd position due to the presence of the amber stop codon and the StrepII-tag would not be included. StrepII-tag affinity beads were incubated with a small amount of cleared lysates and purified Hsp47 control variants. The beads became fluorescent within 5 mins when incubated with $H_{47Y<ONBY}$, indicating that the StrepII-tag had been incorporated at the C-terminus (ONBY present) whereas no fluorescence was observed in truncated version having no StrepII-tag (Figure 11a). The clear lysates were purified using StrepII-tag affinity purification and screened to affirm the presence of StrepII-tag.

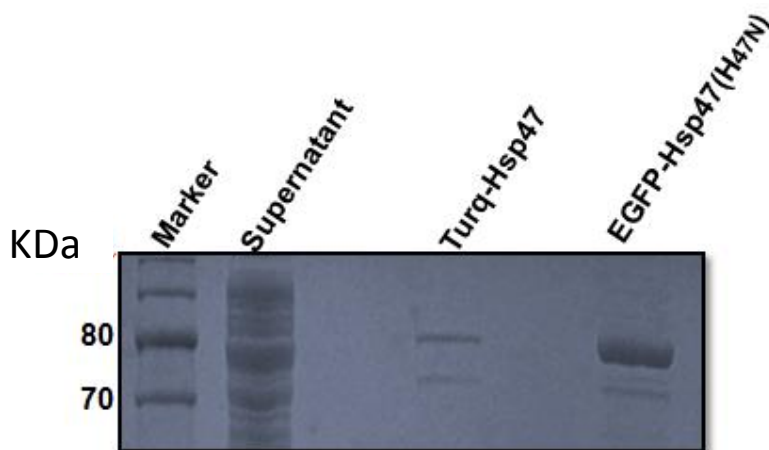


Figure10. 12% SDS PAGE gel of Turquoise and EGFP-Hsp47 (H_{47N}) produced in Clear coli and purified using Strep-Tag affinity

Western Blot was performed labeling StrepII-tag using Alexa488-Streptavidin after affinity purification which showed a clear fluorescent band when ONBY was present during synthesis, and no fluorescence was observed in the truncated version (Figure 12C). This result confirmed the incorporation of ONBY to $H_{47Y<ONBY}$. The yield of the synthesis was 43.56ng from 200ml culture. Two additional mutants of H_{47N} were developed as control proteins for further experiments: (i) $H_{47Y<R}$, with Tyrosine mutated to Arginine at 383 position as an inactive version of H_{47N} ⁷⁴. (ii) H_{47Kdel} where the KDEL sequence at C terminus of H_{47N} was deleted, thereby preventing retrograde delivery of the protein into the ER (Figure 12). The yields of all the variants are included in Table S1.

2.3. Discussion

Photoactivatable Hsp47 was successfully developed using strategy 2. The UAAs were successfully incorporated at 383rd Try position. However, considering H_{47N} yield as 100% only 23.28 % of $H_{47Y<ONBY}$ could be synthesized from 200mL culture. This is due to limitations in dissolving ONBY in the medium to dissolve as in our experienced concentration above 0.4 mM could not be completely dissolved in the medium turning medium it acidic (checked by pH indicator).

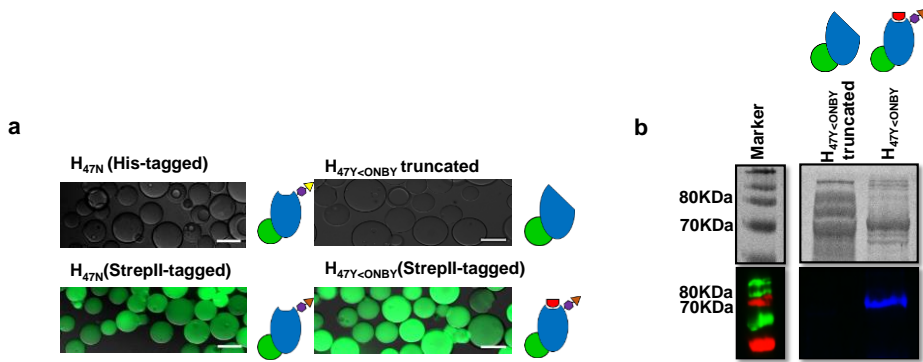


Figure 11. Characterization of Photoactivatable Hsp47 (H_{47Y<ONBY})

a. Microscopy images (merged phase contrast and epifluorescence green channels) of Strep-II-Tagged agarose beads incubated with supernatant of different Hsp47 variants showing the presence or absence of StrepII-tag in the protein structure (Scale bar 100 μ m).
 b. 12% SDS Page gel and Western Blot of purified H_{47Y<ONBY} (truncated and full) stained with Alexa 488 conjugated Streptavidin (blue).

Also, Hsp47 is a heat sensitive protein therefore cooling conditions are required for purification of this protein. The synthetic yield of the photoactivatable version makes it challenging to use for in vitro functional assays. For each bioactivity experiments discussed in next chapter, H_{47 Y<ONBY} had to be freshly synthesized as it is stable for few weeks at -80°C. To circumvent this issue, large cultures of around 1 to 2 L were cultured. However, even more decrease in the yield for about 10 % was observed. Therefore, other strategies need to be explored to develop a stimuli responsive Hsp47 tool.

In this context, alternative approaches to manipulate the molecular design of Hsp47 are 1. use of photo switchable protein like LOV2 J α^{185} and 2. use of enzyme cleavable peptide sequences¹⁸² to mask the active site of the protein turning it temporarily in active. For both approach careful selection of Hsp47 sequences especially at the active site should be examined such that any alteration should not result in loss of Hsp47 permanently.

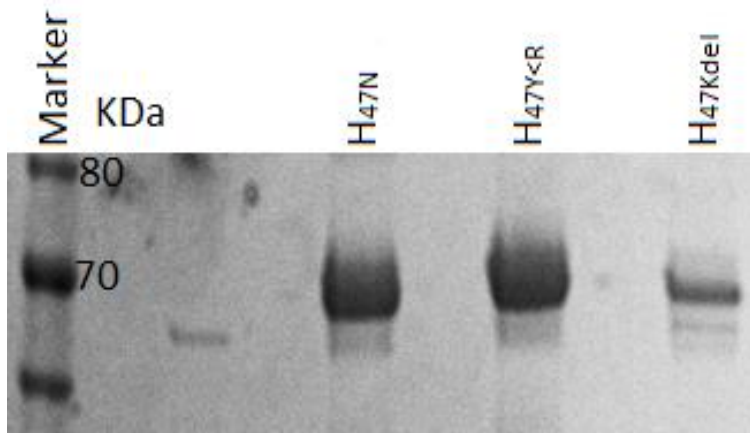
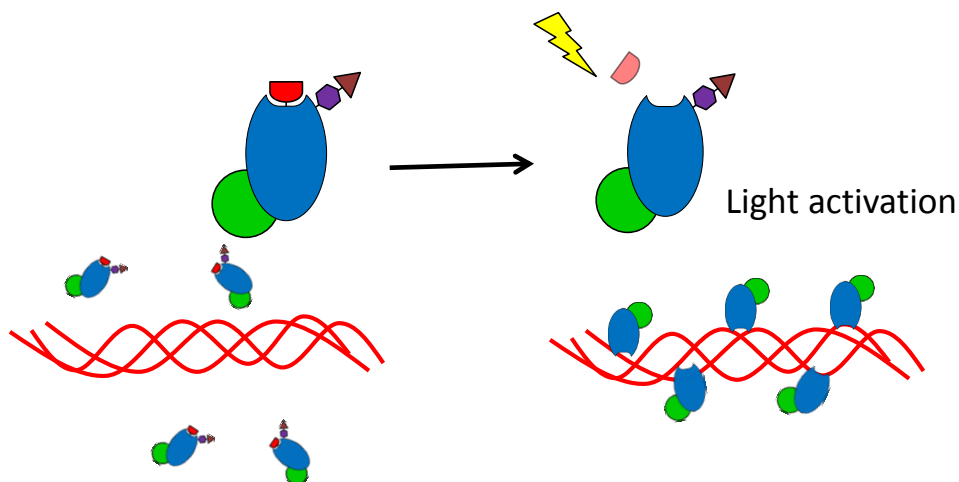


Figure12. 12 % SDS PAGE gel of Hsp47 variants

Chapter 3

Characterization of Photoactivatable Hsp47-Collagen Interactions¹

The functionality of recombinantly synthesized Hsp47 and photoactivatable variants was characterized and quantified based on its interactions with collagen. Biochemical (Protein binding assay and Native PAGE co-localization) and biophysical (Fibrillation Assay and Rheology) techniques were used for this purpose. The restoration of bio functionality upon light exposure is demonstrated and quantified.



¹Parts of this chapter were published in *Advanced Science* (2019), 6,1801982, Essak S. Khan, Shrikrishnan Sankaran, Julieta I. Paez, Christina Muth, Mitchell K. L. Han, Aránzazu del Campo, “Photoactivatable Hsp47: A Tool to Regulate Collagen Secretion and Assembly”

3.1. Introduction

Proteins are the work horses of the cells, especially in the biological processes of inter/intra-cellular communications. These communications are directed through interactions with specific molecular clients such as DNA, RNA, other proteins or small molecules. Most of signal transduction inside and outside the cells is governed by protein-protein interactions. These interactions are stable or transient interactions that largely occur through non-covalent interactions like electrostatic, hydrophobic, van der Waals, etc.

Strategies to study these interactions can be broadly classified into *in vitro*, *in vivo* and *in silico* approaches. *In vitro* approaches include biochemical approaches like Coimmunoprecipitation²³¹, Affinity chromatography²³², Tandem affinity purification-mass spectroscopy (TAP-MS)²³³, Protein micro arrays²³⁴, Protein-fragment complementation, Phage display (H), etc. and biophysical approaches like X-ray crystallography²³⁵, NMR spectroscopy²³⁶, Rheology²³⁷, Isothermal calorimetry (ITC)²³⁸, Circular dichroism spectroscopy (CD)²³⁹, Single molecule optical tweezers²⁴⁰. *In vivo* approach include Yeast 2 hybrid (Y2H) (H). *In silico* approaches include Ortholog-based sequence method, Domain-pairs-based sequence method, Structure-based methods, Gene neighborhood, In silico 2 hybrid (I2H) and Phylogenetic tree²⁴¹.

In vitro assays are defined assays performed outside living organism in a controlled environment to reveal functional and structural principles of protein-protein interactions. For example, coimmunoprecipitation is used to identify a protein's unknown client by studying the binding affinity of known protein to any unknown client from whole cell extract in which protein are in their native confirmations using antibodies raised against them²³¹. Affinity chromatography is a highly sensitive method, which is used to detect the weakest interactions between proteins. Combining both co immunoprecipitation with affinity chromatography results in Pull down assay²³², with which it is possible to identifying novel interacting partner of the known protein. TAP-MS involves double tagging of the protein of interest at the genetic level using affinity and radiolabel tags, followed by a two-step purification and mass spectroscopic analysis^{233, 242}. X-ray crystallography gives insight into the atomic level interaction of protein structures and function. NMR spectrophotometry is a complement to this technique, which detects even very weak interactions²⁴³. CD provides the structural information at secondary structural level and change in conformation on binding to the client or under influence of environmental

factors based on differential absorbance of proteins giving rise to change in degree of ellipticity²³⁹.

In vivo methods allow us to understand protein-protein interactions in their native states using a living system. An example of this approach is the Yeast 2 hybrid (Y2H) (H) assay. In this method a yeast transcription factor protein, which has a DNA Binding Domain (DBD) and an Activation Domain (AD), is hybridized with the protein of interest and its binding partner²⁴⁴. When there is an interaction between the protein of interest and its binding partner, the two domains of transcription factor are in close proximity which activates the transcription of a reporter gene²⁴⁵.

In silico methods are mostly structure based prediction analyses like the phylogenetic tree method, which predicts possible protein-protein interactions based on the evolution history of the protein²⁴⁶. Another example includes Ortholog-based sequence method which is based on the homologous sequence of the query protein in the annotated protein databases with pairwise local sequence algorithm²⁴⁷.

Different methods have been used in the literature to characterize the interaction of Hsp47 with Collagen. Most of them rely on changes in the physical properties of collagen solutions and hydrogels. Collagen extracted from tissues can be dissolved at acidic pH, but forms aggregates at neutral pH at 34-37°C as consequence of the lateral association of collagen helices^{50, 75, 81}. The lateral assembly is driven by electrostatic and hydrogen bond interactions that are sensitive to pH and temperature²⁴⁸. The kinetics of this fibrillation process has been extensively investigated^{81, 84, 99-100, 248-251}. The formation of aggregates leads to changes in the viscosity and optical properties of the collagen solution, which give an indirect readout of the molecular organization.

The fibrillation process has been followed by **turbimetry**, which quantifies the diffraction of light caused by the formation of collagen fibers which is detectable only when mass per unit length is roughly 100 times greater than that of a single monomer which is approximately 300 kDa of size 300nm²⁵¹⁻²⁵². In this assay the absorbance of collagen fibers is measured against time. The

kinetics of two processes involved in collagen assembly has been monitored through this assay: nucleation and fiber growth. These processes occur at different rates, which can be determined from lag and the log phase of the fibrillar kinetics²⁵².

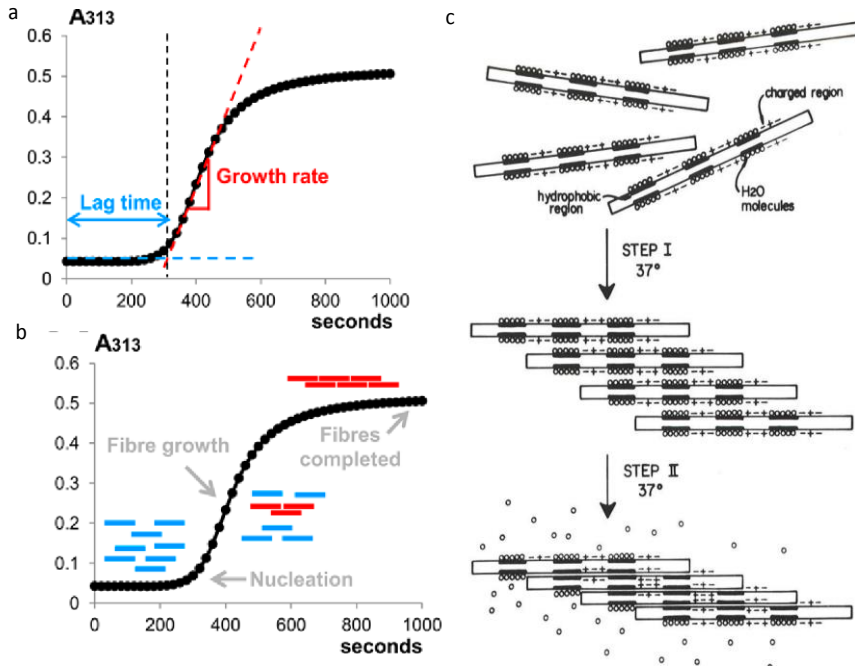


Figure 1. a. Increase of turbidity in a sample containing aggregating collagen monomers in vitro. The initial lag phase is terminated by an increase in absorbance, followed by nucleation time. A sigmoidal growth phase follows, during which nuclei are elongated into fibers by the lateral incorporation of freely diffusing monomers. b. The growth rate can be defined as the slope of the quasi-linear section of the sigmoid, i.e., the slope at the inflection point. The intersection of the tangent with the baseline marks the nucleation time. c. Random monomers of collagen first begin to align in quarter staggered overlap. The alignment is typically due to electrostatic interactions. As the temperature approaches 37°C the hydrogen bonded water molecules shown in circles, clustered around the collagen, “melts” and approaches the nonpolar surfaces. Exclusion of surface helps in interaction of these surfaces with each other. The driving force results from increase in entropy of the system increasing the state of disorder of the system. Reproduced from ⁹⁹ with permissions from ACS.

Initially collagen monomers assemble to form aggregates which have been shown to create phase separation into a random solution phase and an aggregated ordered phase which lowers the free energy. Formation of aggregated state with average molecular weight of 4×10^6 is observed in COL I, II and III collagens. These initial aggregates are referred to as 'Nucleus' and the process is known as nucleation. This is a rate limiting step as it involves deprotonation of carboxylic group and protonation of amines which is followed by electrostatic interactions between charged groups and surface hydrophobicity⁹⁹. It is suggested that the turbimetry measurements are dependent on mass per unit length and when it reached about 100 collagen molecules assembled in this anisotropic nature it can be detectable. The measurements in the plateau region reflect the formation of units about 1.5×10^3 molecules in a fiber cross section¹²⁸.

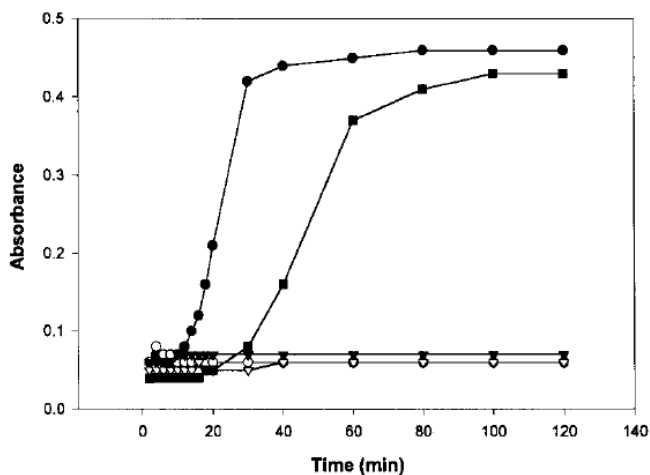


Figure 2. Hsp47 effect on collagen fibrillation monitored using turbimetry. Collagen association into fibrils monitored at 313 nm in the presence or the absence of Hsp47. Upper panel: acid-soluble type I collagen was diluted in 20 mM sodium phosphate buffer (pH 7.4)/50 mM NaCl to a final concentration of 200 $\mu\text{g}/\text{ml}$ (0.6 μM). Molar ratios of Hsp47 to collagen triple helix were as follows: closed circle (0:1); closed square (0.5: 1); closed inverted triangle (1:1); open circle (2:1); open inverted triangle (6: 1). Reproduced from^{53a}.

In the log phase the growth the fibers starts assembling to the nuclei in random directions to form disordered aggregates. This is spontaneous and temperature driven process. (Figure1). Addition of Hsp47 to a collagen solution has been shown to delay the kinetics of the fibrillation process ^{75, 81}. A two fold molar ratio of Hsp47 to collagen results in complete inhibition of collagen fibrillation (Figure 2).

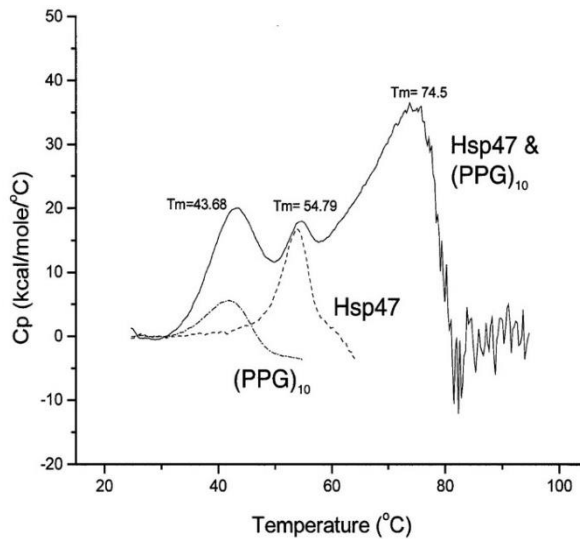


Figure3. The heat capacity of Hsp47s, (PPG)₁₀, and a mixture of both was measured by DSC. Reproduced from ⁸⁴.

Differential Scanning Calorimetry (DSC) has been used to measure the temperature dependence of partial heat capacity of collagen by determining enthalpy. The difference in electrical energy require to raise the temperature of the sample with respect to rise in temperature of the reference solvent is recorded to calculate difference in heat capacity¹¹⁹. Collagen triple helix unfolding and stabilization dynamics can be measured using DSC In this case, the T_m value (melting point of compound) of collagen propeptides dissolved in appropriate buffers is recorded with the change in temperature. One such example is shown in Figure 3. In this case, the T_m of collagen peptides (PPG₁₀) was recorded and on addition of Hsp47 the change is the T_m of the peptides

were observed. Binding of Hsp47 leads to a change in unfolding dynamics prolonging the melting temperature, indicating a stabilization of the collagen triple helices^{75, 84}.

Apart from environmental factors, the composition of collagen subtypes can also influence collagen gelation i.e. influence of one collagen type can affect the gelation kinetics of another. For example, the stiffness of heterotypic networks of collagen drastically changes with change in composition - as shown in Figure 4, when COLV was mixed with Col I and the gelation kinetics were studied, increasing concentration of COL V caused a decrease in the network stiffness²³⁷. Another report suggested that, COL V is also shown to be a dominant regulator of fibrillogenesis, *in vivo*, affirming this finding as long and stiffer fibers can be formed with COL I in association with COLV²⁵³. Therefore, rheology can also be used to study protein-protein interactions and their effect on stiffness of structural proteins like collagen.

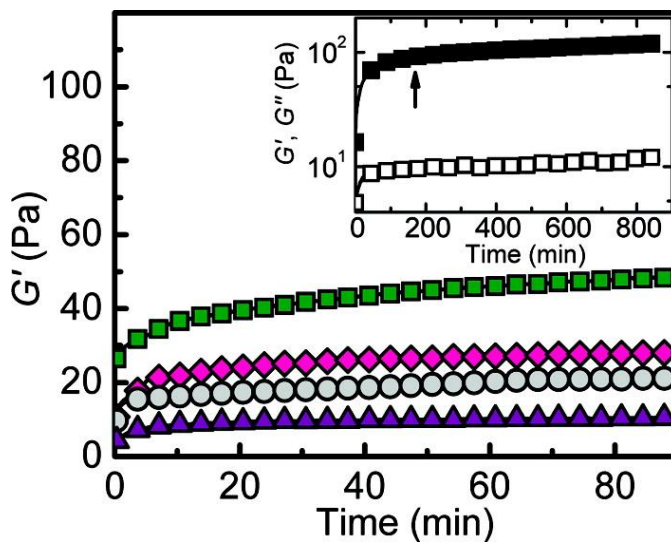


Figure4. The graph shows collagen polymerization behavior with varying proportions of COL I and V keeping total concentration of fixed total collagen concentration of 2 mg/mL measured by considering the time dependence of the elastic modulus of collagen solutions at 37 °C. Symbols denote weight/weight ratios of collagen I to collagen V: 100/0 (green squares), 90/10 (pink diamonds), 80/20 (white circles), and 0/100 (purple triangles). Inset: elastic (solid squares) and viscous (open squares) shear moduli for a 100/0 gel of 3 mg/ml. Reproduced from²³⁷ with permissions from ACS.

In this chapter, *in vitro* characterization of the interaction between the recombinantly produced Hsp47 variants and collagen is characterized. The interaction between Photoactivatable Hsp47 and Collagen before and activation with light is analyzed. For these studies different assays were used: (i) Light induced molecular adsorption of proteins technique (LIMAP) based colocalization assay and Native PAGE western blot. (ii) Study of fibrillation kinetics by turbimetry, (iii) study of collagen gelation by rheology. DSC was not used because of the limitations in yields of Photoactivatable Hsp47 and due to long duration of the assay.

3.2. Results and Discussion

3.2.1. Characterization of Photoactivatable Hsp47 interaction with collagen by binding assay

The binding of the different Hsp47 variants (H_{47N} , $H_{47Y<ONBY}$, $H_{47Y<R}$, H_{47Kdel}) to collagen was studied by Light induced adsorption of protein affinity assay. For this purpose Collagen I was micro patterned on a glass substrate by ²⁵⁴ photo cleaving PEG chains using a photo initiator to expose PLL for collagen binding (10 μ m PRIMO filter masks used). The Hsp47 variants were incubated with the Collagen I micro patterns. The interaction with collagen was visualized by fluorescence microscopy since all proteins were green fluorescence due to EGFP tagging. H_{47N} and H_{47Kdel} showed fluorescent bands indicating interaction with collagen, whereas $H_{47Y<ONBY}$, the negative control, $H_{47Y<R}$, and EGFP did not bind to collagen (Figure 4a). Light irradiation of the $H_{47Y<ONBY}$ solution during incubation (*in situ* activation upon 10 sec exposure at 365 nm) led to appearance of fluorescent bands. This result demonstrates that photochemical activation of $H_{47Y<ONBY}$ renders functional Hsp47 ($H_{47Y<ONBYhv}$), able to bind to collagen. Native PAGE-western blot analysis confirmed these results (Figure 4b). Co-localization of fluorescent antibody labeled bands of collagen and H_{47N} or light-activated $H_{47Y<ONBYhv}$ was observed. Conversely, $H_{47Y<ONBY}$, $H_{47Y<R}$ and EGFP did not co localize with the collagen band, demonstrating no collagen binding.

3.2.2 Characterization of Photoactivatable Hsp47: Collagen interaction by Fibrillation assay

Previous reports have demonstrated that addition of Hsp47 in 2-fold molar excess to a 0.6 μM collagen solution in PBS delays collagen fibrillation at 34°C^{75, 249}. Similar experiments were performed in the presence of Hsp47 variants synthesized in the previous chapter. Turbidity measurements reproduced these results (see Figure 6a).

When using minimum essential medium (MEM) for the experiments, improved gelation was observed, and confirmed by rheology measurements (see Figure 7). For this purpose, 2 mg/mL of rat tail collagen was dissolved in MEM and PBS buffers and the pH was adjusted to 7.4 with 1 M NaOH solution on ice bath. The network of collagen was polymerized in between the plates of a rheometer by increasing the temperature from 4°C to 37°C. The temperature dependence of the shear moduli during polymerization of collagen, polymerized in both buffers, is shown Figure 7. A lag phase was observed in both cases at till ~15°C. The shear moduli began to increase immediately after this temperature, indicating polymerization occurred in both cases. However, the shear modulus drastically increased in collagen prepared in MEM buffer

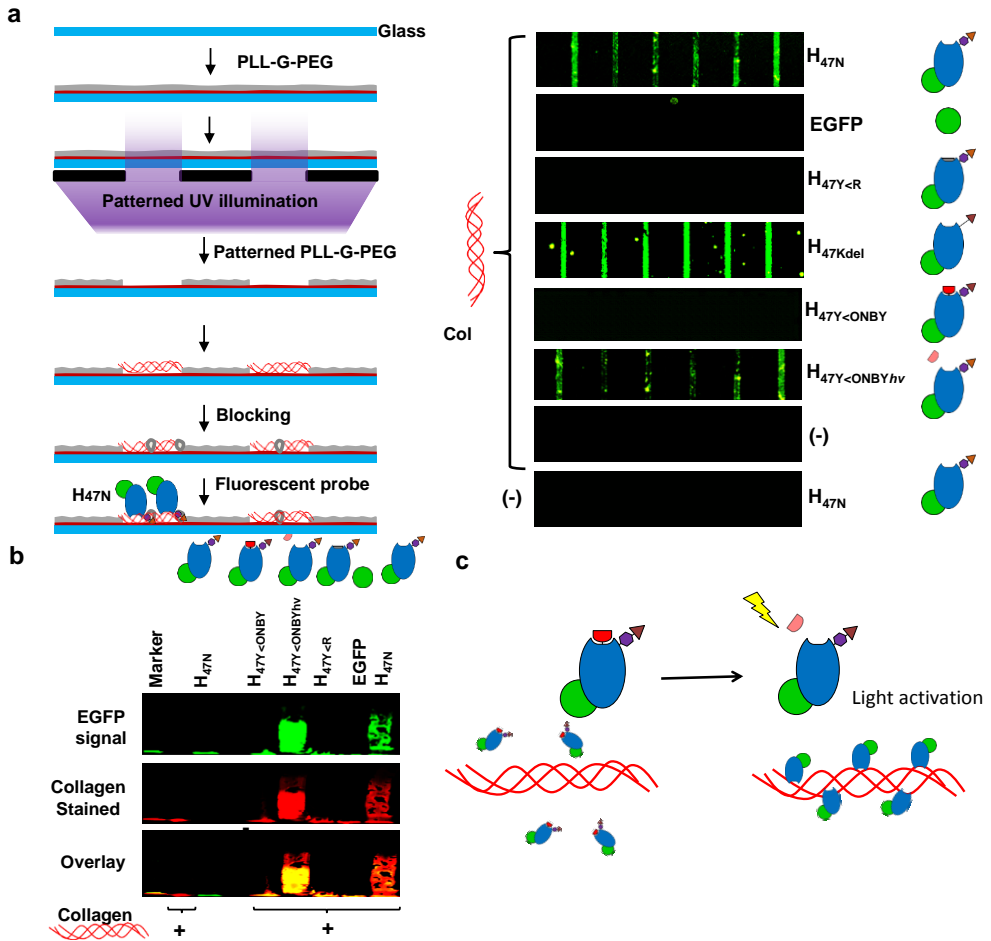


Figure 5. **a.** Schematic of binding assay of Hsp47 and its variants to collagen micro-patterns and fluorescence image of micro-patterning protein-protein affinity assay; **b.** Native PAGE Western Blot of rat tail Collagen Type 1 (200ug/mL, 0.6uM) mixed with H_{47N}, H_{47Y<R47Y<ONBYhv} or H_{47Kdel} (1.2uM), demonstrating co-localization of Hsp47 variants with collagen in binding assays.

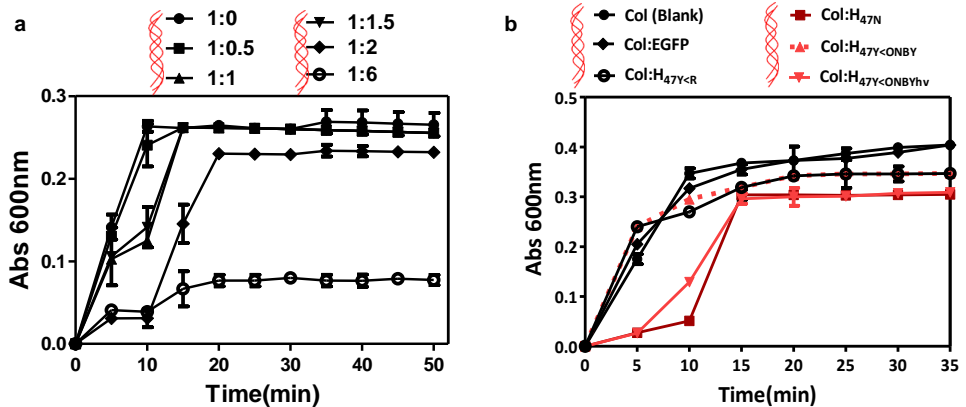


Figure 6. a. Turbidity measurements of Collagen/Hsp47 mixtures of different ratios. The increase in absorbance at 600nm reflects the formation of fibrils. Rat tail collagen (3mg/mL) was diluted to 0.4 mg/ml by addition of MEM Buffer (1x) and was adjusted to pH to 7.5 with sodium hydroxide within 4 min to prevent premature polymerization[27].The 0.4 mg/ml of collagen solution was mixed with H47N at molar ratios of 0.5:1 (H_{47N} (0.3uM): Collagen (0.6uM)), 1:1 (H_{47N} (0.6uM): Collagen (0.6uM)), 2:1 (H_{47N} (1.2uM): Collagen (0.6uM)) and 6:1(H_{47N} (3.6uM): Collagen (0.6uM)) to a final concentration of 0.2 μg/ml. A 0.2 μg/ml collagen solution was used as a positive control. 75μl of each sample were transferred to a plate reader and absorbance was measured at 600 nm for 50 min at 34 °C. The experiments were performed in triplicate. (n = 3 data point representing mean value of technical triplicates of each experiment). **b.** Fibrillogenesis assay by turbidimetry measurements of collagen (200ug/mL, 0.6uM) mixed with H_{47N}, H_{47Y<R}, H_{47Y<ONBYhv} or H_{47Kdel} (1.2μM) at molar ratio 2:1(Hsp47: Collagen) at OD600 values (n=3 data point representing mean value of technical triplicates of each experiment with error bars representing standard deviation).

3.2.2 Characterization of collagen gelation by Rheology assay

Rat tail collagen I with stock concentration of 3mg/ml was diluted in PBS and MEM buffer and the pH was adjusted to 7.5 using 1M NaOH solution on ice. The DHRIII Rheometer was used for studying gelation kinetics by cooling two 8mm diameter parallel plates at 4°C. 50 μl of the collagen solution mixed with either PBS or MEM were placed between two parallel plates. The shear moduli were at frequency ω - 30-0.03 rad/s while temperature was increased to 40°C at 0.1°C/min. The shear modulus of PBS-dissolved collagen was found to be low, indicating poor gelation. MEM is considered more representative of physiological conditions for collagen association and is reported to promote

the formation of fibrils with a native D-banding pattern compared to PBS, which was verified by AFM imaging in the previous report²³⁷. Therefore, MEM buffer was used for further fibrillation assays with Hsp47 variants at concentrations between 0.1 μ M and 1.2 μ M. H_{47Y<ONBY}, H_{47Y<R} and EGFP did not show any effect on fibrillation kinetics of collagen solutions at any tested concentration (Figure 5b). Light-activated H_{47Y<ONBY_{hv}} reduced the rate of collagen fibrillation to a similar extent to H_{47N} at comparable concentrations. These results indicate that H_{47Y<ONBY_{hv}} enables light-triggered interference with lateral association of collagen triple helices and delay of fibril formation.

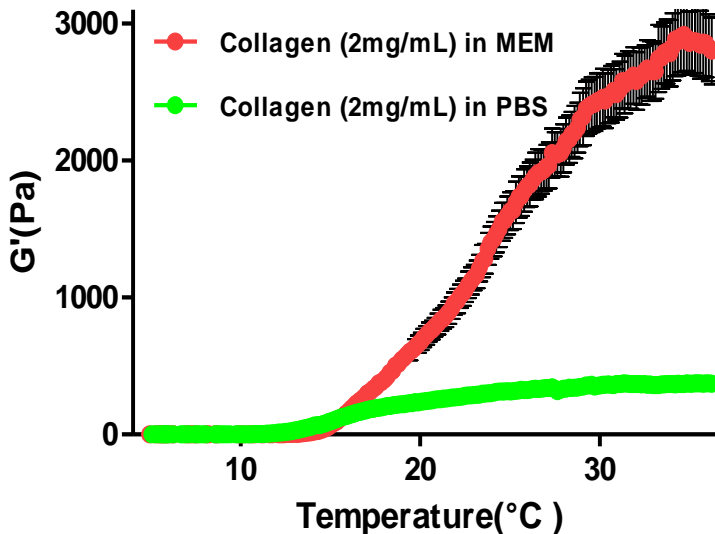


Figure 7. Rat tail collagen (3mg/mL) was diluted to 2 mg/mL concentration with MEM or PBS and was adjusted to pH to 7.5. A DHR III Rheometer (TA Instruments) was used for the measurements. 50 μ l of the collagen solution were placed between two parallel plates of 8 mm diameter cooled at 4°C. The shear moduli (G') were measured at frequency ω - 30-0.03 rad/s while temperature was increased to 40°C at 0.1°C/min.

Attempts were made to study the effect of photoactivatable Hsp47 on unfolding kinetics of collagen using Nano DSC. However, due to large amount of sample requirement and limitation in yields of photo activatable Hsp47, this analysis was not continued.

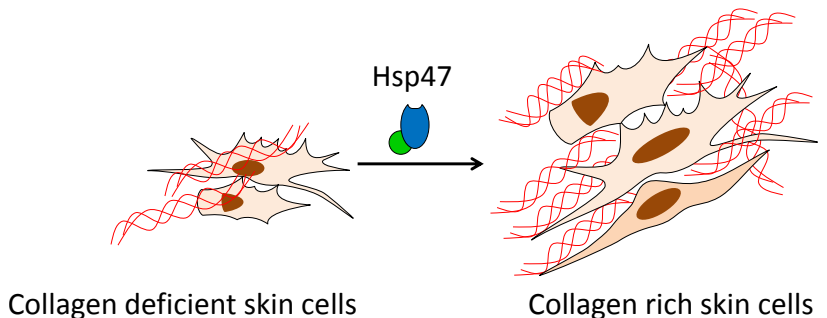
3.3. Conclusions

Photoactivatable Hsp47 (H_{47Y<ONBY}) was characterized *in vitro* by binding and functional assays. Upon light exposure, the H_{47Y<ONBY} turns into functional Hsp47 *in situ*. This was demonstrated by binding of H_{47Y<ONBY} to collagen patterns on light activation. Native PAGE Western blot affirmed this finding by showing colocalization. Fibrillation assay further elucidated the functional activity of H_{47Y<ONBY} by delaying collagen fibrillation kinetics on photo activation. Therefore, the activity of H_{47Y<ONBY} was confirmed.

Chapter 4

Hsp47-induced stimulation of fibrillar collagen deposition in in vitro cultures of skin cells¹

In this chapter, a recently known mechanism to deliver Hsp47 inside the Endoplasmic reticulum of cells within a few hours of incubation via retrograde KDEL receptor-mediated uptake was explored. On exogenous supply of Hsp47 increase in Collagen deposition is demonstrated in vitro. A comparison of different levels of collagen deposition on Hsp47-stimulation in cells from skin tissue was studied in vitro. COL I, III and V are enhanced on Hsp47 delivery in fibroblast, endothelial and epithelial cells. Network collagen IV and fibril-associated collagen XII were not affected by the increased Hsp47 intracellular levels.



¹Parts of this chapter were published in Advanced Science (2019), 6,1801982,Essak S. Khan, Shrikrishnan Sankaran, Julieta I. Paez ,Christina Muth ,Mitchell K. L. Han, Aránzazu del Campo , “Photoactivatable Hsp47: A Tool to Regulate Collagen Secretion and Assembly”

4.1. Introduction

The mechanical properties of skin tissue are determined by the morphology of collagen and elastin fibers in the different layers.^{4, 23, 255} Skin tissue feels soft, but it presents a high tensile strength of 1-20 MPa^{4, 256}. Collagen fibers, being 60-80% of skin dry weight, confer skin its resistance to mechanical stress. The skin consists of three cellular layers: (i) stratified keratinocyte-containing epidermis (outer layer), (ii) fibroblast-containing dermis (middle layer) and (iii) adipocyte-containing hypodermis (lower layer). The collagen composition at each layer is different²⁵⁷⁻²⁵⁸. The basement membrane separating the epidermis and dermis is rich in COL IV. COL I is predominant in the dermal and hypodermal layer, and forms heterotypic structures with other collagens such as COL III and/or V³⁵.

In multiple skin pathologies collagen organization is altered, either genetically or acquired due to environmental factors. Genetic collagen-related skin disorders such as Epidermolysis bullosa (EB)²⁵⁹ and Ehlers-Danlos Syndrome (EDS) are both caused due to mutations in COL I¹²⁹ and/or COL III¹⁸. The patients have fragile skin, blisters and chronic wounds as consequence of reduced collagen levels in the skin tissue due to collagen miss folding, impaired formation of highly organized structures, poor collagen crosslinking, and accelerated collagen degradation¹²⁸. Scurvy and Aging have localized wrinkles and blisters due to weakening of skin structural architecture between dermis and epidermis due to sparse collagen fiber density and extensive degradation of collagen by matrix metalloproteinase^{131, 260}. The existing therapies for these disorders are based on growth factors (e.g. TGF-beta²⁶¹⁻²⁶²) and chemical stimulants (e.g. ascorbic acid²⁶²⁻²⁶⁴, glycolic acid²⁶⁵ and retinol²⁶⁶) to boost the collagen production and matrix deposition. However, these molecules have multiple other roles in the body and the therapies are associated with negative side effects such as promoting abnormal angiogenesis, or inflammatory responses.

In this chapter, the possibility to enhance collagen deposition in cells by uptake of exogenous Hsp47 is tested²⁶⁷. The delivery of recombinant proteins from the medium into the ER of cells was considered a challenge for this objective. Initially, microinjection of the protein into the ER was planned²⁶⁸⁻²⁷⁰. However, during the course of this study a KDEL receptor-mediated endocytosis mechanism capable of transporting proteins containing an ER retention motif (KDEL) to the ER was observed. By including KDEL motif in the recombinantly synthesized H_{47<ONBY>}, the possibility to deliver it to the ER by simple incubation was attempted and successfully achieved.

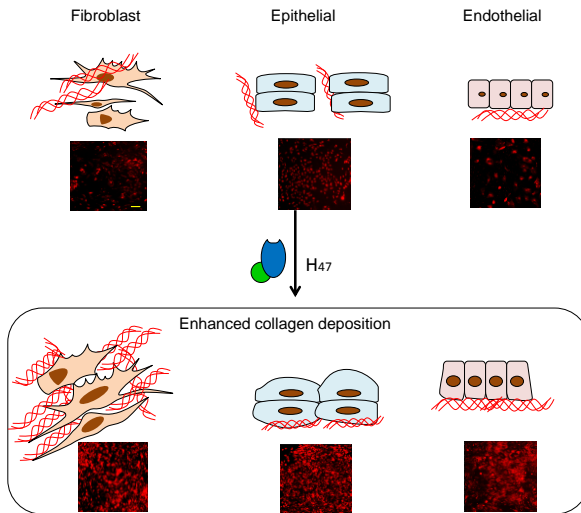


Figure1. Scheme showing enhanced collagen deposition by treatment with recombinant H₄₇. Immunostaining of COL I in fibroblast, epithelial and endothelial cell lines is shown in Red using COL I antibody. Scale: 250µm.

In this chapter the preferential secretion of certain collagen types is studied in different cell types, with a focus in skin cells. For this purpose, Hsp47 uptake and Hsp47-induced collagen deposition is quantified in *in vitro* cultures of skin fibroblasts, epithelial and endothelial cells (Figure 1). The expression and secretion of specific collagen subtypes (COL I, III, IV, V and XII) is analyzed and compared these results among the different cell types.

4.2. Results:

4.2.1. Hsp47 variants can be delivered into ER via KDEL receptor-mediated Endocytosis

Hsp47 is an ER resident protein with a C-terminal KDEL retention motif. This motif is recognized by KDEL receptor after Hsp47 release in the Golgi and is responsible for its retention in the ER²⁷¹. In fact, deletion of KDEL sequence has been shown to block the retention of Hsp47 into the ER.²⁷² The KDEL receptor is also present in the plasma membrane of cells, and has been shown to assist internalization of KDEL containing molecules from the extracellular space²⁷³⁻²⁷⁵. If Hsp47 variants could be delivered to ER using KDEL receptor mediated endocytosis was tested (Fig.1a).

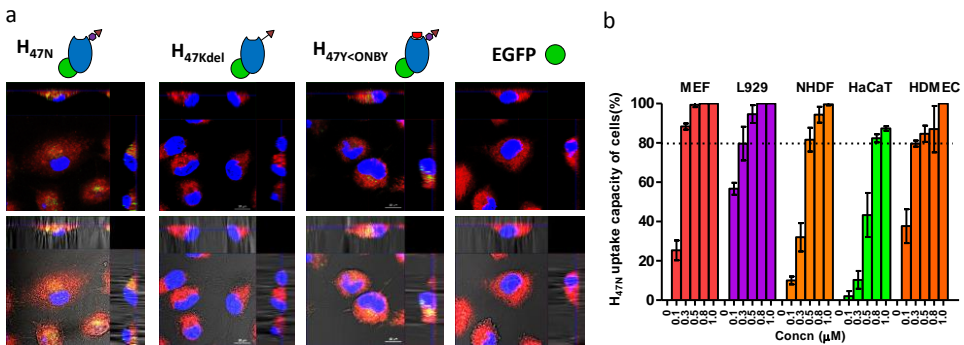


Figure 2. Delivery of Hsp47 variants to ER via KDEL receptor-mediated endocytosis is shown. **a.** Z stack images of L929 cells after incubation with Hsp47 variants showing colocalization of H_{47N} or H_{47Y<ONBY} signal and ER staining. No fluorescence was observed after incubation with EGFP or H_{47KDEL} constructs (blue: DAPI (Nucleus), Green: EGFP (Hsp47 variants), and Red: ER tracker dye); scale bar: 10 μm. **b.** H₄₇ uptake by NHDF, L929, MEF, HaCaT and HDMEC after 3 h incubation with increasing concentrations of H₄₇ in the medium (0.1 μM-1.0 μM). The graph was plotted by quantifying the percentage of cells showing H₄₇ (EGFP green signal) with ER tracker dye (Red signal). 100% H₄₇ uptake of cells indicate that all cells in culture had co-localized signal. Error bars indicate standard deviation of n=3 experiments.

For this purpose, the uptake of Hsp47 was tested in fibroblast (NHDF from human skin dermis, L929 from mouse adipose tissue and MEF from mouse

embryos), epithelial (HaCaT, human epidermal keratinocytes) and endothelial (HDMEC from human dermis) cells as a representative of each layers of skin. Initially, the uptake was characterized with different Hsp47 variants on L929 and MEFs fibroblasts were incubated with Hsp47 variants for 3 h and imaged. Cells incubated with H_{47N} (hereafter mentioned as H47 in this chapter), H_{47Y<R} and H_{47Y<ONBYhv} showed colocalization of the EGFP signal (green in Fig.1) with the ER tracker dye (red), indicating successful uptake of the Hsp47 variant by the cells (see 10X-magnified images in Fig 2). Neither uptake of the H_{47Kdel} variant with deleted KDEL, nor uptake of EGFP was observed after 3 h incubation. In order to optimize the Hsp47 concentration for efficient delivery to fibroblast cells, experiments with concentrations of H_{47N} in the incubation medium between 0.01µM and 1µM were performed. 0.2-0.3µM concentration proved to be the best condition for the delivery of the recombinant constructs (see Figure 3). Protein concentrations above 0.3µM resulted in the formation of protein aggregates on the cell culture substrate. These results demonstrate that the photoactivatable H_{47Y<ONBYhv} can be simply introduced into the ER of cells by short incubation, allowing easy experimental implementation of this tool for the study of Hsp47-specific roles in cellular pathways and collagen assembly.

Next, NHDF, HaCaT and HDMEC cells were incubated with H₄₇ at concentrations between 0.1µM and 1.0 µM after delivery optimization. The cell was cultured at same cell density and incubated with H₄₇ at concentrations between 0.1µM and 1.0 µM. Incubation with lower H₄₇ concentrations showed no detectable fluorescence signal inside the cells. On the other extreme, cells incubated with 1 µM H₄₇ showed fluorescent aggregates on the surface of the culture plate, indicating that saturating levels of H₄₇ might have been achieved and H₄₇ was binding to extracellular collagen deposited by the cells. At the intermediate concentrations accumulation of green fluorescence was detected inside the cells and no aggregates were observed outside of the cells, indicating efficient uptake of H47. The incubation time of 3 h was up taken from our previous experience (Figure S3).

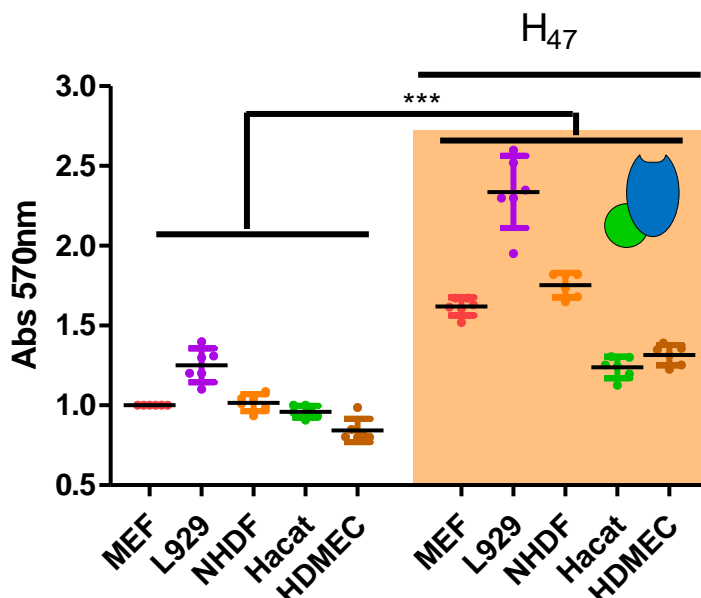


Figure 3. Quantification of collagen deposition using Sirius red assay in the different cell types with error bars represent standard deviation of n-6 independent experiments. The plots were normalized with MEF cells untreated condition as 1. Error bars represent standard deviation from n-3 experiments. Statistical significance for both b and c was analyzed by Tukey test comparing non-treated against H₄₇ treated cells (mean±SD, ANOVA, *** $p < 0.001$).

H₄₇ uptake was visualized by epifluorescence imaging of EGFP green signal inside the cells. Co-localization of H₄₇ and the ER signals confirmed accumulation of the up taken H₄₇ at the ER in a cell types (Figure 2b, S1). No signal was observed when cells were incubated with EGFP alone, indicating that uptake is specific to the H₄₇ sequence and not mediated by the EGFP label (Figure S1and 2).

Next, the uptake of H₄₇ was quantified by counting the percentage of cells with detectable ER- and H₄₇ fluorescent signals after 3 h using Image J software in all cell types. 100% up take indicates that all the cells with labeled ER contained labeled H₄₇. Results show that H₄₇ uptake was concentration dependent and cell type dependent (Figure 2b). An increase in the H₄₇ incubation concentration leads to increased uptake, and >80% uptake was observed for fibroblasts and

endothelial cells at 0.5 μM H₄₇. Saturation levels are achieved at 0.5 and 0.8 μM H₄₇ for MEF and L9329 cells, and at 1 μM H₄₇ for NHDF and HDMECs. HaCaT cells showed the lowest uptake, with maximum uptake values of ca. 80% achieved at >0.8 μM H₄₇ concentrations. This variation is attributed to differences in distribution and density of KDEL receptors on the cell membrane, as it has been reported earlier²⁷⁶.

4.2.2. Increase in collagen production in skin cells in response to Hsp47

Collagen biosynthesis is dependent on the expression level of functional Hsp47. Therefore, the possibility of H₄₇ induced collagen deposition in different cell types after incubation was investigated. For this purpose, cells were seeded for 24 h on tissue culture plastic wells and incubated with 0.5 μM of H₄₇ for 3h. The medium was exchanged and cells were cultured for further 24h. The deposited collagen on the culture plate was labeled with Picro Sirius Red and quantified by spectrophotometry. Sirius red is a strong anionic dye comprising six sulfonate groups that binds preferentially to the cationic groups of the collagen fibers²⁷⁷⁻²⁷⁸. Data were normalized by the value of collagen deposition by MEF cells without any treatment. The fibroblast cell lines MEF, L929 and NHDF showed a 70% -100% increase in collagen deposition when treated with H₄₇. Under the same incubation conditions, the epithelial (HaCaT) and endothelial (HDMEC) cell lines showed 20 and 50% increase in collagen deposition respectively (Figure 3). These results indicate that exogenously supplied H₄₇ induces collagen deposition more effectively in fibroblast cells. This is in agreement with the natural role of fibroblasts as major matrix-producing cells in connective tissue²⁷⁹⁻²⁸⁰.

4.2.3. Increase in varying amount of collagen subtypes in response to Hsp47

The composition of the collagen matrix is tissue-dependent and different cells are expected to produce different collagen types. We investigated to which extent the uptake of exogenous H₄₇ by a cell changed the natural pattern of deposited collagens. For this purpose, H₄₇-treated cultures were decellularized and the remaining matrix layer on the culture plate was stained using antibodies specific for COL I, III, V and XII.

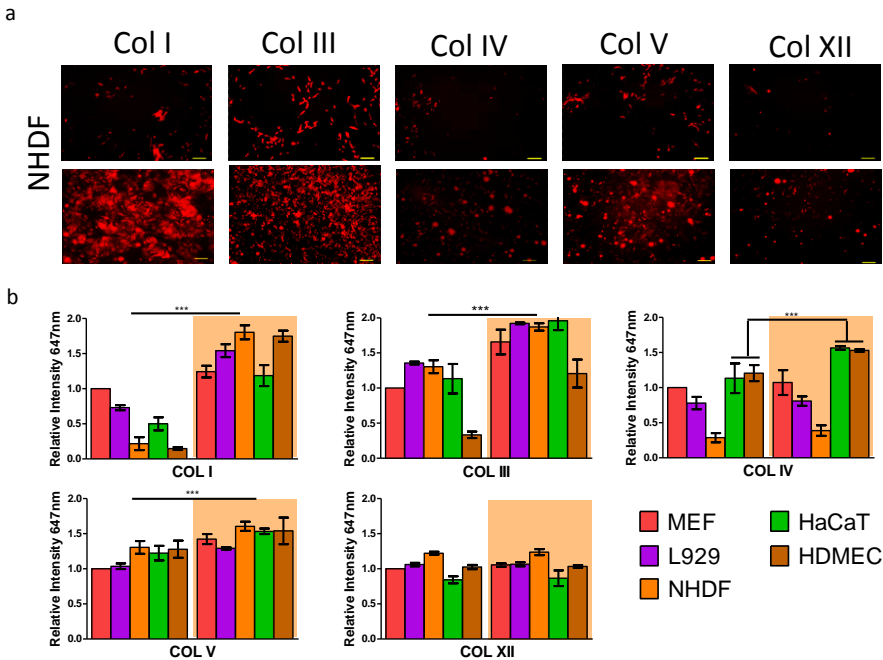


Figure 4. Quantification of H₄₇ stimulated deposition of different collagen subtypes. a. Fluorescence images showing immunostained COL I, III, IV, V and XII in NHDF cells before and after treatment with H₄₇ (Scale – 250µm) **b.** Quantification of deposited COL I, III, IV, V and XII from immunostained images in NHDF, L929, MEF, HaCaT and HDMEC cultures. Data correspond to collagen deposition 24 hours after H₄₇ treatment and controls. The plots were normalized with MEF cells untreated condition as 1. Error bars represent standard deviation from n-3 experiments. Statistical significance was analysed by Tukey test comparing non-treated against H₄₇ treated cells (mean±SD, ANOVA, *** $p < 0.001$).

These collagens were selected based on their abundance in skin tissue and their involvement in skin related disorders, in which they are reduced or mutated. The relative abundance of each collagen subtype was obtained from the fluorescence image of the culture plate. The mean fluorescence intensity value for each collagen subtype was corrected by subtraction of the background (see experimental details), and normalized by the corresponding value obtained in untreated MEF cells. An increase in the deposition of fibrillar COLs I, III and V was observed in all cell types upon H₄₇ treatment, although the

increase in COL I and III were significantly larger in fibroblast. The increase in the deposition of fibrillar collagens I, III and V was significantly higher in fibroblast cultures vs. HaCaT and HDMEC cultures. Conversely, deposition of network COL IV did not show significant changes upon H47 treatment in any cell type (Figure 4 and S2). No changes were observed in the deposition of COL XII either. These results suggest that Hsp47 may not be involved in the secretion of the network forming collagens, like COL IV or fibril-associated collagens, like COL XII. Increased cell spreading in cultures treated with Hsp47 was observed, which is not surprising as collagen is a matrix protein with multiple adhesion sites for the integrin family.

4.3. Discussion

Hsp47 is a collagen-specific chaperone protein with multiple roles in collagen biosynthesis. Expression levels of Hsp47 correlate with collagen production^{77, 97}. Hsp₄₇ has a regulatory role during scar formation in neonatal mouse skin after injury, which indicates that its expression during healing is up regulated *in situ*, in response to injury²⁸¹. These facts indicate that Hsp47 could be an interesting therapeutic target in collagen-related skin disorders, as alternative to non-specific collagen inducers such as TGF β ²⁸², VEGF²⁸³ or ascorbic acid²⁶²⁻²⁶³. Therapeutic use of these molecules to enhance collagen deposition influences other cellular functions such as proliferation^{262-263, 284-285}, differentiation²⁸⁴ and angiogenesis²⁸⁶, leading to undesired side effects. For example, ascorbate increases collagen production by acting as a co-factor to proline and lysine hydroxylases, which are involved in the hydroxylation of procollagen³⁴. However, these enzymes are also involved in the hydroxylation of other matrix proteins, like Elastin or Fibronectin²⁸⁷. In contrast, the unique collagen-specificity of Hsp47 would allow up regulation of collagen deposition, without affecting any other molecule or cellular pathway as known and established in the literature and our observation.

The deposition of fibrillar collagens I and II, and to a less extent fibrillar collagen V was mainly enhanced in all tested cell types. Deposition of network COL IV being the major collagen type in the basement membrane, and fibril-associated COL XII did not increase. The enhancement of fibrillar collagen

deposition vs. other collagen types highlights the supporting role of Hsp47 in the intracellular assembly, stabilization and transport of collagen superstructures. A fibrillar collagen specific stimulation of collagen production could be a positive aspect for a potential Hsp47-derived therapy to enhance natural collagen production in diseases.

It is interesting to compare the efficiency of Hsp47-based enhancement in collagen deposition vs. treatment with other collagen inducers from literature data. In the comparison both the amount of deposited collagen and the time scale at which noticeable deposition occurred is relevant. We anticipate that the comparison is done among different cell types and culture methods and, therefore, numbers can only be taken as indicative. In our data, the deposition of fibrillar COLs I and III in fibroblasts (MEF, L929 or NHDF) was enhanced up to 70% -100% in 24 h. In contrast, ascorbate treatment of primary healthy skin fibroblast increased collagen production by 20-40 % after 4 days of treatment *in vitro* (measured by radioactively labeling procollagen),²⁸⁸ and only 10 % in Hsp47 deficient fibroblast (measured by Sirius red assay)²⁶⁷. Glycolic acid treatment increased collagen production by 48% in a week in human skin fibroblast culture from neonatal foreskin and outgrown cells²⁸⁹ and Vitamin A (retinol) induced a 100% increase in chronological aging skin in human patients *in vivo* after 24 weeks²⁹⁰. This comparison reveals that Hsp47 promotes fast and efficient deposition of fibrillar collagen in comparison with the other molecules, which would be a beneficial feature for a therapeutic use of Hsp47.

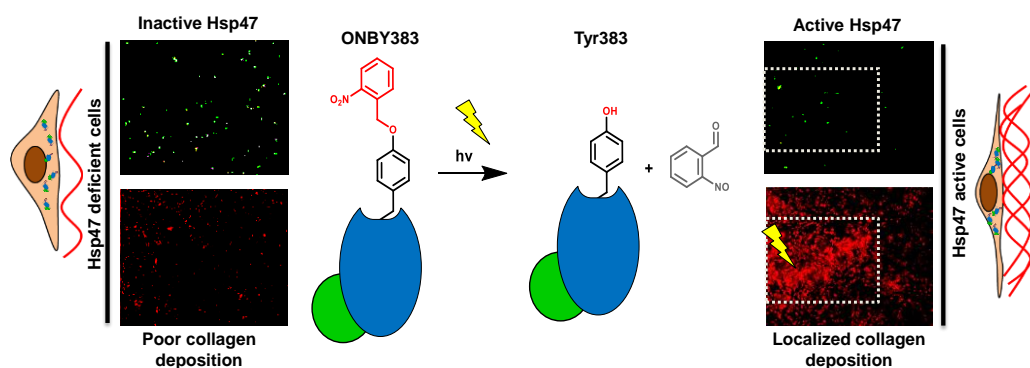
4.5. Conclusions

Recombinant Hsp47 variants were delivered in the ER recently known KDEL receptor mediated endocytosis approach. Skin fibroblast cells showed similar trend in uptake with varying concentration of Hsp47. Skin epithelial and endothelial cells showed a drastic increase in uptake only at 0.5 μ M concentration of Hsp47 in the medium. Exogenous delivery of Hsp47 increases fibrillar collagens I, III and V in all the cells. Modest increase in collagens IV and XII in epithelial and endothelial cells was observed.

Chapter 5

Light regulated collagen deposition in vitro¹

In this chapter, the possibility to activate $H_{47Y<ONBY}$ inside the cells in in vitro cultures will be tested. For this purpose, fibroblasts derived from Hsp47-deficient mouse embryos will be used. After incubation with $H_{47Y<ONBY}$ and controlled light exposure, the deposition of collagen will be imaged and quantified. Collagen deposition levels will be compared with normal fibroblasts and with fibroblasts stimulated with ascorbic acid as chemical inducer. The ability to promote collagen synthesis locally and on demand will be demonstrated.



¹Parts of this chapter were published in Advanced Science (2019), 6,1801982, Essak S. Khan, Shrikrishnan Sankaran, Julieta I. Paez, Christina Muth, Mitchell K. L. Han, Aránzazu del Campo, "Photoactivatable Hsp47: A Tool to Regulate Collagen Secretion and Assembly"

5.1. Introduction

Collagen deposition is a key step during morphogenesis of branched tissues like mammary glands, salivary glands or alveolar ducts, which are formed due to variations in spatial distribution of collagen. For example, collagen deposition is critically involved in alveolar formation and maturation²⁹¹ (Figure1 A, B). In the mammary gland, the axial orientation of the stromal collagen I fibers in the mammary fat pad are essential for branching morphogenesis (Figure1C, D)^{6, 24, 292}.

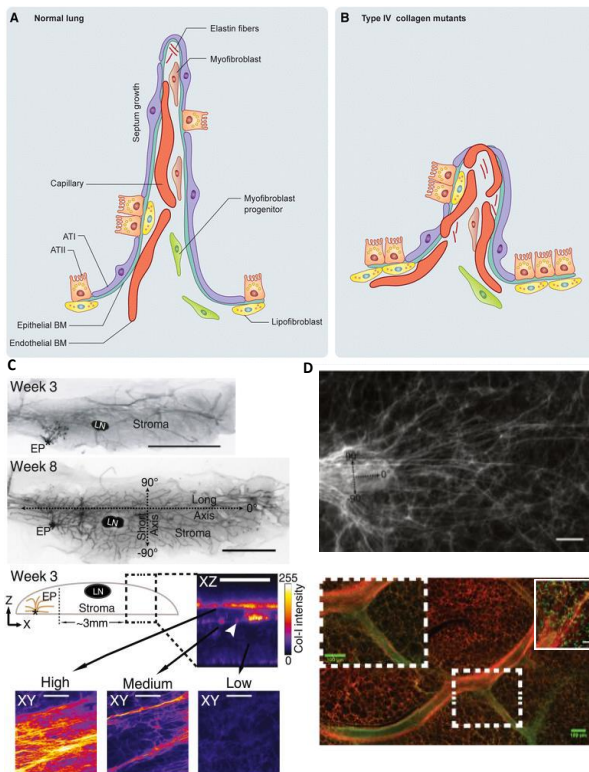


Figure1. Schematic showing alveologensis. **A.** Normal alveolar septum in which alveolar myofibroblast progenitors localized at the base of the septum proliferates, differentiate into alveolar myofibroblast, and migrate where they synthesize elastin. **B.** Type IV collagen mutations cause abnormal septum formation causing and abnormal capillary formation. Myofibroblasts fail to proliferate, differentiate and migrate, causing defects in elastin

deposition. **Axial Collagen I orientation in the branching of mammary glands.** C. Mouse mammary gland at postnatal week 3 and 8. Morphological features showing orientation of (EP), ni(*) and (LN). For orientation analysis, the long axis of registered glands was specified as 0° . **D.** Representative COL-I staining around an epithelial end bud. To compare COL-I orientation relative to branch, long axis is specified (dashed arrows). Reproduced with permissions from ²⁹¹⁻²⁹² from Elsevier.

Spinal cord regeneration after injury is directed by predeposited collagen. During injury, the Wnt pathway of fibroblasts, which controls COL XII transcription, becomes activated. These cells migrate to the site of injury and deposit collagen. The COL XII scaffold guides axon growth to bridge the injury site and is a required step for spinal cord regeneration. This has been demonstrated in a zebra fish model by silencing Wnt pathway or COL XII. In both cases, no functional recovery was observed ²⁹³ (Figure2).

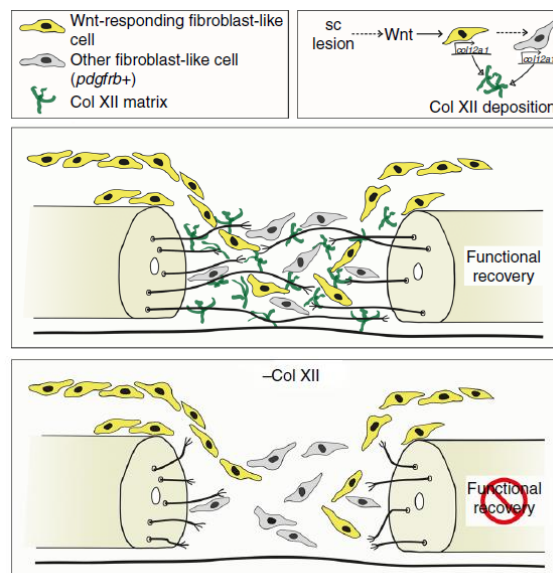


Figure2. Scheme shows deletion of COL XII under the transcriptional control of Wnt pathway of fibroblast-like cells. This leads to poor deposition of COL XII preventing axon regeneration and lack of functional recovery. Reproduced from ²⁹³.

During arterial injury the deposition of collagen promotes arterial tissue remodeling. In disease conditions like atherosclerosis; impaired arterial remodeling causes change in vessel circumference, varying arterial enlargement and leading to collapse of arterial wall promoting atherosclerosis²⁹⁴⁻²⁹⁵. In this case, the increase in collagen deposition has been associated with the increase in Hsp47 levels. After the injury, increase in Hsp47-bound collagen was found at ER/cis-Golgi interface, followed by the formation of extracellular collagen fibers (Figure3)²⁹⁶.

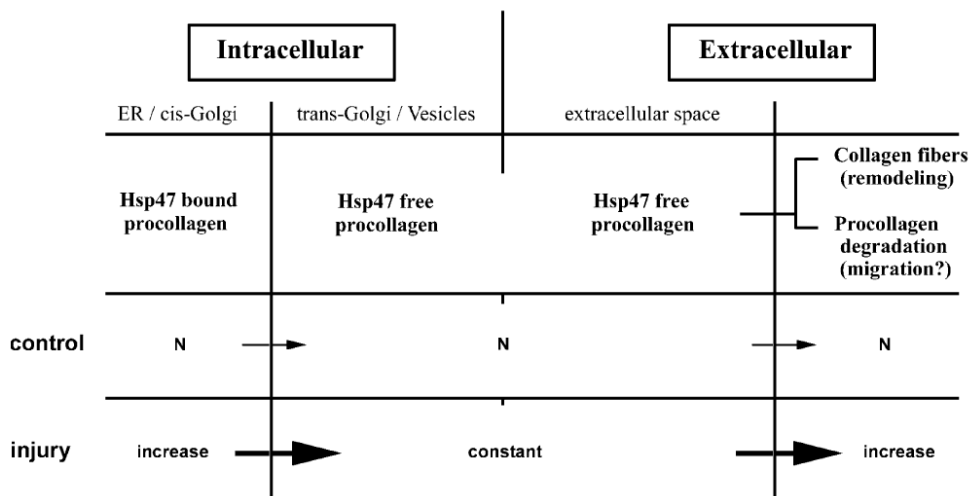


Figure3. Scheme shows Hsp47 and collagen turnover in the arterial injury. In the normal control condition, there is a constant level (small arrow) of procollagen with normal (N) levels intra- and extracellular. After arterial injury, there is an increase in collagen synthesis; also there is increase in Hsp47 bound procollagen. This results in an increase in extracellular collagen fiber content and/or procollagen degradation. However, the free collagen levels remain constant, suggesting a higher throughput of free procollagen (large arrows) after arterial injury. Reproduced from²⁹⁶ with permissions.

In chondrogenesis, mutation in Hsp47 is associated to severe chondrodysplasia and bone deformities with lower levels of COL II and XI²⁹⁷ and misalignment of COL I. In addition, accumulation of misaligned COL I in the intervertebral discs and a decrease in COL II fibers were observed. Under these conditions poor calcification was observed and the formation of endochondral bones which are

severely twisted and shortened was documented²⁹⁸. Hsp47 is therefore imperative for obtaining well-organized cartilage and normal endochondral bone formation as shown in Figure 2^{33, 152}. Collagen deficiency due to Hsp47 mutation or down regulation occurs in several forms of diseases like Osteogenesis imperfecta, Ehlers-Danlos Syndrome, Chondrodysplasias and Alport syndrome. These diseases are studied using Hsp47 deficient mouse models.

An *in vitro* model to study the functional role of Hsp47 was established by Nagata and coworkers⁸³. Deletion of the *Hsp47* gene in mouse lead to lethal mouse embryos with severely affected growth and maturation of skeleton. Poor deposition of COL IV was also observed.

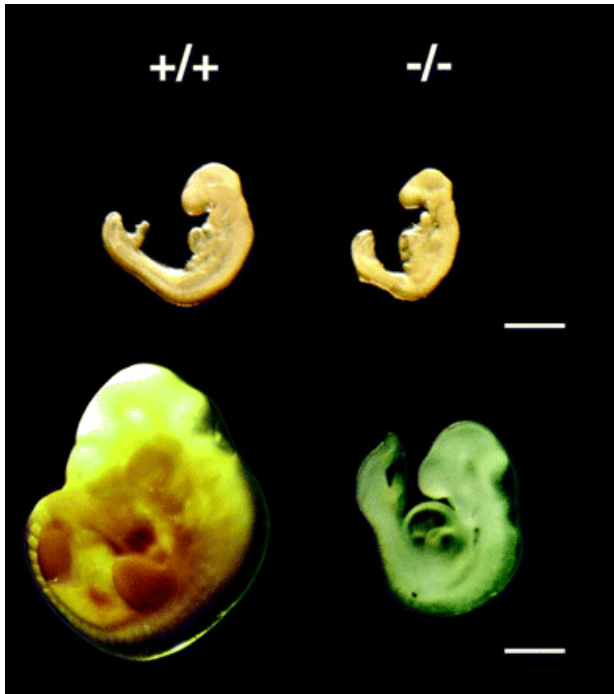


Figure4. Lateral views of 9.5 dpc (e) and 10.5 dpc (f) *Hsp47*^{-/-} homozygous embryos (right) and wild type (+/+) embryos (left). Embryos were observed before (f) and after (e) fixation with 10% formaldehyde. Bars, 1 mm. Reproduced from⁸³.

The embryos died at day 11.5 and showed malformed epithelial tissues and ruptured blood vessels (Figure 3)⁸³. Embryonic fibroblasts from this knockout

model are widely used as cell line for the study of collagen anomalies related to Hsp47^{5, 44, 49, 83, 101-102, 147, 151-152, 272, 299-300}.

In this chapter, Collagen deficient mouse embryonic fibroblasts (MEFs) derived from the Hsp47 knock-out embryo (Hsp47^{-/-}) will be used to study the effect of light-regulated delivery of Photoactivatable Hsp47. Collagen deposition in cell cultures after light exposure will be imaged and quantified. Single cell analysis of collagen distribution in secretory compartments inside the cells on Photoactivatable Hsp47 activation will be analyzed. Spatial definition of collagen deposition in vitro using localized exposure will also be demonstrated.

5.2. Results and Discussion

5.2.1. Increase in COL I, III and V deposition on Hsp47 delivery in Hsp47^{-/-} cells.

To test if Hsp47 increases collagen subtypes production is solely due to Hsp47 delivered exogenous Hsp47^{-/-} cells were chosen. Hsp47^{-/-} cells were delivered with H_{47N} in DMEM medium containing antibiotics for 3 h. After 3 h medium was exchanged and cells were incubated for 24 h for collagen deposition. Both non treated and H₄₇-treated cultures were decellularized and the remaining matrix layer on the culture plate was stained using antibodies specific for COL I, III, V and XII. Collagen subtypes were stained with COL I, III, IV, V and XII specific antibody and epifluorescence imaging was performed using Nikon TA microscope. The relative abundance of each collagen subtype was obtained from the fluorescence image of the culture plate. The mean fluorescence intensity value for each collagen subtype was corrected by subtraction of the background, and normalized by the corresponding value obtained in untreated Hsp47^{-/-} cells (see experimental section).

Deposition of fibrillar COLs I, III and V increased upon H₄₇ treatment. No increase in COL IV and XII was observed, in agreement with previous observations in the other cell lines (Figure 5 a, c, S4). In order to quantify deposited collagen subtypes at higher sensitivity, western blot analysis of the deposited matrix was performed. Hsp47^{+/+} cells were used as control. Higher deposition of COL I, III and V was confirmed, and a very low amount of COL IV

was also detected. Interestingly, similar analysis performed with healthy MEF cells (Hsp47+/+) revealed that these cells produced these collagen types to similar extent as observed in Hsp47-/- cells after H47-induction (Figure 5b). These results demonstrate that treatment of H47 deficient cells with exogenous H₄₇ allows cells to deposit collagen in composition and at levels similar to healthy cells. Taking into account the physiological relevance of matrix composition and properties in cellular behavior *in vivo* we speculate Hsp47 would be ideal tool to trigger fibrillar collagen synthesis on-demand.

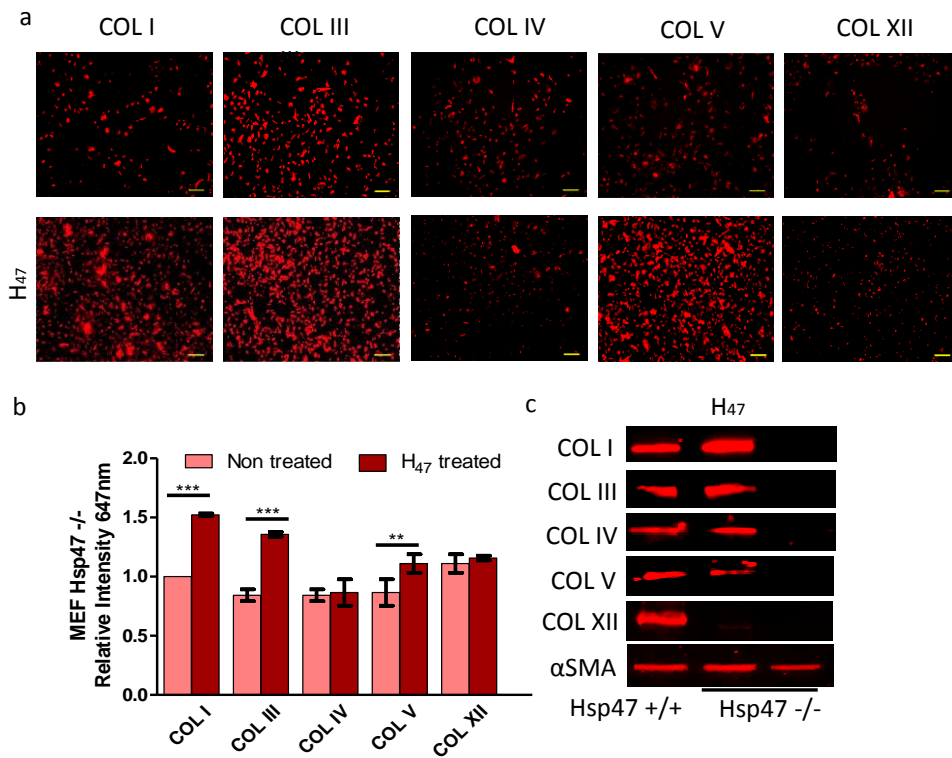


Figure 5. Stimulated deposition of COL I, III and V in Hsp47^{-/-} cells after H₄₇ uptake. **a.** Fluorescence images of immunostained COL I, III, IV, V and XII in MEF Hsp47^{-/-} cells 24 after H₄₇ treatment and controls (Scale – 250μm). **b.** Western blot of COL I, III, IV, V and XII in deposited collagen from MEF Hsp47^{+/+}, Hsp47^{-/-} and Hsp47^{-/-} cultures 24 hours after treatment with 0.5 μM H₄₇. Red bands indicate signal from collagen subtypes specific antibody. **c.** Quantification of deposited COL I, III, IV, V and XII from immuno

staining assays in MEF Hsp47^{-/-} cultures. Error bars representing standard deviation from n-3 experiments in **a** and **c**. The plots in both **a** and **c** assays were normalized by MEF Hsp47^{-/-} cells untreated condition taken as 1. Statistical significance in **a** and **c** was analyzed by Tukey test. Significance was calculated by comparing non treated against Hsp47 treated cells (mean±SD, ANOVA).

5.2.2. Increase in collagen production in Hsp47^{-/-} cell cultures in response to photo activation of H_{47Y<ONBY}

The secretion of collagen by Hsp47^{-/-} cells after incubation with H₄₇ and H_{47Y<ONBY} followed by light exposure was studied. The deposition of collagen was quantified after 24 h using the Sirius Red assay. This dye binds specifically to [Gly-X-Y]_n helices of fibrillar collagen types I to V¹⁰². Hsp47^{-/-} cells incubated with H_{47N} showed a significant increase in collagen production (15-20%) after 24 h (Figure 6). Hsp47^{-/-} cells incubated with H_{47Y<ONBY} did not show increase in collagen production, in agreement with the lack of bio functionality of H_{47Y<ONBY} observed in previous experiments. Exposure (30 sec) of H_{47Y<ONBY} treated cells with 405nm light *in situ* led to higher deposited collagen. Within the concentration range used (estimated as approximately 0.012nM H_{47Y<ONBY} per cell) no cytotoxicity effect due to the nitroso byproduct was observed (Figure 9). Note that the ONB photo removable group has been used in *in vitro* and *in vivo*^{196, 230, 301} applications and no significant cytotoxicity has been associated with the released photoproduct. These results demonstrate bio functionality of H_{47Y<ONBY} intracellularly in response to light activation (Figure.6.b). Ascorbate (Vitamin C) is a widely used chemical inducer for collagen production. Ascorbate affects COL I biosynthesis at translational level by triple helix stabilization^{100, 299, 302}. The collagen deposition levels in Hsp47^{-/-} cells treated with ascorbate were compared with the results obtained from treatment with H_{47N} and H_{47Y<ONBY}. Interestingly, higher levels of collagen production in cells treated with H_{47N} and light exposed H_{47Y<ONBY} were found compared to ascorbate treated cells (Figure.6. b). Addition of ascorbate to cells containing H_{47N} or light exposed H_{47Y<ONBYhv} had a synergistic effect for collagen production (see Figure 6.c, 7).

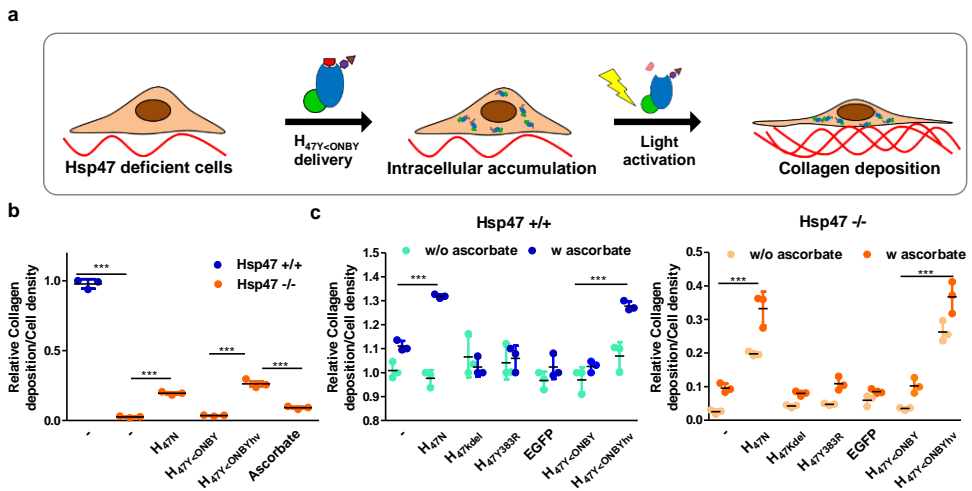


Figure 6. Stimulated collagen deposition using Photoactivatable Hsp47.

a. Scheme showing photo activation of H_{47Y<ONBY} and stimulated collagen deposition in Hsp47 deficient cells. b. Relative collagen deposition in Hsp47 +/+ and Hsp47 -/- cultures treated with Hsp47 variants and ascorbate. c. Relative collagen deposition in Hsp47 +/+ and Hsp47 -/- cultures treated with Hsp47 variants with or without ascorbate. Collagen deposition was calculated using quantified data of Sirius Red Assay at 570 nm (n=3 data point representing mean value of technical triplicates of each experiment with whisker plots representing standard deviation). Statistical significance was analyzed by Tukey test, which shows significant differences between conditions. Significance was calculated by comparing Hsp47 +/+ to Hsp47 -/- and on photo activation of H_{47Y<ONBY} delivered in Hsp47 -/- (mean±SD, ANOVA, *** p<0.001).

When Hsp47 +/+ cells were treated with H_{47N} or with *in situ* activated H_{47Y<ONBY}hv only a slight increase in collagen production was observed (see Figure 6.c, 8). The presence of H_{47N} caused a change in cell morphology of Hsp47-/- cells: spreading was enhanced, possibly due to the interaction with the deposited collagen (Figure S1).

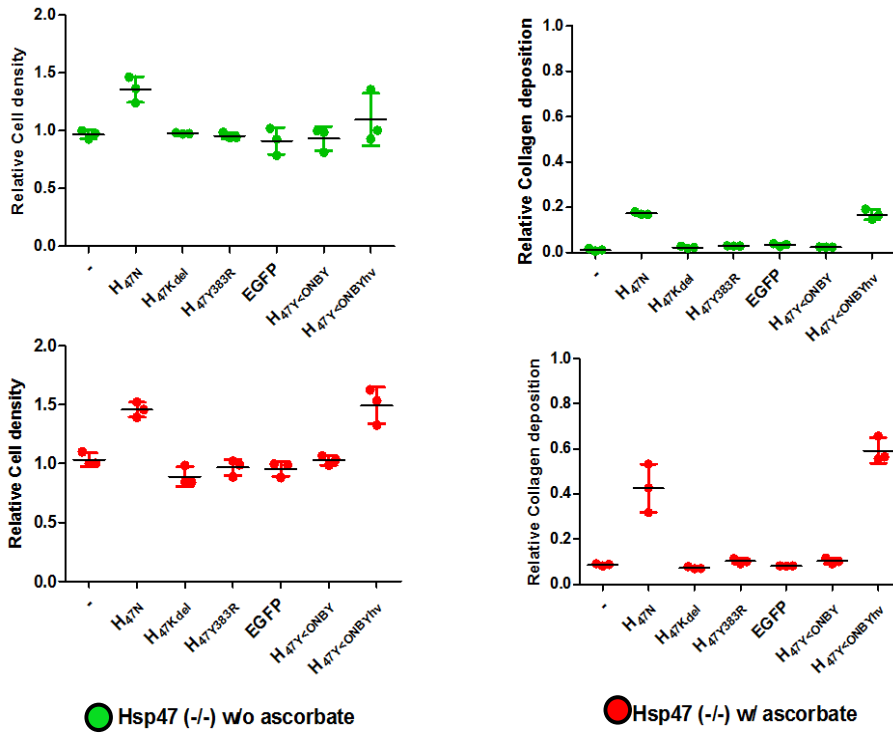


Figure 7. Relative quantification of collagen deposition and Relative Cell Density of MEF Hsp47 $-/-$ in absence (a) and presence of ascorbate (b) with Hsp47 variants. Photo activation of H₄₇Y<ONBY was done *in situ* by irradiating UV light for 30 sec using Nikon Ti-Eclipse microscope at 405 nm wavelength (n=3 data point representing mean value of technical triplicates of each experiment with whisker plots representing standard deviation standard deviation).

Interestingly, proliferation levels in Hsp47 $-/-$ cultures treated with H₄₇N or *in situ* activated H₄₇Y<ONBY were higher than in non-treated cultures (see Figure 6). Together, these results demonstrate the efficiency of exogenous H₄₇<ONBY to up regulate collagen biosynthesis upon light exposure in Hsp47 $-/-$ cells, and to enhance cell spreading in Hsp47 $+/+$ cells (Figure s1).

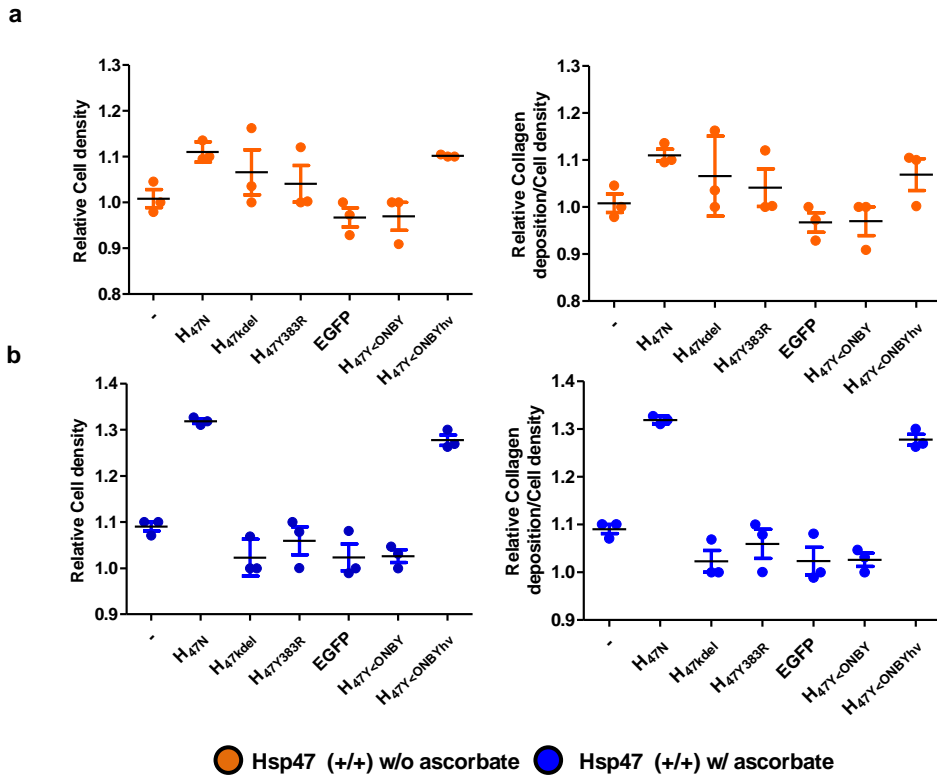


Figure8. Relative quantification of collagen deposition, Relative Cell Density of Hsp47 +/+ in absence (a) and presence of ascorbate(b) with different Hsp47 mutants. Collagen deposition was quantified using Sirius Red Assay. Cell density was counted using DAPI staining of the nucleus and Image J software. Photo activation of H_{47Y<ONBY} was done *in situ* by 30 sec exposure at 405 nm using Nikon Ti-Eclipse microscope at 50% illumination intensity (n=3 data point representing mean value of technical triplicates of each experiment with whisker plots representing standard deviation standard deviation).

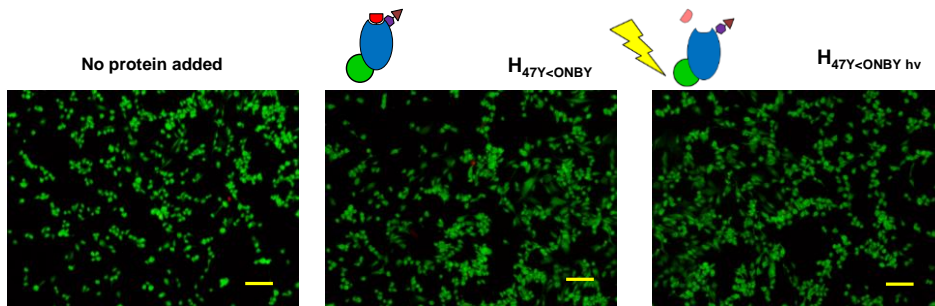


Figure 9. Fluorescence images showing Live-Dead staining of MEF Hsp47 ^{-/-} cells after 24 h of *in situ* photo activation of H_{47Y<ONBY} at 405 wavelength for 30 sec irradiation (Green : Live cells and Red: Dead cells). Scale: 200 μm.

5.2.3. Controlled light exposure allows spatial regulation of collagen production

The potential of H_{47Y<ONBY} for spatially control collagen production through photo activation in cell cultures was tested. For this purpose an assay for imaging collagen deposition on the culture substrates was established. Hsp47 ^{-/-} cells were incubated with the different Hsp47 variants for 3 h. Then the medium was exchanged and cells were cultured for further 24 h, fixed and stained with COL I. For demonstrating the bioactivity of H_{47Y<ONBY} we only considered COL I deposition. Antibody for imaging deposited collagen type I on the culture substrates. H_{47N} and light-exposed H_{47Y<ONBY} showed EGFP fluorescence located in the ER, indicating that the recombinant protein delivered was still present intracellularly after 24 h (Figure 10). This is in agreement with the reported >24 h half-life of Hsp47³⁰⁰. H_{47Y<R} did not show EGFP fluorescence after 24 h, which may be due to degradation because of lack of functional activity over time (Figure.10. b). No fluorescence was observed in substrates with Hsp47 ^{-/-} cells incubated with H_{47Y<R}, H_{47Kdel} or EGFP after collagen staining, whereas fluorescence corresponding to deposited collagen was observed on substrates with cells incubated with H_{47N} (Figure 10.b). These results demonstrate that H_{47Y<ONBY} can be used in cell cultures to increase collagen production at a selected time point.

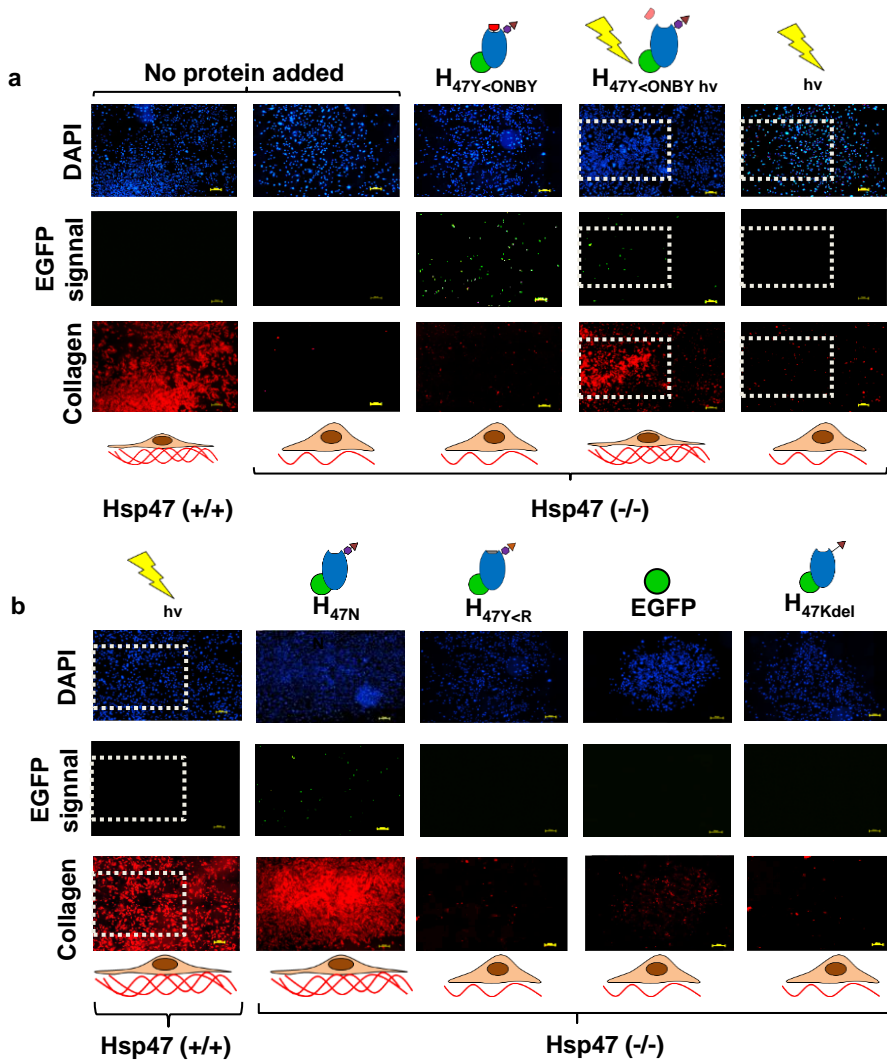


Figure 10. Localized induction of collagen deposition by photo activation of Photoactivatable Hsp47. Immunostaining of MEF Hsp47 $+/+$ and $-/-$ cultures 24 h after treatment with different Hsp47 variants and controls COL 1 Antibody staining in red, Hsp47 variants in green (EGFP), and nuclei in blue (DAPI). a. Hsp47 $+/+$ and $-/-$ having no protein delivery were used as controls. The light exposed areas ($1.8 \times 1.2 \text{ mm}^2$) are highlighted with dotted square. Irradiation wavelength was 405 nm. b. Hsp47 $+/+$ cells

incubated with other inactive mutants did not show enhanced collagen production, whereas cells incubated with H_{47N} showed higher collagen levels. Scale bar: 250um.

In order to test if light-induced collagen deposition can occur in a spatially defined manner, 1.8x1.2mm² areas of the Hsp47^{-/-} cell culture previously incubated with H_{47Y<ONBY} were irradiated for 30 seconds at 405 nm. Higher doses results in cell damage³⁰³. Cells at the exposed areas showed significantly higher collagen deposition (Figure 11.a). Hsp47^{-/-} and Hsp47^{+/+} cells lacking exogenous H_{47Y<ONBY} did not show any increase in collagen staining upon light exposure, indicating that UV irradiation by itself had no effect on collagen production (Figure.11)

In order to evaluate the spatial accuracy of the photo-induced collagen deposition in Hsp47^{-/-} cells treated with H_{47Y<ONBY}, three independent 1.13 mm² areas of the culture were irradiated at 405 nm. Increased collagen deposition within the exposed areas after staining with COL I antibody (Figure 10) with very less deviation in collagen deposition was observed. In addition, cells within the scanned area showed a wider cells having elongated morphology which may be the reason we observe less Nucleus signal. These results demonstrate the possibility to use H_{47Y<ONBY} to photo regulate collagen biosynthesis in cell cultures and build spatially defined collagen networks.

5.2.4. Interactome of procollagen and secretory organelles upon photo activation of H_{47Y<ONBY}

To study the distribution of procollagen within cell compartments upon activation of H_{47Y<ONBY} in individual cells, high resolution imaging of immunostained samples was performed. The rER (rough Endoplasmic reticulum) and the Golgi belong to cell's secretory apparatus involved in the intracellular processing of Procollagen. It has also been suggested that collagen is exchanged between rER and Golgi and it releases from smooth ER (sER)³⁰⁴. Cells were fixed and stained at different time points after light activation. Staining included ER, Golgi apparatus and Col 1 using specific florescent antibodies. Hsp47^{+/+} cells and Hsp47^{-/-} cells without any protein treatment were used as controls.

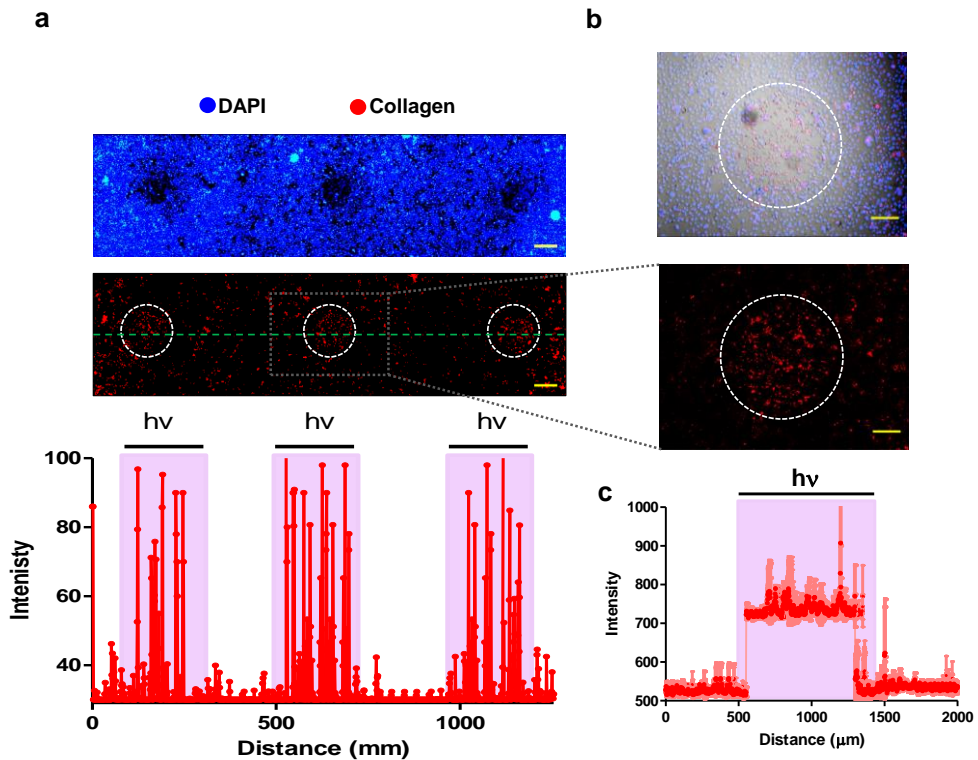


Figure 11. Immunostaining of patterns of collagen deposition in MEF Hsp47 $-/-$ cultures treated with H_{47Y<ONBY} after patterned exposure. The cell culture was incubated with H_{47Y<ONBY} for 3 hours and then medium was changed. Three spots of area 1.32 mm² separated by 4 mm distance were scanned with at 405 nm laser. In order to reveal the illuminated area, a green highlighter ink was used to mark the underside of the 24-well plate. The ink was photo bleached after 3 min UV exposure (Figure S2) and the bleached areas were used as reference for the scanning areas. (a) Fluorescence images of photo patterned areas after staining with DAPI and collagen type I antibody. The photo-patterned areas are highlighted with dotted circles. The scale bar corresponds to 500μm. The graph represents the intensity of the collagen deposited across the horizontal green line. (b) Fluorescence image of collagen deposited by cells in the exposed area and bright field overlay image showing change in cell morphology. Scale bar corresponds to 250μm. (c) Mean intensity and standard deviation of collagen deposition from 3 independent experiments, each having 3 individual light-exposed spots of 1.13 mm² area

Imaging after 2, 4 or 8 h did not show procollagen-specific fluorescence signals.³⁰⁴ This agrees with reported data stating that secretion of fully assembled collagen fibers requires 24 hours^{43, 302, 305}. After 24 h, procollagen signals appeared and co-localized with the ER and Golgi. In order to derive a quantitative measure of co-localization, Pearson's coefficients analysis (r) was calculated based on the plot profiles of average intensity from Nucleus to cell periphery as shown in Figure 11 as blue and red dashed box (where +1 value reflects perfect correlation and any value above 0.8 reflects positive correlation).

Considering the Nucleus as a centroid, a '0-50%' section of intensity profile was calculated from edge of Nucleus up to half the distance till the periphery (brown dashed boxes) and the remaining distance till the periphery was considered as a "50-100%" section (orange dashed boxes). In Hsp47 +/+ cells, 0.95 and 0.90 r-values in the 0-50% section was observed with ER-COL I and Golgi-COL I signals respectively. This suggests that procollagen is distributed within the secretory apparatus surrounding the nucleus. However, in the 50-100% section, COL I was found to co-localize with ER (r=0.93) but not with Golgi (r=0.001). This supports the second pathway of collagen secretion which is quite debatable. In Hsp47 -/- cells, even though a similar co-localization trend was observed in the 0-50% section (ER-COL I r=0.002 and Golgi-COL I r=0.004) (Figure 13), no correlation was observed in the 50-100% section in both ER-COL I (r-value) and Golgi-COL I (r-value) signals. This reveals that procollagen is accumulated around the nucleus in secretory apparatus but does not get transported towards the periphery of the cells for secretion as has been reported previously^{34, 44, 47, 77, 106, 304}.

Hsp47 -/- cells treated with H_{47Y<ONBY}, a similar trend of procollagen distribution as compared to untreated Hsp47 -/- i.e. (0-50 % section -ER-COL I r=0.8976 and Golgi-COL I r= 0.9014 and 50-100% section - r values) was observed. This suggests functionally arrested Hsp47 doesn't allow it to interact with procollagen. Moreover, EGFP signal from H_{47Y<ONBY} was found to have a positive correlation in the 0-50 % section (ER- H_{47Y<ONBY} r=0.8976 and Golgi- H_{47Y<ONBY} r-

0.9014) and poor correlation in the 50-100 % section (r values). This suggests that H_{47Y<ONBY} remains in the ER even though it does not bind to procollagen.

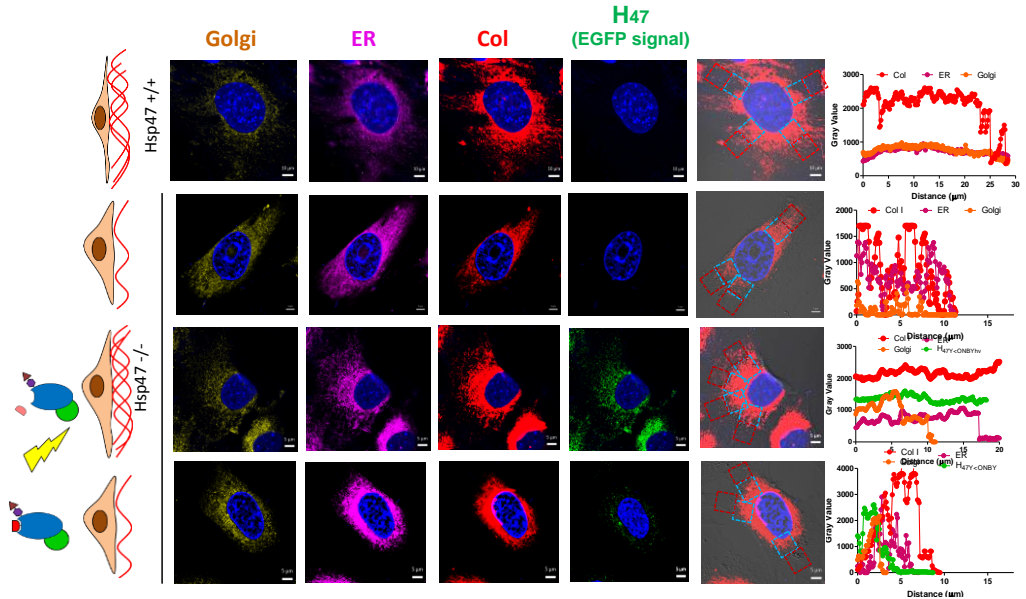


Figure12. Subcellular detection of procollagen at secretory organelles on photo activation of H_{47Y<ONBY}. Immunostaining of Hsp47 +/+, non-activated and light-activated Hsp47 -/- MEF cells treated with H_{47Y<ONBY}. Golgi Antibody is shown in Red, ER tracker Dye in Orange, COL I Antibody in Yellow, Hsp47 signal in green (EGFP), and nuclei in blue (DAPI). Activation was done with 405 nm light. Dotted squares represent the areas considered for Pearson correlation analysis in four different directions (Blue: 0-50% area from nucleus to periphery, Red: 50-100% area from nucleus to periphery of the cells. Intensity profile plots of representative cells from three independent experiments. Scale bars: Hsp47 +/+ -10μm and Hsp47 -/-, Hsp47 -/- active Hsp47 and Hsp47 -/- inactive Hsp47 with 5μm.

This supports our previous observations in the collagen deposition assays (Figure10). Interestingly, a significant correlation in EGFP-COL I signal in 0-50 % section was observed, indicating that both H_{47Y<ONBY} and procollagen are accumulated in the ER near the nucleus, causing ER trafficking (Figure 12). It is important to note that Pearson's correlation analysis is only capable of quantifying the spatial correlation between two signals and cannot evaluate

whether the two molecules are bound to each other. The functional arrest of $H_{47Y<ONBY}$ in Hsp47 $-/-$ cells was further confirmed by the fact that procollagen was seen to be aligned with the ER around the nucleus Golgi apparatus was found around ER in small spots, but no procollagen signal was found overlapping with it.

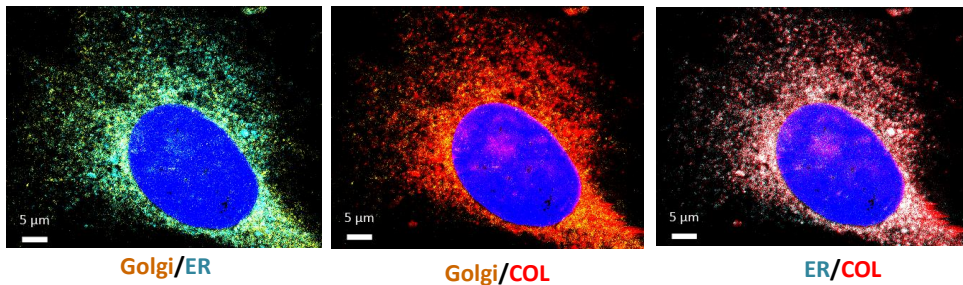


Figure 13. Immunostaining of MEF $-/-$ cells showing procollagen (Red) localizes in the ER (Cyan) around the nucleus whereas not in the Golgi shown in Yellow. This demonstrates ER trafficking of procollagen in Hsp47 $-/-$ cells. Scale – 5 μ m.

On activation of $H_{47Y<ONBY}$ in Hsp47 $-/-$ cells, using 405 nm light, a significant change in procollagen distribution was observed. Procollagen production had increased in the activated cells after 24h. The distribution of collagen was observed from nucleus till the periphery of the cells.

A similar trend in procollagen distribution was observed compared to Hsp47 $+/+$ cells i.e. (0-50 % section -ER-COL I r- 0.8623 and Golgi-COL I r- 0.9014) and (50-100 % section -ER-COL I r- 0.8317 and Golgi-COL I r-0.0012). Also, strong amount of EGFP signal was observed around the nucleus indicating accumulation of Hsp47 here. Increase in cell size was observed, probably since activation of $H_{47Y<ONBY}$ in Hsp47 $-/-$ cells enhances collagen secretion and promotes cell spreading due to increase in deposited collagen (Figure 12, Table 1).

5.3. Conclusions

In conclusion, the ability to promote collagen synthesis on demand, in a spatially defined manner and in disease state cells is demonstrated *in vitro*. *In situ* light exposure allowed light-mediated increase of functional Hsp47

concentration inside the cells, and consequently localized up regulation of collagen production and deposition in cell cultures. Spatial accuracy of collagen deposition was confirmed with patterned light activation of endocytosed photoactivatable Hsp47. Single cells showed increase in procollagen production at a submicron level within secretory organelles. The distribution of procollagen in the secretory apparatus were enhanced on functional activation of our tool, resembling the distribution seen in Hsp47 +/+ cells. Moreover, increase in cell size was observed on activation. We envision that this tool will allow unprecedented studies of collagen synthesis and early assembly. Moreover, photoactivatable Hsp47 might inspire new therapeutic concepts for treating collagen-related defects like Osteogenesis imperfecta, Ehlers–Danlos syndrome, and epidermolysis bullosa by promoting correct folding of collagen. Finally, the possibility of external up regulation of collagen synthesis and deposition might be advantageous for tissue regeneration and rebuilding of the extracellular scaffold.

		Pearson's coefficient r					
n=20	Distance from the Nucleus (%)		ER-Col I	Golgi-Col I	Hsp47-ER	Hsp47-Golgi	Hsp47-Col
Hsp47+/+	0-50		0.9519	0.9014			
	50-100		0.9325	0.0			
Hsp47-/-	0-50		0.9926	0.9153			
	50-100		0.0020	0.0			
	0-50	H _{47Y<ONBY}	0.8976	0.9014	0.9411	0.0076	0.8612
	50-100	H _{47Y<ONBY}	0.0063	0.0	0.0	0.0	0.0
	0-50	H _{47Y<ONBY hv}	0.8623	0.9014	0.9519	0.8317	0.9014
	50-100	H _{47Y<ONBY hv}	0.8317	0.0	0.0005	0.0	0.00

Table1. This table shows Pearson's coefficient analysis of Col I distribution on activation of H_{47Y<ONBY}. n-20 cells from each conditions were used for analysis from three independent experiments

Chapter 6

Stimulated collagen production in keratoconus corneal tissue using Hsp47: a new therapeutic scenario for Keratoconus?

Keratoconus is a corneal disorder due to poor reduction in collagen deposition and poor crosslinking of collagen. Hsp47 has reported to be down regulated in keratoconus cornea, and this is speculated as one of the factors involved in this disorder. In this chapter the therapeutic potential of photoactivatable Hsp47 is demonstrated in ex vivo keratoconus cornea from patients. Photoactivatable Hsp47 was delivered to keratocytes in cornea tissue ex vivo, overcoming interacting with matrix collagen. Localized activation of the protein leads to an increase in the deposition of fibrillar COL I, III and V in ex vivo keratoconus cornea cultures.

6.1. Introduction

Keratoconus is a multifactorial corneal ectasia. It is usually diagnosed from puberty to 30 years of age and often progresses from the fourth decade of life. The prevalence of keratoconus in white Europeans has been estimated to be 1 in 1750 and up to 1 in 450 in South Asians for the age group 10–44 years¹³⁴. Its pathogenesis displays a progressing non-inflammatory softening of the central cornea^{5, 134-135, 306}. This softening is related to impaired synthesis and crosslinking of collagen fibrils with consequent changes in the morphology of the collagen matrix, and to a bulging of the central portion of the cornea in a cone shape^{135-136, 307-308}. This results in localized corneal thinning, irregular astigmatism and visual impairment³⁰⁹.

Corneal tissue is composed of different cell types in a layered arrangement. The outer epithelial layer acts as a physical barrier to pathogens and is separated from the middle layer by the Bowman's layer rich in COL IV.³¹⁰ The middle layer (stroma) consists of a fibrous collagen matrix with a thickness of 465.4 ± 36.9 μm . Stromal fibroblasts (keratocytes) are responsible for the deposition and remodeling of this collagen matrix. The innermost layer is the endothelium, separated from the stroma by the Descemet's membrane^{307-308, 311-312}. In healthy individuals, the frontal stratified epithelial layer consists of type I, VI, VII, XII and XIII collagens, which are all decreased in keratoconus cornea^{5, 136, 307-308, 311}. The stromal layer contains mainly collagen types I and V, and lower amounts of collagen type VI, XII, XIII, XIV and XXIV. In keratoconus cornea, a reduction in type I, III, IV, V and XII collagens is reported¹³⁵. Mutations in prolyl and lysyl hydroxylases, necessary for the hydroxylation of proline and lysine residues in the collagen triple helix, are associated to keratoconus disease^{36, 248}. Hydroxylation is essential for the crosslinking of collagen fibrils³¹³. The low crosslinking in keratoconus stroma is behind the softening and thinning of the stroma, which becomes deformed and protrudes towards the outer epithelial layer at the ocular pressure^{135, 313}.

Therapeutic approaches to treat KC at early stages are based on UV-mediated crosslinking of the cornea collagen matrix using riboflavin¹³⁶. This treatment

stabilizes the collagen matrix and leads to improved organization of the collagen fibrils and down regulation of matrix metalloproteases like MMP-1, 3 and 9. However, cross-linking decreases viability, promotes apoptosis and inhibits proliferation of keratocytes³¹⁴. Moreover, the inflammatory response and scarring associated to KC due to myofibroblastic transformation of keratocytes is also not prevented by UV crosslinking^{306, 315}. Treatment of keratoconus disease in more advanced states requires corneal implants and transplants which clears a line of vision of 1 or 2 and still requires contact lenses.

The chaperone protein Hsp47 is down-regulated in keratoconus fibroblasts¹⁵³. Hsp47 has been shown to promote wound healing without scar formation and proper alignment of collagen fibers in neonatal skin after injury²⁸¹. In this chapter, the ability of H_{47Y<ONBY} to mediate light-driven stimulation of collagen deposition in cornea explants is tested. Note that this is not possible by treatment with native Hsp47, since it would remain attached to the collagen in the extracellular matrix. Effective delivery of H_{47Y<ONBY} into keratocytes in human normal cornea (NC) and keratoconus cornea (KC) will be demonstrated, and no interference with the extracellular matrix of the tissue. *In situ* and on-demand functional activation of H_{47Y<ONBY} with light is shown, followed by collagen secretion and matrix remodeling in the cornea *ex vivo*. COL I, III and V were showed significant increase on functional activation of H_{47Y<ONBY} whereas COL IV and XII showed modest increase.

6.2. Results and Discussions

6.2.1. Hsp47 uptake by NC and KC keratocytes in 2D cultures leads to increased collagen expression and secretion of fibrillar collagens I, III and V

The uptake of H₄₇ by primary human cornea derived stromal fibroblasts was first tested. Normal and KC keratocytes were incubated with EGFP-labeled H₄₇ for 3 h, fixed and stained for ER and cell nucleus. As control, cells were also incubated with EGFP. NC and KC keratocytes incubated with H_{47N} showed co-localization of the fluorescent signals corresponding to H_{47N} and to the ER, indicating successful uptake of the H_{47N} by these cells (see Figure S1a). No fluorescence was observed in cultures incubated with EGFP, which does not contain a KDEL sequence, supporting the evidence that H_{47N} endocytosis occurs specifically via the KDEL receptor. Experiments performed at different incubation concentrations of H_{47N} (0.01 μM -1 μM) showed that the optimal concentration was 0.5 μM (Figure S1). Concentrations above 0.5 μM resulted in the formation of H_{47N} aggregates on the cell culture substrate.

To determine the bioactivity of the endocytosed H_{47N}, the collagen deposition levels of H_{47N}-treated NC and KC keratocytes were evaluated by Sirius Red assay²⁷⁷ and compared with non-treated controls. NC keratocytes treated with H₄₇ showed a significant increase in collagen production (≈20%) 3 days after treatment.

A modest increase was detected in the first and second days after the treatment. KC keratocytes deposited 40% less collagen than NC keratocytes, and H_{47N} treatment induced a ca. 30% increase in collagen deposition (Figure 1b). The reported half-life of Hsp47 inside the cells is more than 24h³¹⁶. Our observations are in agreement with this finding. The observed increased deposition of collagen confirms that endocytosed H_{47N} remains functional for 2-3 days inside the cornea fibroblasts. In KC keratocytes, lower expression levels of COL I, III, IV, V and XII have been reported¹³⁵. To test if treatment with exogenous H₄₇ stimulates expression of these collagens, changes in mRNA levels of collagen subtypes was determined using Q-PCR analysis with appropriate primers.

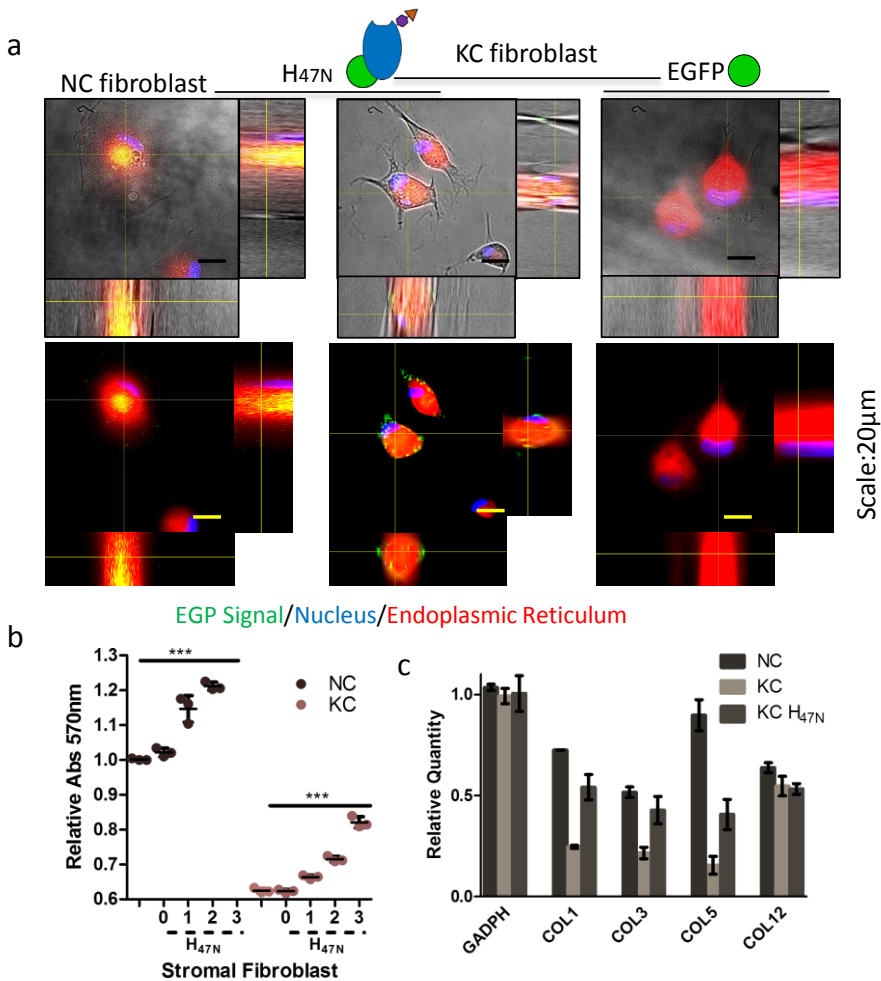


Figure1. Increase in collagen production of keratocytes in 2D culture after incubation with H_{47N}. **a.** Microscopy Z stack images of NC and KC stromal fibroblast cells (keratocytes) after incubation with H_{47N} showing colocalization of H_{47N} signal and ER staining. Incubation with EGFP did not lead to intracellular fluorescence. Blue: DAPI (Nucleus), Green: EGFP (H_{47N}) and Red: ER tracker Dye. Scale bar: 20 µm. **b.** Relative collagen deposition in NC and KC cultures after 3 days of treatment with H_{47N}. Collagen deposition was quantified using the Sirius Red Assay at 570 nm (n=3 data point representing mean value of technical triplicates of each experiment with whisker plots representing standard

deviation). Statistical significance was analyzed by Tukey test. Significance was calculated by comparing non treated vs. treated cells (mean±SD, ANOVA, *** p<0.001). **c.** Q-PCR results of gene expression levels of collagen subtypes 24 h after delivery of H_{47N}. Error bars indicates standard derivation of three independent experiments (n-3).

Increased expression levels of fibrillar collagens I, III and V were found after treatment with H_{47N}. No increase in the expression of network-forming collagen COL IV and fibril associated collagen XII was observed after H_{47N} treatment (Figure 1c). These results suggest that H₄₇ mainly supports secretion of fibrillar collagens in KC keratocytes. Similar results have been observed in in vitro cultures with other cell types¹³⁵.

6.2.2. Photoactivatable Hsp47 can be delivered to keratocytes in corneal explants

Collagen is a major component of the extracellular matrix in natural tissues. Therefore, treatment of natural tissues with soluble Hsp47 would lead to retention of the protein at the extracellular matrix and no delivery to the cells. H_{47Y<ONBY}, where the affinity for collagen is temporally inhibited, does not interact with matrix collagen. Therefore, this could open the possibility to deliver Hsp47 into the cells within tissues. This possibility was tested using cornea tissue explants from postmortem patients. 4 Explants were sliced into three pieces each and pinned on a PDMS-coated wells within 6 well plates. Tissue pinning should replicate the tensional state of corneal tissue *in vivo*, under ocular fluid pressure (Figure 2).

Corneal fragments were incubated with H_{47N} and H_{47Y<ONBY} at 0.5 μM concentration for 5 h. After delivery, the tissues were fixed with PFA and sucrose treatment, cryosectioned and immunostained with COL I antibody. Epifluorescence imaging showed homogeneous distribution of H_{47N} within the cornea co localized with the signal from matrix collagen I staining. Conversely, H_{47Y<ONBY} signal was located inside the keratocytes, accumulated around the nuclei and did not co-localize with the signal from the matrix collagen (Figure 3). These results confirm that H_{47Y<ONBY} can be delivered to cornea cells in

cornea explants due to its inhibited affinity to collagen through the mutated 383Tyr residue.

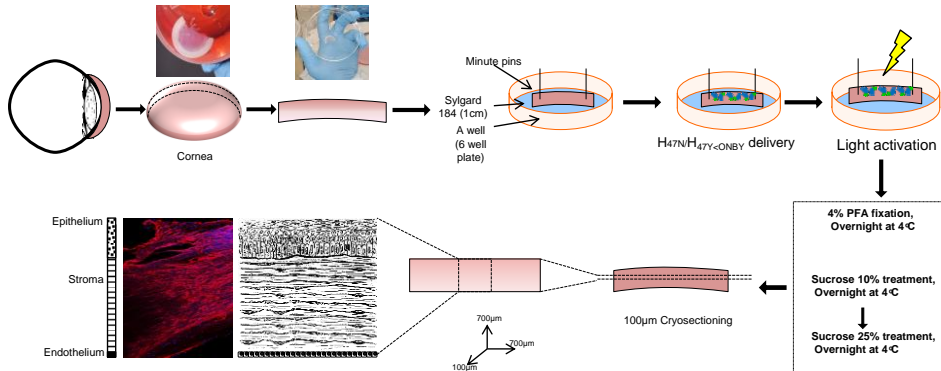


Figure 2. a. Scheme reflects the experimental protocol for the delivery of Hsp47 to ex vivo cornea cultures, and the following histological analysis of collagen deposition. Cornea explant is pinned on a Sylgard coated well in a 6 well plate using minute pins. Hsp47 variants were incubated for 5 h in cell culture medium. Subsequently, samples were fixed, cryosectioned and immunostained. Corneas were fixed with 4% PFA and treated with increasing concentrations of sucrose (10-25%) before embedding for Cryosectioned. Sections were stained with Col I Antibody in red. Hsp47 variants are green (EGFP), and nuclei are stained in blue (DAPI).

6.2.3. Light-stimulated deposition of matrix collagen in KC cornea after H_{47Y<ONBY>} treatment

The ability of intracellular H_{47Y<ONBY>} to stimulate collagen deposition in cornea tissue after light activation was then tested. For this purpose pinned NC and KC were first incubated for 5 h with H_{47Y<ONBY>}. A defined area (2.5x0.75mm²) was then scanned with a 405 nm (3mW/cm²) LED laser for 1 min and the cornea was maintained in culture for 3 days. Collagen deposition was analyzed by second harmonic generation (SHG) imaging of the irradiated area after cryo slicing the cornea tissue at day 3. Control experiments without H_{47Y<ONBY>} treatment were also performed.

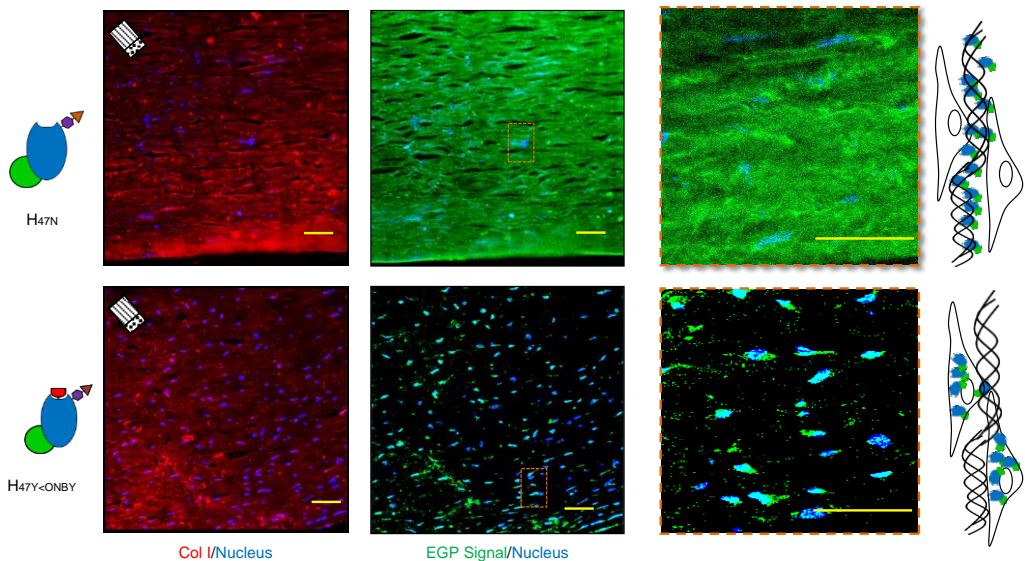


Figure3. Delivery of H₄₇ and H_{47Y<ONBY} to cornea tissue *ex vivo*. Epifluorescence images of NC cornea after incubation with H_{47N} or H_{47Y<ONBY} for 5 h and staining with COL I antibody (red). H₄₇ was retained at the extracellular collagen matrix, whereas H_{47Y<ONBY} (Green) was up taken by the cell and localized at the ER (Blue: DAPI (Nucleus), Green: EGFP and Red: ER tracker Dye) Scale bar: 250 μ m.

Figure 4a shows the SHG image of collagen in not treated NC. Uniform, highly aligned and superimposed fibers of 5-20 μ m diameter were observed. The alignment and uniformity of collagen in cornea tissue are essential for maintaining optical transparency and provide the biomechanical prerequisites necessary to sustain shape and strength³¹⁷⁻³¹⁸. When imaged at the same conditions, KC showed a weak SHG signal, as indication of poorly organized collagen structures (Figure 4a). No individual fibers could be distinguished in the SHG image. The observed morphologies in NC and KC are in agreement with reported data, confirming that our methodology to *ex vivo* culture cornea tissue and to do SHG imaging of collagen are adequate³¹⁸.

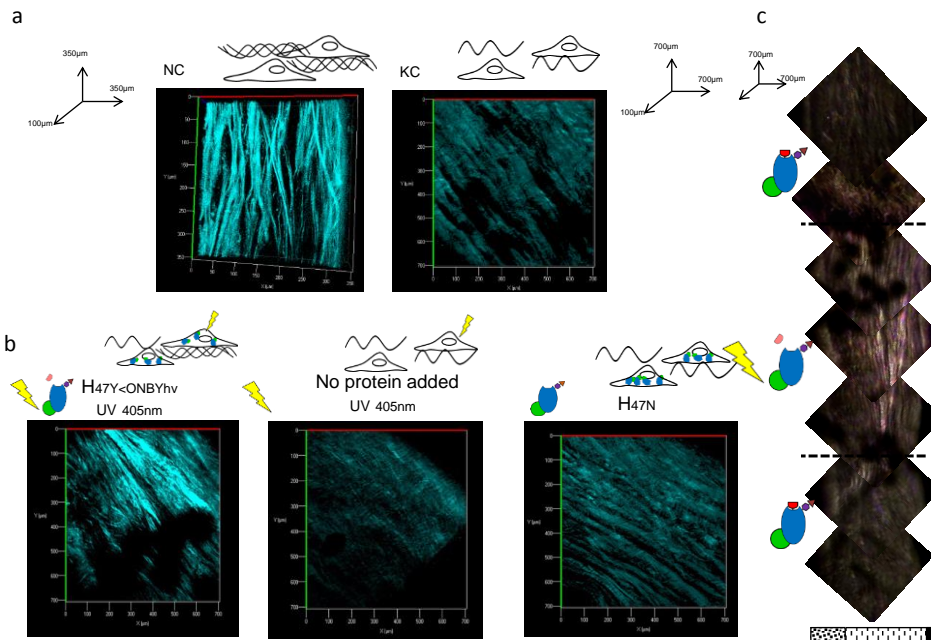


Figure4. Light stimulation of collagen deposition in KC using H_{47Y<ONBY}. SHG images of collagen fibers in: **a.** NC showing superimposed and aligned collagen fibers and in KC showing weak SHG intensity and low collagen alignment. **b.** KC after light exposure; after treatment with H_{47Y<ONBY} and light exposure; and after treatment with H_{47N} and light exposure. Increased deposition of collagen was only observed when cells were treated with H_{47Y<ONBY} and illuminated. **c.** KC after treatment with H_{47Y<ONBY} and localized light exposure showing increase in collagen deposition and ordered collagen structures only at the irradiated area (2.5x0.75 mm², highlighted with black lines). The bar in each image shows the orientation of cornea (Small dotted area-Epithelial, Dashed area-Stromal and Black line: Endothelium).

Figure 4d shows the SHG image of KC corneal fragments incubated with H_{47Y<ONBY} irradiated and cultured for 3 days. A significantly stronger SHG signal was obtained and an improved organization of the collagen fibers was visible. The areas of the tissue which were not exposed showed the same weak SHG

signal as in non-treated KC (Figure 4d). UV exposure on untreated KC corneas did not show any change in collagen morphology, indicating that the irradiation did not affect the tissue (Figure 4b). H_{47N} treated KC tissues did not show any improvement in collagen deposition, which we associate to the retention of the protein in the extracellular space. Altogether these results demonstrate the ability of H_{47Y<ONBY} in combination with light to stimulate matrix collagen deposition in corneal explants with morphological features resembling those of collagen in normal corneas.

6.2.4. Deposited collagen in H_{47Y<ONBY} treated KC showed high degree of alignment

In order to characterize the degree of alignment of the deposited collagen, the samples were characterized by polarization light microscopy (PLM)¹¹⁵. The anisotropy of collagen fibers makes them birefringent¹¹⁷. Birefringence (B) is the difference in refractive index between the two orthogonal axes of an anisotropic object ($\Delta n_1 - \Delta n_2$) as mentioned by Weiss and coworkers in Protoplasma, 2010. The optical retardation of the sample, which is an experimental indication of the molecular order and orientation of the birefringent structures, corresponds to the birefringence value multiplied by the thickness of the sample^{80, 319} (Figure 5). The mean optical retardance values were generated using the Polscope software from 8 images from 3 independent experiments. The relative optical retardance value was normalized by the highest retardance value of NC sample, taken as 100%.

Birefringence measurements of NC tissue yielded higher optical retardation than on KC tissues which showed ~25% retardation, indicating a stronger orientation of the collagen fibers (Figure 5a). Treatment of KC tissues with H_{47Y<ONBY} and photo activation lead to collagen structures with increased optical retardation, up to 85% (Figure c). These results indicate that functional activation of H_{47Y<ONBY} inside keratocytes of KC tissue produced correctly folded and aligned collagen fibers. Non-activated areas in the same tissue retained low optical retardation (Figure 5).

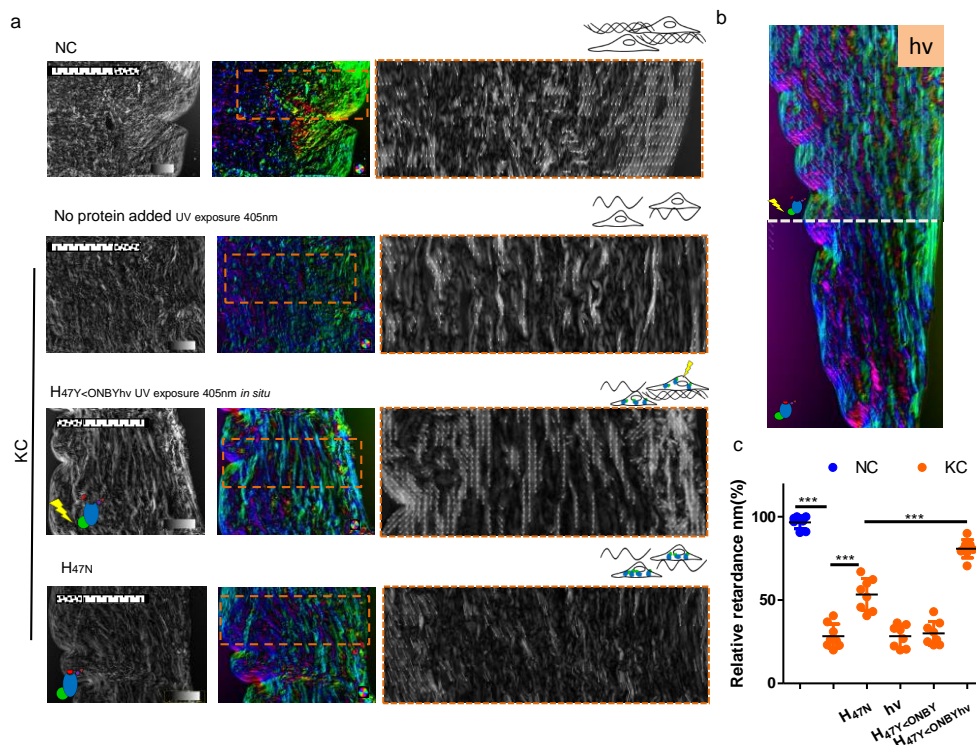


Figure 5. Deposition of oriented collagen fibers upon localized activation of H_{47Y<ONBY} in NC and KC tissues by polarization optical microscopy imaging (LC-PolScope). a. NC and KC tissues treated with H_{47Y<ONBY} after light-activation, and corresponding controls. Optical retardation signal per pixel are shown from dark to white color LC-PolScope orientation images encoding the slow optical axis per pixel are shown as pie diagram. b. Orientation image encoding the slow optical axis per pixel along with vectors show localized aligned fibers in the KC treated with H_{47Y<ONBY} and activated on light exposure (half of the cornea is expose to 405nm light for 1 min).c. Graph represents relative retardance in NC and KC cornea in different conditions. (n=8 data point representing mean value of 8 images from technical triplicates of each experiment with whisker plots representing standard deviation). Statistical significance was analyzed by Tukey test. Significance was calculated by comparing non treated vs. treated cells (mean±SD, ANOVA, *** p<0.001).

Light exposure of KC tissue without Hsp47 treatment did not change the alignment of collagen fibers. In the same line, KC tissues treated with H_{47N} did not show improved directionality of collagen fibers either with modest increase in optical retardation up to 50 % (Figure 5a). These results indicate that H_{47Y<ONBY} enables on-demand and spatially confined deposition of aligned collagen fibers in cornea tissue (Figure 5a).

6.2.5. Fibrillar collagens type I, II and V are preferentially deposited in cornea tissue after treatment with H_{47Y<ONBY} and photo activation

Hsp47 has been reported to bind to fibrillar COL I, II, III and V⁷⁴. What type of collagens are preferentially deposited in cornea tissues after local activation of H_{47Y<ONBY} was evaluated. For this purpose NC, KC and H_{47Y<ONBY} -treated KC tissues were fixed 3 days after incubation and immuno stained for COL I, III, IV, V and XII with specific antibodies (Figure 6). COL I, III, IV, V and XII were found in NC and KC tissues, though lower fluorescence intensity was observed for the five collagen types in KC tissues. KC treated with H_{47Y<ONBY} showed no changes in collagen deposition vs. KC tissue. Light irradiation of H_{47Y<ONBY} treated KC to light (405nm) lead to increased deposition of COL I, III and V in the exposed areas (Figure 6). No changes were observed for COL IV and XII. These results indicate that the exogenous administration of H₄₇ via light activated H_{47Y<ONBY} to KC tissue triggers production of fibrillar collagens. KC treated with H₄₇ showed a small increase in deposited collagen (Figure S2), indicating that only increased intracellular H₄₇ can effectively interact with the collagen biosynthesis process. Note that similar findings were also observed in keratocyte cultures. Altogether, these findings suggest that photoactivatable H₄₇ can be regarded as potential therapeutic tool to rescue functional collagen matrices in keratoconus corneas by inducing photo regulated deposition of COL I, III and V.

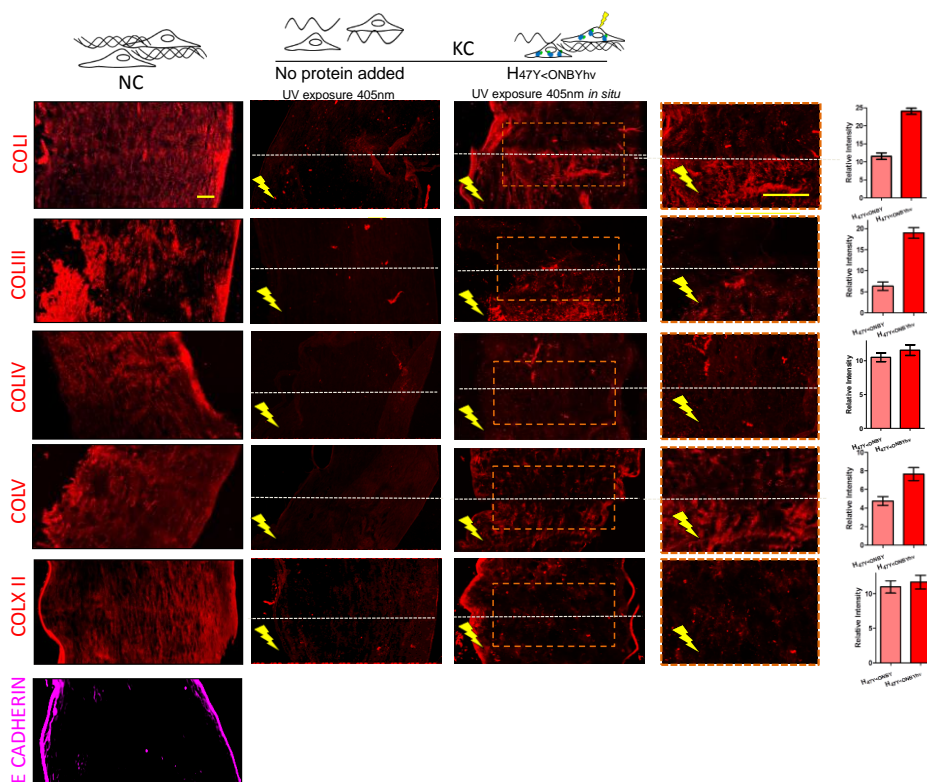


Figure6. Light-stimulated deposition of different collagen subtypes. Fluorescence images of NC, KC and KC treated with H_{47Y-ONBY} after 3 days of culture. Samples were immunostained with antibodies for COL I, III, IV, V and XII (in red). The light exposed areas are highlighted with yellow light blot. The orange dashed line square area is zoomed in the adjacent figure. Plot profile indicates increase in red signal intensity from COL I, III and V and no increase in IV and XII. Scale bar: 250um.

6.3. Discussion

Treatment of KC tissue with exogenous H_{47Y<ONBY} and light allowed stimulation of keratocytes to deposit fibrillar collagen *ex vivo*. The presented results provide a conclusive proof that delivery and activation of H_{47Y<ONBY} enhance thickening of collagen fibers in cornea tissue while retaining their natural parallel arrangement as revealed by the SHG images. The specificity of Hsp47 for collagen makes this approach highly interesting to study and eventually for therapeutic treatment of diseases associated with alterations in the deposition or stability of fibrillar collagen. Deeper studies and applications of H_{47Y<ONBY} for these purposes require, however, additional studies and eventually modifications in the molecular design of our tool.

End-point imaging of cornea tissue samples via SHG and polarization microscopy after fixing and cryosectioning provided information regarding collagen fiber density and orientation. Variations in collagen morphology between H₄₇ stimulated and un-stimulated sections of the same tissue fragment could be visualized by these methods. However, this method does not allow differentiation between the existing and new synthesized collagen in the images. Quantification and analysis of the properties of the deposited collagen (i.e. type, crosslinking or degradation rate) require other methods. Very recently a new strategy for quantification of newly synthesized collagen has been reported³²⁰. By stably knocking-in a probe collagen gene in which procollagen is fused to a photo switchable probe, Dendra2. The monomeric version of this fluorescent protein is green-to-red photo convertible. This strategy allows distinguishing between newly synthesized collagen and preexisting collagen by fluorescence imaging. Another relevant feature is that the genetic construct is engineered within Exon 1 of procollagen 1 $\alpha 2$ domain, such that the fluorescent protein doesn't affect triple helix formation and cannot be cleaved during fiber formation. In this way, collagen processing can be traced from intra to extracellular level. In future work this strategy could be used to quantify the rates and extents of collagen deposition in corneal tissues when stimulated by our photoactivatable Hsp47.

One advantage but also possible limitation to the therapeutic application of this approach is the use of light to control the activity of H_{47Y<ONBY} in the tissue. On the one H_{47Y<ONBY} allows easy external regulation of the pharmacokinetic profile in the tissue using a light source. On the other hand it requires light protection of the tissue with orange light filters when activation is not desired until it gets enzymatically degraded. Another limitation is that it requires UV light for activation, and UV light has a low penetration depth in tissues. This is not an issue for cornea, as it is transparent, but it is an issue for all other tissues. The use of other photo removable groups for Tyr which are sensitive to NIR light, which has higher penetration depth in tissue, is not straightforward since the tools for genetic encoding are not available. An alternative could be to engineer an enzymatic cleavable moiety. For example, CNA35, a collagen binding probe was engineered with a cyclization of protease inhibitor domain between its two binding domain N1 and N2 which can be cleaved on addition of proteases³²¹.

Hsp47 has largely been considered as a therapeutic target in cancer. Knockdown of Hsp47 expression reduces collagen levels and inhibits tumor proliferation and metastasis by reducing fibrosis^{98, 150}. Hsp47 inhibitors for therapeutic treatment of fibrosis are in development²⁷⁷. In contrast with this scenario, this study explores the application of exogenous Hsp47 to enhance collagen production. The development of the photoactivatable H_{47Y<ONBY}, with a tunable affinity for collagen, was crucial for this purpose, as it does not interact with matrix collagen in the tissue and it allows intracellular delivery. This approach is not specific for KC disease or cornea tissue, and should be tested in other examples of collagen disorders in the future. Relevant scenarios could be EDS or Epidermolysis bullosa in skin, or eventually osteoporosis and osteoarthritis in bones were mutations in Hsp47 occur in some variants of the diseases^{18, 74, 129, 259, 322}. Hsp47 is a naturally occurring protein, it is collagen specific, is readily up taken by cells in tissue without the need of delivery vehicles, and has a life time of 1-2 days³¹⁶. These features make it highly attractive as possible therapeutic molecule for medical application.

6.4. Conclusions

Hsp47 is a collagen specific protein involved in the biosynthesis of collagen. This protein is down regulated in KC, a disease state that is associated with a distorted collagen matrix of the cornea tissue. The recombinantly produced, photoactivatable H_{47Y<ONBY} is a H₄₇ variant with low affinity for collagen. When incubated with cornea tissue, this protein does not interact with matrix collagen and is uptake by keratocytes and accumulates in the ER within 3 hours. Light exposure of cornea tissue after treatment with H_{47Y<ONBY} leads to increased deposition of fibrillar collagens type I, II and V. Site-selective exposure of H_{47Y<ONBY} treated cornea allows for localized remodeling of the extracellular collagen matrix *in situ*. This possibility was demonstrated in *ex vivo* KC, inspiring future therapeutic concepts for keratoconus and other collagen-associated diseases.

Conclusions and Outlook

In this PhD thesis, a photoactivatable variant of Hsp47 (H_{47Y<ONBY}) was developed, tested and applied to enhance collagen deposition in a collagen-deficient disorder (keratoconus). The following general conclusions can be extracted from this work:

1. The substitution of Tyr383 of Hsp47 by the non-natural light-responsive o-nitro benzyl tyrosine (ONBY) rendered Hsp47 inactive toward collagen binding, and allowed its light-regulation at selected time points and sites after cellular uptake. The affinity loss of the mutated protein also prevented interaction with extracellular collagen, and allowed delivery of Hsp47 to cells within corneal tissue explants. This feature is particularly interesting, as it allows considering the mutated Hsp47 for use in therapeutics.
2. Hsp47 is up taken by cells in *in vitro* cultures and also tissue explants via KDEL receptor mediated endocytosis by simple incubation of Hsp47 in the medium. This finding establishes a generalized strategy for delivering proteins precisely to ER of the cells.
3. Hsp47 treatment leads to increased secretion of fibrillar COL I, III and V in skin cell lines *in vitro* within a 24h time scale after exogenous supply of the protein. Modest increase in non-fibrillar COL IV and XII was observed in skin epithelial and endothelial cell lines. This suggests that Hsp47 can be used as a collagen stimulant targeting skin based collagenopathies like brittle bone diseases, EDS and chronic skin wounds irrespective of whether there is a defect in endogenous Hsp47 or not.
4. Administration of H_{47Y<ONBY} allowed light-stimulated secretion of collagen in Hsp47 negative cells *in vitro*. The activation of collagen production in disease-state cells opens a possibility of localized

deposition of collagen on demand. This is a relevant finding from tissue engineering perspective to repair damaged tissues locally.

5. Due to its temporary functional arrest, it was possible to deliver photoactivatable Hsp47 precisely inside corneal cells. Upon site specific activation of this tool by light, localized increase in fibrillar collagen was demonstrated in *ex vivo* damaged corneal tissues from keratoconus patients. These results demonstrate the therapeutic potential of this tool to treat keratoconus disorder in human patients. Further investigations will be carried out to evaluate whether corneal function can be restored using this strategy.

Photoactivatable Hsp47 can enable unprecedented fundamental studies of collagen biosynthesis and matrix biology, and inspire new therapeutic concepts for tissue regeneration.

Annexure

Supporting Information:

FileUp

MSF: 421 Type: P Check: 7992 ..

Name: Homo oo Len: 421 Check: 684 Weight: 0.0
Name: Rattusnorvegicus oo Len: 421 Check: 4859 Weight: 10.0
Name: Mus oo Len: 421 Check: 3917 Weight: 10.0
Name: Canislupus oo Len: 421 Check: 1504 Weight: 10.0
Name: Gallusgallus oo Len: 421 Check: 1217 Weight: 10.0
Name: Zebrafish oo Len: 421 Check: 3540 Weight: 10.0
Name: Goldfish oo Len: 421 Check: 5498 Weight: 10.0
Name: Melonfly oo Len: 421 Check: 5970 Weight: 10.0
Name: ChannelCatfish oo Len: 421 Check: 2938 Weight: 10.0
Name: Amazonparrot oo Len: 421 Check: 2619 Weight: 10.0
Name: Brandtsbat oo Len: 421 Check: 2759 Weight: 10.0
Name: Greenseaturtle oo Len: 421 Check: 8976 Weight: 10.0
Name: Rockdove oo Len: 421 Check: 557 Weight: 10.0
Name: Squerrillikeanimal oo Len: 421 Check: 3579 Weight: 10.0
Name: Yak oo Len: 421 Check: 940 Weight: 10.0
Name: Blackfruitbat oo Len: 421 Check: 2467 Weight: 10.0
Name: Nakedmolerat oo Len: 421 Check: 796 Weight: 10.0
Name: ChineseHamester oo Len: 421 Check: 3110 Weight: 10.0
Name: Damaralandmolerat oo Len: 421 Check: 2798 Weight: 10.0
Name: Mediterraneanfruitfly oo Len: 421 Check: 3130 Weight: 10.0
Name: Australian oo Len: 421 Check: 6134 Weight: 10.0//

Homo	MRSLLLLSAF	CLLEAALAAE	VKKPAAAAAP	GTAEKLSPKA	ATLAERSAGL
Rat	.MRSLLLGTL	CLLAVALAAE	VKKPVEATAP	GTAEKLSska	TTLAERSTGL
Mus	.MRSLLLGTL	CLLAVALAAE	VKKPLEAAAP	GTAEKLSska	TTLAERSTGL
Cani	MRLLLLLNTC	CLLAVVLAEE	VKKPAAAAAP	GSAEKLSPKA	ATLAERSAGL
GallMQIFLVL	ALCGLAAAVP	SEDRKLSDKA	TTLADRSTTL
ZebMWVSSLI	ALCLLAVAVS	GEDKKLSTHA	TSMADTSANL
GolMLVSSV	LLCLLATVSG	..DKALSSHA	SILADNSANF
MelMEALKIT	YKLERQFLVK	FLFVLGATAL
ChanMWVKFLV	GLCLLASVGA	..DKKLSSHA	TILADNSANL
AmazMWIILVL	ALCGLAAAVP	SEDRKLSDKA	TTLADRSTTL
Bran	MRSLLLLTSF	CLLAMALAAE	VKKPAAPAAP	GTAEKLSPKA	TTLAERSAGL
GreeMWVTNLL	ALCALVAAVP	SEDKKLSDKA	AALADRSTTL
RocMWIILV	LALCGLAAAV	PSEDRKLSDK	ATTADRSTT
Sque	MRSLLLLSTF	CLLALAG...VLAELSPK	AATLAERSAG
Yak	MRALLLISTI	CLLARALAAE	VKKPAAAAAP	.GTAEKLSPK	AATLAERSAG
Blac	MRSLLLLSTF	CLLAITLAAE	VKKPAVAAAA	PGTGEKLSPK	AATLAERSAG
Nake	MRLLLLLGTG	SLLAVALAAE	VKKPAAAAAP	G.TAEKLSSK	AATLAERSAG
Chin	.MRSLLLLASF	CLLAVALAAE	VKKPVEAAAP	G.TAEKLSSK	ATTLAERSTG
Dama	MRLLLLLGTG	SLLAVALAAE	VKKPAAVAAP	G.TAEKLSSK	AATLAERSAG
MediMMAYTY	RHKLQIYFIA	QILCTVWLTA
AustMGMKL	ILLSLLICV	KSEPVLKQ	GPILGDSTVN

Homo	AFSLYQAMAK	DQAVENILVS	PVVVASSLGL	VSLGGKATTA	SQAKAVLSAE
Rat	AFSLYQAMAK	DQAVENILLS	PLVVASSLGL	VSLGGKATTA	SQAKAVLSAE
Mus	AFSLYQAMAK	DQAVENILLS	PLVVASSLGL	VSLGGKATTA	SQAKAVLSAE
Cani	AFSLYQAMAK	DQAVENILLS	PVVVASSLGL	VSLGGKATTA	SQAKAVLSAE
Gal	AFNLYHAMAK	DKNMENILLS	PVVVASSLGL	VSLGGKATTA	SQAKAVLSAD
Zeb	AFNLYHNVAK	EKGLENILIS	PVVVASSLGM	VAMGSKSSTA	SQVKSILKAD
Gol	AFNLYHNLAK	EKDIENIVIS	PVVVASSLGL	VALGGKSNTA	SQVKTVLSAT
Mel	AYGQDDGFAQ	D...DNVYSW	YILDVTRILQ	NAESNIVVSP	SNIRALLKTP
Chan	AFDLYHNMAK	EKDMENILIS	PVVVASSLGL	VALGGKASTA	SQVKTVLSGN
Amaz	AFNLYXAMAK	DKNMENILLS	PVVVASSLGL	VSLGGKATTA	SQAKAVLSAD
Bran	AFSLYQAMAK	DQAVENILLS	PVVVASSLGL	VSLGGKATTA	SQAKAVLSAE
Gree	AFNLYHTMAK	DKNMENILVS	PVVVASSLGL	VSLGGKATTA	SQAKAVLSAD
Roc	LAFNLYHAMA	KDK..NMENI	LLSPVVVASS	LGLVSLGGKA	ATASQAKAVL
Sque	LAFSLYQAMA	KDQ..AVENI	LLSPVVVASS	LGLVSLGGKA	ATASQAKAVL
Yak	LAFSLYQAMA	KDQ..AVENI	LLSPVVVASS	LGLVSLGGKA	ATASQAKAVL
Blac	LAFSLYQAMA	KDQ..AVENI	LLSPVVVASS	LGLVSLGGKA	TTASQAKAVL
Nake	LAFSLYQAMA	KDQ..AVENI	LLSPVVVASS	LGLVSLGGKA	ATASQAKAVL
Chin	LAFSLYQAMA	KDQ..AVENI	LLSPLVVASS	LGLVSLGGKA	TTASQAKAVL
Dama	LAFSLYQAMA	KDQ..AVENI	LLSPVVVASS	LGLVSLGGKA	ATASQAKAVL
Medi	TVCGESDKYS	EDEVVNENNV	LAWYILDVSQ	ILQNSKVNTI	LSP...MNL
Aust	LGLSLYQMTI	KDQKLRSQL	LFSPVVVASS	LGVMMSGAKD	KTAKQVKSLL

Homo	QLRDEEVHAG	LGELLRSLSN	STARNTWKL	GSRLYGPSSV	SFADDFVRSS
Rat	KLRDEEVHTG	LGELLRSLSN	STARNTWKL	GSRLYGPSSV	SFADDFVRSS
Mus	KLRDEEVHTG	LGELLRSLSN	STARNTWKL	GSRLYGPSSV	SFADDFVRSS
Cani	QLRDEEVHAG	LGELLRSLSN	STARNTWKL	GSRLYGPSSV	SFAEDFVRSS
Gal	KLNDYVHSG	LSELLNEVSN	STARNTWKI	GNRLYGPASI	NFADDFVKNS
Zeb	ALKDEHLHTG	LSELLTEVSD	PQTRNTWKI	SNRLYGPSSV	SFAEDFVKNS
Gol	TVKDEQLHSG	LSELLTEVSN	STARNTWKI	SNRLYGPSSV	SFVDNFLKSS
Mel	PSMN..LRFG	FDEKTMGL..	...QNVIFAE	SNMILNNP..DTL
Chan	KVKDENLHSG	LAELLSEVSN	PKERNVTWKI	TNRLYGPSSV	SFSEDFVKNS
Amaz	KLNDYVHSG	LSELLNEVSN	STARNTWKI	GNRLYGPASI	NFADDFVKNS
Bran	QLRDEEVHAG	LGELLRSLSN	STARNTWKL	GSRLYGPSSV	SFAEDFVRSS
Gree	KLNDYIHHG	LSELLNEVSN	STARNTWKL	GNRLYGPSSI	SFAEDFVKSS
Roc	SADKLNDDYL	HSGLSELLNE	VSNSTARNT	WKIGNRLYGP	ASINFADDFV
Sque	SAEQLRDEEV	HAGLGELLRS	LSNSTARNVT	WKLGSRLYGP	SSVSFAEDFV
Yak	SAEQLRDDEV	HAGLGELLRS	LSNSTARNVT	WKLGSRLYGP	SSVSFAEDFV
Blac	SAEQLRDEEV	HAGLGELLRS	LSNNTARNVT	WKLGSRLYGP	SSVSFAEDFV
Nake	SAEQLRDEEV	HAGLGELLRS	LSNSTARNVT	WKLGSRLYGP	SSVSFAEDFV
Chin	SAEKLREDEV	HTGLGELLRS	LSNSTARNVT	WKLGSRLYGP	SSVNFAEDFV
Dama	SAEQLRDEEV	HTGLGELLRS	LSNSTARNVT	WKLGSRLYGP	SSVSFAEDFV
Medi	KTPAIVDLRF	GADN.EMEGI	NMILAESRRS	LSRP.....
Aust	NIN.LNDDTL	HPAFSELLNE	VSNETARNNT	WKIGNCLYAP	TSVNVRRDDFV

Homo	KQHYNCEHSK	INFRDKRSAL	QSINEWAAQT	TDGKLPVTK	DVERTDGALL
Rat	KQHYNCEHSK	INFRDKRSAL	QSINEWASQT	TDGKLPVTK	DVERTDGALL
Mus	KQHYNCEHSK	INFRDKRSAL	QSINEWASQT	TDGKLPVTK	DVERTDGALL
Cani	KQHYNCEHSK	INFRDKRSAL	QSINEWAAQT	TDGKLPVTK	DVERTDGALL
Gal	KKHYNYEHSK	INFRDKRSAL	KSINEWAAQT	TDGKLPVTK	DVEKTDGALI
Zeb	KKHYNYEHSK	INFRDKRSAL	NSINEWAAKT	TDGKLPEITK	DVKNTDGAMI
Gol	KKHYNCEHSK	INFRDKRSAL	KAINDWASKS	TDGKLPVTK	DVEKTDGAMI

Mel	EWFYDCKIQE	TSFTDKKKLI	TSINDWSENI	ADQTIILKSSE	MILKEENLQV
Chan	KKHYKYEHAK	INFRDKKSAV	NAINEWASKS	TDGKLPEVTK	DVEKTDGAMI
Amaz	KKHYNYEHSK	INFRDKRSAL	KSINEWAAQT	TDGKLPEVTK	DVEKTDGALI
Bran	KLHYNCEHSK	INFRDKRSAL	QSINEWASQT	TDGKLPEVTK	EVERTDGALL
Gree	KKHYNYEHSK	INFRDKRSAL	KSINEWASQT	TNGKLEPVTT	NVEKTDGALI
Roc	KNSKKHYNYE	HSKINFRDKR	SALKSINewa	AQTTDgklpe	VTKDVEKTDG
Sque	RSSKQHYNCE	HSKINFRDKR	SALQSINewa	AQTTGGKLPE	VTSdVERTDG
Yak	RSSKQHYNCE	HSKINFRDKR	SALQSINewa	AQTTDgklpe	VTKDVERTDG
Blac	RSSKQHYNCE	HSKINFRDKG	SALQSINewa	AQTTDgklpe	VTKEVERTDG
Nake	RSSKQHYNCE	HSKINFRDKR	TALQSINewa	AQTTDgklpe	VTKDVERTDG
Chin	HSSKQHYNCE	HSKINFRDKR	SALQSINewa	SQTTDgklpe	VTKDVERTDG
Dama	RSSKQHYNCE	HSKINFRDKR	SALQSINewa	AQTTDgklpe	VTKDVERTDG
Medi	ENVEMFYNTK	IQEISFADTA	NHLVMINDWG	KRVTNEEFPK	LIESNSSLKN
Aust	QKTKTHYKYD	HSQINFKDQR	SALRSINQWA	SQATEGKLSE	ITAALSSTDG

Homo	VNAMFFKPHW	DEKFHHKMVD	NRGFMVTRSY	TVGVMMHRT	GLYNYDDEK
Rat	VNAMFFKPHW	DEKFHHKMVD	NRGFMVTRSY	TVGVTMMHRT	GLYNYDDEK
Mus	VNAMFFKPHW	DEKFHHKMVD	NRGFMVTRSY	TVGVTMMHRT	GLYNYDDEK
Cani	VNAMFFKPHW	DEKFHHKMVD	NRGFMVTRSY	TVGVTMMHRT	GLYNYDDEK
Gal	VNAMFFKPHW	DEKFHHKMVD	NRGFMVTRSY	TVGVPMHRT	GLYNYDDEA
Zeb	VNAMFFKPHW	DEKSHHKMVD	NRGFLVTRSH	TVSVPMMHRT	GIYGFYEDTE
Gol	INAMFYKPHW	DEQFHHKMVD	NRGFLVHRSY	TVSVPMMHRT	GIYGLFDTT
Mel	LILNMLNFKE	TLQINFKYTL	NATFHERPDS	TIVLPAVETT	EYLKYLDSQI
Chan	INAIIFYKPHW	DEQFHHQMVD	NRAFLVHRSY	TVSVPMMHRT	GIYGFYDDTA
Amaz	VNAMFFKPHW	DEKFHHKMVD	NRGFMVSRYS	TVGVPMHRT	GLYNYDDET
Bran	VNAMFFKPHW	DERFHHKMVD	NRGFMVTRSY	TVGVTMMHRT	GLYNYDDEK
Gree	VNAMFFKPHW	EERFHHKMVD	NRGFMVTRSY	TVGVPMHRT	GLYNYDDEA
Roc	ALIVNAMFFK	PHWDEKFHHK	MVDNRGFMVT	RSYTVGVPM	HRTGLYNYD
Sque	ALLVNAMFFK	PHWDERFHHK	MVDNRGFMVT	RSYTVGVMT	HRTGLYNYD
Yak	ALLVNAMFFK	PHWDERFHHK	MVDNRGFMVT	RSYTVGVMT	HRTGLYNYD
Blac	ALLVNAMFFK	PHWDERFHHK	MVDNRGFMVT	RSYTVGVMT	HRTGLYNYD
Nake	ALLVNAMFFK	PHWDEKFHHK	MVDNRGFMVT	RSYTVGVMT	HRTGLYNYD
Chin	ALLVNAMFFK	PHWDEKFHHK	MVDNRGFMVT	RSYTVGVMT	HRTGLYNYD
Dama	ALLVNAMFFK	PHWDEKFHHK	MVDNRGFMVT	RSYTVGVMT	HRTGLYNYD
Medi	LQVLIILNMFH	FVETLEINFK	YTANLLFYIT	PKQRTKVPVAV	ETTEYLKYL
Aust	AFIINANYFK	PHWDESFQQT	MVDKRGFIIT	RTHTVSIIPMM	HQIRLCNYYE

Homo	EKLQIVEMPL	AHKLSSLIIL	MPHHVEPLER	LEKLLTKEQL	KIWMGKMQKK
Rat	EKLQIVEMPL	AHKLSSLIIL	MPHHVEPLER	LEKLLTKEQL	KIWMGKMQKK
Mus	EKLQIVEMPL	AHKLSSLIIL	MPHHVEPLER	LEKLLTKEQL	KIWMGKMQKK
Cani	EKLQIVEMPL	AHKLSSLIIL	MPHHVEPLER	LEKLLTKEQL	KIWMGKMQKK
Gal	EKLQIVEMPL	AHKLSSMIFI	MPNHVEPLER	VEKLLNREQL	KTWASKMKKR
Zeb	NRFLIVSMPL	AHKKSSMIFI	MPYHVEPLDR	LENLLTRQQL	DTWISKLEER
Gol	NNLLVLDMAL	AHKMSSIVFI	MPYHVESLER	VEKLLTRQQL	NTWISKMEQR
Mel	LDAKILELPY	SNGLYFYII	LPHTKQGVIE	TINNLGYEQL	TRIEWMKKER
Chan	NSFFVLEMP	AHKKSSVIFI	MPYHVESLER	LEKMLTRKQL	DIWQSKMEQK
Amaz	EKLQIVEMPL	AHKLSSMIFI	MPNHVEPLER	VEKLLNREQL	KTWAGKMKKR
Bran	EKLQIVEMPL	AHKLSSLIIL	MPHHVEPLER	LEKMLTKEQL	KIWMGKMQKR
Gree	EKLQIVEMPL	AHKLSSMIFI	MPNHVEPLER	VEKLLTREQL	KTWIGKLLKR
Roc	DETEKLQVVE	MPLAHKLSSM	IFIMPNHVEP	LERVEKLLNR	EQLKTWAGKM

Sque	DEKEKLQIVE	MPLAHKLSSL	IIIMPHHVEP	LERLEKLLTK	EQLKTWMGKM
Yak	DEKEKLQWVE	MPLAHKLSSL	IIIMPHHVEP	LERLEKLLTK	EQLKVVMGKM
Blac	DEKEKMQIVE	MPLAHKLSSL	IILMPHHVEP	LERLEKMLTK	EQLKIWMGKM
Nake	DEKEKVQILE	MPLAHKLSSL	IILMPHHVEP	LERLEKLLTK	EQLKAWTGKL
Chin	DEKEKLQILE	MPLAHKLSSL	IILMPHHVEP	LERLEKLLTK	EQLKAWMGKM
Dama	DEKEKVQILE	MPLAHKLSSL	IILMPHHVEP	LERLEKLLTK	EQLKVVMGKM
Medi	SQMLDAKILQ	LPYSNG.FSM	YILLPHTKAG	LNELLSILGF	EQLKRLQWMM
Aust	DNANSLQVLE	LPLSHKHSSM	IFIMTKHIEP	LARLEKLLTK	EQLNTWIGKL

Homo	AVAISLPKGV	VEVTHDLQKH	LAGLGLTEAI	DKNKADLSRM	SGKKDLYLAS
Rat	AVAISLPKGV	VEVTHDLQKH	LAGLGLTEAI	DKNKADLSRM	SGKKDLYLAS
Mus	AVAISLPKGV	VEVTHDLQKH	LAGLGLTEAI	DKNKADLSRM	SGKKDLYLAS
Cani	AVAISLPKGV	VEVTHDLQKH	LAGLGLTEAI	DKNKADLSRM	SGKKDLYLAS
Gal	SVAISLPKVV	LEVSHDLQKH	LADLGLTEAI	DKTADLSKI	SGKKDLYLSN
Zeb	AVAISLPKVS	MEVSHDLQKH	LGELGLTEAV	DKPKADLSNI	SGKKDLYLSN
Gol	AVAVSLPKVS	VEVSHDLQKH	LTELGLTEAV	DKAKADLSNI	SGKKDLYLSN
Mel	RVNVVMPTEFK	YHFITNMREH	IQKN...SA	HRFDVDFEPA	FG.VETKIN
Chan	AVAVSLPKIS	MEVSHNLQKY	LGELGVTEAV	DKTADLSNI	SGKKDLYLAN
Amaz	SVAISLPKVV	LEVSHDLQKH	LADLGLTEAI	DKTADLSKI	SGKKDLYLSN
Bran	AVAISLPKGV	VEVTHDLQKH	LAGLGLTEAI	DKNKADLSRM	SGKKDLYLAS
Gree	AVAISLPKVS	LEVSHDLQKH	LADLGLTEAM	DKNKADLSKI	SGKKDLYLSN
Roc	KKRSVAISLP	KVVLEVSHDL	QKHLADLGLT	EADTKADL	SKISGKKDLY
Sque	QTKAVAISLP	KGVVEVTHDL	QKHLATLGLT	EADKNKADL	SRMSGKKDLY
Yak	QKKAVAISLP	KGVVEVTHDL	QKHLAGLGLT	EADKNKADL	SRMSGKKDLY
Blac	QKKAVAISLP	KGVVEVTHDL	QKHLAGLGLT	EADKNKADL	SRMSGKKDLY
Nake	QKKAVAISLP	KGVVEVTHDL	QKHLAGLGLT	EADKNKADL	SRMSGKKDLY
Chin	QKKAVAISLP	KGVVEVTHDL	QKHLAGLGLT	EADKNKADL	SRMSGKKDLY
Dama	QKKAVAISLP	KGVVEVTHDL	QKHLAGLGLT	EADTKADL	SRMSGKKDLY
Medi	EVRNVNVLMP	TFKYSFITNL	KEDILDK...	.SDHRFDSDF	ENSFSKEKDF
Aust	ERHTVSVSLP	KVNLEVSHDL	QKYLQELGLT	EAVDNKADF	SGITGKKNLH

Homo	VFHATAFELD	TDGNPFQDI	YGREELRSPK	LFYADHPFIF	LVRDTQSGSL
Rat	VFHATAFEWD	TEGNPFQDI	YGREELRSPK	LFYADHPFIF	LVRDNQSGSL
Mus	VFHATAFEWD	TEGNPFQDI	YGREELRSPK	LFYADHPFIF	LVRDNQSGSL
Cani	VFHATAFEWD	TEGNPFQDI	YGREELRSPK	LFYADHPFIF	LVRDTQSGSL
Gal	VFHAAALEWD	TDGNPYDADI	YGREEMRNPK	LFYADHPFIF	MIKDSKTNSI
Zeb	VFHASSELEWD	TEGNPFDPISI	FGSEKMRNPK	LFYADHPFIF	LVKDNKTNSI
Gol	VFHASAMEWD	TEGNPPDTSI	YGTDLKTPK	LFYADHPFIF	LVKDKKTNSI
Mel	IFQTTLVQFD	GSG.RARVED	YEKIRTTKYE	RFHVRPFAF	YIKEKSTGRI
Chan	VFHASAFEWD	IAGNPADTSI	FGTDKVNPK	LFYVDHPFIF	LVKDKSTGSI
Amaz	VFHAAALEWD	TEGNPYDADI	YGREEMRNPK	LFYADHPFIF	MIKDSKTNSI
Bran	VFHATAFEWD	TEGNPFQDI	YGREELRSPK	LFYADHPFIF	LVRDSQTGSL
Gree	VFHAAALEWD	TEGNPFDAI	YGREEMRNPK	LFYADHPFVF	VIKDNKTNSI
Roc	LSNVFHATAL	EWDTEGNPYD	ADIYGREEMR	NPKLFYADHP	FIFMIKDNKT
Sque	LASVFHATAF	ELDTEGNPFD	QDIYGREELR	SPKLFYADHP	FIFLVRDTQS
Yak	LASVFHATAF	EWDTDGNPFD	QDIYGREELR	SPKLFYADHP	FIFLVRDTQS
Blac	LASVFHATAF	EWDTEGNPFD	QDIYGREELR	SPKLFYADHP	FIFLVRDSQS
Nake	LASVFHATAF	EWDTEGNPFD	QDIYGREELR	SPKLFYADHP	FIFLVRDTQS
Chin	LASVFHATAF	EWDTDGNPFD	QDIYGREELR	SPKLFYADHP	FIFLVRDNQS
Dama	LASVFHATAF	EWDTEGNPFD	QDIYGREELR	SPKLFYADHP	FIFLVRDTQS
Medi	LN.IFKVAAI	SFNGTGKPRV	EDYQNIR.SA	KYEKFHVDRP	FVYYIEN.KY

```

Aust      LSGMLHATAI DWDTEGNQFD QDWNSPEITK SAKV FYADHA YIFLIRDNKT

Homo      LFIGRLVRPK GDKMRDEL
Rat       LFIGRLVRPK GDKMRDEL
Mus       LFIGRLVRPK GDKMRDEL
Cani      LFIGRLVRPK GDKMRDEL
Gal       LFIGRLVRPK GDKMRDEL
Zeb       LFIGRLVRPK GDKMRDEL
Gol       LFMGRLVQPK GDKMRDEL
Mel       VCIGKVLNPV Q.....
Chan      LFIGRLVRPK GEKMRDEL
Amaz      LFIGRLVRPK GDKMRDEL
Bran      LFIGRLVRPK GDKMRDEL
Gree      LFIGRLVKPK GDKMRDEL
Roc       NSILFIGRLV RPKGDKMRDEL
Sque      GSLLFIGRLV RPKGDKMRDEL
Yak       GSLLFIGRLV RPKGDKMRDEL
Blac      GSLLFIGRLV RPKGDKMRDEL
Nake      GSLLFIGRLV RPKGDKMRDE L
Chin      GSLLFIGRLV RPKGDKMRDE L
Dama      GSLLFIGRLV RPKGDKMRDE L
Medi      GEIVCIGKVE NPEQ.....
Aust      NSILLIGRLV KPKSNDHDEL .

```

Figure S1. Multiple sequence alignment of Hsp47 showing conserved residues in different species. The KDEL sequence is highlighted in Green, active site 383 Y is highlighted in Blue, Histidine involved in protonation are highlighted in Red. RCL loop in Grey and Aspartic acid and Histidine are highlighted in Yellow and Pink.

Chapter 2

Sr.No	Title	Detail Plasmid & Genetic Construct	Yield (200 mL culture)
1	H ₄₇	cHsp47strepPJexp411	183.26 ng (with impurities)
2	H _{47N}	EGFPHsp47strepTagpeT28a EGFPHsp47strepTagpBAD	207.8 µg 65.98 ng
3	H _{47Y<ONBYhv}	EGFPHsp47strepTag383TAGMutpBAD	43.56 ng
4	H _{47Kdel}	EGFPHsp47strepTag C terminal KDEL Deletion peT28a	65.98ng
5	H _{47Y<R}	EGFPHsp47strepTag MutY383R peT28a	45.85 ng
6	EGFP	EGFPpeT28a	359.95 ng

Table S1. Yield of the synthesis of Hsp47 mutants calculated from absorbance measurement using Nano drop UV spectrophotometer.

Sr.No	Title	Detail Plasmid & Genetic Construct	Primers
1	H _{47N}	EGFPHsp47strepTagpeT28a	tttGAATTCATGCTGAGCCCGAAAGCC
			tttCTCGAGTTATTTCTCAAATTGCGGGTGG
		EGFPHsp47strepTagpBAD	tttCCATGGTGAGCAAGGCGAG
			tttCTCGAGTTATTTCTCAAATTGCGGGTGG
2	H _{47Y<ONBY}	EGFPHsp47strepTag383TAGMutpBAD	AGCTGTTTTagGCGGATCATCCG
			TCGGGAACGCAGCTCTT
3	H _{47KDEL}	EGFPHsp47strepTag C terminal KDEL Deleted peT28a	CTGGAATCCGCTTGGAGC
			GTCGCCCTTTGGACGGAC
4	H _{47Y<R}	EGFPHsp47strepTag MutY383R peT28a	GAAGCTGTTTcgCGCGATCATCC
			GGGGAACGCAGCTCTCA
5	EGFP	EGFPpeT28a	CTGGAATCCGCTTGGAGC
			GTCGCCCTTTGGACGGAC

Table S2. Primers used for developing H_{47YN}, H_{47Y<ONBY} and other mutants.

hsp47

ATG CGC TCC CTC CTG CTT CTC AGC GCC TTC TGC CTC CTG GAG GCG GCC CTG GCC GCC GAG GTG AAG AAA CCT GCA GCC GCA GCA GCT CCT GGC ACT GCG GAG AAG
TTG AGC **CCG** AAG GCG GCC **ACG** CTT GCC GAG CGC AGC GCC GGC CTG GCC TTC AGC TTG TAC CAG GCC ATG GCC AAG GAC CAG GCA GTG GAG AAC ATC CTG GTG TCA
GGG GTG GTG GTG GCG TCG TCG **GUA** **GGG** CTC GTG TCG CTG GGC GGC AAG GCG ACC **ACG** GCG TCG CAG GCC AAG GCA GTG CTG AGC GCC GAG CAG CTG GCG GAC
GAG GAG GTG CAC GCC GGC CTG GGC GAG CTG CTG GCG TCA CTC AGC AAC TCC **ACG** GCG GCG AAC GTG ACC TGG AAG CTG GGC AGC **CGA** CTG TAC **GGA** **ACT** AGC
TCA GTG AGC TTC GCT GAT GAC TTC GTG GCG AGC AGC AAG CAG CAC TAC AAC TGC GAG CAC TCC AAG ATC AAC TTC GCG GAC AAG GCG AGC GCG CTG CAG TCC ATC
AAC GAG TGG GCC GCG CAG ACC ACC GAC GGC AAG CTG **ACT** GAG GTC ACC AAG GAC GTG GAG GCG **ACG** GAC GGC GCC CTG **GUA** GTC AAC GCC ATG TTC TTC AAG
CCA CAC TGG GAT GAG AAA TTC CAC CAC AAG ATG GTG GAC AAC CGT GGC TTC ATG GTG ACT **CGG** TCC TAT ACC GTG GGT GTC ATG ATG CAC **CGG** ACA GGC CTC TAC
AAC TAC TAC GAC GAC GAG AAG GAA AAG CTG CAA ATC GTG GAG ATG **ACT** CTG GCC CAC AAG CTC TCC AGC CTC ATC ATC CTC ATG **ACT** CAT CAC GTG GAG CCT CTC
GAG GCG CTT GAA AAG CTG **GUA** ACC AAA GAG CAG CTG AAG ATC TGG ATG **GGG** AAG ATG CAG AAG AAG GCT GTT GCC ATC TCC TTG **GGG** AAG GGT GTG GTG GAG GTG
ACC CAT GAC CTG CAG AAA CAC CTG GCT **GGG** CTG GGC CTG ACT GAG GCC ATT GAC AAG AAC AAG GCC GAC TTG TCA GCG ATG TCA GGC AAG AAG GAC CTG TAC CTG
GCC AGC GTG TTC CAC GCC ACC GCC TTT GAG TTG GAC ACA GAT GGC AAC **ACT** TTT GAC CAG GAC ATC TAC **GGG** GCG GAG GAG CTG GCG AGC **ACT** AAG CTG TTC TAC
GCC GAC CAC **ACT** TTC ATC TTC **GUA** GTG **GGG** GAC ACC CAA AGC GGC TCC CTG **GUA** TTC ATT **GGG** GCG CTG GTC **GGG** CCT AAG GGT GAC AAG ATG **CGA** GAC GAG TTA

FiguresS1.31 Rare codon analysis of Hsp47 in *E.coli*

Experimental Materials and Methods:

Experimental Materials & Methods:

Strategy 1:

Cloning and Expression of Human Hsp47 (hHsp47):

The IMPACT system was used for expression of hHsp47. Truncated version of hHsp47 cDNA (1-378 R a.a) (BB1) and full length hHsp47 were sub cloned into pMiniT vector, finally it was cloned into pTXB1 vector (New England Bio labs) (such that the truncated version was constructed just before Intein protein gene in between Nde1 and Sap1 site). The expression was induced in BL21(DE3) cells grown to an OD600 of 0.6 –0.7 by adding 0.1mM, 0.5 mM, 1mM isopropyl- β -D-thio-galactoside (IPTG) and shaking for 5 h at 37 °C, 8 hr at 30° C , 16 hr at 25° C and 18 hr at 15° C. The protein condition using 0.1 mM and 15 degree for 18 hr solved the solubility issue of preventing inclusion bodies formation up to certain extent. However, it was difficult to purify this small amount of protein using chitin beads affinity purification approach. Initially buffer recommended by manufacturer's protocol was used for purification of truncated version of hHsp47 i.e. Lysis buffer & column buffer (20 mM Na-HEPES pH 8.5, 500 mM NaCl ,1 mM EDTA ,Nonionic detergents (0.2% Tween 20) and protease inhibitors [PMSF (20 μ M)]. To avoid degradation of protein due to oxidation about 1 mM of TCEP [tris-(2-carboxyethyl) phosphine] added. The truncated version of protein was cleaved using on column cleavage buffer (20 mM Na-HEPES pH 8.5 , 500 mM NaCl,50 mM 2-mercaptoethanesulfonic acid) was used. For purification of full length hHsp47 the cells were harvested using Lysis buffer & column buffer (20 mM Tris HCL pH 8.5, 500 mM NaCl ,1 mM EDTA ,Nonionic detergents (0.2% Tween 20) and pro-tease inhibitors [PMSF (20 μ M)] , 1 mM of TCEP [tris-(2-carboxyethyl)phosphine]). The protein was cleaved using on column cleavage buffer (20 mM Tris HCl pH 8.5 , 500 mM NaCl,50 mM DTT or β -mercaptoethanol) .

Due to restriction with the synthesis of photo caged peptide of about (41 mer); the truncated hHs47 was design to have Arg at its C terminus end. But unfortunately it's cleavage conditions were difficult for Hsp47 to withstand the temperature (23 °C for 40 hrs).³²³ In order to facile the protein extraction and cleavage procedure another approach was used which included harvesting the T7 express cells using Lysis Buffer (100 mM TrisHCl (pH 7.5), 500 mM NaCl , 0.5 mM EDTA , 0.1%(v/v) Tween 20) following which the unbound proteins on the chitin beads were washed 10-15 times the bed volume of beads with Wash Buffer 1 (50 mM TrisHCl (pH 7.4) ,1000 mM NaCl,0.5% (v/v) Tween 20) and then 5 times using Wash Buffer 2 (sodium phosphate buffer(pH 7.4) ,50 mM NaCl) .The proteins bound onto the beads were incubated with Elution buffer. To optimize the cleavage conditions following conditions were studied by incubating the protein in three different elution buffers containing (A: Sodium phosphate buffer(pH 7.4) ,50 mM NaCl, 100mM MESNA, B: Sodium phosphate buffer(pH 7.4), 50 mM NaCl,100mM β Mercaptoethanol; C: Sodium phosphate buffer(pH 7.4),50 mM NaCl,100mM DTT) Fig.³²⁴ In order to improve the expression of full length hHsp47, it was further cloned into p RSETB plasmid using BamH1 and EcoR1 site .³²⁵ The positive clone was confirmed by sequencing and was transformed into T7 express cells. This did not help much as most of the protein was still found in the inclusion bodies even though the induction and expression studies were performed. Also, full length version of hHsp47 and truncated hHsp47+Intein was cloned in pTriX-mcherry-Lov2-Ja vector (Addgene 81041) using BamH1 and HindIII site such that

mcherry was attached at the N terminus of hHsp47 to improve the solubility. This construct was transformed into Rosetta-gami 2(DE3) pLacI having p RARE plasmid for gene optimization which could slightly help in expressing truncated version of hHsp47. The p RSETB and pTrix constructs were purified using Ni-NTA His-Tag affinity purification approach.

Strategy 2:

Cloning and purification

The psfGFP150TAGPyIT-His6pBad plasmid encoding for MbPyIT and C-terminal hexahistidine-tagged sfGFP, with an amber stop codon at position 150 (pBad), and pBK-ONBYRS expressing MbPylS mutant was a gift from Prof. Dr. Jason Chin, Medical Research Council Laboratory of Molecular Biology, University of Cambridge, UK¹⁹⁵. A construct encoding amino acids 36–418 of the canine Hsp47 (canine SERPINH1 mRNA, NCBI accession NM_001165888), cloned into the pJExpress vector with a C-terminal Strep II tag was gift from Prof. Dr. Ulrich Baumann, University of Cologne, Germany³²⁶.

The canine-derived synthetic Hsp47 gene from pJExpress plasmid was cloned in pET28a plasmid at the C terminus of EGFP gene using EcoRI and XhoI sites and transformed in NEB5 α cells using manufacturer's protocol (NEB C29871). Colonies were picked up and insert screening was performed using colony PCR and confirmed with sequencing following which positively cloned constructs were selected and were further cloned into psfGFP150TAGPyIT-His6pBad plasmid at NcoI and XhoI site to develop pEGFPHsp47StrepIItagpBad construct. This construct was used to optimize protein expression conditions and was used as a backbone for developing the final construct pEGFPHsp47TAG 383 StrepIItagpBad construct (described later). Colonies were picked up and insert screening was performed using colony PCR approach and sequencing following which positively cloned constructs were selected and transformed into One shot top10 cells for protein expression using strepTag2 purification. Transformed cells were grown to OD600 of 0.8 in LB medium containing kanamycin (Kan) (25 μ g/ml) and tetracycline (Tet) (12.5 μ g/ml). These cells were pelleted and the medium was exchanged in sterile environment with pre-warmed Terrific broth containing kanamycin (25 μ g/ml) and tetracycline (12.5 μ g/ml) and protein expression was induced after half an hour with 0.2 % arabinose at 37°C / 250 rpm. After induction, the cultures were incubated for 1 hour at 37°C / 250 rpm following which it was kept at 25-30°C / 180 rpm cells overnight. The cultured cells were harvested and pellets stored at -80 °C. Cells were resuspended in lysis buffer (50 mM Tris ·HCl (pH 7.5), 150 mM NaCl, 100 μ M PMSF, 4 mM DTT) and lysed by sonication. Cleared lysates were loaded onto 1 ml Streptactin Superflow high capacity binding column (IBA) and eluted with 2.5 mM (D)-desthiobiotin in lysis buffer excluding PMSF.

For the expression of photoactivatable Hsp47 (H_{47Y<ONBY}), E. coli TOP10 cells co-transformed with pBK-ONBYRS and pEGFPHsp47TAG 383 StrepTagIIPBad (encoding for N terminal EGFP tagged cHsp47 and C-terminal strepIItag with an amber stop codon (TAG) at position 383). The TAG mutation at 383rd position was incorporated with NEB Q5 site-directed mutagenesis kit using manufacturer's protocol (NEB E0554S). Transformed cells were incubated overnight with shaking at 37°C in LB supplemented with Kan (25 μ g/ml) and Tet (12.5 μ g/ml). The overnight culture was diluted 1:100 in two separate volumes of terrific broth (TB) supplemented with the same concentration of

antibiotics and incubated with shaking at 37°C. At OD600= 0.8 bacteria were isolated by centrifugation and re-suspended in equal volumes of warm TB supplemented with the same concentration of antibiotics, in the presence or absence of 0.4 mM of O-[(2-Nitrophenyl)methyl]-L-tyrosine hydrochloride (Santa Cruz Biotech). After 30 min, protein expression was induced with the addition of arabinose at a final concentration of 0.2% (w/v). Induction studies were performed with different temperature conditions after induction incubation for 1 hour at 37°C / 250 rpm following with 25-30°C / 180 rpm cells overnight was chosen as optimized expression condition. The cultured cells were harvested and pellets stored at -80 °C. Cells were resuspended in lysis buffer (50 mM Tris ·HCl (pH 7.5), 150 mM NaCl, 100 µM PMSF) and lysed by sonication. 20µL of the clear lysates were taken incubated with 5 µL of Strep II tagged agarose beads (IBA Life sciences) for 5 min. Previously purified H_{47N} (His-tagged) and H_{47N} (strepIItagged) were used as controls. The beads were then spun down at 1000 rcf for 30 s and washed 2 times with PBS. For purification, cleared lysates were loaded onto 1 ml Strepactin Superflow high capacity binding column (IBA Life sciences) and eluted with 2.5 The bead solutions were placed in 96 well-plate wells and imaged using the Nikon Ti-Eclipse microscope. mM (D)-desthiobiotin in lysis buffer excluding PMSF. The soluble fraction for both H_{47N} and H_{47Y<ONBY} was concentrated and purified further by gel filtration (Superdex S75; GE Healthcare) in buffer A [20 mM Hepes (pH 7.5), 300 mM NaCl, 4 mM DTT]. The strepIItag at C terminus was chosen as a selection marker for ONBY incorporation which was confirmed by Alexa 488 labeled Streptavidin against the strepIItag at the C terminus of H_{47Y<ONBY}. The bacteria which were not fed with ONBY in the medium produced truncated or incomplete H_{47Y<ONBY} because of the TAG mutation. A Western Blot was performed by running protein samples on SDS page. The 12% SDS PAGE gel was transferred using blotting chamber to PVDF membrane. The Blotted PVDF Membrane was blocked with Blocking buffer (0.5% milk powder in PBST (0.1 w/v)) for 20 mins. The excess blocking buffer was washed of three times using PBST (0.1 w/v) and then stained using labeled Fluorescent Alexa 488 streptavidin with a dilution of 1:500 for 20 mins. The excess streptavidin was washed of three times using PBST (0.5 w/v) and image RGB Blot in Gel doc.

In order to have controls for protein and cell based assays the N-terminal E GFP tagged cHsp47 pet28a plasmid were modified to develop variants. The variants were a. EGFP-Hsp47 383 Y<R pet28a (encoding H_{47Y<R} with Tyrosine mutated to Arginine at 383rd position).b. KDEL del EGFP-Hsp47 pet28a (encoding H_{47Kdel} without KDEL sequence at the C terminus). All the mutants were developed using NEB site-directed mutagenesis kit (NEB E0554S) and transformed into NEB 5 α cells for plasmid extraction and sequencing analysis. Positive clones were transformed in BL21 (DE3) Clear coli cells for His-tagged Ni-NTA chromatography. Expression was induced in BL21 (DE3) cells grown to an OD600 of 0.6–0.7 by adding 0.5 mM isopropyl-β-d-thio-galactoside and shaking overnight at 25 °C. Cells were resuspended in lysis buffer (300 mM NaCl, 10 mM imidazole, 20 mM Tris, pH 8) and lysed by sonication. Cleared lysate was purified by Ni-NTA affinity chromatography (Ni-NTA superflow; Qiagen). The soluble fraction was concentrated and purified further by gel filtration (Superdex S75; GE Healthcare) in buffer A [20 mM Hepes (pH 7.5), 300 mM NaCl, and 4 mM DTT]. EGFP-pet28a was purified using same approach.

Chapter 3

Experimental Materials and Methods:

Collagen micro patterned affinity binding assay with Hsp47 variants

Collagen micro patterns were made by adapting a reported protocol^{254, 327}. Glass cover-slips were cleaned by 5 min air plasma treatment (Harrick Plasma, Ithaca, NY, USA). In a 20×20×0.25 μm³ Poly(dimethylsiloxane) (PDMS) membrane having square, nine 3×3 mm² wells. The PDMS membrane was placed on the plasma treated cover-slip. In each 3×3 mm² well, 5 μL of a 0.1 mg/mL PLL-g-PEG (PLL (20)-g [3.5]-PEG (5), SuSoS AG, Dübendorf, Switzerland) solution in phosphate buffered saline (PBS) was incubated for 1 h. Next, the wells were incubated with 5μL of photo initiator (4-benzoylbenzyltrimethyl ammonium chloride) solution (custom synthesis by Sigma-Aldrich outsourced to SinoChem, China) for 1 minute. A wide field mass less UV projection was employed for making 10 μm patterns for 10 sec having 50%intensity at 365 nm wavelength. The optical projection system is based on a standard epi-fluorescence inverted microscope (Nikon Ti-Eclipse microscope, Nikon Instrument, France) coupled with a Digital Light Processing device (Texas-Instrument DLP Discovery 4100 UV) including a DMD (PRIMO unit) to generate spatially modulated excitation patterns^{254, 327}.The UV exposure cleaves the PEG chains at the exposed sites on the substrate. After extensive rinsing with PBS, the micro wells were filled with 10 μL of 200ug/mL rat tail collagen I (Fisher Scientific) in H₂O (Diluted from Rat tail collagen stock of 3mg/mL). Collagen adsorbs on the UV exposed areas. The wells with the collagen patterns were incubated for 10 mins with 1μM solutions of H_{47N}, H_{47Y<R}, H_{47Kdel}, H_{47Y<ONBY} or EGFP in PBS. For *in situ* photo activation of H_{47Y<ONBY}, the well filled with H_{47Y<ONBY} was irradiated 10 s with a PRIMO unit at 365 nm and 50% intensity. Fluorescence imaging was done using a Nikon Ti-Eclipse microscope.

Native PAGE Western Blot

3mg/mL rat tail collagen Type 1 (Fischer Scientific) was diluted in sterile D/W to a concentration of 200ug/mL. H_{47N}, H_{47Y<R}, H_{47Y<ONBY}, H_{47Y<ONBYhv}, H_{47Kdel} and EGFP solutions at 1.2μM concentration were mixed with collagen solutions in 2:1 ratio. The samples were incubated overnight at 4°C. 20ul were run in Native PAGE 4-16% Bis-Tris Protein Gel (Invitrogen).The proteins were blotted on PVDF membrane for WB. Anti-Collagen Type I (RABBIT) Antibody - 600-401-103-0.1 (Rockland antibodies and assays), Secondary; Goat anti-Rabbit IgG (H+L) Highly Cross-Adsorbed Secondary Antibody, Alexa Fluor 647(Invitrogen) in 1:500 dilution were used for WB.

Fibrillation Assay

Collagen Type I solution (3mg/mL, Fisher Scientific) was diluted to 0.4 mg/ml with minimal essential medium (MEM) Buffer (1x) and pH was adjusted to 7.5 with 1 M sodium hydroxide (Sigma-Aldrich). This process has to be done within 4 min to prevent premature polymerization.²³⁷ The collagen solution was mixed with 1.2 mM solutions of H_{47N}, EGFP, H_{47Y<R}, H_{47Y<ONBY} or H_{47Y<ONBY_{hV}} in MEM at molar ratio 1:2. The final concentration of collagen was 0.2 µg/ml(0.6 µM). A 0.2 µg/ml collagen solution was also used as a positive control. 100µl of the COL/Hsp47 variant mixture were transferred to a precooled 96 well plate and absorbance at 600 nm was recorded with a Spectra Max UV plate reader during 40 min. The optical density of the Collagen solution at 600 nm was measured under different conditions. This wavelength does not interfere with the UV spectrum of ONBY. The H_{47Y<ONBY} solution was irradiated at 365 nm for 5 mins for activation.

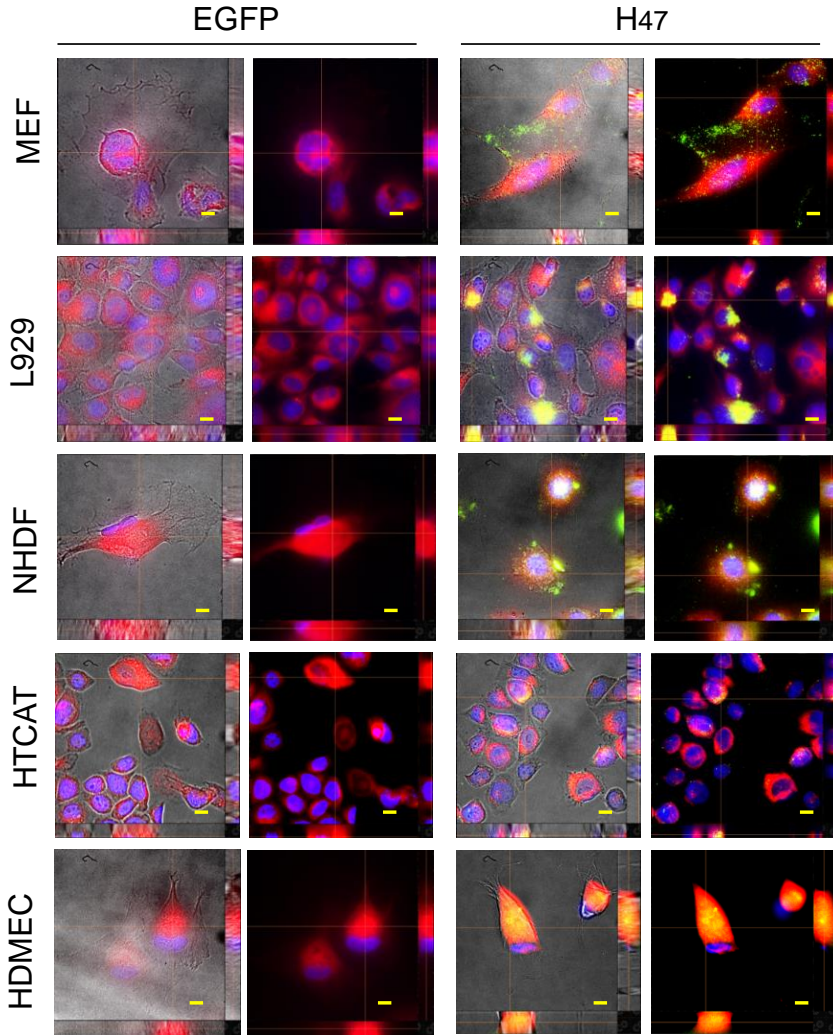
Rheology assay

For Rheology measurements Rat tail collagen (3mg/mL) (Thermo fisher Scientific) was diluted to 2 mg/mL concentration in MEM or PBS and was neutralized to pH to 7.5 with sodium hydroxide within 4 min. DHRIII Rheometer (TA Instruments) was used for the measurements of 50 µl of the collagen solution placed between two parallel plates of 8 mm diameter cooled at 4°C. The shear moduli (G') were measured at frequency ω - 30-0.03 rad/s while temperature was increased to 40°C at 0.1°C/min.

Statistical analysis

In Fibrillation Assay and Rheology each data point represents the technical mean of (n=3) experiments including standard deviation represented by error bars. The data were plotted with the absorbance values. All the experiments are performed in triplicates.

Chapter 4



C

Figure S1. Z stack images of NHDF, L929, MEF, HaCaT and HDMEC after incubation with H47 for 3 h. Images show co localization of H47 and ER signals. (Blue: DAPI (Nucleus), Green: (Hsp47), and Red: ER tracker dye). Right side: H47 treated cell lines. Left side: EGFP treated cell lines. Scale: 20 μm .

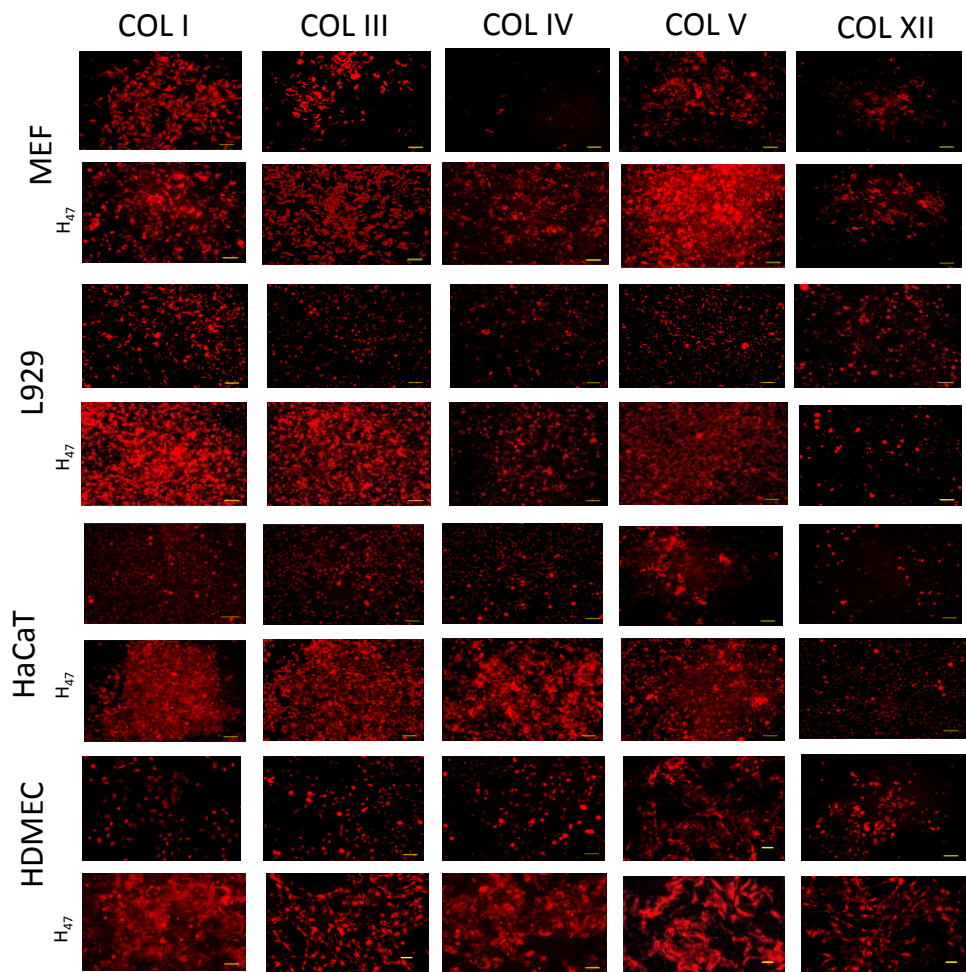


Figure S2. Immunostaining of COL I, III, IV, V and XII deposited in MEF, L929, HaCaT and HDMEC cultures after incubation with H47 and corresponding controls. (Scale corresponds to 250 μ m).

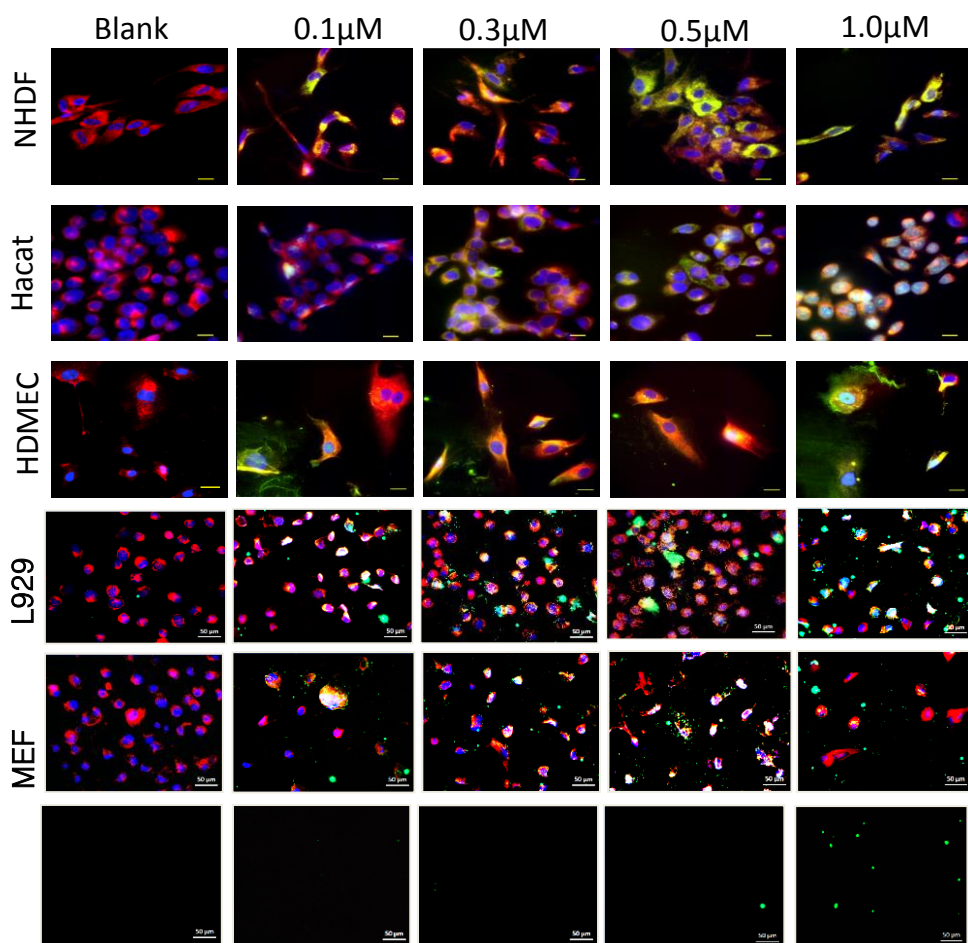


Figure S3. Immunostaining of ER with ER tracker dye shown in Red in NHDF, HaCaT, HDEMIEC, L929 and MEF cells treated with different concentration of H₄₇. (Scale corresponds to 50 μ m).

Experimental details:

Cell delivery assay

Hsp47^{+/+} and Hsp47^{-/-} MEFs derived from Lethal Mouse Embryos [2] were gifted by Prof. Dr. Kazuhiro Nagata, Kyoto Sangyo University, Japan, L929 fibroblasts (ATCC CRL-6364), NHDF (Promo Cell C-12302), HaCaT (ATCC® PCS-200-011) and HDMEC (Promo Cell C-12210) were purchased from commercial suppliers.

MEF, L929, NHDF and HaCaT cells were seeded on 15 well Ibidi μ -Slide Angiogenesis plate (20,000 cells per well) with DMEM GlutaMax (Gibco) containing 10% fetal bovine serum (FBS; Gibco) and Penicillin-Streptomycin (Pen-strep) antibiotic. HDMEC cells were seeded using 199medium with endothelial growth supplement (Gibco), 10% fetal bovine serum (FBS; Gibco) and Pen-strep antibiotics (20,000 cells per well) After 24 h, cells were incubated with varying concentration of H₄₇ (0.1 μ M-1 μ M) for 3 h. After incubation, the medium was removed and cells were washed once with sterile Assay buffer (1X) provided in the kit. Dual staining solution (for nucleus and ER) was prepared by mixing 1 μ l of ER tracker dye (ER Staining Kit - Red Fluorescence - Cytopainter (ab139482)) with 1 μ l of DAPI in 1 ml of ER Assay buffer (1X) provided in the kit. The cells were incubated with 60 μ l of Dual staining solution per well at 37°C for 1 h. Cells were washed with Assay buffer (1X) once, fixed with 4% PFA for 10 mins and washed three times with Assay buffer (1X). All the experiments were done in triplicate.

Quantification of H₄₇ uptake by different cell types

Imaging of the cell cultures was performed using Nikon NT microscope (60X objective). The number of cells showing both H₄₇ signal with ER tracker signal were counted and represented in percentage. Maximum of 100% was considered if all cells showed EGFP green signal from H₄₇ with ER signal. This analysis was performed on all cell types. All the analysis was done using Image J and graphs were plotted using graph prism software for three independent experiments for each cell types.

Sirius Red Assay for quantification of Collagen deposition and Immuno-staining

Cells were cultured in 24 well plate for 24 hours (50K cells per well). Cells were incubated with 0.5 μ M solutions of H₄₇ in DMEM and M191medium for 3 h, followed by medium exchange and cultured for 24 h. For Sirius Red assay cells were fixed using Bouin solution (75% picric acid, 10% formalin, and 5% acetic acid) (Sigma HT10132). Collagen deposited in the wells was stained by incubating with 0.1% Sirius red in picric acid (ab150681) for 1 h and washing with 0.01 N HCl. The matrix was dissolved in 0.1 N NaOH and the absorption of the slurry was measured at 570 nm using a Biolumin960k

spectrophotometer^[1, 2e] The absorbance values (Figure 3 in manuscript) were normalized by the value of collagen deposition from untreated MEF cells.

For immunostaining the cultures were decellularized using a previously established protocol ^[3], fixed and stained with Collagen-specific antibodies. Cultures were treated with 0.5% Triton X-100 and 20mM NH₄OH for 5 min at 37 °C for decellularization The deposited matrix on the culture substrate was blocked with 5% Goat serum in PBS and stained for COL I,III,IV,V and XII with primary antibodies as recommended by supplier (Rabbit polyclonal anti-type I collagen, 600-401-103-0.1 (Rockland), Collagen III Polyclonal Antibody (Thermo fisher, PA5-34787), Anti-COL4A3 antibody (Sigma,HPA042064-100UL), Anti-Collagen V antibody (ab7046), Anti-COL12A1 antibody (Sigma,HPA070695) (dilution 1:200 for all the antibodies)). Samples were washed 3 times with PBS and stained with secondary antibody (goat anti-Rabbit IgG (H+L) Highly Cross-Adsorbed Secondary Antibody, Alexa Fluor 647, A-21245 (dilution 1:200)). For analysis, the mean gray value of fluorescent intensity was measured for each collagen subtypes and subtracted from background mean gray value of fluorescent intensity by imaging cells stained with only secondary antibody. Results were normalized by taking untreated MEF cells as 1.

Statistical significance

For Sirius Red assay (n=6) number of experiment were performed and plotted with graphs including whisker plots representing standard deviation for MEF, L929, NHDF, HaCaT and HDMEC. For immunostaining quantification IMAGE J was used to quantify mean intensity profile of stained matrices in all cell types treated with and without H₄₇ with bar plots including error bars indicating standard deviation. In both assays the data were normalized with respect to collagen deposited in MEF untreated as 1. Statistical significance was analyzed by Tukey test, which shows significant differences between conditions. Significance was calculated by comparing non treated vs. treated cells (mean±SD, ANOVA, *** p<0.001).

Chapter 5

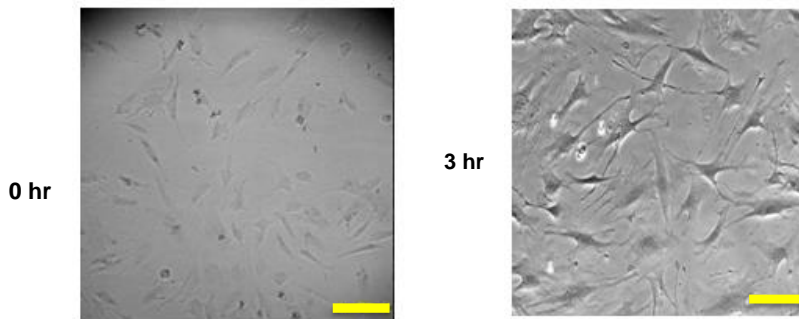


Figure S1. Bright field images of Hsp47 (+/+) cells showing changes in cell morphology 3 hours after delivery of H₄₇ (Scale:100 μ m).

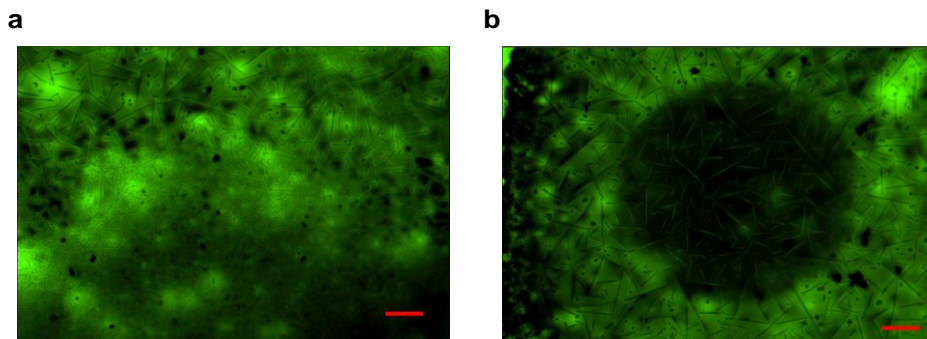


Figure S2: a. Fluorescence image of plastic 24 well plate bottom (which one) coated with fluorescent green highlighter ink (Pelikan Text marker 490). **b.** A 1.13 mm² area of this surface was photo bleached for 3 mins by UV exposure at 405 nm (Scale.200 μ m)

Experimental Materials and Methods:

Immunostaining and Western blot for collagen subtypes on Hsp47 delivery

Hsp47^{+/+} and Hsp47^{-/-} cells were cultured in 24 well plate for 24 hours (50K cells per well). Cells were incubated with 0.5 μ M solutions of H47 in DMEM and M191 medium for 3 h, followed by medium exchange and cultured for 24 h. For immunostaining the cultures were decellularized using a previously established protocol [3], fixed and stained with Collagen-specific antibodies. Cultures were treated with 0.5% Triton X-100 and 20mM NH₄OH for 5 min at 37 °C for decellularization. The deposited matrix on the culture substrate was blocked with 5% Goat serum in PBS and stained for COL I,III,IV,V and XII with primary antibodies as recommended by supplier (Rabbit polyclonal anti-type I collagen, 600-401-103-0.1 (Rockland), Collagen III Polyclonal Antibody (Thermo fisher, PA5-34787), Anti-COL4A3 antibody (Sigma,HPA042064-100UL), Anti-Collagen V antibody (ab7046), Anti-COL12A1 antibody (Sigma,HPA070695) (dilution 1:200 for all the antibodies)). Samples were washed 3 times with PBS and stained with secondary antibody (goat anti-Rabbit IgG (H+L) Highly Cross-Adsorbed Secondary Antibody, Alexa Fluor 647, A-21245 (dilution 1:200)). For analysis, the mean gray value of fluorescent intensity was measured for each collagen subtypes and subtracted from background mean gray value of fluorescent intensity by imaging cells stained with only secondary antibody. Results were normalized by taking untreated MEF Hsp47^{-/-} cells as 1. In MEF Hsp47^{-/-} untreated cells were considered as 1. This analysis was performed in Image J.

For Western blot, deposited collagen from cells cultured in presence and in the absence of H₄₇ was suspended in 2mL RIPA Buffer and 200 μ L. Before this step, the collagen deposited was decellularized using above mentioned protocol. Protease inhibitor and mixed with Lameli buffer (4x stock concentration). The samples were loaded into SDS-Gels and run at 150V for 80mins. The 12% SDS PAGE gels were transferred using blotting chamber to PVDF membranes. The Blotted PVDF Membranes were blocked with Blocking buffer (0.5% milk powder in PBST (0.1 w/v)) for 20 mins. The excess blocking buffer was washed off three times using PBST. The PVDF membranes were incubated overnight at 4°C with: rabbit polyclonal anti-type I collagen (Rockland, 600-401-103-0.1), Collagen III Polyclonal Antibody (Thermo fisher, PA5-34787), Anti-COL4A3 antibody (Sigma, HPA042064-100UL), anti-Collagen V antibody (ab7046), or anti-COL12A1 antibody (Thermo fisher, HPA070695) at 1:200 dilution. For α -Smooth Muscle (α -SMA) condition cells were not decellularized and antibodies used were Anti-Actin, α -Smooth Muscle - Cy3 (C6198) On the following day the excess was washed off three times using PBST (0.5 w/v) and the sample was stained with secondary antibody for 1 h at room temperature (Goat anti-Rabbit IgG (H+L) Highly Cross-Adsorbed Secondary Antibody, Alexa Fluor 647, A-21245

(dilution 1:200)) (1:500 dilution). The PVDF membrane after staining was visualized under Gel Doc. All the experiments were done in triplicate.

Sirius Red Assay for quantification of Collagen deposition and Immunostaining for H_{47Y<ONBY}

Hsp47^{+/+} and Hsp47^{-/-} MEFs derived from Lethal Mouse Embryos were gifted by Prof. Dr. Kazuhiro Nagata, Kyoto Sangyo University, Japan^{77, 100, 145, 328-330}. Cells were cultured in 24 well plate with high glucose DMEM Glutamax(Gibco) containing 10% FBS (Gibco), w/o or w/ ascorbic acid phosphate (0.1mM) (Ascorbate), and antibiotics for 24 hours (25K cells per well). Cells were incubated with 0.3 μ M solutions of Hsp47 variants or EGFP in medium for 3 h, followed by medium exchange w/ or w/o ascorbate, and cultured for additional 24 h. After PBS washing, cells were fixed using Bouin solution (75% picric acid, 10% formalin, and 5% acetic acid) (Sigma HT10132). Collagen deposited in the wells was stained by incubation with 0.1% Sirius red in picric acid (ab150681) for 1 h and washing with 0.01 N HCl and 0.1 N NaOH¹⁴⁵. Collagen deposition was quantified at 570 nm using a Biolumin960k spectrophotometer. Results were normalized by taking Hsp47 (+/+) as 1. Cell Counting was performed using Image J with references to DAPI stained cells. All the analysis was performed in triplicate.

To test the cytotoxicity of ONBY on activation of H_{47Y<ONBY}, a live-dead cell staining assay was performed. Hsp47^{-/-} cells were incubated with H_{47Y<ONBY} and activated (H_{47Y<ONBYhv}) *in situ* UV exposure for 30 seconds at 405 nm with 50% intensity. H_{47Y<ONBY} added and no protein added conditions were used as controls. After 24 h, cells were treated with 1 mL of PBS containing 40 μ L of Propidium iodide (Stock concentration 2mg/mL in H₂O) and 12 μ L of Fluorescein diacetate (Stock concentration 5mg/mL in DMSO) for 5 mins. Cells were washed with PBS and imaged using Nikon Ti-Eclipse microscope.

For investigating the potential of H_{47Y<ONBY} for spatiotemporal control Hsp47^{+/+} and Hsp47^{-/-} cells (25K cells per well) were cultured in 24 well plates with high glucose DMEM Glutamax (Gibco) containing 10% FBS (Gibco), 0.1 mM ascorbate, and antibiotics. After 24 h, cells were incubated with 0.3 μ M solution of H_{47N}, H_{47Y<ONBY}, H_{47Kdel} or EGFP in DMEM medium for 3 h. Afterwards the solution was exchanged by DMEM Glutamax with ascorbate and cells were cultured for further 24 h. The wells containing H_{47Y<ONBY} were irradiated at 405 nm using Ti-Nikon Microscope with laser power of 50% intensity for 30 seconds (\sim 37mW exposure over the total exposed area i.e.1.7W/cm² (measured using ILX Light wave OMM-68108 Optical Multimeter) which is equivalent to energy of 51.2 J/cm²) with 10X objective exposed in an area of about 1.8x1.2mm², an hour after medium exchange. After 24 h cells were fixed and immuno stained against collagen with Primary; Rabbit polyclonal anti-type I collagen, 600-401-103-0.1 (Rockland; dilution

1:200), Secondary; Goat anti-Rabbit IgG (H+L) Highly Cross-Adsorbed Secondary Antibody, Alexa Fluor 647, A-21245 (dilution 1:200) and stained Nucleus with DAPI (Thermo fisher). Microscopic images were taken with Nikon Ti-Eclipse microscope. All the experiments were done in triplicates.

To study the deviation in spatial deposition of collagen on photo-activation of H_{47Y<ONBY}, we cultured Hsp47^{-/-} cells and delivered H_{47Y<ONBY}. After 3 h the medium was exchanged in normal medium. A 1.13 mm² area (diameter=1.2mm) was irradiated on Hsp47^{-/-} cell culture previously incubated with H_{47Y<ONBY} for 30 seconds at 405 nm with 50% intensity an hour after medium exchange at 3 different spots having a distance of 4mm between the spots using 20X objective. To determine the area that was irradiated through this method, we marked the underside of a 24-well plate with a green highlighter ink (Pelikan Text marker 490) which was then photo bleached by 3 min UV exposure with similar intensity and area. The photo bleached was considered as a reference in all the experiments. A time lapse bright field (UV protection filters installed) microscopy was performed with Nikon Ti-Eclipse microscope for 24h. Cells were fixed using 4% PFA and stained for collagen 1 using the protocol mentioned above. Fluorescence imaging was done using a Nikon Ti-Eclipse microscope using 4X objective. All the experiments were done in triplicates.

For single cells analysis, Hsp47^{+/+} and Hsp47^{-/-} cells (20K cells per well) were cultured in 15 wells IBIDI Angiogenesis slides with high glucose DMEM Glutamax (Gibco) containing 10% FBS (Gibco), and antibiotics. After 4 h, cells were incubated with 0.3 μM solution of H_{47Y<ONBY} in DMEM medium for 3 h. One set of wells containing H_{47Y<ONBY} were irradiated at 405 nm using Ti-Nikon Microscope with laser power of 50% intensity for 30 seconds with 20X objective, an hour after medium exchange. Next the solution was exchanged by DMEM Glutamax and cells were cultured for further 24 h. After 24 h cells were fixed and immuno stained against collagen with Primary; Rabbit polyclonal anti-type I collagen, 600-401-103-0.1 (Rockland; dilution 1:200), Secondary; Goat anti-Rabbit IgG (H+L) Highly Cross-Adsorbed Secondary Antibody, Alexa Fluor 647, A-21245 (dilution 1:200), Golgi apparatus with Golgin-97 Monoclonal Antibody (CDF4) (1:200 dilutions, Thermo fisher A-21270), ER with ER Staining Kit - Red Fluorescence Cytopainter (ab139482) and stained Nucleus with DAPI (Thermo fisher). Microscopic images were taken with confocal microscope. All the experiments were done in triplicates.

Statistics and Reproducibility

For MEF Hsp47^{-/-} three independent experiments were performed. For immunostaining quantification IMAGE J was used to quantify mean intensity profile of stained matrices in all cell types treated with and without H47 with bar plots including error bars indicating standard deviation. The data were normalized to MEF Hsp47^{-/-} untreated cells were

considered as 1. Statistical significance was analyzed by Tukey test, which shows significant differences between conditions. Significance was calculated by comparing non treated vs. treated cells (mean±SD, ANOVA, *** $p < 0.001$).

For Sirius Red assay each data point represents technical triplicates. (n=4) number of experiment was performed and plotted the graphs including whisker plots representing standard deviation by normalizing all the conditions with respect to Hsp47 (+/+) as 1. The samples sizes for all biochemical assays, imaging and immunoblotting reported have a sample sizes (n=3). All independent quantitative experiments were started from cell cultures. The quality of these quantitative datasets is assessed by the standard deviation value of all the measured and are provided in each main and supplementary dataset. The value of $p < 0.05$ was used for statistical significance. A one-way ANOVA with a Tukey test of the variance was used to determine the statistical significance between groups. The statistical significance difference was set to * $\alpha < 0.05$, ** $\alpha < 0.01$, *** $\alpha < 0.001$. For quantitative measurements to study distribution of procollagen I with secretory organelles and H_{47Y<ONBY}, Pearson's correlation (r) was performed. All the plot profiles were generated using Image J plot profile function. Pearson's coefficients were calculated on the plot profiles of average intensity from Nucleus to cell periphery (were +1 value reflects perfect correlation and any value above 0.8 reflects positive correlation). These were performed on 20 cells in each condition from 3 independent experiments. Nucleus was assigned as a centroid and '50%' section of intensity profile was calculated from edge of Nucleus to half distance till the periphery (shown in brown dashed box) and total distance was considered as 100% (shown in orange dashed box). This was performed in four different directions from the Nucleus for each cell. In Hsp47 +/+ 0.95 and 0.90 r values at 50% distance was observed with ER-COL I and Golgi-COL I signal.

Chapter 6

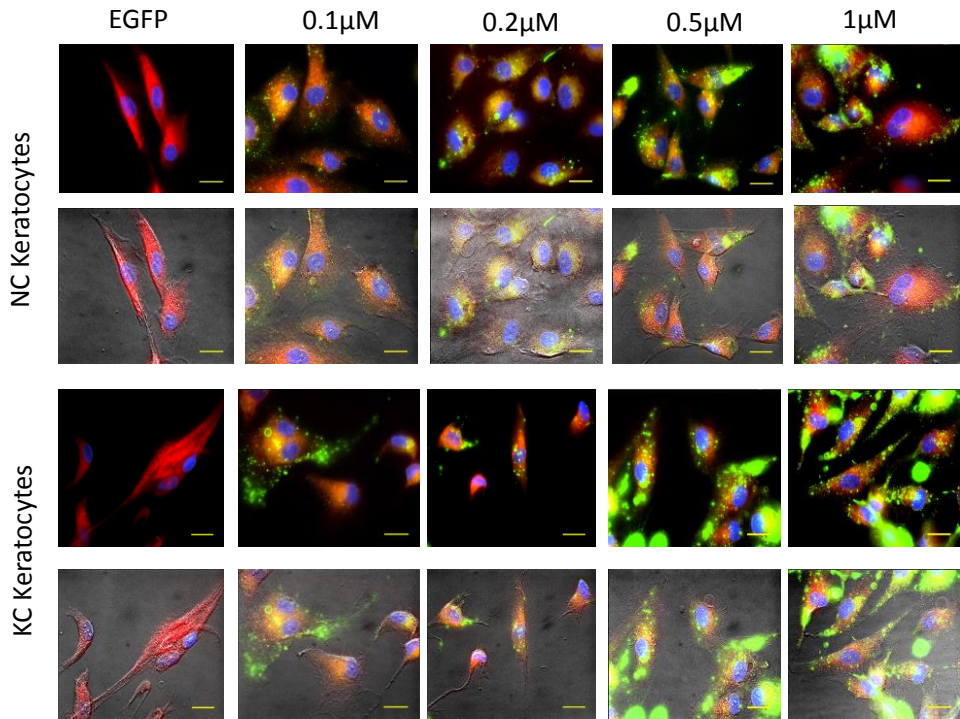


Figure S1. Microscopy images of NC and KC keratocytes after incubation with different concentration of H_{47N} (i.e. 0.1-1μM) showing colocalization of H_{47N} signal and ER staining. No fluorescence was observed after incubation with EGFP (Blue: DAPI (Nucleus), Green: EGFP (H_{47N}) and Red: ER tracker Dye) Scale bar: 20 μm.

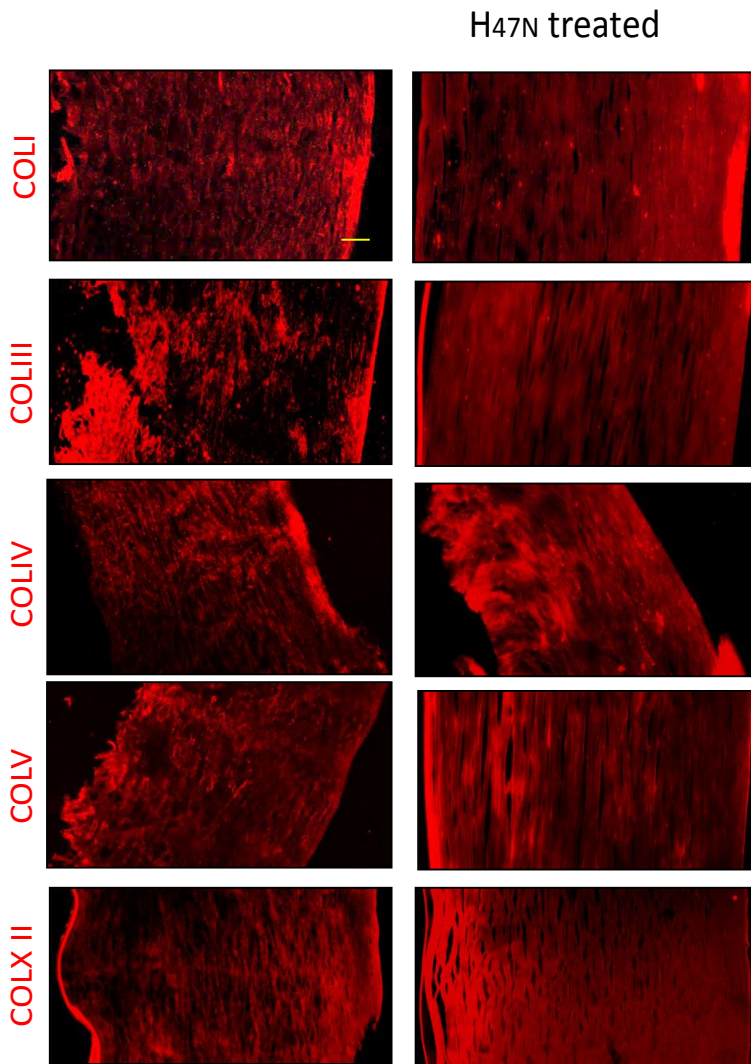


Figure S2: Immunostaining of NC and KC treated with H_{47N} 3days after treatment. COL I, III, IV, V and XII Antibody are stained in red showing very low increase in collagen subtypes signal. Scale bar: 250um

COL IA1	GAACGCGTGCATCCCTTGT (20 bp) GAACGAGGTAGTCTTTCAGCAACA (24 bp)	http://www.rtpriimerdb.org/assay_report.php?assay_id=1089
COLIIIAI	AACACGCAAGGCTGTGAGACT (21 bp) GCCAACGTCCACACCAAATT (20 bp)	http://www.rtpriimerdb.org/assay_report.php?assay_id=1090
COLIVAI	CACCCTCCCCCTTCTACTC (20bp) GCCCAGAGAATGCACCTG (18bp)	https://www.ncbi.nlm.nih.gov/pmc/articles/PMC3081799/
COL VAI	CACAACCTGCCTGATGGAATAACA (24 bp) GCAGGGTACAGCTGCTTGGT (20 bp)	http://www.rtpriimerdb.org/assay_report.php?assay_id=1091
COLXII	CAGTGAGGTGGATAGTGGATTTAG (25bp) AGTGTTGGGTTCCCTGTGAG (21bp)	https://www.ncbi.nlm.nih.gov/gene/?term=Homo+sapiens+COL12A1
GAPDH	GTCAAGGCTGAGAACGGGAA (20bp) GCTTCACCACCTTCTTGATG (20bp)	https://iovs.arvojournals.org/article.aspx?articleid=2127403

Table1. Q- PCR primers for mRNA expression of keratocytes,

Experimental Procedures

Delivery of H_{47N} variants to keratinocyte cultures

NC and KC fibroblast cells were seeded on 12 well μ -Slide Angiogenesis plates (Ibidi) with DMEM GlutaMax medium containing 10% fetal bovine serum (FBS; Gibco), and antibiotics (20K cells per well). 30 mins after seeding, cells were incubated with 0.1-1.0 μ M solution of H_{47N} variants in DMEM. After 3 h incubation the medium was removed and cells were washed once with sterile assay buffer (1x). Dual staining of ER and nuclei was done by mixing 1 μ l of ER tracker (ER Staining Kit - Red Fluorescence - Cytopainter (ab139482)) with 1 μ l of DAPI in 1 ml of ER Assay buffer (1X) provided in the kit. The cells were incubated with 60ul of Dual staining solution per well at 37°C for ½ hr. Cells were washed with Assay buffer (1X) once. Cells were fixed with 4% PFA for 10 mins. All the experiments were done in triplicate.

Sirus Red assay

NC and KC cells were cultured in 24 well plate with DMEM Glutamax (Gibco) containing 10% FBS (Gibco), and antibiotics for 24 hours (25K cells per well). Cells were incubated with 0.3 μ M solutions of H_{47N} in medium for 3 h, followed by medium exchange, and cultured for 24 h. Cells were washed with PBS and fixed using Bouin solution (75% picric acid, 10% formalin, and 5% acetic acid) (Sigma HT10132). Staining was done by incubation with 0.1% Sirius Red in picric acid (ab150681) for 1 h and washing with 0.01 N HCl and 0.1 N NaOH²⁷⁷. Collagen deposition was quantified at 570 nm using a Biolumin960k spectrophotometer. Results were normalized by taking untreated NC stromal fibroblast as 1. All the analysis was performed in triplicate.

QPCR assay for determining collagen subtypes expression levels

NC and KC stromal fibroblasts were seeded on 6 well plates in duplicates. One set of KC stromal fibroblasts was previously incubated with 0.3 μ M of H_{47N} for 3 h. All cells (NC, KC and H_{47N} treated KC stromal fibroblast) were incubated for another 24h. Total RNA isolation was conducted using PureLink™ RNA Mini Kit (Thermo fisher, 12183018A). RT-PCR was performed using with EXPRESS SYBR™ GreenER™ qPCR Super mix, universal (Thermofisher, 1178401K). The primers of all the genes are mentioned in Table S1.

Ethical considerations

The study with human cornea explants was approved by the Ethics Committee of Saarland (no 48/19), and informed consent was obtained from all participants. Only patients with an

age older than 18 years were included in the study. 8 NC and 3 KC were used in the study. Corneas after surgery were transferred in DMEM medium after surgery and kept at 37°C.

Sample Preparation and Immunostaining of NC and KC

Sylgard 184 coated plates were used to pin the cornea tissue and keep it under tension. 45 ml of Silicone Elastomer Base were mixed with 5 ml Silicone Curing Agent in a 50 ml tube with hands for 10 mins. 1.5 ml of Sylgard mixture was poured into each well to form a ~2mm-thick film covering the whole well and avoiding air bubbles. The 6 well plates were kept at 55°C in an oven overnight to crosslink Sylgard. NC and KC immersed in the DMEM medium containing 10% FBS and antibiotics were cut into three pieces and pinned on the Sylgard coated plates using Stainless steel minute pins (Fine Science tools, 26002-10).

NC and KC cornea were incubated with Hsp47 variants in DMEM medium with 10% FBS and antibiotics for 5 h. Tissue samples were fixed in 4 %PFA in PBS (4°C) overnight, incubated in 10 and 25 % of sucrose in PBS overnight, and then embedded in CryoGlue (#30001101, SLEE medical GmbH, Germany). Embedded samples were frozen and stored at 80 °C. For cryosectioning samples were incubated for 5 min at -20°C in the chamber of the cryostat SLEE MNT (SLEE medical GmbH, Germany). Sections of 15 to 100 µm were conducted, depending on experiment. Tissues were mounted on Menyel-Glaser Super frost Plus glass slides (ThermoFisher) and stained for different collagen types with primary antibodies (Rabbit polyclonal anti-type I collagen, 600-401-103-0.1 (Rockland; dilution 1:200)). Samples were washed 3 x with PBS and stained with secondary antibody (Goat anti-Rabbit IgG (H+L) Highly Cross-Adsorbed Secondary Antibody, Alexa Fluor 647, A-21245 (dilution 1:200)). Nuclei were stained with DAPI (Thermo fisher).

For Second Harmonic Generation (SHG), polarization optical microscopy and immunostaining, corneas were incubated for 5 h with Hsp47 variants, followed by 3 days incubation in normal medium. For photo activation of KC treated with H_{47Y<ONBY} the wells were irradiated at 405 nm using a Ti-Nikon Microscope at 50% laser power (3mW/cm², measured using Silver Line UV Radiometer) during 1 min using a 10X objective. The irradiation step was done one hour after medium exchange. For SHG imaging a 2.5x10.75mm² area was illuminated.

For polarization microscopy experiments and immunostaining one half of the KC was illuminated. After exposure, the corneas were cultured for 3 days by changing the medium every day, fixed. For polarization samples without any staining was used.

For immunostaining experiments, collagen with Primary; Rabbit polyclonal anti-type I collagen, 600-401-103-0.1 (Rockland), Collagen III Polyclonal Antibody (ThermoFisher,

PA5-34787), Anti-COL4A3 antibody (Sigma, HPA042064-100UL) , Anti-Collagen V antibody (ab7046), Anti-COL12A1 antibody (Thermofisher, HPA070695) (dilution 1:200 for all the antibodies), Secondary; Goat anti-Rabbit IgG (H+L) Highly Cross-Adsorbed Secondary Antibody, Alexa Fluor 647, A-21245 (dilution 1:200) and stained. No staining was performed for polarization microscopy. Tissues were embedded in PBS for imaging. All the experiments were done in triplicates.

Microscopy

A Zeiss LSM Confocal microscopy with 60x objective and Nikon TA microscope with 20x objective were used. For SHG imaging a 2-photon Zeiss LSM 710 was used. 800 nm pulsed laser was used for excitation and a 400/5 nm band pass filter was used for emission. Polarization Light Microscopy (PLM) imaging was done in a LC-PolScope image processing system (CRI, LOT-Oriel, Darmstadt, Germany) mounted on a Zeiss inverse microscope (Zeiss Observer Z1, Göttingen, Germany) equipped with A-Plan 10x/0.25Ph1 objectives. Prior to specimen analysis, the background image was captured under identical conditions as the corneal samples. The optical retardation indicates the relative phase shift between two orthogonally polarized light waves after traversing an optically anisotropic material in this case collagen fibers, whereas the orientation mode refers to the orientation of its slow optical axis (azimuth)⁸⁰. The orientations of slow-axis vectors were determined by using the Abrio imaging software. All acquisitions of polarized images were performed at 546 nm using a standard Abrio filter. The mean optical retardance values are generated by the software in NC, KC and KC treated with H_{47N} and H_{47Y<ONBY} and light activated H_{47Y<ONBY}_{hv} samples. For subtracting signal from background initial calibration was performed on the glass slide without sample.

Statistics and Reproducibility

For Sirius Red assay each data point represents technical triplicates. We performed (n=4) number of experiment and plotted the graphs including whisker plots representing standard deviation by normalizing all the conditions with respect to NC untreated as 1. Statistical significance was analyzed by Tukey test, which shows significant differences between conditions. Significance was calculated by comparing non treated vs. treated cells (mean±SD, ANOVA, *** p<0.001). For QPCR the data is represented as bars with error bars showing standard deviation. The quality of these quantitative datasets is assessed by the standard deviation value of all the measured. For calculation of relative retardance in polarization measurement assay optical retardance values from 8 images from n-3 independent experiment were performed and highest retardance value from NC were considered as 100% and all the data were normalized to it. Graph plotted including whisker plots indicates whisker plot representing standard deviation and Statistical significance was

analyzed by Tukey test shows significant differences between conditions. Significance was calculated by comparing non treated vs. treated cells (mean \pm SD, ANOVA, *** p<0.001). The samples sizes for all biochemical assays, imaging and immunoblotting reported have a sample sizes (n=3). All independent quantitative experiments were started from cell and tissue cultures

References

1. Frantz, C.; Stewart, K. M.; Weaver, V. M., The extracellular matrix at a glance. *J Cell Sci* **2010**, *123* (Pt 24), 4195-200.
2. Badylak, S. F., The extracellular matrix as a biologic scaffold material. *Biomaterials* **2007**, *28* (25), 3587-93.
3. Jarvelainen, H.; Sainio, A.; Koulu, M.; Wight, T. N.; Penttinen, R., Extracellular matrix molecules: potential targets in pharmacotherapy. *Pharmacol Rev* **2009**, *61* (2), 198-223.
4. A.Holzapfel, G., Biomechanics of Soft Tissue. Holzapfel, G. A., Ed. BIOMECH PREPRINT SERIES: 2000.
5. Goebels, S.; Eppig, T.; Wagenpfeil, S.; Cayless, A.; Seitz, B.; Langenbacher, A., Staging of keratoconus indices regarding tomography, topography, and biomechanical measurements. *Am J Ophthalmol* **2015**, *159* (4), 733-8.
6. Schedin, P.; Keely, P. J., Mammary gland ECM remodeling, stiffness, and mechanosignaling in normal development and tumor progression. *Cold Spring Harb Perspect Biol* **2011**, *3* (1), a003228.
7. Suki, B.; Bates, J. H., Extracellular matrix mechanics in lung parenchymal diseases. *Respir Physiol Neurobiol* **2008**, *163* (1-3), 33-43.
8. Wynn, T. A.; Ramalingam, T. R., Mechanisms of fibrosis: therapeutic translation for fibrotic disease. *Nat Med* **2012**, *18* (7), 1028-40.
9. Bonnans, C.; Chou, J.; Werb, Z., Remodelling the extracellular matrix in development and disease. *Nature Reviews Molecular Cell Biology* **2014**, *15* (12), 786-801.
10. Zimmermann, W. H., Tissue Engineering of a Differentiated Cardiac Muscle Construct. *Circulation Research* **2001**, *90* (2), 223-230.
11. Weber, K. T., Cardiac interstitium in health and disease: The fibrillar collagen network. *Journal of the American College of Cardiology* **1989**, *13* (7), 1637-1652.
12. Singh, B.; Fleury, C.; Jalalvand, F.; Riesbeck, K., Human pathogens utilize host extracellular matrix proteins laminin and collagen for adhesion and invasion of the host. *FEMS Microbiology Reviews* **2012**, *36* (6), 1122-1180.
13. Doyle, A. D.; Yamada, K. M., Mechanosensing via cell-matrix adhesions in 3D microenvironments. *Experimental Cell Research* **2016**, *343* (1), 60-66.
14. Badylak, S. F., Regenerative medicine and developmental biology: The role of the extracellular matrix. *The Anatomical Record Part B: The New Anatomist* **2005**, *287B* (1), 36-41.
15. Schaefer, L.; Schaefer, R. M., Proteoglycans: from structural compounds to signaling molecules. *Cell Tissue Res* **2010**, *339* (1), 237-46.
16. Harvey Lodish , A. B., Paul Matsudaira, Chris A. Kaiser, Monty Krieger, Matthew P. Scott, Lawrence Zipursky, James Darnell "*Integrating Cells Into Tissues*". *Molecular Cell Biology* 5th ed.; WH Freeman and Company.: New York.

17. Zhang, C.; Ji, Q.; Yang, Y.; Li, Q.; Wang, Z., Exosome: Function and Role in Cancer Metastasis and Drug Resistance. *Technol Cancer Res Treat* **2018**, *17*, 1533033818763450.
18. Myllyharju, J.; Kivirikko, K. I., Collagens and collagen-related diseases. *Annals of Medicine* **2009**, *33* (1), 7-21.
19. Sluijter, J. P.; Smeets, M. B.; Velema, E.; Pasterkamp, G.; de Kleijn, D. P., Increased collagen turnover is only partly associated with collagen fiber deposition in the arterial response to injury. *Cardiovasc Res* **2004**, *61* (1), 186-95.
20. Wise, S. G.; Weiss, A. S., Tropoelastin. *Int J Biochem Cell Biol* **2009**, *41* (3), 494-7.
21. Smith, M. L.; Gourdon, D.; Little, W. C.; Kubow, K. E.; Eguiluz, R. A.; Luna-Morris, S.; Vogel, V., Force-induced unfolding of fibronectin in the extracellular matrix of living cells. *PLoS Biol* **2007**, *5* (10), e268.
22. Shoulders, M. D.; Raines, R. T., Collagen Structure and Stability. *Annual Review of Biochemistry* **2009**, *78* (1), 929-958.
23. Boerboom, R. A.; Krahn, K. N.; Megens, R. T. A.; van Zandvoort, J., M. A. M.; Merckx, M.; Bouten, C. V. C., High resolution imaging of collagen organisation and synthesis using a versatile collagen specific probe. *J. Struct. Biol.* **2007**, *159* (3), 392-399.
24. Varner, V. D.; Nelson, C. M., Cellular and physical mechanisms of branching morphogenesis. *Development* **2014**, *141* (14), 2750-9.
25. Glowacki, J.; Mizuno, S., Collagen scaffolds for tissue engineering. *Biopolymers* **2008**, *89* (5), 338-44.
26. Byers, P. H.; Pyott, S. M., Recessively inherited forms of osteogenesis imperfecta. In *Annual Review of Genetics*, 2012; Vol. 46, pp 475-497.
27. Margadant, C.; Sonnenberg, A., Integrin-TGF- β crosstalk in fibrosis, cancer and wound healing. *EMBO reports* **2010**, *11* (2), 97-105.
28. Pannu, J.; Nakerakanti, S.; Smith, E.; Dijke, P. t.; Trojanowska, M., Transforming Growth Factor- β Receptor Type I-dependent Fibrogenic Gene Program Is Mediated via Activation of Smad1 and ERK1/2 Pathways. *Journal of Biological Chemistry* **2007**, *282* (14), 10405-10413.
29. Yamamoto, N.; Kinoshita, T.; Nohata, N.; Yoshino, H.; Itesako, T.; Fujimura, L.; Mitsuhashi, A.; Usui, H.; Enokida, H.; Nakagawa, M.; Shozu, M.; Seki, N., Tumor-suppressive microRNA-29a inhibits cancer cell migration and invasion via targeting HSP47 in cervical squamous cell carcinoma. *International Journal of Oncology* **2013**, *43* (6), 1855-1863.
30. Birk, D. E.; Bruckner, P., Collagen Suprastructures. In *Collagen*, 2005; pp 185-205.
31. Ricard-Blum, S.; Ruggiero, F.; van der Rest, M., The Collagen Superfamily. In *Collagen*, 2005; pp 35-84.
32. Brinckmann, J., Collagens at a Glance. In *Collagen*, 2005; pp 1-6.
33. Helena Kuivaniemi, 2 Gerard Tromp,1 and Darwin J. Prockop, Mutations in Fibrillar Collagens (Types I, II, III, and XI), Fibril-Associated Collagen (Type IX), and Network-Forming Collagen (Type X) Cause a Spectrum of Diseases of Bone, Cartilage, and Blood Vessels. *Human Mutation* **1997**, *9*, 300-315.

34. Ishikawa, Y.; Bachinger, H. P., A molecular ensemble in the rER for procollagen maturation. *Biochim Biophys Acta* **2013**, 1833 (11), 2479-91.
35. Ricard-Blum, S., The collagen family. *Cold Spring Harb Perspect Biol* **2011**, 3 (1), a004978.
36. Ansorge, H. L.; Meng, X.; Zhang, G.; Veit, G.; Sun, M.; Klement, J. F.; Beason, D. P.; Soslowsky, L. J.; Koch, M.; Birk, D. E., Type XIV Collagen Regulates Fibrillogenesis: premature collagen fibril growth and tissue dysfunction in null mice *J Biol Chem* **2009**, 284 (13), 8427-38.
37. Wenstrup, R. J.; Florer, J. B.; Brunskill, E. W.; Bell, S. M.; Chervoneva, I.; Birk, D. E., Type V collagen controls the initiation of collagen fibril assembly. *J Biol Chem* **2004**, 279 (51), 53331-7.
38. Bruckner, P., Suprastructures of extracellular matrices: paradigms of functions controlled by aggregates rather than molecules. *Cell Tissue Res* **2010**, 339 (1), 7-18.
39. BR, O., Collagen IX. *Int J Biochem Cell Biol* **1997**, 29 (4), 555-8.
40. Amenta, P. S.; Scivoletti, N. A.; Newman, M. D.; Sciancalepore, J. P.; Li, D.; Myers, J. C., Proteoglycan-collagen XV in human tissues is seen linking banded collagen fibers subjacent to the basement membrane. *J Histochem Cytochem* **2005**, 53 (2), 165-76.
41. Gordon, M. K.; Hahn, R. A., Collagens. *Cell Tissue Res* **2010**, 339 (1), 247-57.
42. Villone, D.; Fritsch, A.; Koch, M.; Bruckner-Tuderman, L.; Hansen, U.; Bruckner, P., Supramolecular interactions in the dermo-epidermal junction zone: anchoring fibril-collagen VII tightly binds to banded collagen fibrils. *J Biol Chem* **2008**, 283 (36), 24506-13.
43. Yeung, C.-Y. C.; Garva, R.; Pickard, A.; Chang, J.; Holmes, D. F.; Lu, Y.; Mallikarjun, V.; Swift, J.; Adamson, A.; Calverley, B.; Meng, Q. J.; Kadler, K. E., Circadian Clock Regulation of the Secretory Pathway. *bioRxiv 304014* **2018**.
44. Greenspan, D. S., Biosynthetic Processing of Collagen Molecules. In *Collagen. Topics in Current Chemistry*, 2005; Vol. 247, pp 149-183.
45. Schwarz, R. I., Collagen I and the fibroblast: High protein expression requires a new paradigm of post-transcriptional, feedback regulation. *Biochemistry and Biophysics Reports* **2015**, 3, 38-44.
46. Gilkes, D. M.; Chaturvedi, P.; Bajpai, S.; Wong, C. C.; Wei, H.; Pitcairn, S.; Hubbi, M. E.; Wirtz, D.; Semenza, G. L., Collagen Prolyl Hydroxylases Are Essential for Breast Cancer Metastasis. *Cancer Research* **2013**, 73 (11), 3285-3296.
47. Kumar, S.; Sevilla, C. A.; Dalecki, D.; Hocking, D. C., Regional Fibronectin and Collagen Fibril Co-Assembly Directs Cell Proliferation and Microtissue Morphology. *Plos One* **2013**, 8 (10), e77316.
48. Nagai N, H. M.; S, I.; E, A.; T, M.; N, H., Embryonic lethality of molecular chaperone hsp47 knockout mice is associated with defects in collagen biosynthesis. *J Cell Biol* **2000**, 150, 1499-506.
49. Natsume, T.; Koide, T.; Yokota, S.; Hirayoshi, K.; Nagata, K., Interactions between collagen-binding stress protein HSP47 and collagen. Analysis of kinetic parameters by surface plasmon resonance biosensor. *J Biol Chem* **1994**, 269 (49), 31224-8.

50. Oecal, S.; Socher, E.; Uthoff, M.; Ernst, C.; Zaucke, F.; Sticht, H.; Baumann, U.; Gebauer, J. M., The pH-dependent Client Release from the Collagen-specific Chaperone HSP47 Is Triggered by a Tandem Histidine Pair. *Journal of Biological Chemistry* **2016**, 291 (24), 12612-12626.
51. Sivakumar, P., New insights into extracellular matrix assembly and reorganization from dynamic imaging of extracellular matrix proteins in living osteoblasts. *Journal of Cell Science* **2006**, 119 (7), 1350-1360.
52. Thomson, C. A.; Ananthanarayanan, V. S., A Method for Expression and Purification of Soluble, Active Hsp47, a Collagen-Specific Molecular Chaperone. *Protein Expression and Purification* **2001**, 23 (1), 8-13.
53. Fidler, A. L.; Boudko, S. P.; Rokas, A.; Hudson, B. G., The triple helix of collagens - an ancient protein structure that enabled animal multicellularity and tissue evolution. *J Cell Sci* **2018**, 131 (7).
54. J.J. Nietfeld, A. K., The function of ascorbate with respect to prolyl 4-hydroxylase activity. *Biochimica et Biophysica Acta*, **1981**, 657, 159-167.
55. R. Myllyla, E. R. K.-S., K.I. Kivirikko, The role of ascorbate in the prolyl hydroxylase reaction. *Biochem. Biophys. Res. Commun* **1978**, 83, 441-448.
56. ErnestHausmann, Cofactor requirements for the enzymatic hydroxylation of lysine in a polypeptide precursor of collagen. *Biochimica et Biophysica Acta (BBA) - Protein Structure* **1967**, 133 (3), 591-593.
57. Marini, J. C.; Cabral, W. A.; Barnes, A. M.; Chang, W., Components of the collagen prolyl 3-hydroxylation complex are crucial for normal bone development. *Cell Cycle* **2007**, 6 (14), 1675-81.
58. D. C.John, M. E. G., N. J.Bulleid, Cell-free synthesis and assembly of prolyl 4-hydroxylase: the role of the beta-subunit (PDI) in preventing misfolding and aggregation of the alpha-subunit. *EMBO J* **1993**, 12 (4), 1587-1595.
59. Lindert, U.; Weis, M. A.; Rai, J.; Seeliger, F.; Hausser, I.; Leeb, T.; Eyre, D.; Rohrbach, M.; Giunta, C., Molecular Consequences of the SERPINH1/HSP47 Mutation in the Dachshund Natural Model of Osteogenesis Imperfecta. *J Biol Chem* **2015**, 290 (29), 17679-89.
60. Schegg, B.; Hulsmeier, A. J.; Rutschmann, C.; Maag, C.; Hennet, T., Core glycosylation of collagen is initiated by two beta(1-O)galactosyltransferases. *Mol Cell Biol* **2009**, 29 (4), 943-52.
61. Sricholpech, M.; Perdivara, I.; Nagaoka, H.; Yokoyama, M.; Tomer, K. B.; Yamauchi, M., Lysyl hydroxylase 3 glucosylates galactosylhydroxylysine residues in type I collagen in osteoblast culture. *J Biol Chem* **2011**, 286 (11), 8846-56.
62. Lars H. Engelholm, S. I., Henrik J. Jurgensen, Thore Hillig, Daniel H. Madsen, Boye S. Nielsen and Niels Behrendt, The collagen receptor uPARAP/Endo180. *Frontiers in Bioscience* **2009**, 14, 2103-2114.
63. Ishikawa, Y.; Vranka, J. A.; Boudko, S. P.; Pokidysheva, E.; Mizuno, K.; Zientek, K.; Keene, D. R.; Rashmir-Raven, A. M.; Nagata, K.; Winand, N. J.; Bachinger, H. P., Mutation in cyclophilin B that causes hyperelastosis cutis in American Quarter Horse does not affect peptidylprolyl cis-trans isomerase activity but shows altered

- cyclophilin B-protein interactions and affects collagen folding. *J Biol Chem* **2012**, 287 (26), 22253-65.
64. Ishikawa, Y.; Vranka, J.; Wirz, J.; Nagata, K.; Bachinger, H. P., The rough endoplasmic reticulum-resident FK506-binding protein FKBP65 is a molecular chaperone that interacts with collagens. *J Biol Chem* **2008**, 283 (46), 31584-90.
 65. J Engel, D. J. P., The Zipper-Like Folding of Collagen Triple Helices and the Effects of Mutations that Disrupt the Zipper. *Annual Review of Biophysics and Biophysical Chemistry* **1991**, 20, 137-152.
 66. Kurt J. Doege , J. H. F., Folding of Carboxyl Domain and Assembly of Procollagen I. **1986**, 261 (19), 8924-893.
 67. Neil J. Bulleid, J. A. D., Janice F. Lees, The C-propeptide domain of procollagen can be replaced with a transmembrane domain without affecting trimer formation or collagen triple helix folding during biosynthesis. *The EMBO Journal* **1997**, 16, 6694-6701.
 68. Koide, T.; Nagata, K., Collagen Biosynthesis. In *Collagen*, 2005; pp 85-114.
 69. Bernard, M. P.; Myers, J. C.; Chu, M. L.; Ramirez, F.; Eikenberry, E. F.; Prockop, D. J., Structure of a cDNA for the pro.alpha.2 chain of human type I procollagen. Comparison with chick cDNA for pro.alpha.2(I) identifies structurally conserved features of the protein and the gene. *Biochemistry* **2002**, 22 (5), 1139-1145.
 70. Bernard, M. P.; Chu, M. L.; Myers, J. C.; Ramirez, F.; Eikenberry, E. F.; Prockop, D. J., Nucleotide sequences of complementary deoxyribonucleic acids for the pro.alpha.1 chain of human type I procollagen. Statistical evaluation of structures that are conserved during evolution. *Biochemistry* **2002**, 22 (22), 5213-5223.
 71. Boudko, S. P.; Zientek, K. D.; Vance, J.; Hacker, J. L.; Engel, J.; Bachinger, H. P., The NC2 domain of collagen IX provides chain selection and heterotrimerization. *J Biol Chem* **2010**, 285 (31), 23721-31.
 72. Ishikawa, Y.; Wirz, J.; Vranka, J. A.; Nagata, K.; Bachinger, H. P., Biochemical characterization of the prolyl 3-hydroxylase 1.cartilage-associated protein.cyclophilin B complex. *J Biol Chem* **2009**, 284 (26), 17641-7.
 73. Ohnishi, S.; Sumiyoshi, H.; Kitamura, S.; Nagaya, N., Mesenchymal stem cells attenuate cardiac fibroblast proliferation and collagen synthesis through paracrine actions. *FEBS Lett* **2007**, 581 (21), 3961-6.
 74. Widmer, C.; Gebauer, J. M.; Brunstein, E.; Rosenbaum, S.; Zaucke, F.; Drogemuller, C.; Leeb, T.; Baumann, U., Molecular basis for the action of the collagen-specific chaperone Hsp47/SERPINH1 and its structure-specific client recognition. *Proc Natl Acad Sci U S A* **2012**, 109 (33), 13243-7.
 75. Thomson, C. A.; Ananthanarayanan, V. S., Structure-function studies on hsp47: pH-dependent inhibition of collagen fibril formation in vitro. *J Biol Chem*.
 76. Ishida, Y.; Nagata, K., Hsp47 as a collagen-specific molecular chaperone. In *Methods in Enzymology*, 2011; Vol. 499, pp 167-182.
 77. Ishida, Y.; Kubota, H.; Yamamoto, A.; Kitamura, A.; Bachinger, H. P.; Nagata, K., Type I collagen in Hsp47-null cells is aggregated in endoplasmic reticulum and

- deficient in N-propeptide processing and fibrillogenesis. *Mol Biol Cell* **2006**, 17 (5), 2346-55.
78. Takaki Koide, S. A., Kazuhiro Nagata, Substrate Recognition of Collagen-specific Molecular Chaperone HSP47. *J.Biol.Chem.* **1999**, 274, 34523-34526.
 79. Koide, T.; Asada, S.; Takahara, Y.; Nishikawa, Y.; Nagata, K.; Kitagawa, K., Specific recognition of the collagen triple helix by chaperone HSP47: Minimal structural requirement and spatial molecular orientation. *Journal of Biological Chemistry* **2006**, 281 (6), 3432-3438.
 80. Eder, M.; Lutz-Meindl, U.; Weiss, I. M., Non-invasive LC-PolScope imaging of biominerals and cell wall anisotropy changes. *Protoplasma* **2010**, 246 (1-4), 49-64.
 81. Nishikawa, Y.; Takahara, Y.; Asada, S.; Shigenaga, A.; Otaka, A.; Kitagawa, K.; Koide, T., A structure-activity relationship study elucidating the mechanism of sequence-specific collagen recognition by the chaperone HSP47. *Bioorg Med Chem* **2010**, 18 (11), 3767-75.
 82. Koide, T.; Nishikawa, Y.; Asada, S.; Yamazaki, C. M.; Takahara, Y.; Homma, D. L.; Otaka, A.; Ohtani, K.; Wakamiya, N.; Nagata, K.; Kitagawa, K., Specific recognition of the collagen triple helix by chaperone HSP47. II. The HSP47-binding structural motif in collagens and related proteins. *J Biol Chem* **2006**, 281 (16), 11177-85.
 83. Nagai, N.; Hosokawa, M.; Itoharu, S.; Adachi, E.; Matsushita, T.; Hosokawa, N.; Nagata, K., Embryonic Lethality of Molecular Chaperone Hsp47 Knockout Mice Is Associated with Defects in Collagen Biosynthesis. *The Journal of Cell Biology* **2000**, 150 (6), 1499-1506.
 84. Dafforn, T. R.; Della, M.; Miller, A. D., The molecular interactions of heat shock protein 47 (Hsp47) and their implications for collagen biosynthesis. *J Biol Chem* **2001**, 276 (52), 49310-9.
 85. Robert E. Burgeson, N. P. M., Louann W. Murray, Keith G. Dungan, Douglas R Keene and Lynn T. Sakai The Structure of Type VII Collagen. *Annals of the Newyork Academy of Sciences* **1985**, 460 (1).
 86. Ishikawa, Y.; Boudko, S.; Bachinger, H. P., Ziploc-ing the structure: Triple helix formation is coordinated by rough endoplasmic reticulum resident PPIases. *Biochim Biophys Acta* **2015**, 1850 (10), 1983-93.
 87. Malhotra, V.; Erlmann, P., The pathway of collagen secretion. *Annu Rev Cell Dev Biol* **2015**, 31, 109-24.
 88. Saito, K.; Katada, T., Mechanisms for exporting large-sized cargoes from the endoplasmic reticulum. *Cell Mol Life Sci* **2015**, 72 (19), 3709-20.
 89. Saito, K.; Chen, M.; Bard, F.; Chen, S.; Zhou, H.; Woodley, D.; Polischuk, R.; Schekman, R.; Malhotra, V., TANGO1 facilitates cargo loading at endoplasmic reticulum exit sites. *Cell* **2009**, 136 (5), 891-902.
 90. Ishikawa, Y.; Ito, S.; Nagata, K.; Sakai, L. Y.; Bachinger, H. P., Intracellular mechanisms of molecular recognition and sorting for transport of large extracellular matrix molecules. *Proc Natl Acad Sci U S A* **2016**, 113 (41), E6036-E6044.
 91. Wilson, D. G.; Phamluong, K.; Li, L.; Sun, M.; Cao, T. C.; Liu, P. S.; Modrusan, Z.; Sandoval, W. N.; Rangell, L.; Carano, R. A.; Peterson, A. S.; Solloway, M. J., Global

- defects in collagen secretion in a Mia3/TANGO1 knockout mouse. *J Cell Biol* **2011**, 193 (5), 935-51.
92. Ahmed, U. Investigation into the structure and function of Hsp47 University of Birmingham, 2009.
 93. Bianchi, F. T.; Camera, P.; Ala, U.; Imperiale, D.; Migheli, A.; Boda, E.; Tempia, F.; Berto, G.; Bosio, Y.; Oddo, S.; LaFerla, F. M.; Taraglio, S.; Dotti, C. G.; Di Cunto, F., The collagen chaperone HSP47 is a new interactor of APP that affects the levels of extracellular beta-amyloid peptides. *PLoS One* **2011**, 6 (7), e22370.
 94. Macdonald, J. R.; Bachinger, H. P., HSP47 binds cooperatively to triple helical type I collagen but has little effect on the thermal stability or rate of refolding. *J Biol Chem* **2001**, 276 (27), 25399-403.
 95. Thomson, C. A.; Tenni, R.; Ananthanarayanan, V. S., Mapping Hsp47 binding site(s) using CNBr peptides derived from type I and type II collagen. *Protein Sci* **2003**, 12 (8), 1792-800.
 96. Mamoru Satoh, K. H., Shin-ichi Yokota, Nobuko Hosokawa, and Kazuhiro Nagata, Intracellular Interaction of Collagen-specific Stress Protein HSP47with Newly Synthesized Procollagen *The Journal of Cell Biology* **1996**, 133, 469-483.
 97. Kuroda, K.; Tsukifujii, R.; Shinkai, H., Increased expression of heat-shock protein 47 is associated with overproduction of type I procollagen in systemic sclerosis skin fibroblasts. *J Invest Dermatol* **1998**, 111 (6), 1023-8.
 98. Ito, S.; Nagata, K., Roles of the endoplasmic reticulum-resident, collagen-specific molecular chaperone Hsp47 in vertebrate cells and human disease. *J Biol Chem* **2019**, 294 (6), 2133-2141.
 99. Dewavrin, J. Y.; Abdurrahim, M.; Blocki, A.; Musib, M.; Piazza, F.; Raghunath, M., Synergistic rate boosting of collagen fibrillogenesis in heterogeneous mixtures of crowding agents. *J Phys Chem B* **2015**, 119 (12), 4350-8.
 100. Makareeva, E.; Leikin, S., Procollagen triple helix assembly: an unconventional chaperone-assisted folding paradigm. *PLoS One* **2007**, 2 (10), e1029.
 101. Thomson, C. A.; Tenni, R.; Ananthanarayanan, V. S., Mapping Hsp47 binding site(s) using CNBr peptides derived from type I and type II collagen. *Protein Science* **2003**, 12 (8), 1792-1800.
 102. Shinya Ito, K. O., Koh Takeuchi, Motoki Takagi , Masahito Yoshida, Takatsugu Hirokawa, Shoshiro Hirayama, Kazuo Shin-ya, Ichio Shimada, Takayuki Doi, Naoki Goshima, Tohru Natsume,; Nagata, a. K., A small-molecule compound inhibits a collagen-specific molecular chaperone and could represent a potential remedy for fibrosis. *J Biol Chem* **2017**, 292 (49), 20076-20085.
 103. Kadler, K. E., Fell Muir Lecture: Collagen fibril formation in vitro and in vivo. *Int J Exp Pathol* **2017**, 98 (1), 4-16.
 104. Canty, E. G.; Lu, Y.; Meadows, R. S.; Shaw, M. K.; Holmes, D. F.; Kadler, K. E., Coalignment of plasma membrane channels and protrusions (fibripositors) specifies the parallelism of tendon. *J Cell Biol* **2004**, 165 (4), 553-63.

105. Kalson, N. S.; Starborg, T.; Lu, Y.; Mironov, A.; Humphries, S. M.; Holmes, D. F.; Kadler, K. E., Nonmuscle myosin II powered transport of newly formed collagen fibrils at the plasma membrane. *Proc Natl Acad Sci U S A* **2013**, *110* (49), E4743-52.
106. Engvall, E., Molecular assembly, secretion, and matrix deposition of type VI collagen. *The Journal of Cell Biology* **1986**, *102* (3), 703-710.
107. Young, B. B.; Zhang, G.; Koch, M.; Birk, D. E., The roles of types XII and XIV collagen in fibrillogenesis and matrix assembly in the developing cornea. *J Cell Biochem* **2002**, *87* (2), 208-20.
108. Karl E. Kadler, D. F. H., John A. Trotter, John A. Chapman Collagen fibril formation. *Biochem. J.* **1996**, *316*, 1-11.
109. Holmes, D. F., Chapman, J. A., Prockop, D. J. and Kadler, K. E., Growing tips of type I collagen fibrils formed in vitro are near-paraboloidal in shape, implying a reciprocal relationship between accretion and diameter. *Proc Natl Acad Sci U S A* **1992**, *89*, 9855-9859.
110. Kadler, K. E., Hojima, Y. and Prockop, D. J., Collagen fibrils in vitro grow from pointed tips in the C- to N-terminal direction. *Biochem. J.* **1990**, *268*, 339-343.
111. Esposito, C.; Caputo, I., Mammalian transglutaminases. Identification of substrates as a key to physiological function and physiopathological relevance. *FEBS J* **2005**, *272* (3), 615-31.
112. Avery, N. C.; Bailey, A. J., The effects of the Maillard reaction on the physical properties and cell interactions of collagen. *Pathol Biol (Paris)* **2006**, *54* (7), 387-95.
113. Mostaco-Guidolin, L.; Rosin, N. L.; Hackett, T. L., Imaging Collagen in Scar Tissue: Developments in Second Harmonic Generation Microscopy for Biomedical Applications. *Int J Mol Sci* **2017**, *18* (8).
114. Chen, X.; Nadiarynk, O.; Plotnikov, S.; Campagnola, P. J., Second harmonic generation microscopy for quantitative analysis of collagen fibrillar structure. *Nat Protoc* **2012**, *7* (4), 654-69.
115. Arun Gopinathan, P.; Kokila, G.; Jyothi, M.; Ananjan, C.; Pradeep, L.; Humaira Nazir, S., Study of Collagen Birefringence in Different Grades of Oral Squamous Cell Carcinoma Using Picrosirius Red and Polarized Light Microscopy. *Scientifica (Cairo)* **2015**, *2015*, 802980.
116. da Silva Dde, F.; Vidal Bde, C.; Zezell, D. M.; Zorn, T. M.; Nunez, S. C.; Ribeiro, M. S., Collagen birefringence in skin repair in response to red polarized-laser therapy. *J Biomed Opt* **2006**, *11* (2), 024002.
117. Jan, N. J.; Grimm, J. L.; Tran, H.; Lathrop, K. L.; Wollstein, G.; Bilonick, R. A.; Ishikawa, H.; Kagemann, L.; Schuman, J. S.; Sigal, I. A., Polarization microscopy for characterizing fiber orientation of ocular tissues. *Biomed Opt Express* **2015**, *6* (12), 4705-18.
118. Q. Qiu, M. S., M. Kawaja, X. Shen, J. E. Davies, Attachment, morphology, and protein expression of rat marrow stromal cells cultured on charged substrate surfaces. *Journal of Biomedical Materials* **1998**, 98.

119. Abraham, L. C.; Zuenä, E.; Perez-Ramirez, B.; Kaplan, D. L., Guide to collagen characterization for biomaterial studies. *J Biomed Mater Res B Appl Biomater* **2008**, *87* (1), 264-85.
120. McMullan, D., Scanning electron microscopy 1928–1965. *Scanning* **1995**, *17* (3), 175-185.
121. Detamore, M. S.; Orfanos, J. G.; Almarza, A. J.; French, M. M.; Wong, M. E.; Athanasiou, K. A., Quantitative analysis and comparative regional investigation of the extracellular matrix of the porcine temporomandibular joint disc. *Matrix Biol* **2005**, *24* (1), 45-57.
122. Cocks, E.; Taggart, M.; Rind, F. C.; White, K., A guide to analysis and reconstruction of serial block face scanning electron microscopy data. *J Microsc* **2018**, *270* (2), 217-234.
123. Aper, S. J.; van Spreuwel, A. C.; van Turnhout, M. C.; van der Linden, A. J.; Pieters, P. A.; van der Zon, N. L.; de la Rambelje, S. L.; Bouten, C. V.; Merckx, M., Colorful protein-based fluorescent probes for collagen imaging. *PLoS One* **2014**, *9* (12), e114983.
124. Hwang, J.; Huang, Y.; Burwell, T. J.; Peterson, N. C.; Connor, J.; Weiss, S. J.; Yu, S. M.; Li, Y., In Situ Imaging of Tissue Remodeling with Collagen Hybridizing Peptides. *ACS Nano* **2017**, *11* (10), 9825-9835.
125. McCaughey, J.; Stevenson, N. L.; Cross, S.; Stephens, D. J., ER-to-Golgi trafficking of procollagen in the absence of large carriers. *J Cell Biol* **2019**, *218* (3), 929-948.
126. Pepperkok, D. J. S. a. R., Imaging of procollagen transport reveals COPIdependent cargo sorting during ER-to-Golgi transport in mammalian cells. *Journal of Cell Science* **2002**, *115* (6), 1149-1160.
127. Pickard, A.; Adamson, A.; Lu, Y.; Chang, J.; Garva, R.; Hodson, N.; Kadler, K., Collagen assembly and turnover imaged with a CRISPR-Cas9 engineered Dendra2 tag. *bioRxiv* 331496 **2018**.
128. Coulombe, P. A.; Kerns, M. L.; Fuchs, E., Epidermolysis bullosa simplex: a paradigm for disorders of tissue fragility. *J Clin Invest* **2009**, *119* (7), 1784-93.
129. Kuivaniemi H, T. G., Prockop DJ, Mutations in fibrillar collagens (types I, 11, 111, and XI), fibril-associated collagen (type IX), and network-forming collagen (type X) cause a spectrum of diseases of bone, cartilage, and blood vessels. *Hum Mutat* **1997**, *9*, 300-15.
130. Shirley, E. D.; Demaio, M.; Bodurtha, J., Ehlers-danlos syndrome in orthopaedics: etiology, diagnosis, and treatment implications. *Sports Health* **2012**, *4* (5), 394-403.
131. Robertson, W. V., B., The effect of ascorbic acid deficiency on the collagen concentration of newly induced fibrous tissue. *J Biol Chem* **1952**, *198*, 403-408.
132. Mario Chojkier, R. S., Beverly Peterkofsky, Specifically Decreased Collagen Biosynthesis in Scurvy Dissociated from an Effect on Proline Hydroxylation and Correlated with Body Weight Loss. *J Clin Invest.* **1983**, *72* (3), 826–835.
133. Rabinowitz, Y. S., Keratoconus. *Surv Ophthalmol* **1998**, *42* (4).
134. Gore, D. M.; Shortt, A. J.; Allan, B. D., New clinical pathways for keratoconus. *Eye (Lond)* **2013**, *27* (3), 329-39.

135. Katarzyna A. Wojcik, J. B., Jerzy Szaflik, Jacek P. Szaflik, Role of biochemical factors in the pathogenesis of keratoconus. *Acta Biochim Pol.* **2014**, 61 (1).
136. Mohammadpour, M.; Heidari, Z.; Hashemi, H., Updates on Managements for Keratoconus. *J Curr Ophthalmol* **2018**, 30 (2), 110-124.
137. Bonnemann, C. G., The collagen VI-related myopathies: muscle meets its matrix. *Nat Rev Neurol* **2011**, 7 (7), 379-90.
138. Mahajan, V. B.; Olney, A. H.; Garrett, P.; Chary, A.; Dragan, E.; Lerner, G.; Murray, J.; Bassuk, A. G., Collagen XVIII mutation in Knobloch syndrome with acute lymphoblastic leukemia. *Am J Med Genet A* **2010**, 152A (11), 2875-9.
139. Cury, M.; Zeidan, F.; Lobato, A. C., Aortic disease in the young: genetic aneurysm syndromes, connective tissue disorders, and familial aortic aneurysms and dissections. *Int J Vasc Med* **2013**, 2013, 267215.
140. Blair-Levy, J. M.; Watts, C. E.; Fiorentino, N. M.; Dimitriadis, E. K.; Marini, J. C.; Lipsky, P. E., A type I collagen defect leads to rapidly progressive osteoarthritis in a mouse model. *Arthritis Rheum* **2008**, 58 (4), 1096-106.
141. Feng, Y.; Egan, B.; Wang, J., Genetic Factors in Intervertebral Disc Degeneration. *Genes Dis* **2016**, 3 (3), 178-185.
142. Nichols, S. K. R. K. P. W. L., Acquired von Willebrand Disease. *Mayo Clin Proc.* **2002**, 77, 181-187.
143. Udén, A.; Nilsson, I. M.; Willner, S., Collagen-Induced Platelet Aggregation and Bleeding Time in Adolescent Idiopathic Scoliosis. *Acta Orthopaedica Scandinavica* **2009**, 51 (1-6), 773-777.
144. Ishida, Y.; Nagata, K., Hsp47 as a collagen-specific molecular chaperone. In *Methods in Enzymology*, 2011; Vol. 499, pp 167-182.
145. Ito, S. e. a., A small-molecule compound inhibits a collagen-specific molecular chaperone and could represent a potential remedy for fibrosis. *J Biol Chem* **2017**, 292 (49), 20076-20085.
146. Wynn, T. A., Cellular and molecular mechanisms of fibrosis. *J Pathol* **2008**, 214 (2), 199-210.
147. Hagiwara, S.; Nakamura, K.; Hamada, H.; Sasaki, K.; Ito, Y.; Kuribayashi, K.; Sato, T.; Sato, Y.; Takahashi, M.; Kogawa, K.; Kato, J.; Terui, T.; Takayama, T.; Matsunaga, T.; Taira, K.; Niitsu, Y., Inhibition of type I procollagen production by tRNAVal CTE-HSP47 ribozyme. *Journal of Gene Medicine* **2003**, 5 (9), 784-794.
148. Zhu, J.; Xiong, G.; Fu, H.; Evers, B. M.; Zhou, B. P.; Xu, R., Chaperone Hsp47 Drives Malignant Growth and Invasion by Modulating an ECM Gene Network. *Cancer Research* **2015**, 75 (8), 1580-1591.
149. Sepulveda, D.; Rojas-Rivera, D.; Rodriguez, D. A.; Groenendyk, J.; Kohler, A.; Lebeaupin, C.; Ito, S.; Urra, H.; Carreras-Sureda, A.; Hazari, Y.; Vasseur-Cognet, M.; Ali, M. M. U.; Chevet, E.; Campos, G.; Godoy, P.; Vaisar, T.; Bailly-Maitre, B.; Nagata, K.; Michalak, M.; Sierralta, J.; Hetz, C., Interactome Screening Identifies the ER Luminal Chaperone Hsp47 as a Regulator of the Unfolded Protein Response Transducer IRE1alpha. *Mol Cell* **2018**, 69 (2), 238-252 e7.

150. Zhu, J.; Xiong, G.; Fu, H.; Evers, B. M.; Zhou, B. P.; Xu, R., Chaperone Hsp47 Drives Malignant Growth and Invasion by Modulating an ECM Gene Network. *Cancer Res* **2015**, *75* (8), 1580-91.
151. Christiansen, H. E.; Schwarze, U.; Pyott, S. M.; AlSwaid, A.; Al Balwi, M.; Alrasheed, S.; Pepin, M. G.; Weis, M. A.; Eyre, D. R.; Byers, P. H., Homozygosity for a Missense Mutation in SERPINH1, which Encodes the Collagen Chaperone Protein HSP47, Results in Severe Recessive Osteogenesis Imperfecta. *American Journal of Human Genetics* **2010**, *86* (3), 389-398.
152. Masago, Y.; Hosoya, A.; Kawasaki, K.; Kawano, S.; Nasu, A.; Toguchida, J.; Fujita, K.; Nakamura, H.; Kondoh, G.; Nagata, K., The molecular chaperone Hsp47 is essential for cartilage and endochondral bone formation. *J Cell Sci* **2012**, *125* (Pt 5), 1118-28.
153. Foster, J. W.; Shinde, V.; Soiberman, U. S.; Sathe, G.; Liu, S.; Wan, J.; Qian, J.; Dauoud, Y.; Pandey, A.; Jun, A. S.; Chakravarti, S., Integrated Stress Response and Decreased ECM in Cultured Stromal Cells From Keratoconus Corneas. *Invest Ophthalmol Vis Sci* **2018**, *59* (7), 2977-2986.
154. Dafforn, T. R.; Della, M.; Miller, A. D., The Molecular Interactions of Heat Shock Protein 47 (Hsp47) and Their Implications for Collagen Biosynthesis. *Journal of Biological Chemistry* **2001**, *276* (52), 49310-49319.
155. Hosokawa, N.; Takechi, H.; Yokota, S.-i.; Hirayoshi, K.; Nagata, K., Structure of the gene encoding the mouse 47-kDa heat-shock protein (HSP47). *Elsevier Science Gene* **1993**, *126*, 187-193.
156. The Kruppel-like factor Zf9 and proteins in the Sp1 family regulate the expression of HSP47, a collagen-specific molecular chaperone. *J Biol Chem* **2002**, *277* (47), 44613-22.
157. Pang, X. Y.; Cui, W. M.; Liu, L.; Zhang, S. W.; Lv, J. P., Gene knockout and overexpression analysis revealed the role of N-acetylmuramidase in autolysis of *Lactobacillus delbrueckii* subsp. *bulgaricus* Ij-6. *PLoS One* **2014**, *9* (8), e104829.
158. Agrawal, N.; Dasaradhi, P. V.; Mohammed, A.; Malhotra, P.; Bhatnagar, R. K.; Mukherjee, S. K., RNA interference: biology, mechanism, and applications. *Microbiol Mol Biol Rev* **2003**, *67* (4), 657-85.
159. Rakhit, R.; Navarro, R.; Wandless, T. J., Chemical biology strategies for posttranslational control of protein function. *Chem Biol* **2014**, *21* (9), 1238-52.
160. P. Muller, Glossary of terms used in physical organic chemistry (IUPAC Recommendations 1994). *Pure and Applied Chemistry* **2009**, *66* (5), 1077-1184.
161. Bertozzi, G. A. L. a. C. R., Chemoselective ligation reactions with proteins, oligosaccharides and cells. *Trends Biotech* **1998**, *16*.
162. Chen, X.; Wu, Y. W., Selective chemical labeling of proteins. *Org Biomol Chem* **2016**, *14* (24), 5417-39.
163. Lang, K.; Chin, J. W., Bioorthogonal reactions for labeling proteins. *ACS Chem Biol* **2014**, *9* (1), 16-20.

164. Nicholas J. Agard, J. M. B., Jennifer A. Prescher, Anderson Lo, and Carolyn R. Bertozzi, A Comparative Study of Bioorthogonal Reactions with Azides. *ACS Chemical Biology* **2006**, *10*.
165. Breinbauer, R.; Kohn, M., Azide-alkyne coupling: a powerful reaction for bioconjugate chemistry. *ChemBiochem* **2003**, *4* (11), 1147-9.
166. V. V. Rostovtsev, L. G. G., V. V. Fokin, K. B. Sharpless, A Stepwise Huisgen Cycloaddition Process: Copper(i)-Catalyzed Regioselective TMLigation of Azides and Terminal Alkynes. *Angew. Chem. Int. Ed.* **2002**, *41*, 2596.
167. Serwa, R.; Majkut, P.; Horstmann, B.; Swiecicki, J.-M.; Gerrits, M.; Krause, E.; Hackenberger, C. P. R., Site-specific PEGylation of proteins by a Staudinger-phosphite reaction. *Chemical Science* **2010**, *1* (5).
168. M. Robert J. Vallée, P. M., Ina Wilkening, et al, Staudinger-Phosphonite Reactions for the Chemoselective Transformation of Azido-Containing Peptides and Proteins. *Org. Lett.* **2011**, *13* (20), 5540.
169. Saxon E, B. C., Cell surface engineering by a modified Staudinger reaction. *Science* **2000**, *287* (5460), 2007-2010.
170. J. M. Baskin, J. A. P., S. T. Laughlin, N. J. Agard, P. V. Chang, I. A. Miller, A. Lo, J. A. Codelli, C. R. Bertozzi, Copper-free click chemistry for dynamic in vivo imaging. *Proc. Natl. Acad. Sci.* **2007** *104*, 16793.
171. Ning, X.; Guo, J.; Wolfert, M. A.; Boons, G. J., Visualizing metabolically labeled glycoconjugates of living cells by copper-free and fast huisgen cycloadditions. *Angew Chem Int Ed Engl* **2008**, *47* (12), 2253-5.
172. C.W. Tornøe, C. C., M. Meldal, Peptidotriazoles on Solid Phase: [1,2,3]-Triazoles by Regiospecific Copper(I)-Catalyzed 1,3-Dipolar Cycloadditions of Terminal Alkynes to Azides. *J. Org. Chem* **2002**, *67*, 3057.
173. Muir, T. W., Semisynthesis of proteins by expressed protein ligation. In *Annual Review of Biochemistry*, 2003; Vol. 72, pp 249-289.
174. Yi, L.; Abootorabi, M.; Wu, Y. W., Semisynthesis of prenylated Rab GTPases by click ligation. *ChemBioChem* **2011**, *12* (16), 2413-2417.
175. McGrath, N. A.; Raines, R. T., Chemoselectivity in chemical biology: Acyl transfer reactions with sulfur and selenium. *Accounts of Chemical Research* **2011**, *44* (9), 752-761.
176. Philip E. Dawson, T. W. M., Ian Clark-Lewis, Stephen B. H. Kent, Synthesis of Proteins by Native Chemical Ligation. *Science* **1994**, 266.
177. Haase, C.; Seitz, O., Extending the scope of native chemical peptide coupling. *Angew Chem Int Ed Engl* **2008**, *47* (9), 1553-6.
178. Haase, C.; Rohde, H.; Seitz, O., Native chemical ligation at valine. *Angew Chem Int Ed Engl* **2008**, *47* (36), 6807-10.
179. Henager, S. H.; Chu, N.; Chen, Z.; Bolduc, D.; Dempsey, D. R.; Hwang, Y.; Wells, J.; Cole, P. A., Enzyme-catalyzed expressed protein ligation. *Nat Methods* **2016**, *13* (11), 925-927.

180. Hong Wu, Z. H., Xiang Qin Liu, Protein trans-splicing by a split intein encoded in a split DnaE gene of *Synechocystis* sp. PCC6803. *Proc. Natl. Acad. Sci. USA* **1998**, 95 (9226–9231).
181. Philip E. Dawson, T. W. M., Ian Clark-Lewis, Stephen B. H. Kent, Synthesis of Proteins by Native Chemical Ligation. *Science* **1994**, 226.
182. Mao, H.; Hart, S. A.; Schink, A.; Pollok, B. A., Sortase-mediated protein ligation: a new method for protein engineering. *J Am Chem Soc* **2004**, 126 (9), 2670-1.
183. Nguyen, G. K.; Wang, S.; Qiu, Y.; Hemu, X.; Lian, Y.; Tam, J. P., Butelase 1 is an Asx-specific ligase enabling peptide macrocyclization and synthesis. *Nat Chem Biol* **2014**, 10 (9), 732-8.
184. Heck, T.; Faccio, G.; Richter, M.; Thony-Meyer, L., Enzyme-catalyzed protein crosslinking. *Appl Microbiol Biotechnol* **2013**, 97 (2), 461-75.
185. Shannon M. Harper, L. C. N., Kevin H. Gardner, Structural Basis of a Phototropin Light Switch. *SCIENCE* **2003**, 301, 1541-44.
186. Olson, D. S. G. a. A. J., Structural symmetry and protein function *Annu. Rev. Biophys. Biomol. Struct.* **2000**, 29, 105-53.
187. Grusch, M.; Schelch, K.; Riedler, R.; Reichhart, E.; Differ, C.; Berger, W.; Ingles-Prieto, A.; Janovjak, H., Spatio-temporally precise activation of engineered receptor tyrosine kinases by light. *EMBO J* **2014**, 33 (15), 1713-26.
188. Nihongaki, Y.; Suzuki, H.; Kawano, F.; Sato, M., Genetically engineered photoinducible homodimerization system with improved dimer-forming efficiency. *ACS Chem Biol* **2014**, 9 (3), 617-21.
189. Bugaj, L. J.; Spelke, D. P.; Mesuda, C. K.; Varedi, M.; Kane, R. S.; Schaffer, D. V., Regulation of endogenous transmembrane receptors through optogenetic Cry2 clustering. *Nat Commun* **2015**, 6, 6898.
190. Liu, Q.; Tucker, C. L., Engineering genetically-encoded tools for optogenetic control of protein activity. *Curr Opin Chem Biol* **2017**, 40, 17-23.
191. Wu, Y. I.; Frey, D.; Lungu, O. I.; Jaehrig, A.; Schlichting, I.; Kuhlman, B.; Hahn, K. M., A genetically encoded photoactivatable Rac controls the motility of living cells. *Nature* **2009**, 461 (7260), 104-8.
192. Pham, E.; Mills, E.; Truong, K., A synthetic photoactivated protein to generate local or global Ca(2+) signals. *Chem Biol* **2011**, 18 (7), 880-90.
193. Paonessa, F.; Crisculo, S.; Sacchetti, S.; Amoroso, D.; Scarongella, H.; Pecoraro Bisogni, F.; Carminati, E.; Pruzzo, G.; Maragliano, L.; Cesca, F.; Benfenati, F., Regulation of neural gene transcription by optogenetic inhibition of the RE1-silencing transcription factor. *Proc Natl Acad Sci U S A* **2016**, 113 (1), E91-100.
194. Xin X. Zhou, H. K. C., Amy J. Lam, Michael Z. Lin., Optical Control of Protein Activity by Fluorescent Protein Domains. *Science* **2012**, 338 (6108), 810-814.
195. Arbely, E.; Torres-Kolbus, J.; Deiters, A.; Chin, J. W., Photocontrol of Tyrosine Phosphorylation in Mammalian Cells via Genetic Encoding of Photocaged Tyrosine. *Journal of the American Chemical Society* **2012**, 134 (29), 11912-11915.

196. Deiters, A.; Groff, D.; Ryu, Y.; Xie, J.; Schultz, P. G., A Genetically Encoded Photocaged Tyrosine. *Angewandte Chemie International Edition* **2006**, *45* (17), 2728-2731.
197. Wu, N.; Deiters, A.; Cropp, T. A.; King, D.; Schultz, P. G., A Genetically Encoded Photocaged Amino Acid. *J. AM. CHEM. SOC* **2004**, *126*, 14306-14307.
198. Givens, R. S.; Jung, A.; Park, C.-H.; Weber, J. r.; Bartlett, W., New Photoactivated Protecting Groups. 7.p-Hydroxyphenacyl: A Phototrigger for Excitatory Amino Acids and Peptides. *American Chemical Society* **1997**, (119), 8369-8370.
199. Lang, K.; Chin, J. W., Cellular incorporation of unnatural amino acids and bioorthogonal labeling of proteins. *Chem Rev* **2014**, *114* (9), 4764-806.
200. Liu, C. C.; Schultz, P. G., Adding new chemistries to the genetic code. *Annu Rev Biochem* **2010**, *79*, 413-44.
201. Neumann, H., Rewiring translation - Genetic code expansion and its applications. *FEBS Lett* **2012**, *586* (15), 2057-64.
202. Reinkemeier, C. D.; Girona, G. E.; Lemke, E. A., Designer membraneless organelles enable codon reassignment of selected mRNAs in eukaryotes. *Science* **2019**, *363* (6434).
203. Ryu, Y.; Schultz, P. G., Efficient incorporation of unnatural amino acids into proteins in *Escherichia coli*. *Nat Methods* **2006**, *3* (4), 263-5.
204. Xie, J.; Schultz, P. G., An expanding genetic code. *Methods* **2005**, *36* (3), 227-38.
205. Liu, W.; Brock, A.; Chen, S.; Chen, S.; Schultz, P. G., Genetic incorporation of unnatural amino acids into proteins in mammalian cells. *Nat Methods* **2007**, *4* (3), 239-44.
206. Wang L, B. A., Herberich B, Schultz P., Expanding the Genetic Code of *Escherichia coli*. *Science* **2001**, *301*, 964-7.
207. Chou, C.; Young, D. D.; Deiters, A., A light-activated DNA polymerase. *Angew Chem Int Ed Engl* **2009**, *48* (32), 5950-3.
208. Chou, C.; Young, D. D.; Deiters, A., Photocaged t7 RNA polymerase for the light activation of transcription and gene function in pro- and eukaryotic cells. *Chembiochem* **2010**, *11* (7), 972-7.
209. Deiters, A.; Groff, D.; Ryu, Y.; Xie, J.; Schultz, P. G., A genetically encoded photocaged tyrosine. *Angew Chem Int Ed Engl* **2006**, *45* (17), 2728-31.
210. Wu, N.; Deiters, A.; Cropp, T. A.; King, D.; Schultz, P. G., A genetically encoded photocaged amino acid. *J Am Chem Soc* **2004**, *126* (44), 14306-7.
211. Lemke, E. A.; Summerer, D.; Geierstanger, B. H.; Brittain, S. M.; Schultz, P. G., Control of protein phosphorylation with a genetically encoded photocaged amino acid. *Nat Chem Biol* **2007**, *3* (12), 769-72.
212. Chen, P. R.; Groff, D.; Guo, J.; Ou, W.; Cellitti, S.; Geierstanger, B. H.; Schultz, P. G., A facile system for encoding unnatural amino acids in mammalian cells. *Angew Chem Int Ed Engl* **2009**, *48* (22), 4052-5.
213. Nguyen, D. P.; Mahesh, M.; Elsasser, S. J.; Hancock, S. M.; Uttamapinant, C.; Chin, J. W., Genetic encoding of photocaged cysteine allows photoactivation of TEV protease in live mammalian cells. *J Am Chem Soc* **2014**, *136* (6), 2240-3.

214. Hemphill, J.; Chou, C.; Chin, J. W.; Deiters, A., Genetically encoded light-activated transcription for spatiotemporal control of gene expression and gene silencing in mammalian cells. *J Am Chem Soc* **2013**, *135* (36), 13433-9.
215. Xuan, W.; Yao, A.; Schultz, P. G., Genetically Encoded Fluorescent Probe for Detecting Sirtuins in Living Cells. *J Am Chem Soc* **2017**, *139* (36), 12350-12353.
216. David, R.; Richter, M. P.; Beck-Sickinger, A. G., Expressed protein ligation. Method and applications. *Eur J Biochem* **2004**, *271* (4), 663-77.
217. Chin, J. W., Expanding and Reprogramming the Genetic Code of Cells and Animals. *Annual Review of Biochemistry* **2014**, *83* (1), 379-408.
218. Lang, K.; Chin, J. W., Cellular Incorporation of Unnatural Amino Acids and Bioorthogonal Labeling of Proteins. *Chemical Reviews* **2014**, *114* (9), 4764-4806.
219. Adams, S. R.; Tsien, R. Y., Controlling the cell chemistry with caged compounds. *Annu. Rev. Physiol* **1993**, (55), 755-784.
220. Schoepfer, R., The pRSET family of T7 promoter expression vectors for Escherichia coli. *Gene* **1993**, *124*, 83-85.
221. David, R.; Richter, M. P. O.; Beck-Sickinger, A. G., Expressed protein ligation. *European Journal of Biochemistry* **2004**, *271* (4), 663-677.
222. Wu, Y.; Zhou, Y.; Song, J.; Hu, X.; Ding, Y.; Zhang, Z., Using green and red fluorescent proteins to teach protein expression, purification, and crystallization. *Biochemistry and Molecular Biology Education* **2008**, *36* (1), 43-54.
223. Waseem, A.; Aper, S. J. A.; van Spreuwel, A. C. C.; van Turnhout, M. C.; van der Linden, A. J.; Pieters, P. A.; van der Zon, N. L. L.; de la Rambelje, S. L.; Bouten, C. V. C.; Merckx, M., Colorful Protein-Based Fluorescent Probes for Collagen Imaging. *Plos One* **2014**, *9* (12), e114983.
224. Wood, D. W.; Camarero, J. A., Intein applications: from protein purification and labeling to metabolic control methods. *J Biol Chem* **2014**, *289* (21), 14512-9.
225. Cui, C.; Zhao, W.; Chen, J.; Wang, J.; Li, Q., Elimination of in vivo cleavage between target protein and intein in the intein-mediated protein purification systems. *Protein Expr Purif* **2006**, *50* (1), 74-81.
226. Singla, N.; Himanen, J. P.; Muir, T. W.; Nikolov, D. B., Toward the semisynthesis of multidomain transmembrane receptors: modification of Eph tyrosine kinases. *Protein Sci* **2008**, *17* (10), 1740-7.
227. Chou, C.; Deiters, A., Light-activated gene editing with a photocaged zinc-finger nuclease. *Angew Chem Int Ed Engl* **2011**, *50* (30), 6839-42.
228. MA145-ClearColi-BL21-DE3-Electocompetent-Cells. Genomics, L., Ed. Lucigen Genomics: 2019.
229. Snapp, E., Design and use of fluorescent fusion proteins in cell biology. *Curr Protoc Cell Biol* **2005**, Chapter 21, 21 4 1-21 4 13.
230. Arbely, E.; Torres-Kolbus, J.; Deiters, A.; Chin, J. W., Photocontrol of tyrosine phosphorylation in mammalian cells via genetic encoding of photocaged tyrosine. *J Am Chem Soc* **2012**, *134* (29), 11912-5.
231. Verhelst, J.; De Vlieger, D.; Saelens, X., Co-immunoprecipitation of the Mouse Mx1 Protein with the Influenza A Virus Nucleoprotein. *J Vis Exp* **2015**, (98).

232. Kaleka, K. S.; Petersen, A. N.; Florence, M. A.; Gerges, N. Z., Pull-down of calmodulin-binding proteins. *J Vis Exp* **2012**, (59).
233. Guillaume Rigaut, A. S., Berthold Rutz, Matthias Wilm, Matthias Mann¹, and Bertrand Séraphin, A generic protein purification method for protein complex characterization and proteome exploration. *Nat Biotech* **1999**, *17*, 1030-32.
234. Schreiber, G. M. a. S. L., Printing proteins as microarrays for high-throughput function determination. *Science* **2000**, *289* (5485), 1760-1763.
235. Urakubo, Y.; Ikura, T.; Ito, N., Crystal structural analysis of protein-protein interactions drastically destabilized by a single mutation. *Protein Sci* **2008**, *17* (6), 1055-65.
236. Gell, D. A.; Kwan, A. H.; Mackay, J. P., NMR Spectroscopy in the Analysis of Protein-Protein Interactions. In *Modern Magnetic Resonance*, 2017; pp 1-34.
237. Piechocka, I. K.; van Oosten, A. S.; Breuls, R. G.; Koenderink, G. H., Rheology of heterotypic collagen networks. *Biomacromolecules* **2011**, *12* (7), 2797-805.
238. Michael M. Pierce, C. S. R., Barry T. Nall, Isothermal Titration Calorimetry of Protein-Protein Interactions. *Methods* **1999**, *19*, 213-221.
239. Circular Dichroism to Study Protein Interactions. In *Current Protocols in Protein Science* John Wiley & Sons, Inc: 2006; Vol. 20.10.1-20.10.18.
240. Jiao, J.; Rebane, A. A.; Ma, L.; Zhang, Y., Single-Molecule Protein Folding Experiments Using High-Precision Optical Tweezers. *Methods Mol Biol* **2017**, *1486*, 357-390.
241. Rao, V. S.; Srinivas, K.; Sujini, G. N.; Kumar, G. N., Protein-protein interaction detection: methods and analysis. *Int J Proteomics* **2014**, *2014*, 147648.
242. Rohila, J. S.; Chen, M.; Cerny, R.; Fromm, M. E., Improved tandem affinity purification tag and methods for isolation of protein heterocomplexes from plants. *Plant J* **2004**, *38* (1), 172-81.
243. O'Connell, M. R.; Gamsjaeger, R.; Mackay, J. P., The structural analysis of protein-protein interactions by NMR spectroscopy. *Proteomics* **2009**, *9* (23), 5224-32.
244. Young, K. H., Yeast Two-Hybrid: So Many Interactions, (in) So Little Time ... *Biology of Reproduction* **1998**, *58*, 302-311.
245. J. Keith Joung, E. I. R., Carl O. Pabo, A bacterial two-hybrid selection system for studying protein-DNA and protein-protein interactions. *Proceedings of the National Academy of Sciences* **2000**, *97* (13), 7382-7387.
246. Bork, I. L. P., Interactive Tree Of Life (iTOL): an online tool for phylogenetic tree display and annotation. *Bioinformatics* **2007**, *23* (1), 127-128.
247. Jahangiri-Tazehkand, S.; Wong, L.; Eslahchi, C., OrthoGNC: A Software for Accurate Identification of Orthologs Based on Gene Neighborhood Conservation. *Genomics Proteomics Bioinformatics* **2017**, *15* (6), 361-370.
248. Carina Ploetz, E. I. Z., David E.Birk Collagen Fibril Assembly and Deposition in the Developing Dermis: Segmental Deposition in Extracellular Compartments. *Journal of Structural Biology* **1991**, *106*, 73-81.
249. Abdul-Wahab, M. F.; Homma, T.; Wright, M.; Olerenshaw, D.; Dafforn, T. R.; Nagata, K.; Miller, A. D., The pH sensitivity of murine heat shock protein 47

- (HSP47) binding to collagen is affected by mutations in the breach histidine cluster. *J Biol Chem* **2013**, 288 (6), 4452-61.
250. Barbara R. Williams, A. G., Donald C. Poppke, Karl A. Piez, Collagen fibril formation. *J.Biol.Chem* **1978**, 253, 6578-6585.
 251. de Wild, M.; Pomp, W.; Koenderink, G. H., Thermal memory in self-assembled collagen fibril networks. *Biophys J* **2013**, 105 (1), 200-10.
 252. Silver, F. H.; Birk, D. E., Kinetic Analysis of Collagen Fibrillogenesis: I. Use of Turbidity-Time Data. *Collagen and Related Research* **1983**, 3 (5), 393-405.
 253. Sun, M.; Chen, S.; Adams, S. M.; Florer, J. B.; Liu, H.; Kao, W. W.; Wenstrup, R. J.; Birk, D. E., Collagen V is a dominant regulator of collagen fibrillogenesis: dysfunctional regulation of structure and function in a corneal-stroma-specific Col5a1-null mouse model. *J Cell Sci* **2011**, 124 (Pt 23), 4096-105.
 254. Strale, P. O.; Azioune, A.; Bugnicourt, G.; Lecomte, Y.; Chahid, M.; Studer, V., Multiprotein Printing by Light-Induced Molecular Adsorption. *Adv Mater* **2016**, 28 (10), 2024-9.
 255. Lynne T. Smith, K. A. H., Joseph A. Madri, Collagen Types I, III, and V in Human Embryonic and Fetal Skin.
 256. Koppenol, D. C.; Vermolen, F. J.; Niessen, F. B.; van Zuijlen, P. P. M.; Vuk, K., A biomechanical mathematical model for the collagen bundle distribution-dependent contraction and subsequent retraction of healing dermal wounds. *Biomech Model Mechanobiol* **2017**, 16 (1), 345-361.
 257. Uhlen, M.; Fagerberg, L.; Hallstrom, B. M.; Lindskog, C.; Oksvold, P.; Mardinoglu, A.; Sivertsson, A.; Kampf, C.; Sjostedt, E.; Asplund, A.; Olsson, I.; Edlund, K.; Lundberg, E.; Navani, S.; Szigartyo, C. A.; Odeberg, J.; Djureinovic, D.; Takanen, J. O.; Hober, S.; Alm, T.; Edqvist, P. H.; Berling, H.; Tegel, H.; Mulder, J.; Rockberg, J.; Nilsson, P.; Schwenk, J. M.; Hamsten, M.; von Feilitzen, K.; Forsberg, M.; Persson, L.; Johansson, F.; Zwahlen, M.; von Heijne, G.; Nielsen, J.; Ponten, F., Proteomics. Tissue-based map of the human proteome. *Science* **2015**, 347 (6220), 1260419.
 258. Edqvist, P. H.; Fagerberg, L.; Hallstrom, B. M.; Danielsson, A.; Edlund, K.; Uhlen, M.; Ponten, F., Expression of human skin-specific genes defined by transcriptomics and antibody-based profiling. *J Histochem Cytochem* **2015**, 63 (2), 129-41.
 259. Kajbafzadeh, A. M.; Elmi, A.; Mazaheri, P.; Talab, S. S.; Jan, D., Genitourinary involvement in epidermolysis bullosa: clinical presentations and therapeutic challenges. *BJU Int* **2010**, 106 (11), 1763-6.
 260. Phillip, J. M.; Aifuwa, I.; Walston, J.; Wirtz, D., The Mechanobiology of Aging. *Annu Rev Biomed Eng* **2015**, 17, 113-141.
 261. Pan, X.; Chen, Z.; Huang, R.; Yao, Y.; Ma, G., Transforming growth factor beta1 induces the expression of collagen type I by DNA methylation in cardiac fibroblasts. *PLoS One* **2013**, 8 (4), e60335.
 262. JC Gessin , L. B., JS Gordon JS, R.G.Berg, Regulation of collagen synthesis in human dermal fibroblasts in contracted collagen gels by ascorbic acid, growth factors, and inhibitors of lipid peroxidation. *Exp. Cell Res.* **1993**, 206, 283-290.

263. Pullar, J. M.; Carr, A. C.; Vissers, M. C. M., The Roles of Vitamin C in Skin Health. *Nutrients* **2017**, *9* (8).
264. S, R. S.; R, P.; P, S.; J, T.; rews, Effect of vitamin C on collagen biosynthesis and degree of birefringence in polarization sensitive optical coherence tomography (PS-OCT). *African Journal of Biotechnology* **2008**, *7* (12), 2049-2054.
265. S.J Kim, J. H. P., D.H Kim,Y.Ho,H.I. Maibach, Increased In Vivo Collagen Synthesis and In Vitro Cell Proliferative Effect of Glycolic Acid. *Dermatologic Surg* **1998**, *24* (10), 1054-1058.
266. Ganceviciene, R.; Liakou, A. I.; Theodoridis, A.; Makrantonaki, E.; Zouboulis, C. C., Skin anti-aging strategies. *Dermatoendocrinol* **2012**, *4* (3), 308-19.
267. Khan, E. S.; Sankaran, S.; Paez, J. I.; Muth, C.; Han, M. K. L.; Del Campo, A., Photoactivatable Hsp47: A Tool to Regulate Collagen Secretion and Assembly. *Adv Sci (Weinh)* **2019**, *6* (9), 1801982.
268. FitzHarris, G.; Marangos, P.; Carroll, J., Changes in endoplasmic reticulum structure during mouse oocyte maturation are controlled by the cytoskeleton and cytoplasmic dynein. *Dev Biol* **2007**, *305* (1), 133-44.
269. Lippincott-Schwartz, J., Kinesin is the motor for microtubule-mediated Golgi-to-ER membrane traffic [published errata appear in J Cell Biol 1995 Mar;128(5):following 988 and 1995 May;129(3):893]. *The Journal of Cell Biology* **1995**, *128* (3), 293-306.
270. Miles, S.; McManus, H.; Forsten, K. E.; Storrie, B., Evidence that the entire Golgi apparatus cycles in interphase HeLa cells: sensitivity of Golgi matrix proteins to an ER exit block. *J Cell Biol* **2001**, *155* (4), 543-55.
271. Mirco Capitani; Sallese, M., The KDEL receptor: New functions for an old protein. *FEBS Letters* **2009**, 3863–3871.
272. Satoh, M., Intracellular interaction of collagen-specific stress protein HSP47 with newly synthesized procollagen. *The Journal of Cell Biology* **1996**, *133* (2), 469-483.
273. Björn Becker, M. R. S., Domenik Rammo, Tobias Bubel, Ludger Santen & Manfred J. Schmitt, Cargo binding promotes KDEL receptor clustering at the mammalian cell surface. *Scientific Reports* **2016**.
274. Alice Chen, T. H., Carole Mikoryak, Rockford K. Draper Retrograde transport of protein toxins under conditions of COPI dysfunction. *Biochimica et Biophysica Acta* **1589** **2002**, 124-139.
275. Björn Becker, A. B., Esther Gießelmann, Julia Dausend, Domenik Rammo, Nina C. Müller, Emilia Tschacksch, Miriam Steimer, Jenny Spindler, Ute Becherer, Jens Rettig, Frank Breinig & Manfred J. Schmitt, H/KDEL receptors mediate host cell intoxication by a viral A/B toxin in yeast. *Scientific Reports* **2016**, 1-11.
276. Becker, B.; Shaebani, M. R.; Rammo, D.; Bubel, T.; Santen, L.; Schmitt, M. J., Cargo binding promotes KDEL receptor clustering at the mammalian cell surface. *Sci Rep* **2016**, *6*, 28940.
277. Ito, S.; Ogawa, K.; Takeuchi, K.; Takagi, M.; Yoshida, M.; Hirokawa, T.; Hirayama, S.; Shin-Ya, K.; Shimada, I.; Doi, T.; Goshima, N.; Natsume, T.; Nagata, K., A small-molecule compound inhibits a collagen-specific molecular chaperone and could represent a potential remedy for fibrosis. *J Biol Chem* **2017**, *292* (49), 20076-20085.

278. Corrine R. Kliment, J. M. E., Lauren P. Crum, Tim D. Oury, A novel method for accurate collagen and biochemical assessment of pulmonary tissue utilizing one animal. *Int J Clin Exp Pathol* **2011**, 4 (4), 349-355.
279. Cole, M. A.; Quan, T.; Voorhees, J. J.; Fisher, G. J., Extracellular matrix regulation of fibroblast function: redefining our perspective on skin aging. *J Cell Commun Signal* **2018**, 12 (1), 35-43.
280. Fisher, G. J.; Varani, J.; Voorhees, J. J., Looking older: fibroblast collapse and therapeutic implications. *Arch Dermatol* **2008**, 144 (5), 666-72.
281. Wang, Z. L.; Inokuchi, T.; Ikeda, H.; Baba, T. T.; Uehara, M.; Kamasaki, N.; Sano, K.; Nemoto, T. K.; Taguchi, T., Collagen-binding heat shock protein HSP47 expression during healing of fetal skin wounds. *Int J Oral Maxillofac Surg* **2002**, 31 (2), 179-84.
282. Johnston, E. F.; Gillis, T. E., Transforming growth factor beta-1 (TGF-beta1) stimulates collagen synthesis in cultured rainbow trout cardiac fibroblasts. *J Exp Biol* **2017**, 220 (Pt 14), 2645-2653.
283. Lu, Y.; Azad, N.; Wang, L.; Iyer, A. K.; Castranova, V.; Jiang, B. H.; Rojanasakul, Y., Phosphatidylinositol-3-kinase/akt regulates bleomycin-induced fibroblast proliferation and collagen production. *Am J Respir Cell Mol Biol* **2010**, 42 (4), 432-41.
284. Liu, Y.; Li, Y.; Li, N.; Teng, W.; Wang, M.; Zhang, Y.; Xiao, Z., TGF-beta1 promotes scar fibroblasts proliferation and transdifferentiation via up-regulating MicroRNA-21. *Sci Rep* **2016**, 6, 32231.
285. Moses, D. H. L., TGF-P Regulation of Epithelial Cell Proliferation. *Mol. Reprod. Dev.* **1992**, 32, 179-184.
286. Trompezinski, S., Berthier-Vergnes, O. , Denis, A. , Schmitt, D. and Viac,J, Comparative expression of vascular endothelial growth factor family members, VEGF-B, -C and -D, by normal human keratinocytes and fibroblasts. *Experimental Dermatology* **2004**, 13, 98-105.
287. Jeffrey M. Davidson, P. A. L., Ornella Zoia†, Daniela Quaglino, Jr.,MariaGabriella Giro, Ascorbate Differentially Regulates Elastin and Collagen Biosynthesis in Vascular Smooth Muscle Cells and Skin Fibroblasts by Pretranslational Mechanisms. *J.Biol.Chem* **1997**, 272, 345-352.
288. Murad, S.; Tajima, S.; Johnson, G. R.; Sivarajah, A.; Pinnell, S. R., Collagen Synthesis in Cultured Human Skin Fibroblasts: Effect of Ascorbic Acid and Its Analogs. *Journal of Investigative Dermatology* **1983**, 81 (2), 158-162.
289. Seong-Jin Kim. Jong-Jin Kim, J.-H. P., Do-Heong-Jin Kim, Jong-Hyuk Park, Do-Hyun Kim, Young-Ho Won, Howard I.Maibach Increased In Vivo Collagen Synthesis and In Vitro Cell Proliferative Effect of Glycolic Acid. *Dermatol Surg* **1998**, 24, 1054 -1058.
290. Varani; Gary J. Fisher; John J. Voorhees; Sewon Kang, R. K. H. S. R. K. W. E. S. S. C. V. N. H. T. A. H. A. L. K. J. D. N. J., Improvement of Naturally Aged Skin With Vitamin A (Retinol). *ARCH DERMATOL* **2007**, 143, 606-612.
291. Loscertales, M.; Nicolaou, F.; Jeanne, M.; Longoni, M.; Gould, D. B.; Sun, Y.; Maalouf, F. I.; Nagy, N.; Donahoe, P. K., Type IV collagen drives alveolar epithelial-

- endothelial association and the morphogenetic movements of septation. *BMC Biol* **2016**, *14*, 59.
292. Brownfield, D. G.; Venugopalan, G.; Lo, A.; Mori, H.; Tanner, K.; Fletcher, D. A.; Bissell, M. J., Patterned collagen fibers orient branching mammary epithelium through distinct signaling modules. *Curr Biol* **2013**, *23* (8), 703-9.
293. Wehner, D.; Tsarouchas, T. M.; Michael, A.; Haase, C.; Weidinger, G.; Reimer, M. M.; Becker, T.; Becker, C. G., Wnt signaling controls pro-regenerative Collagen XII in functional spinal cord regeneration in zebrafish. *Nat Commun* **2017**, *8* (1), 126.
294. Lopes, J.; Adiguzel, E.; Gu, S.; Liu, S. L.; Hou, G.; Heximer, S.; Assoian, R. K.; Bendeck, M. P., Type VIII collagen mediates vessel wall remodeling after arterial injury and fibrous cap formation in atherosclerosis. *Am J Pathol* **2013**, *182* (6), 2241-53.
295. S. Glagov , H. S. B., Y. Sakaguchi, C.A. Goudet, R.P. Vito, Mechanical determinants of plaque modeling, remodeling and disruption. *Atherosclerosis* **1997**, *131 Suppl* (S13-S14).
296. Sluijter, J., Increased collagen turnover is only partly associated with collagen fiber deposition in the arterial response to injury. *Cardiovascular Research* **2004**, *61* (1), 186-195.
297. Shi-Wu Li, D. J. P. c., Heikki Helminen, Reinhard Fassler, Tuomo Lapvetelainen, Kari Kiraly, Alpo Peltarri, Jari Arokoski, Hui Lui, Machiko Arita, and Jaspal S. Khillan, Transgenic mice with targeted inactivation of the $\alpha 1(\text{I})$ gene for collagen 11 develop a skeleton with membranous and periosteal bone but no endochondral bone. *Genes and development* **1995**, *9* (2821-2830).
298. Mackie, E. J.; Ahmed, Y. A.; Tatarczuch, L.; Chen, K. S.; Mirams, M., Endochondral ossification: how cartilage is converted into bone in the developing skeleton. *Int J Biochem Cell Biol* **2008**, *40* (1), 46-62.
299. Gilkes, D. M.; Chaturvedi, P.; Bajpai, S.; Wong, C. C.; Wei, H.; Pitcairn, S.; Hubbi, M. E.; Wirtz, D.; Semenza, G. L., Collagen prolyl hydroxylases are essential for breast cancer metastasis. *Cancer Res* **2013**, *73* (11), 3285-96.
300. Nakai, A., Involvement of the stress protein HSP47 in procollagen processing in the endoplasmic reticulum. *The Journal of Cell Biology* **1992**, *117* (4), 903-914.
301. Kenneth D. Philipson, J. P. G., Gabriel S. Brandt, Dennis A. , Incorporation of caged cysteine and caged tyrosine into a transmembrane segment of the nicotinic ACh receptor. *American Journal of Physiology-Cell Physiology* **2001**, *281*:1, C195-C206.
302. Schwarz, R. I., Collagen I and the fibroblast: high protein expression requires a new paradigm of post-transcriptional, feedback regulation. *Biochem Biophys Rep* **2015**, *3*, 38-44.
303. Ramakrishnan, P.; Maclean, M.; MacGregor, S. J.; Anderson, J. G.; Grant, M. H., Cytotoxic responses to 405nm light exposure in mammalian and bacterial cells: Involvement of reactive oxygen species. *Toxicol In Vitro* **2016**, *33*, 54-62.
304. Canty, E. G.; Kadler, K. E., Procollagen trafficking, processing and fibrillogenesis. *J Cell Sci* **2005**, *118* (Pt 7), 1341-53.

305. Pickard, A.; Adamson, A.; Lu, Y.; Chang, J.; Garva, R.; Hodson, N.; Kadler, K., Collagen assembly and turnover imaged with a CRISPR-Cas9 engineered Dendra2 tag. **2018**.
306. Stachon, T.; Stachon, A.; Hartmann, U.; Seitz, B.; Langenbucher, A.; Szentmary, N., Urea, Uric Acid, Prolactin and fT4 Concentrations in Aqueous Humor of Keratoconus Patients. *Curr Eye Res* **2017**, *42* (6), 842-846.
307. Gordon-Shaag, A.; Millodot, M.; Shneor, E.; Liu, Y., The genetic and environmental factors for keratoconus. *Biomed Res Int* **2015**, *2015*, 795738.
308. You, J.; Corley, S. M.; Wen, L.; Hodge, C.; Hollhumer, R.; Madigan, M. C.; Wilkins, M. R.; Sutton, G., RNA-Seq analysis and comparison of corneal epithelium in keratoconus and myopia patients. *Sci Rep* **2018**, *8* (1), 389.
309. Mahadevan, R.; Arumugam, A. O.; Arunachalam, V.; Kumaresan, B., Keratoconus - a Review from a Tertiary Eye-Care Center☆. *Journal of Optometry* **2009**, *2* (4), 166-172.
310. Torricelli, A. A.; Singh, V.; Santhiago, M. R.; Wilson, S. E., The corneal epithelial basement membrane: structure, function, and disease. *Invest Ophthalmol Vis Sci* **2013**, *54* (9), 6390-400.
311. Rong, S. S.; Ma, S. T. U.; Yu, X. T.; Ma, L.; Chu, W. K.; Chan, T. C. Y.; Wang, Y. M.; Young, A. L.; Pang, C. P.; Jhanji, V.; Chen, L. J., Genetic associations for keratoconus: a systematic review and meta-analysis. *Sci Rep* **2017**, *7* (1), 4620.
312. Sridhar, M. S., Anatomy of cornea and ocular surface. *Indian J Ophthalmol* **2018**, *66* (2), 190-194.
313. Khaled, M. L.; Helwa, I.; Drewry, M.; Seremwe, M.; Estes, A.; Liu, Y., Molecular and Histopathological Changes Associated with Keratoconus. *Biomed Res Int* **2017**, *2017*, 7803029.
314. Hovakimyan, M.; Guthoff, R. F.; Stachs, O., Collagen cross-linking: current status and future directions. *J Ophthalmol* **2012**, *2012*, 406850.
315. Song, X.; Stachon, T.; Wang, J.; Langenbucher, A.; Seitz, B.; Szentmary, N., Viability, apoptosis, proliferation, activation, and cytokine secretion of human keratoconus keratocytes after cross-linking. *Biomed Res Int* **2015**, *2015*, 254237.
316. Nakai, A.; Satoh, M.; Hirayoshi, K.; Nagata, K., Involvement of the stress protein HSP47 in procollagen processing in the endoplasmic reticulum. *J Cell Biol* **1992**, *117* (4), 903-14.
317. Young, R. D.; Knupp, C.; Pinali, C.; Png, K. M.; Ralphs, J. R.; Bushby, A. J.; Starborg, T.; Kadler, K. E.; Quantock, A. J., Three-dimensional aspects of matrix assembly by cells in the developing cornea. *Proc Natl Acad Sci U S A* **2014**, *111* (2), 687-92.
318. Meek, K. M., Corneal collagen-its role in maintaining corneal shape and transparency. *Biophys Rev* **2009**, *1* (2), 83-93.
319. Spiesz, E. M.; Kaminsky, W.; Zysset, P. K., A quantitative collagen fibers orientation assessment using birefringence measurements: calibration and application to human osteons. *J Struct Biol* **2011**, *176* (3), 302-6.

320. Adam Pickard, A. A., Yinhui Lu, Joan Chang, Richa Garva, Nigel Hodson, Karl E. Kadler, Collagen assembly and turnover imaged with a CRISPR-Cas9 engineered Dendra2 tag. *bioRxiv* **2018**, 331496.
321. Breurken, M.; Lempens, E. H.; Merckx, M., Protease-activatable collagen targeting based on protein cyclization. *Chembiochem* **2010**, *11* (12), 1665-8.
322. Razzaque, M., Expression profiles of collagens, HSP47, TGF- β 1, MMPs and TIMPs in epidermolysis bullosa acquisita. *Cytokine* **2003**, *21* (5), 207-213.
323. NEB. IMPACT Kit Instruction manual 2016 2016.
324. Tarasava, K.; Freisinger, E., An optimized intein-mediated protein ligation approach for the efficient cyclization of cysteine-rich proteins. *Protein Engineering, Design and Selection* **2014**, *27* (12), 481-488.
325. Sydor, J. R.; Mariano, M.; Sideris, S.; Nock, S., Establishment of Intein-Mediated Protein Ligation under Denaturing Conditions: C-Terminal Labeling of a Single-Chain Antibody for Biochip Screening. *Bioconjugate Chem* **2002**, *13*, 707-712.
326. Oecal, S.; Socher, E.; Uthoff, M.; Ernst, C.; Zaucke, F.; Sticht, H.; Baumann, U.; Gebauer, J. M., The pH-dependent Client Release from the Collagen-specific Chaperone HSP47 Is Triggered by a Tandem Histidine Pair. *J Biol Chem* **2016**, *291* (24), 12612-26.
327. Douglass, M. R.; Lee, B. L.; Strale, P.-O.; Azioune, A.; Bugnicourt, G.; Lecomte, Y.; Chahid, M.; Studer, V., Light-induced quantitative microprinting of biomolecules. In *Emerging Digital Micromirror Device Based Systems and Applications IX*, 2017.
328. Greenspan, D. S., Biosynthetic Processing of Collagen Molecules. In *Collagen*, 2005; pp 149-183.
329. He, W.; Dai, C., Key Fibrogenic Signaling. *Curr Pathobiol Rep* **2015**, *3* (2), 183-192.
330. Ito, S.; Nagata, K., Biology of Hsp47 (Serpin H1), a collagen-specific molecular chaperone. *Semin Cell Dev Biol* **2017**, *62*, 142-151.

List of Publications

Published

1. **Essak S Khan**, Shrikrishnan Sankaran, Julieta I. Paez, C. Muth, Mitchell. K. L. Han, Aranzazu del Campo, *Photoactivatable Hsp47: A Tool to Regulate Collagen Secretion and Assembly*, *Adv. Sci.* 2019, 1801982.
2. Yoo Jin Oh, **Essak S Khan**, Aranzazu del Campo, Peter Hinterdorfer, Bin Li, *Nano scale Characteristics and Antimicrobial Properties of (SI-ATRP)-Seeded Polymer Brush Surfaces*, *ACS Appl. Mater. Interfaces* 2019, Accepted.
3. **Essak S Khan**, Shrikrishnan Sankaran, Lorena LLontop, Aranzazu del Campo, *Hsp47: Exogenous supply of Hsp47 triggers fibrillar collagen deposition in skin cell cultures in vitro. (under review at BMC Mol and Cell Biol)* <https://www.biorxiv.org/content/10.1101/803791v1>

In preparation

1. **Essak S Khan**, Jennifer Kasper, Shrikrishnan Sankaran, Tanja Stachon, Aranzazu del Campo, *Stimulated collagen production in corneal tissue using Hsp47: a new therapeutic scenario for Keratoconus?*
2. **Essak S Khan***, Shrikrishnan Sankaran*, Gülistan Kocer, Christina Muth, Aranzazu del Campo *Bio interface for optoregulation of HER2 induced EMT in breast cancer.*
3. **Essak S Khan***, Shrikrishnan Sankaran*, Christina Muth, Aranzazu del Campo, *Photoactivatable ZH affibody for optoregulation of HER2 induced EMT in breast cancer.*

***Authors equally contributed to the work.**

Scientific Talks

1. Parker H. Petit Institute for Bioengineering and Bioscience at Georgia Institute of Technology, Atlanta, Georgia (July 2019)
Title: Photo responsive molecules to control and regulate tissue homeostasis
2. Gordon Research Seminar on Collagen, Colby-Sawyer College, New London, NH, USA. (2019), Discussion leader
Title: Collagen scaffolds in health and diseases.
3. Seminar "Bio interfaces" at the INM – Leibniz Institute for New Materials, Saarbrücken, DE (2019).
Title: Photoactivatable Hsp47: A tool to regulate collagen deposition in collagen disorders.
4. FEBS Advanced Lecture Course "Extracellular Matrix: Cell Regulation, Epigenetics & Modeling", University of Patras, GR (2018).
Title: "Optoregulation of the Assembly and Remodeling of Collagen and its associated diseases"
5. Gordon Research Conference & Seminar on Collagen, Colby-Sawyer College, New London, NH, USA. 2017
Title: "Photoactivatable Hsp47: An optogenetic Tool to Control and Regulate Collagen Assembly and Tumor Microenvironment"

Poster Presentations

1. Gordon Research Seminar on Collagen, Colby-Sawyer College, New London, NH, USA (2019).
Title: *Enhanced collagen biosynthesis: A new approach to tissue repair.*
2. 2018 international Symposium on Chemical Biology, Geneva, CH (2018).
Title: *Photoactivatable Hsp47: an optogenetic tool to control & regulate collagen assembly & Tumor microenvironment*
3. Gordon Research Seminar on Collagen, Colby-Sawyer College, New London, NH, USA (2017).
Title: *Optoregulation of collagen assembly and tumor microenvironment.*
4. CNIO-"la Caixa" Foundation Frontiers Meeting, Molecular Chaperones in Cancer, Centro Nacional de Investigaciones Oncológicas (CNIO), Madrid, ESP. (2017)
Title: *Photoactivatable Hsp47: a tool to regulate collagen assembly and tumor microenvironment*
5. Cellular physics conference 2017, Saarbrücken, DE (2016)

Title: "Photoactivatable Hsp47: A photo responsive tool to control collagen assembly and remodeling"

Workshops

1. Flow Cytometry Workshop, Universität des Saarlandes, Center of Integrative Physiology and Molecular Medicine (CIPMM), Homburg, DE
2. Cell culture course workshop, Pormocell, Heidelberg, DE

Doctoral researcher at Dynamic Biomaterials group,

INM-Leibniz Institute for New Materials,

Saarbrücken, Germany (DE)

E-mail Address	essakkhan@gmail.com	Work Address	INM –Leibniz Institute for New Materials, Campus D2 2 66123 Saarbrücken DE
Work E-mail Address	essak.khan@leibniz-inm.de		
Telephone No.	+49 15217118853;		
Date of Birth	24 January 1993	Nationality	Indian

EDUCATION**2016-2019**

PhD, Dynamic Biomaterials, INM Leibniz Institute for New Materials and Saarland University, DE

Thesis: Optoregulation of collagen deposition and remodelling using photoactivatable Hsp47. (Current)

Thesis Supervisor: Prof. Dr. Aránzazu del Campo

Synthesis of photoactivatable Hsp47, biochemical characterization of light-triggered Hsp47-collagen interaction. Demonstration of light-triggered collagen deposition in in vitro culture and ex-vivo tissues (keratoconnus cornea). Collagen imaging with confocal, SHG and STED microscopy.

Collaboration in additional projects:

Bio interface for optoregulation of HER2-induced EMT in breast cancer.

Study of Bacterial interactions at Nano scale

2014-2015

Master Thesis in Technology in Biotechnology, Chemistry Department, IIT Bombay, Mumbai, IN

Thesis defended with *first division*

Master Thesis: Investigation of regulatory cascade governing tylosin production in *Streptomyces fradiae* using systems biology approach

Thesis Supervisors: Prof. dr. Ruchi Anand, Dr. Sandip Kar

Study of the intracellular Tylosin antibiotic signalling cascade in *S. Fradiae* using protein engineering approaches and mathematical modelling. Assays to quantify protein-client interactions and analysis of protein half-life.

2010-2014

Master of Technology [Integrated] in Biotechnology, School of Biotechnology and Bioinformatics, D. Y. Patil University, Navi-Mumbai, IN.

RESEARCH INTEREST

I am interested in developing bioengineering tools to promote tissue engineering and regeneration by employing techniques from biomaterials perspective.

OTHER PUBLICATIONS

Novel quantitative assay for estimation of ketone bodies in diabetic urine,

Essak S Khan, P. Karanjkar &, V.N. Ravi Kishore. V, *International Journal of Scientific & Engineering Research*, 2016, 7, 9.

SKILLS

Optogenetics: Molecular cloning and probing, photoactivatable protein engineering ;

Cell Biology: 2D and 3D cell cultures, human tissue cultures (cornea and tendon);

Advanced microscopy techniques: LIMAP (Light induced molecular adsorption of proteins), Confocal, SHG, STED microscopy and Polarization Microscopy.

Physicochemical techniques like QCM, Nano-DSC, ITC, UV and Fluorescence spec, surface immobilization of proteins e.g. click chemistry, PEG and PAAM hydrogel;

Biomaterials characterization methods: Rheology;

Biochemistry techniques: Q-PCR, Native-PAGE Western blots, IP and IHC;

Bioinformatics techniques Molecular docking, structure predictions, mathematical modelling using differential equations.

AWARDS AND SCHOLARSHIP

- 2018 ISMB (International society of Matrix Biology) travel grant for Young scientist.
- 2014-2015 Stipend based masters dissertation scholarship, IRCTC, IIT Bombay, Mumbai, India
- 2015 Department of Biotechnology, India scholarship for PhD.
- 2010 All India Pre medical test (AIPMT), CBSE, Delhi
All India Engineering Entrance Examination (AIEEE), CBSE, Delhi
National Aptitude Test in Architecture (NATA), Council of Architecture (COA), Government of India.

OTHER CONFERENCES

- 2013 Annual biotechnology program, Haffkinse Institute, Parel, Mumbai, IN
- 2012 Hands on training on FISH, Karyotyping and IVF, Jaslok hospital, Mumbai, IN
- 2011 Conference on Phylogenetic Evolution Studies, BARC (Bhabha Atomic Research Centre), Mumbai, IN
- 2010 Conference on Computational Neuroscience, SIBACA, Shingad Institute, IN

INTERNSHIPS AND EMPLOYMENT:

- 2014 – 2015 Research Intern, Structural Biochemistry Lab & Systems Biology Lab, Department of Chemistry, IIT Bombay, Mumbai
- 2014 – 2015 Assited Lecturers of Basic Anatomy & Physiology;
Ocular Biochemistry & Pharmacology;
Ocular Basic Anatomy & Physiology & Biochemistry;
Netra Mandir Optometry Institute, Netra Mandir Hospital, Mumbai , India.

SUPERVISION OF STUDENTS

1.Assistant in Lab courses:Biopolymers Practical Course at University Saarland 2017, 2018.

2.Supervision of internship students:

Simon Hehn, Summer Internship, Ecole de Biologie Industrielle (EBI), FR, 2018

Project title: Developing light responsive angiogenic growth factor secretion in non pathogenic *E.coli*.

Lorena Llontop, Internship, Biotechnology, TU Kaiserslautern, DE, 2019

Project title: Hsp47 triggered collagen deposition in fibroblast,epithelial and endothelial cell cultures.

OTHER ACTIVITIES

Class representative, MTI Class,2012

Coordinator and Liaison Executive, Biointerns, Placement and Internship Committee, DYPU,School of biotechnology and bioinformatics,2013-14.

